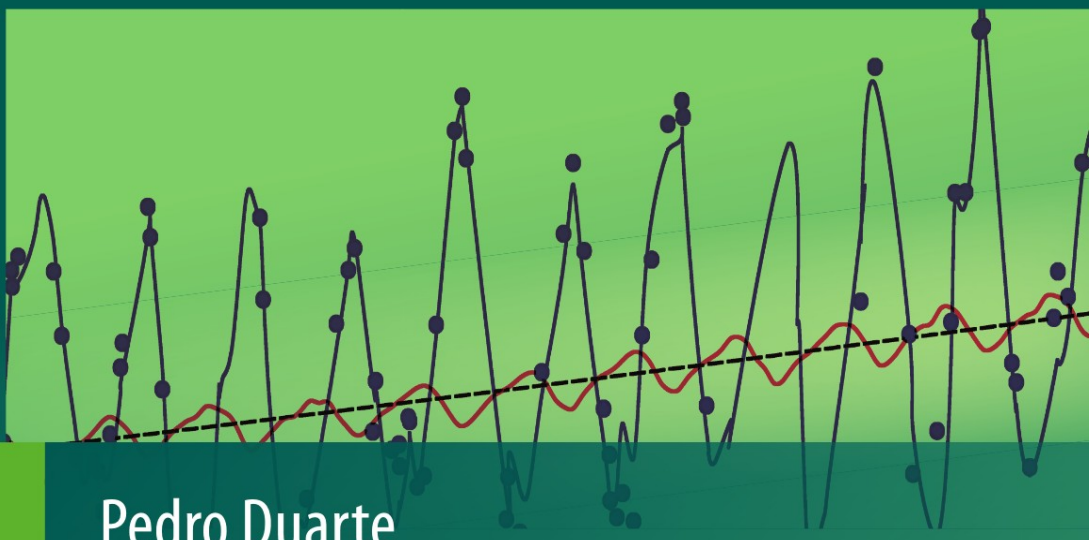

Pedro Duarte
J. Magdalena Santana-Casiano
Editors

Oceans and the Atmospheric Carbon Content

Springer

Oceans and the Atmospheric Carbon Content

Pedro Duarte · J. Magdalena Santana-Casiano
Editors

Oceans and the Atmospheric Carbon Content

Springer

Editors
Pedro Duarte
University Fernando
Pessoa, Porto
Portugal
pduarte@ufp.edu.pt

J. Magdalena Santana-Casiano
Department of Chemistry
University of Las Palmas de Gran Canaria
Spain
jmsantana@dqui.ulpgc.es

ISBN 978-90-481-9820-7 e-ISBN 978-90-481-9821-4
DOI 10.1007/978-90-481-9821-4
Springer Dordrecht Heidelberg London New York

Library of Congress Control Number: PCN applied for

Preface

Most of the chapters of this book were presented as oral communications at the Seasink conference that was held at University Fernando Pessoa, Oporto, Portugal, between the 26th and the 28th of June 2008. The main objective of this conference was to discuss the role of the oceans as a sink for most of the residues from human activities. The conference had several sessions devoted to such topics as organic and inorganic compounds and their effects, global changes, regional approaches to pollution problems and future prospects with respect to the assessment of human impacts upon the marine environment. Some time before the conference, we were invited by Springer to prepare a book on part of the conference topics. Considering the communications presented at the conference and the actuality of issues related to climate change and all its direct and indirect effects upon the oceans, it seemed a good opportunity to prepare a book about the role of the oceans as a carbon sink. In the 2007 synthesis report prepared by the Intergovernmental Panel on Climate Change (IPCC) it is stated that:

> Warming of the climate system is unequivocal, as is now evident from observations of increases in global average air and ocean temperatures, widespread melting of snow and ice and rising global average sea level

In spite of the fact that some people within the scientific community remain skeptical about the causes and the relevance of climate change patterns, there seems to be, at least, a reasonable doubt about its existence and its consequences upon the biosphere. Therefore, it seems reasonable to follow the precautionary principle and try to anticipate and mitigate those consequences. Historically, there is an important time lag between the environmental alerts raised by the scientific community and the political response of human society to those alerts, as discussed in the book "Limits to Growth" by Meadows et al., published in 2004. It is perhaps time to reduce the mentioned time lag and we hope that this book may give a small, yet honest contribution to it.

Globally, the oceans act as a CO_2 sink, as suggested in recent literature. However, this sink role is based on the quantification of CO_2 air–sea exchanges with a low spatial resolution. An important issue is quantifying the source/sink CO_2 role of continental shelves, mostly in near shore urban and industrial high density areas, which emit CO_2 more intensely to the atmosphere. It has been suggested that worldwide the

continental shelf acts as a very important CO_2 sink – "the continental shelf pump hypothesis". However, this hypothesis deserves further investigation, due to the very low spatial and temporal resolution of available data on CO_2 fluxes and to our limited knowledge about the benthic contribution to these fluxes.

Another important issue is to understand the way in which the ocean CO_2 sink may be impacted both by increasing CO_2 levels and global warming. It is expectable that CO_2 fluxes are influenced by upwelling, land drainage, sea surface warming and pH decreasing trends. A pH variation in the ocean could have an important ecological impact as a result of changes in the marine ecosystem and biogeochemical cycles of the elements. Processes that may be changed include organism calcification, carbon and nutrient assimilation, primary production and trace metal speciation. Physiologic and biogeochemical processes tend to be temperature dependent and, therefore, increasing temperature may induce changes in those processes and, consequently, on biologic consumption/production CO_2 processes. Changing temperature may lead to changes in the geographic ranges of several species with potentially important feedbacks to the carbon biogeochemical cycle as well. Furthermore, on one hand, increasing temperature will contribute to saturation of sea water with respect to CO_2, enhancing net efflux from the water to the atmosphere, on the other hand, the opposite effect takes place upon increase of atmospheric CO_2 levels. The awareness raised by the consequences of increasing the so-called greenhouse gases is stimulating the development of several carbon dioxide sequestration technologies and there is already a European directive (Directive 2009/31/EC of the European Parliament and of the council of 23 April 2009) regulating the application of geological storage of carbon dioxide. It is expected that oceans will be used as a ground for some of the mentioned technologies and it is important to anticipate their potential impacts.

This book is divided in eight chapters. Chapter 1 describes the climate variability in the north-western Iberian Peninsula during the last deglaciation, based on a high-resolution pollen analysis in cores retrieved from the Douro estuary and it is also a contribution towards chronologically synchronizing data sets from different origins. It is important to have knowledge about natural and human-induced climate variability to improve projections of future climate changes. Chapter 2 addresses the potential impact of carbon dioxide from a large metropolitan area over the adjacent coastal zone, using an atmospheric dispersion model, and it stresses the importance of having high resolution atmospheric carbon dioxide data to estimate accurately air–sea CO_2 exchanges. Chapter 3 is an in-depth review of present- day carbon dioxide fluxes in the coastal ocean and their potential feedbacks under global climate change, emphasizing the role of coastal oceans as a CO_2 sink and their vulnerability to climate change. Chapter 4 addresses some detailed aspects of phytoplankton community responses to climate change with emphasis on decreasing pH trends in sea water and its ecological effects. Chapter 5 discusses pH decrease and its effects on sea-water chemistry from a 10 year time-series at the ESTOC station, located approximately 100 km north of the islands of Gran Canaria and Tenerife. Chapter 6 presents results on the effect of pH decreases on metal bioaccumulation in the sediments. Chapter 7 analyses possible consequences of

increasing temperatures and pH changes on contaminant cycling. Finally, Chapter 8 presents an application of the Weight-of-Evidence approach for environmental quality assessment regarding the geological sequestration of CO_2 in sediments above sub-seabed geological formations to determine effects of possible leaks.

Results presented and discussed in the chapters of this book suggest that important changes may be occurring in the oceans, as a result of the carbon dioxide increase in the atmosphere, and point to possible effects of these changes over the next decades and their complex synergies with physical, chemical, biological and ecotoxicological phenomena. Furthermore, some of the chapters draw our attention to the necessary precautions regarding the application of some of the technologies used to mitigate problems arising from CO_2 increase in the atmosphere. In synthesis, the contents of this book draw our attention to the importance of dealing with observed global change trends and their effects upon the oceans using an interdisciplinary approach due to their complexity and interlinks between different areas of knowledge.

Contents

1 Climate Variability in the North-Western Iberian Peninsula During the Last Deglaciation 1
Filipa Naughton, Teresa Drago, Maria Fernanda Sanchez-Goñi, and Maria Conceição Freitas

2 Impact of Oporto Metropolitan Area Carbon Dioxide Emissions over the Adjacent Coastal Zone 23
Rogério Carvalho, Nelson Barros, and Pedro Duarte

3 Present Day Carbon Dioxide Fluxes in the Coastal Ocean and Possible Feedbacks Under Global Change 47
Alberto V. Borges

4 Aspects of Phytoplankton Communities Response to Climate Changes 79
Maria da Graça Cabeçadas, Maria José Brogueira, Maria Leonor Cabeçadas, Ana Paula Oliveira, and Marta Cristina Nogueira

5 pH Decrease and Effects on the Chemistry of Seawater 95
Juana Magdalena Santana-Casiano and Melchor González-Dávila

6 Effects of Sediment Acidification on the Bioaccumulation of Zn in *R. Philippinarum* 115
Inmaculada Riba, Enrique García-Luque, Judit Kalman, Julián Blasco, and Carlos Vale

7 Contaminant Cycling Under Climate Change: Evidences and Scenarios 133
Carlos Vale, João Canário, Miguel Caetano, Laurier Poissant, and Ana Maria Ferreira

8 The Use of Weight of Evidence for Environmental Quality Assessment in Sediments Above Sub-Seabed Geological Formations for the Storage of Carbon Dioxide 157
Tomás-Ángel DelValls Casillas, Diana Fernández de la Reguera Tayá, Maria Inmaculada Riba López, and Jesus María Forja Pajares

Index 173

Chapter 1
Climate Variability in the North-Western Iberian Peninsula During the Last Deglaciation

Filipa Naughton, Teresa Drago, Maria Fernanda Sanchez-Goñi, and Maria Conceição Freitas

Abstract Vegetation reconstruction from north-western Portugal estuarine cores reflects millennial- to centennial-scale climate variability during the Last Glacial–Interglacial Transition (LGIT) in the Douro basin. These vegetation cover changes match perfectly the climatic pattern detected in the North Atlantic region and in Greenland. Changes between high and weak forested phases in the Douro basin are associated with warm and cold episodes, respectively.

The first warm episode, the Bölling, occurring within the LGIT, follows the Oldest Dryas episode (terrestrial equivalent of the marine Heinrich 1 event) and was characterised by the expansion of pine, oak and birch. Subsequently, a rapid climate reversal was revealed by the contraction of that arboreal association and increase of herbaceous *taxa* probably reflecting the centennial-scale Older Dryas episode (one of the well-known Intra Bölling-Allerød cold events). The Allerød event, representing the subsequent warming phase, was characterised by the expansion of alder followed by pine. Afterwards, an abrupt cooling occurred, evidenced by the replacement of temperate trees (pine and oak) by herbaceous plants (compositae and grasses), reflecting

F. Naughton (✉)
Unidade de Geologia Marinha, Laboratorio Nacional de Energia e Geologia, Aptdo 7586, 2721-866 Amadora, Portugal INETI, Lisboa, Portugal
e-mail: filipa.naughton@ineti.pt

T. Drago
Instituto Nacional de Recursos Biológicos I.P, IPIMAR, Av. 5 de Outubro, 8700-305 Olhão, Portugal
e-mail: tdrago@ipimar.pt

M.F. Sanchez-Goñi
EPHE, Environnements et Paléoenvironnements Océaniques (UMR CNRS 5805 EPOC), Bordeaux 1 University, Av. des Facultés, 33405 Talence, France
e-mail: mf.sanchezgoni@epoc.u-bordeaux1.fr

M.C. Freitas
Departamento e Centro de Geologia, Faculdade de Ciências, Universidade de Lisboa, Bloco C6, 3º piso, Campo Grande 1749-016 Lisboa, Portugal
e-mail: cfreitas@fc.ul.pt

P. Duarte and J.M. Santana-Casiano (eds.), *Oceans and the Atmospheric Carbon Content*,
DOI 10.1007/978-90-481-9821-4_1,

the Younger Dryas cold event. Finally, the end of the LGIT was characterised by a maximal expansion of temperate and humid forest (birch, oak, pine, ashes, alder), as likely being the result of the climate improvement that characterises the present-day interglacial, the Holocene.

Keywords Climate variability • North-western Iberian Peninsula • Douro estuary • Sedimentation • Vegetation • Forest • Pollen • Glacial–Interglacial transition • Deglaciation • Bölling • Dryas episode • Allerød event • Holocene

1.1 Introduction

Human activities have produced substantial changes in the Earth's climate system since the last century. Knowledge about natural and human-induced climate variability is essential to improve projections of future climate changes. Over the last million years, the earth's climate system has experienced several cyclic shifts of different amplitudes, duration and temporal scales. Oscillations between glacial and interglacial conditions were mainly controlled by changes in the distribution of sunlight on Earth associated with features of the Earth's orbit (e.g. Imbrie et al. 1992) while large, abrupt and widespread millennial-scale climatic changes, known as the Dansgaard-Oeschger events (Dansgaard et al. 1993) were mainly triggered by North Atlantic oceanographic changes (Broecker 1994; Bond et al. 1999). During the last deglaciation (20–6 ka), an increase of the Northern Hemisphere summer insolation resulted in melting of high-latitude ice sheets and, consequently, in rises of sea-level (Imbrie et al. 1992). Superimposed on this global warming trend and, in particular, during the Last Glacial-Interglacial Transition (LGIT) (15–11.5 ka), a millennial-scale climate variability has been detected in the North Atlantic, European archives and Greenland ice records (e.g. Mangerud et al. 1974; Lehman and Keigwin 1992; Alley et al. 1993; Dansgaard et al. 1993). Both orbital and suborbital induced climate variability of the last deglaciation is well expressed in pollen records from the north-western Iberian margin (core MD03-2697: 42°09′59N, 09°42′10W; 2,164 m depth and core MD99-2331: 42°09′00N, 09°40′90W; 2,110 m depth) (Naughton 2007; Naughton et al. 2007a). Vegetation changes in the north-western Iberian Peninsula are synchronous with those reflected by the marine proxy data (e.g. Sea Surface Temperatures-SST) from the same deep-sea core (Naughton 2007; Naughton et al. 2007a). In these records, the warm episode known as Bölling-Allerød (terrestrial equivalent of the Greenland interstadial 1-GIS1: Johnsen et al. 2001; Lowe et al. 2001, 2008) is bracketed by two cold events: the Oldest Dryas which is the terrestrial equivalent of the marine Heinrich event 1 (Naughton et al. 2007a) and of the Greenland stadial 2-GS2 (Johnsen et al. 2001; Lowe et al. 2001) and the Younger Dryas which is the terrestrial counterpart of Greenland stadial 1-GS1 detected in marine and ice cores (e.g. Johnsen et al. 2001; Lowe et al. 2001; Lehman and Keigwin 1992; Naughton et al. 2007a). A sub

millennial-scale cold episode, named Older Dryas, was firstly identified in northern European pollen sequences (e.g. Mangerud et al. 1974), occurring in between the Bölling and the Allerød warm events. The multi-proxy record from the north-western Iberian margin (Naughton et al. 2007a) did not, however, detect this event. Indeed, the Older Dryas event is sometimes difficult to identify and its existence in central and southern Europe has been a subject of debate over the past few decades (see Sanchez Goñi 1996). The lack of evidence of this particular cold event in several central and southern Europe pollen records could be due to low time resolution studies and/or because the vegetation was not sensitive enough to rapidly respond to this relatively abrupt cold event (Sanchez Goñi 1996). However, recent central European paleoclimatic records have documented two century-scale cold events during the Bölling-Allerød warm period (B-A), identified as Older Dryas and intra-Allerød events (Von Grafenstein et al. 1999; Brauer et al. 2000). High time resolution (centennial-scale) pollen records from the Paris Basin (north of France) (Pastre et al. 2000, 2003; Limondin-Lozouet et al. 2002) and lake Lautrey (eastern France) (Peyron et al. 2005; Magny et al. 2006) permitted identification of a cold episode within the Bölling-Allerød, which has been attributed to the Older Dryas event. There are also evidences of two rapid dry episodes within the Bölling-Allerød interstadial in the western tropical and sub-tropical North Atlantic region (e.g. Hughen et al. 1996; Willard et al. 2007). In the northern Iberian Peninsula, most of the well-known pollen sequences (Allen et al. 1996; Peñalba et al. 1997; Muñoz Sobrino et al. 2004) do not record vegetation cover changes during the Older Dryas event. However, further south, the Serra da Estrela pollen records (Portugal) show an abrupt cooling episode which authors associate with the Older Dryas event (Van der Knaap and Van Leewen 1997).

The Serra da Estrela is the only region of Portugal consisting of lakes with continuous sedimentation offering the possibility to document the vegetation history of the Mediterranean biogeographical region since the last deglaciation. No lake records from northern Portugal are available so far to document vegetation changes in the Atlantic biogeographical region during the last deglaciation. Only marine and relatively continuous estuarine pollen records reflecting the regional pollen signature from the northern hydrographical basins can help us to document past vegetation changes in that region.

The aim of this work is to document vegetation responses of northern Portugal to the climate variability that characterises the mid- and end-stages of the last deglaciation (16. 5–6 ka) in the North Atlantic region (e.g. Lehman and Keigwin 1992; Naughton et al. 2007a) and to determine whether the vegetation of this region has changed during the Older Dryas event. For this, we will perform a high resolution (centennial- time scale) pollen analysis in two cores retrieved from the Douro estuary. Previous analyses (sedimentological and micropaleontological) on both cores, have shown several environmental changes in the Douro estuary, such as the displacement of the river main channel during the last deglaciation which was mainly triggered by substantial global sea-level changes (Drago et al. 2006; Naughton et al. 2007b). Furthermore, a detailed description of pollen data reflecting the Holocene period has been previously published in Naughton et al. (2007b).

1.2 Environmental Settings

The Douro estuary is located in the north-western Portuguese coast (41°09′00″N; 8°38′00″W) being nourished by several tributaries, such as the Douro, Coa, Tua, Tâmega, Balsemão and Sousa rivers, which compose the Douro hydrographic basin (Fig. 1.1). This basin is wide (area of 97.682 km^2) and characterised by a heterogeneous

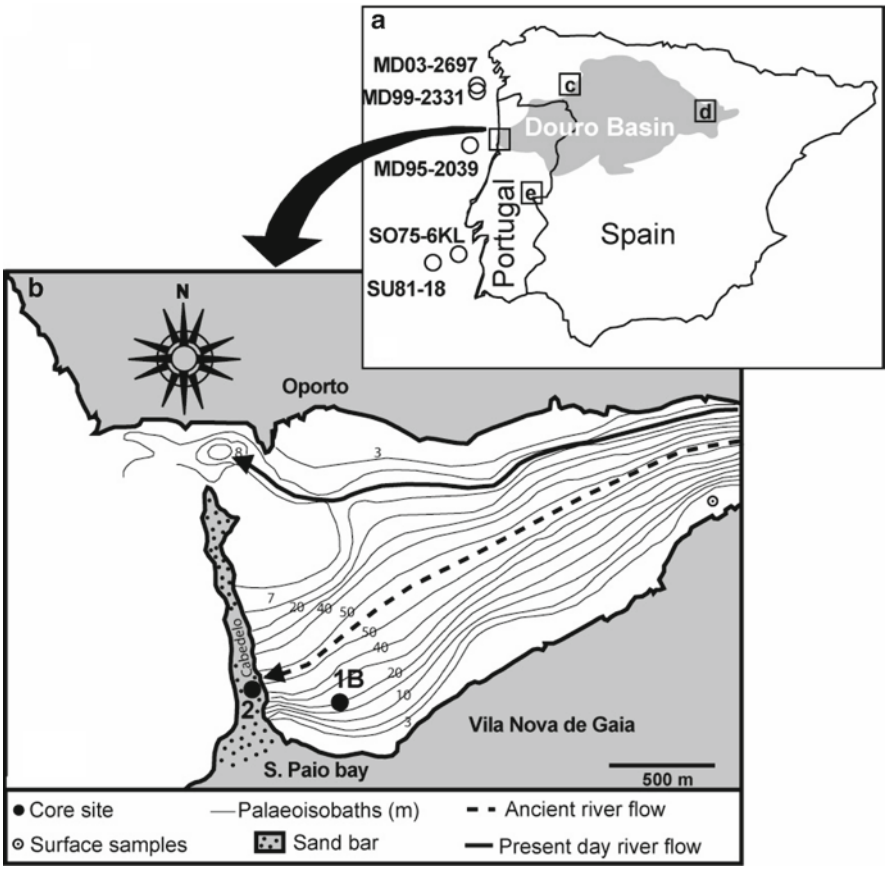

Fig. 1.1 Study area: (**a**) Iberian Peninsula and Douro basin; (**b**) Douro estuary. Dark points represent core sites used in this work; white circles reflect marine pollen sequences (MD03-2697: Naughton 2007; Naughton et al. 2007a; MD99-2331: Naughton 2007; Naughton et al. 2007a, MD95-2039: Roucoux et al. 2005; SU81-18: Turon et al. 2003; SO75-6KL: Boessenkool et al. 2001) and squares c, d and e illustrate the well know reference pollen sequences from Iberian Peninsula (Laguna de la Roya: Allen et al. 1996; Laguna de las Sanguijuelas and lleguna: Muños Sobrino et al. 2004; Quintanar de la Sierra: Peñalba et al. 1997 and Serra da Estrela: Van der Knaap and Van Leeven 1997). Dark lines represent the palaeoisobathic curves defined by Carvalho and Rosa (1988). The dashed line represents the ancient direction of the river main channel flow and the bold dark line the present day river main channel flow. This palaeobathymetric map shows the palaeovalley of the Douro river

geomorphology which results in a complex climate regime. In the west, the climate is strongly influenced by the sea, being humid (annual rainfall average ranges from 1,200 to 2,500 mm) and mild (annual temperature average ranges from 11°C to 15°C). The eastern sector is characterised by a more continental climate with large temperature ranges (cold winters and hot summers), being dryer than the western sector (average annual rainfall ranges from 400 to 1,200 mm) (Loureiro et al. 1986). These climatic patterns generate a complex distribution of vegetation in the Douro basin (Pina Manique 1957; Costa et al. 1998). The continental climate favours the expansion of evergreen oaks (*Quercus ilex* and *Quercus suber*), deciduous oaks (*Quercus pyrenaica* and *Quercus faginea*) and *Juniperus* spp. while the oceanic influence is the predominating Quercion occidentale assemblage (*Quercus robur* and *Q. suber*) (Braun-Blanquet et al. 1956). The river margins are colonized by demanding water requirement species such as *Alnus glutinosa*, *Fraxinus angustifolia*, *Ulmus* spp., *Salix* spp. and *Populus* spp. and the estuary surrounding area is dominated by Poaceae and Ericaceae. The spread of both *Pinus pinaster* and *Eucalyptus globulus* has been induced by man.

The Douro basin is influenced by north-western prevailing winds favouring the transport of pollen grains, mainly by rivers, until the Douro estuary (Naughton et al. 2007a). The mean annual draining is 22.400×10^6 m^3, equivalent to 710 m^3/s of mean annual discharge, with a maximum of 3,000 m^3/s and a minimum of 50 m^3/s (Loureiro et al. 1986).

1.3 Material and Methods

Two cores (1B and 2) were retrieved by rotary drilling in the Douro estuary (Fig. 1.1) using permanent water injection (see Drago et al. 2006; Naughton et al. 2007b). Core 2 attained 43.49 m (–39.19 m in Ordnance Datum–OD which is a coordinate system for heights above mean sea level) and core 1B attained 17.40 m (–13.90 m OD), respectively. Core 2 was retrieved in the paleoriver main channel while core 1B in its southern slope (Fig. 1.1) (Drago et al. 2006).

1.3.1 Radiometric Dating

Six accelerator mass spectrometer (AMS) ^{14}C dates on organic material were obtained in the Beta Analytic, Inc (Table 1.1). All AMS ^{14}C dated levels were calibrated using CALIB Rev 5.0 program and the intcal 04.14c dataset (Stuiver and Reimer 1993; Stuiver et al. 2005). We used the 95.4% (2 sigma) confidence intervals and their relative areas under the probability curve as well as the median probability of the probability distribution (Telford et al. 2004) as suggested by Stuiver et al. (2005). Conventional AMS dates are presented in yr BP (years before present: AD1950) and calibrated dates in "a" (age).

Table 1.1 Conventional radiocarbon and calibrated dates of the Douro estuary cores

Lab code	Core- depth (m)	Core- depth (m) OD	Material	Conv. AMS ^{14}C (kyr BP)	Error	95.4% (2σ) Cal BP age ranges	Cal BP age median probability (ka)
Beta-154313	Core 1B 10.64/10.65	Core 1B –7.14/–7.15	Organic matter	5,750	40	6449 BP:6651 BP	6,548
Beta-174809	Core 1B 11.83/11.84	Core 1B –8.33/–8.34	Organic matter	6,050	60	6741 BP:7029 BP	6,903
Beta-154314	Core 1B 17.40/17.41	Core 1B –13.90 /13.91	Organic matter	9,490	60	10579 BP:10881 BP	10,770
Beta-174810	Core 2 27.08/27.09	Core 2 –22.74/–22.75	Organic matter	9,230	50	10249 BP:10524 BP	10,395
Beta-161372	Core 2 36.66/36.67	Core 2 –32.32/–32.33	Organic matter	10,310	80	11806 BP:12398 BP	12,131
Beta-154315	Core 2 43.40/43.41	Core 2 –39.06/–39.07	Organic matter	13,730	90	15961 BP:16792 BP	16,351

1.3.2 Pollen Analysis

Sixty eight (68) and 40 samples from cores 1B and 2, respectively, were treated for pollen analysis. Sample preparation technique follows Desprat (2005). An exotic spike (Lycopodium) of known concentration has been added to each sample to calculate the total pollen concentrations. After chemical treatments (cold 10%, 25% and 50% HCl; cold 40% and 70% HF), the samples were sieved through a 10 μm nylon mesh screen and mounted in bidistillate glycerine. Pollen and spores were counted using a Zeiss Axioscope light microscope at x550 and x1250 (oil immersion) magnifications. Pollen identifications were achieved via comparison with specialist atlases (Reille 1992) as well as with the EPOC-Bordeaux 1 University reference pollen collection. A minimum of 300 pollen grains (excluding aquatic plants, spores, indeterminate and unknown pollen grains), 100 *Lycopodium* grains and 20 pollen types were counted in each of the 108 samples analysed, to obtain statistically reliable pollen spectra (Rull 1987; Maher 1981). Seven samples from the bottom of core 2 were sterile.

Pollen percentages were calculated based on the main pollen sum which excludes aquatic plants, spores, indeterminate and unknown pollen. We also determined arboreal pollen (AP) and Non Arboreal pollen (NAP) percentages. AP includes: *Pinus*, *Alnus*, *Betula*, *Corylus*, *Quercus suber*-type, deciduous *Quercus*-type, *Quercus ilex*-type, *Salix*, *Fraxinus*, *Hedera helix*, *Olea*, Rhamnaceae, *Pistacia* and *Cistus* while NAP is composed of: *Ephedra*, Chenopodiaceae, *Artemisia*, *Taraxacum*, *Aster*, Caryophyllaceae, *Centaurea Helianthemum*, Lamiaceae, Brassicaceae, Ranunculaceae, *Asphodelus*, *Euphorbia*, Fabaceae, *Polygonum*, *Rumex*, Rosaceae, Apiaceae, Boraginaceae, Cyperaceae, Crassulaceae, Primulaceae, *Calluna*, Ericaceae, Poaceae and *Plantago*.

1.4 Results and Discussion

Pollen records from cores 2 and 1B (Figs. 1.2 and 1.3) provide information about vegetation and climate changes during the mid- and end-stages of the last deglaciation in north-western Portugal. Radiometric dating confirms that the analysed interval age ranges from 13.730 ± 90 to 5.750 ± 40 kyr BP (which represent in calibrated ages the interval between 16.351 and 6.548 ka).

1.4.1 The Oldest Dryas (Heinrich Event 1)

The interval between the bottom of core 2, i.e. –39.07 m OD (Ordnance Datum) (13.730 ± 90 kyr BP: 16.351 ka), and –37.7 m OD, is composed of an important pollen hiatus.

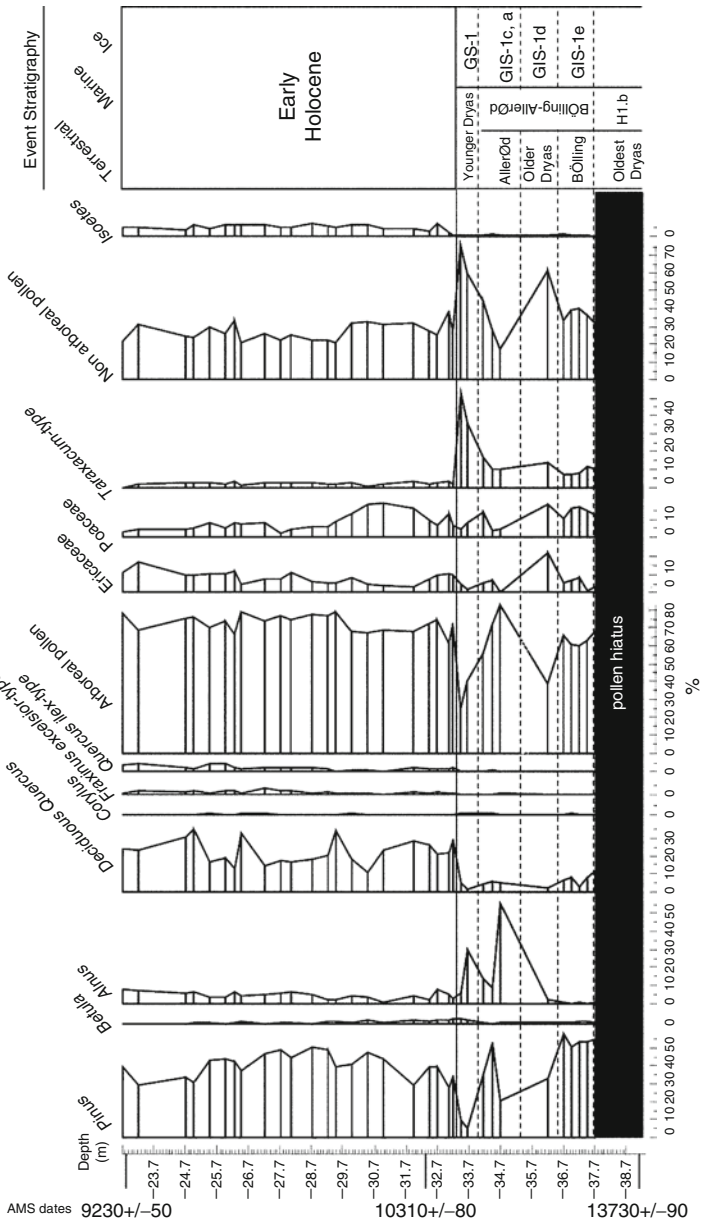

Fig. 1.2 Synthetic pollen diagram of core 2. Core depth is described in Ordnance datum (OD). Three accelerator mass spectrometer (AMS) ^{14}C dates which reflect conventional radiocarbon ages are represented in the left side of this diagram. Arboreal pollen percentages reflect the trees and shrubs which are represented in its left side. Non-arboreal pollen percentages reflect the herbaceous plants represented in its left side. The typical terrestrial, marine and ice stratigraphy represented in the right side of the diagram is correlated with the major vegetation oscillations. H1.b: second phase of the marine Heinrich event 1; GIS: Greenland interstadials (warm events); GS: Greenland stadials (cold events)

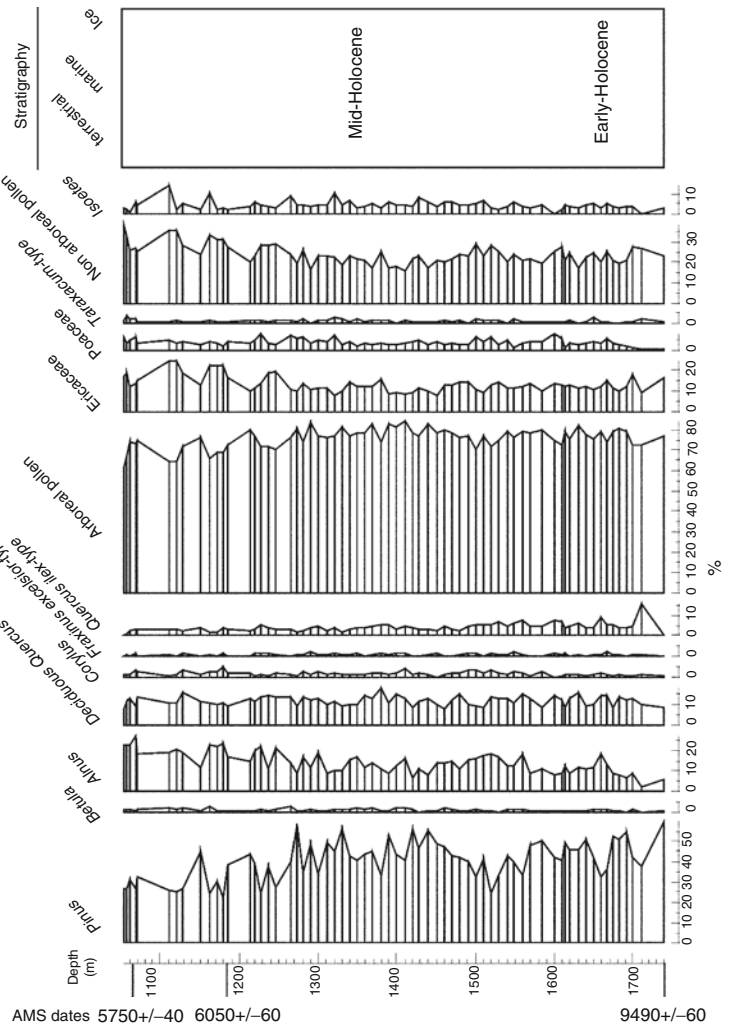

Fig. 1.3 Synthetic pollen diagram of core 1B. Core depth is described in Ordnance datum (OD). Three accelerator mass spectrometer (AMS) ^{14}C dates which reflect conventional radiocarbon ages are represented in the left side of this diagram. Arboreal pollen percentages reflect the trees and shrubs which are represented in its left side. Non-arboreal pollen percentages reflect the herbaceous plants represented in its left side. The typical terrestrial, marine and ice stratigraphy are represented in the right side of the diagram

This hiatus is associated with a coarse-sandy deposit related with fluvial processes (Drago et al. 2006) which prevents good preservation of pollen grains. It is well known that the destruction and damage of pollen grains during their fluvial transport is likely the result of oxidation, desiccation and fragmentation in temporary depositional sites along the transport path (Campbell 1991) and/or due to the increase of episodes of clast-pollen collisions (Fall 1987). The deposition of this relatively coarse material in the Douro paleoriver started at around 13.80 kyr BP (16.35 ka), facilitating the marine transgression which occurred during the last deglaciation (Drago et al. 2006). Further south, the infill of both the Santo André lagoon and the Guadiana paleoriver started at around 14.00 kyr BP (16.50 ka) (Boski et al. 2002; Freitas et al. 2002, 2003; Cearreta et al. 2003; Santos and Sanchez Goñi 2003) confirming that most of the southern European river paleovalleys sedimentary filling took place at the end of the last glacial period (e.g. Dabrio et al. 2000; Shennan et al. 2005; Zazo et al. 2008).

Although pollen grains are not preserved in the basement of the Douro estuary record, marine pollen sequences MD03-2697 and MD99-2331 from the Galician margin (Fig. 1.1) provide detailed information about vegetation cover and climate during the Heinrich event 1 in the north-western Iberian margin and the adjacent landmasses (Naughton et al. 2007a, 2009). The last episode of massive iceberg discharges in the North Atlantic region (Heinrich 1988) occurred between 15.1 ± 0.7 and 13.4 ± 0.3 kyr BP (Elliot et al. 2002) (18.5 and 15.6 ka: Naughton et al. 2009) and those icebergs attained the Iberian margin (e.g. Bard et al. 2000; de Abreu et al. 2003; Turon et al. 2003) mainly during the second phase of Heinrich event 1 (Naughton et al. 2007a, 2009). The impact of Heinrich event 1 in the western Iberian margin was complex and characterised by two main phases: the first phase was marked by an extreme atmospheric (pine and temperate forest decrease) and oceanic cooling associated with an increase of precipitation and high river discharges while the second one was less cold and very dry allowing the development of open landscapes with pine (Naughton et al. 2009). The radiocarbon dating obtained in the bottom of the Douro estuary core 2 (13.80 kyr BP: 16.35 ka) suggests that the beginning of the Douro estuary infill started during the second phase of Heinrich 1 event (identified in the adjacent Galician margin deep-sea cores: Naughton et al. 2007a, 2009). The particular cold conditions detected within Heinrich events in Europe, including in the Iberian Peninsula, were triggered by a slowdown of the thermohaline circulation leading to the introduction of high quantities of meltwater from icebergs into the ocean (e.g., Rahmstorf 1995; Broecker and Hemming 2001; Clark et al. 2002; Vellinga and Wood 2002; Timmermann et al. 2005). On the other hand, the increasing dry conditions detected after 17 ka are likely the result of a northward displacement of the North Atlantic jet-stream precluding the arrival of moisture in Iberia associated to the westerlies (Naughton et al. 2009).

1.4.2 The Last Glacial–Interglacial Transition (LGIT)

In the last decade, great efforts have been made to synchronise chronologically data sets from ice core, marine and land records for comparing regional palaeoclimatic

reconstructions of the Last Glacial Interglacial Transition (LGIT) on a common timescale, in order to understand past ice-sea-atmosphere interactions and feedbacks (INTIMATE group: INTegration of Ice core, MArine and TErrestrial records) (Lowe et al. 2008). Several studies have shown that substantial changes of sea surface temperatures (SST) in the North Atlantic region were probably synchronous with the air temperatures variability in Greenland during the LGIT (Hughen et al. 1996; Lea et al. 2003). Furthermore, high-resolution studies based on direct sea-land correlation of deep-sea cores retrieved in the western Iberian margin have demonstrated that the North Atlantic SST variability was contemporaneous with vegetation changes in the Iberian Peninsula in the same period (Turon et al. 2003; Naughton et al. 2007a, 2009). This suggests that Iberian Peninsula vegetation has probably contemporaneously responded to the climate variability that characterizes the LGIT in the North Atlantic region and in Greenland. Although there is only one single radiocarbon date at the top of the LGIT interval in core 2, we will assume, therefore, that the Douro basin vegetation has synchronously responded to the North Atlantic and Greenland atmospheric changes between 15 and 11.5 ka following the INTIMATE event stratigraphy (Björck et al. 1998; Walker et al. 1999; Lowe et al. 2001, 2008).

The LGIT is right expressed in core 2 between –37.7 and –33.0 m OD (Fig. 1.2) and is marked by abrupt vegetation changes which are related with the Bölling, the Older Dryas, the Allerød and the Younger Dryas events (Mangerud et al. 1974).

1.4.2.1 The Bölling-Allerød Interstadial

The Bölling

The high percentages of arboreal pollen (AP) (60–70%) detected in core 2, between –37.7 and –36.5 m OD, reflect the beginning of temperate forest expansion in the north of Portugal as likely a response to the first warming phase that characterises the onset of the Bölling period (at around 15 and 14.1 ka), or the Greenland interstadial 1e (GIS-1e) following the INTIMATE event stratigraphy (Björck et al. 1998; Walker et al. 1999; Lowe et al. 2001; 2008) (Fig. 1.2). Pine (*Pinus*), followed by oak (deciduous *Quercus*) and birch (*Betula*) are the main trees spreading out through this period in the Douro basin (Fig. 1.2). This vegetation succession has also been detected in other continental pollen sequences from the north-western Iberian Peninsula (Laguna de la Roya and Sanabria March: Allen et al. 1996; Quintanar de la Sierra: Peñalba et al. 1997; Laguna de las Sanguijuelas: Muños Sobrino et al. 2004), Serra de Estrela (Van der Knaap and Van Leeven 1997) and in the pollen sequences from western Iberian margin cores such as MD95-2039 (Roucoux et al. 2005), SU81-18 (Turon et al. 2003) and in MD03-2697 (Naughton et al. 2007a) (Fig. 1.1) at the beginning of the Bölling-Allerød interstadial. The atmospheric temperature increase that characterises the onset of the Bölling-Allerød interstadial is synchronous with the

increase of Sea Surface Temperatures (SST) (Naughton et al. 2007a). Both the orbitally induced increase in northern summer insolation (Berger 1978) and the strengthening of the thermohaline circulation (McManus et al. 2004; Gherardi et al. 2005) contributed to the warming of the north-western Iberian margin and adjacent landmasses.

The Older Dryas

The increase of non-arboreal pollen percentages (NAP) (>60%) at –36.2 m OD reflects an episode of temperate forest contraction probably related with a decrease of atmospheric temperatures (Fig. 1.2). Although there is one single sample recording this forest contraction, the pollen association observed in the adjacent layers (at –36.7 and –34.7 m OD) is distinct from that observed at –36.2 m OD. This suggests that level 36.2 m OD represents a real cooling. The stratigraphic control provided by core 2 is very weak, consisting of a single radiocarbon date for the LGIT interval, preventing the establishment of a good stratigraphical correlation between this cold episode and one specific Intra Bölling-Allerød cold event (the Older Dryas: 14 ka and the intra-Allerød cold event: 13.2 ka) (Lowe et al. 2008) detected in the Greenland ice cores. The Older Dryas and the intra-Allerød cold event correspond to the sub-phases (d) and (b) of the Greenland interstadial 1 (GIS-1d and GIS-1b) following the INTIMATE event stratigraphy proposed by Björck et al. (1998) and Walker et al. (1999). They are frequently difficult to identify in low-resolution sedimentary sequences (with more than 100 years of time scale) because such a centennial-scale cold event occurred in a short time period (less than 100 years) as it is demonstrated in the $\delta^{18}O$ record from Greenland ice cores (Lowe et al. 2001, 2008).

However, the vegetation pattern, reflected by a decrease of *Pinus*, deciduous *Quercus* and *Betula* suggests that this cold event could be more likely related with the Older Dryas rather than with the intra-Allerød cold event. Indeed, the Serra da Estrela pollen sequences also detect a decrease of arboreal pollen percentages, including pine (*Pinus*) and birch (*Betula*) during the Older Dryas event (Van der Knaap and Van Leewen 1997). A similar vegetation pattern is recorded in the marine pollen sequence from the Galician margin within the Bölling-Allerød Interstadial (Fig. 1.1) (Naughton et al. 2007a). However, this vegetation signature has not been correlated yet with the Older Dryas. A higher resolution study, with less than 100 years of time resolution, of both marine and terrestrial proxy data from core MD03-2697 together with additional radiocarbon measurements would be needed to confirm the synchronous decrease of deciduous *Quercus* trees and SST values at the time of the Older Dryas event.

Other records from the western subtropical mid-latitudes such as that from Tampa Bay in Florida reveal two abrupt dry episodes reflected by rapid changes in the vegetation cover (in less than 50 years) during the Bölling-Allerød interstadial which have been correlated with the Older Dryas and the intra-Allerød cold period (Willard et al. 2007). All these evidences suggest that such rapid

cold events occurred not only in the high-latitudes of the northern hemisphere but also in the sub-tropical North Atlantic region. Although the causes triggering this relative cooling are still unknown, Renssen et al. (2000) suggest that variations in solar irradiance could have played a much more prominent role in forcing climate changes during these centennial-scale climate variabilities occurring within the LGIT.

The Allerød

An increase of arboreal pollen percentages, attaining 80% of the total pollen content, is detected between –35.3 and –34.0 m OD (Fig. 1.2). The re-expansion of arboreal *taxa* indicates an episode of climate improvement which can be associated with the Allerød period (at around 13.9 and 12.9 ka) related with the sub-phases (c) and (a) of the Greenland interstadial 1 (GIS-1c/1a) following the INTIMATE event stratigraphy proposed by Björck et al. (1998) and Walker et al. (1999). In particular, alder (*Alnus*) percentages increase, attaining a maximum of about 50% at around –34.7 m OD, being then replaced by pine (*Pinus*). Alder is a tree of wet and mild environments such as river sides and flood plains, requiring high light intensity along with abundant moisture conditions (Bennett and Birks 1990). In the Greenland ice cores this phase occurred after the well-known meltwater pulse 1A (MWP-1A) (Fairbanks 1989; Bard et al. 1990). The massive and abrupt rise in sea level by some 16–24 m, followed by a slowdown episode, could have favoured the high sedimentation found in the Douro river main channel, triggering the flood of the main channel margins. This situation, jointly with the increase of moisture conditions and temperatures, could create conditions suitable for the development of great areas of alder fen-woods in the Douro river valley floodplain. The spread of *Alnus* during the Allerød has been detected in other regions such as in the Wolin Island, north-west Poland (Latałowa and Borówka 2006), and in lakes in the north of Russia (Andreev and Tarasov 2007).

Following this, *Alnus* was replaced by *Pinus*.

1.4.2.2 The Younger Dryas

The strong decrease in arboreal pollen (AP = 40% to 20%), between –34.0 and –33.4 m OD, marks the onset of the Younger Dryas (YD) cold episode in the north of Portugal. Indeed, although the high latitude summer insolation attained its maximum values at around 13 ka, a sudden extreme cold episode occurred between 12.9 and 11.7 ka reflecting the YD event. The Younger Dryas cold event has been considered as the most abrupt incident of almost full returning to glacial conditions during the last deglaciation (Broecker 1994, 2000). This event was first documented by plant macrofossil analysis from Scandinavia by a brief re-expansion of a cold-tolerant plant called *Dryas octopetala* (Jenssen 1935) and then in several lacustrine sediments of Europe (e.g. Lotter et al. 1992; Goslar et al. 1993), in several North Atlantic marine deep sea cores (e.g. Bard et al. 1987; Lehman and Keigwin 1992;

Bond et al. 1993; Rasmussen et al. 1996; Sikes and Keigwin 1996) and in the Greenland ice cores (e.g. Alley et al. 1993; Dansgaard et al. 1993; Meese et al. 1997). Evidence of the YD event has also been recorded in north-eastern America and eastern Canada (Peteet et al. 1990; Mott et al. 1986; Levesque et al. 1993), in the British Columbia (Mathewes et al. 1993) and further south in the subtropics such as in the Gulf of Mexico and California (Flower and Kennett 1990; Keigwin and Jones 1990; Teller 1990) and in the tropical region (Colombia, Cariaco basin, Bolivian Ice cores) (van Geel and van der Hammen 1973; Hughen et al. 1996; Thompson et al. 1998). This cold episode was defined as the Greenland stadial 1 (GS-1) event, following the INTIMATE event stratigraphy (Björck et al. 1998; Walker et al. 1999; Lowe et al. 2001, 2008). The causes triggering this climate reversal are still under debate (e.g. Teller et al. 2002; Carlson et al. 2007; Bradley and England 2008) but there is a consensus about the resulted reduction of the North Atlantic thermohaline circulation (e.g. Broecker and Denton 1990; McManus et al. 2004) leading to an abrupt cooling over Europe and north-central America.

In the north of Portugal, the YD event is characterised by the replacement of trees such as the pine (*Pinus*) and oak (deciduous *Quercus*) with herbaceous plants and in particular by Poaceae followed by *Taraxacum*-type pollen (Compositae family) (Fig. 1.2). This particular change in the vegetation cover, associated with an important atmospheric and oceanic cooling episode, has also been documented in some north-western Iberian margin pollen sequences during previous glacial–interglacial transitions such as from Marine Isotopic Stage (MIS) 10–9 (Desprat 2005; Desprat et al. 2009); MIS 8–7 (Desprat et al. 2006), and from MIS 6–5 (Sanchez Goñi et al. 2005), before the major forested phases that characterises MIS 9, MIS 7 and MIS 5 interglacial periods (Desprat et al. 2007). Although there is a substantial contraction of the temperate forest, *Alnus* (alder) woodlands played an important role in the vegetation cover of the Douro region during the YD. Conversely, the marine pollen sequence from the north-western Iberian margin (Naughton et al. 2007a) does not detect any expansion of alder but rather of semi-desert plants suggesting an increase of continental dryness during the Younger Dryas event. Therefore, the expansion of alder in the Douro basin suggests a flooding episode of the Douro river margins rather than likely being the result of a climate improvement episode (increasing temperatures). The expansion of alder during the Younger Dryas cold event has been largely documented in some French lake sequences (David 1993, 2001). Other lake sequences from eastern France (Jura Mountains and Pre-Alps) and the Swiss Plateau shows a substantial lake level rise within the Younger Dryas (Magny and Bégeot 2004). This suggests that the increasing of inundated areas around these lakes would probably contribute to the expansion of alder in those regions.

1.4.3 The Early-Holocene and the End of the Last Deglaciation

The substantial increase of total arboreal pollen percentages (AP > 60%) at around –33.4 m OD marks the beginning of the present-day Interglacial period (Holocene)

in the Douro basin (Figs. 1.2 and 1.3). The expansion of birch (*Betula*), oak (deciduous *Quercus*), pine (*Pinus*) and other forest compounds such as ashes (*Fraxinus excelcior*-type), alder (*Alnus*) and evergreen oaks (*Quercus ilex*-type) reflects an important increase of temperatures and moist conditions in north Portugal (Figs. 1.2 and 1.3). The continuous presence of *Isoetes* spores in the Douro estuary starts at around –33.4 m OD. This further demonstrates the onset of the present-day interglacial period in the Douro basin. A similar vegetation pattern, characterising the early-Holocene period, has been recorded in the marine pollen sequence from the Galician margin (Fig. 1.1) and is contemporaneous with an increase of sea surface temperatures in the North Atlantic and with still maxima of high-latitude summer insolation (Naughton et al. 2007a). Most of the Iberian Peninsula and Iberian margin pollen sequences detect an onset of the major forested period at around 10.3 kyr BP (Fig. 1.1) (e.g. Allen et al. 1996; Peñalba et al. 1997; Boessenkool et al. 2001; Turon et al. 2003; Muñoz Sobrino et al. 2004; Naughton 2007). Therefore, the radiocarbon date obtained at –32.32 m OD (10.3 kyr BP) in core 2 seems to be too old when compared with the vegetation data which delimits the beginning of the Holocene at around –33.0 m OD. This suggests that the sediment level (–32.32 m OD) used for dating was probably contaminated with old organic matter material.

The vegetation evolution in the Douro basin does not, however, show any millennial-scale variability between 10.3 and 5.75 kyr BP (12.1–6.55 ka). Although the Holocene has been considered as a period of relatively stable climate (with no abrupt changes in temperature and precipitation) when compared with the previous glacial and the LGIT periods, a series of millennial-scale climatic shifts have been detected in several detailed paleoclimate records from Greenland ice cores, North Atlantic deep-sea sediments and European Lakes (e.g. O'Brien et al. 1995; Bond et al. 1997; Mayewski et al. 2004; Magny et al. 2006). This millennial-scale climate variability within the Holocene period is characterised by temperature changes of about 1–2°C (Wiersma and Renssen 2005; Davis et al. 2003). Although there are some episodes in which oak (deciduous *Quercus*) is replaced by pine, between 10.3 and 9.2 kyr BP (12.13–10.4 ka) (Fig. 1.2) and there is a slight decrease of arboreal pollen just before 6.0 kyr BP (6.9 ka) (Fig. 1.3) the quantity of arboreal pollen remains mostly constant. One hypothesis that we can put forward is that the weak temperature change that characterises this interglacial period would not substantially affect the vegetation of the Douro estuary. However, further north in the north-western French margin, pollen-based temperature estimates from a shelf core show that vegetation from western France seems to respond to the Holocene millennial-scale climate variability (Naughton et al. 2007c). Also, the pollen record from the Guadiana estuary (southern Iberian Peninsula) detects some short-lived episodes of increasing dryness which have been correlated with the cold events detected in the North Atlantic region (Fletcher et al. 2007). At the same latitude, but in eastern North America, pollen sequences from Chesapeake Bay reflect a quasi-periodic correlation between vegetation changes and rapid climate coolings documented by various proxies (Willard et al. 2005). This suggests that vegetation from mid-latitude regions of the northern

hemisphere seems to have responded to the millennial-scale climate variability of the Holocene. Therefore other hypotheses must be invoked to explain the weak vegetation change signal recorded in the Douro estuary. It is known that Iberian Peninsula coastal areas, including their estuaries, have been directly affected by sea level changes during the Holocene (e.g. Dabrio et al. 2000; Boski et al. 2002, 2007; Freitas et al. 2002, 2003; Drago et al. 2006; Naughton et al. 2007b; Zazo et al. 2008). Indeed, estuarine transgression can trigger landward margin edge forward, increasing therefore the capacity of pollen grains input from the estuary borders. Although it has been previously demonstrated that the pollen signal from the Douro estuary mainly reflects an integrated image of the regional vegetation that colonize the Douro basin during the early- and mid-Holocene (Naughton et al. 2007b), it is possible that geomorphological changes in the Douro estuary related with sea-level fluctuations trigger relative changes in the pollen source area masking the climate-regional pollen signal.

1.5 Conclusion

The high resolution pollen analysis (centennial time scale) performed in two sedimentary sequences from the Douro estuary (north-western Portugal) allows the detection of major Douro basin vegetation changes during the Last Glacial-Interglacial Transition (LGIT) associated with the abrupt climate changes described for the North Atlantic region and Greenland. An important pollen hiatus is detected in the bottom of the Douro estuary as likely the result of particular environmental conditions which preclude pollen preservation during the final stages of the marine Heinrich 1 event (marine equivalent of the terrestrial Oldest Dryas). Following this, abrupt vegetation changes are detected during the LGIT in the Douro basin. The Bölling warm period was marked by the expansion of pine, oak and birch and the Allerød by alder and pine. An episode of temperate forest contraction (pine, oak and birch), reflecting an episode of atmospheric cooling, is sandwiched by the two warmed forested phases (Bölling and Allerød). This episode seems to be associated with the centennial-scale Older Dryas event. The Younger Dryas cold event is particularly well expressed in the Douro estuary record, by an episode of temperate forest contraction and herbaceous plants expansion. The particular vegetation pattern reflected by the replacement of pine and oak by Compositae plants and grasses is representative of the most extreme cold episode that precedes the major forested episode of the Holocene. The major early- and mid-Holocene forested phases are characterised by a strong expansion of pine and birch and temperate trees such as deciduous oak and ash, alder and evergreen oak reflecting the increase of temperature and moisture in the north of Portugal. The north of Portugal vegetation response to the millennial-scale climate variability detected elsewhere in the North Atlantic region is not recorded in the high resolution pollen analysis of the Douro estuarine cores. Therefore, a high resolution palynological study in marine deep-sea

cores would be needed in order to evaluate the impact of Holocene millennial-scale changes on the vegetation of northern Portugal.

Acknowledgments This study has been financed by the Fundação para a Ciência e a Tecnologia (FCT) in the framework of the project "Envi-Changes"-Late Quaternary Environmental Changes From Estuary and Shelf Sedimentary Record (PLE/12/00), of the post-doc grant SFRH/BPD/36615/2007, and by two projects integrated in a French-Portuguese bilateral collaboration (PESSOA and ICCTI-IFREMER). We gratefully acknowledge César de Andrade for all the support and enlightening discussions along the Envi-Changes project. Thanks are also due to Marie-Hélène Castéra for palynological treatments.

References

Allen JRM, Huntley B, Watts WA (1996) The vegetation and climate of northwest Iberia over the last 14 000 yr. J Quat Sci 11:125–147

Alley RB, Meese DA, Shuman CA, Gow AJ, Taylor KC, Grootes PM, White JWC, Ram M, Waddington ED, Mayewski PA, Zielinski GA (1993) Abrupt increase in Greenland snow accumulation at the end of the Younger Dryas event. Nature 362:527–529

Andreev AA, Tarasov PE (2007) Pollen records, postglacial: Northern Asia. In: Elias S (ed) Encyclopedia of quaternary science, vol 4. Elsevier, Amsterdam, The Netherlands:pp 2721–2729

Bard E, Arnold M, Maurice P, Duprat J, Moyes J, Duplessy JC (1987) Retreat velocity of the North-Atlantic polar front during the last deglaciation determined by 14C accelerator mass spectrometry. Nature 328:791–794

Bard E, Hamelin B, Fairbanks RG, Zindler A (1990) Calibration of the ^{14}C timescale over the past 30,000 years using mass spectrometric U-Th ages from Barbados corals. Nature 345:405–410

Bard E, Rostek F, Turon JL, Gendreau S (2000) Hydrological impact of Heinrich events in the subtropical northeast Atlantic. Science 289:1321–1324

Bennett KD, Birks HJB (1990) Postglacial history of alder (*Alnus glutinosa* (L.) Gaertn) in the British Isles. J Quat Sci 5:123–133

Berger AL (1978) Long-term variations of daily insolation and Quaternary climatic changes. J Atmos Sci 35:2362–2367

Björck S, Walker MJC, Cwynar LC, Johnsen S, Knudsen K-L, Lowe JJ, Wohlfarth B (1998) An event stratigraphy for the last termination in the North Atlantic region based on the Greenland ice core record: A proposal by the INTIMATE group. J Quat Sci 13:283–292

Boessenkool KP, Brinkhuis H, Schonfeld J, Targarona J (2001) North Atlantic sea-surface temperature changes and the climate of western Iberia during the last deglaciation; A marine palynological approach. Glob Planet Change 30:33–39

Bond G, Broecker W, Johnsen S, McManus J, Labeyrie L, Jouzel J, Bonani G (1993) Correlations between climate records from North Atlantic sediments and Greenland ice. Nature 365:143–147

Bond G, Showers W, Cheseby M, Lotti R, Almasi P, deMenocal P, Priore P, Cullen H, Hajdas I, Bonani G (1997) A pervasive millenial-scale cycle in North Atlantic Holocene and glacial climates. Science 278:1257–1266

Bond GC, Showers W, Elliot M, Evans M, Lotti R, Hajdas I, Bonani G, Johnson S (1999) "The North Atlantic's 1–2 kyr climate rhythm: relation to Heinrich events, Dansgaard/Oeschger cycles and the little ice age". In: Clark PU, Webb RS, Keigwin LD (eds) Mechanisms of global change at millennial time scales, Geophysical monograph, vol 112. American Geophysical Union, Washington DC, pp 59–76

Boski T, Moura D, Veiga-Pires C, Camacho S, Duarte D, Scott DB, Fernandes SG (2002) Postglacial sea-level rise and sedimentary response in the Guadiana Estuary, Portugal/Spain border. Sediment Geol 150:103–122

Boski T, Camacho S, Moura D, Fletcher W, Wilamowski A, Veiga-Pires C, Correia V, Loureiro C, Santana P (2008) Chronology of the sedimentary processes during the postglacial sea level rise in two estuaries of the Algarve coast, Southern Portugal. Estuar Coast Shelf Sci 77:230–244

Bradley RS, England JH (2008) The Younger Dryas and the Sea of Ancient Ice. Quat Res 70:1–10

Brauer A, Günter C, Johnsen SJ, Negendank JFW (2000) Land-ice teleconnections of cold climatic periods during the last Glacial/Interglacial transition. Clim Dyn 16:229–239

Braun-Blanquet J, Pinto da Silva AR, Rozeira A (1956) Résultats de deux excursions géobotaniques à travers le Portugal septentrional et moyen. II. Chenaies à feuilles caduques (Quercion occidentale) et chenaies à feuilles persistentes (Quercion faginea) au Portugal. Agronomia Lusititana 18:167–234

Broecker WS (1994) Massive iceberg discharges as triggers for global climate change. Nature 372:421–424

Broecker WS (2000) Abrupt climate change: Causal constraints provided by the paleoclimate record. Earth Sci Rev 51:137–154

Broecker WS, Denton GH (1990) What drives glacial cycles? Sci Am, January 262:48–56

Broecker WS, Hemming H (2001) Climate swings come into focus. Science 294:2308–2309

Campbell ID (1991) Experimental mechanical destruction of pollen grains. Palynology 15:29–33

Carlson AE, Clark PU, Haley BA, Klinkhammer GP, Simmons K, Brook EJ, Meissner KJ (2007) Geochemical proxies of North American freshwater routing during the Younger Dryas cold event. PNAS 104:6556–6561

Cearreta A, Cachão M, Cabral MC, Bao R, Ramalho MJ (2003) Lateglacial and Holocene environmental changes in Portuguese coastal lagoons 2: Microfossil multiproxy reconstruction of the Santo Andre coastal area. Holocene 13:447–458

Clark PU, Pisias NG, Stocker TF, Weaver AJ (2002) The role of the thermohaline circulation in abrupt climate change. Nature 415:863–869

Costa JC, Aguiar C, Capelo JH, Lousã M, Neto C (1998) Biogeografia de Portugal continental. Quercetea 0, ALFA, FIP (eds), 56 pp

Dabrio CJ, Zazo C, Goy JL, Sierro FJ, Borja F, Lario J, González JA, Flores JA (2000) Depositional history of estuarine infill during the Late Pleistocene–Holocene postglacial transgression. Mar Geol 162:381–404

Dansgaard W, Johnsen SJ, Clausen HB, Dahl-Jensen D, Gundestrup NS, Hammer CU, Hvidberg CS, Steffensen JP, Sveinbjörnsdottir AE, Jouzel J, Bond G (1993) Evidence for general instability of past climate from a 250-kyr ice-core record. Nature 364:218–220

David F (1993) Developpement des aulnes dans les Alpes francaises du nord. Comptes Rendus Académie des Sciences, Paris 316(Série II):1815–1822

David F (2001) Le tardiglaciaire des Ételles (Alpes françaises du Nord) : Instabilité climatique et dynamique de végétationThe late-glacial sequence of Les Ételles (Northern French Alps): Climate instability and vegetation dynamics. Comptes Rendus de l'Académie des Sciences – Series III – Sciences de la Vie, 324:373–380

Davis BAS, Brewer S, Stevenson AC, Guiot J, Data Contributors (2003) The temperature of Europe during the Holocene reconstructed from pollen data. Quat Sci Rev 22:1701–1716

de Abreu L, Shackleton NJ, Schonfeld J, Hall M, Chapman M (2003) Millennial-scale oceanic climate variability off the Western Iberian margin during the last two glacial periods. Mar Geol 196:1–20

Desprat S (2005) Réponses climatiques marines et continentales du SW de l'Europe lors des derniers interglaciaires et des entrées en glaciation. PhD thesis, Bordeaux 1 University, Bordeaux (France), 282 pp

Desprat S, Sánchez Goñi MF, Turon J-L, Duprat J, Malaizé B, Peypouquet J-P (2006) Climatic variability of Marine Isotope Stage 7: Direct land-sea-ice correlation from a multiproxy analysis of a northwestern Iberian margin deep-sea core. Quat Sci Rev 25:1010–1026

Desprat S, Sánchez Goñi MF, Naughton F, Turon J-L, Duprat J, Malaizé B, Peypouquet J-P (2007) Climate variability of the last five isotopic interglacials: Direct land-sea-ice correlation from the multiproxy analysis of north western Iberian margin deep-sea cores. In: Sirocko F, Litt T, Claussen M, Sánchez Goñi MF (eds) The climate of past interglacials, Elsevier publications. Dev Quat Sci 7:277–288

Desprat S, Sánchez Goñi MF, Duprat J, Cortijo E, McManus JF (2009) Millennial-scale climatic variability between 340 000 and 270 000 years ago in SW Europe: Evidence from a NW Iberian margin pollen sequence. Clim Past Discuss 4:375–414

Drago T, Freitas C, Rocha F, Moreno J, Cachão M, Naughton F, Fradique C, Araujo F, Silveira T, Oliveira A, Cascalho J, Fatela F (2006) Palaeoenvironmental evolution of estuarine systems during the last 14000 years- the case of Douro estuary (NW Portugal). J Coast Res 39:7 pp

Elliot M, Labeyrie L, Duplessy J-C (2002) Changes in North Atlantic deep-water formation associated with the Dansgaard-Oeschger temperature oscillations (60–10 ka). Quat Sci Rev 21:1153–1165

Fairbanks R (1989) A 17,000-year glacio-eustatic sea-level record: Influence of glacial melting rates on the Younger Dryas event and deep-ocean circulation. Nature 342:637–642

Fall PL (1987) Pollen taphonomy in a canyon stream. Quat Res 28:393–406

Fletcher W, Boski T, Moura D (2007) Palynological evidence for environmental and climatic change in the lower Guadiana valley (Portugal) during the last 13,000 years. Holocene 17:479–492

Flower BP, Kennett JP (1990) The Younger Dryas cool episode in the Gulf of Mexico. Paleoceanography 5:949–961

Freitas MC, Andrade C, Cruces A (2002) The geological record of environmental changes in southwestern Portuguese coastal lagoons since the Lateglacial. Quat Int 93–94:161–170

Freitas MC, Andrade C, Rocha F, Tassinari C, Munhá JM, Cruces A, Vidinha J, Marques da Silva C (2003) Lateglacial and Holocene environmental changes in Portuguese coastal lagoons 1: The sedimentological and geochemical records of the Santo André coastal area. Holocene 13:433–446

Gherardi JM, Labeyrie L, McManus JF, Francois R, Skinner LC, Cortijo E (2005) Evidence from the Northeastern Atlantic basin for variability in the rate of the meridional overturning circulation through the last deglaciation. Earth Planet Sci Lett 240:710–723

Goslar T, Kuc T, Ralska-Jasiewiczowa M, Rozanski K, Arnold M, Bard E, van Geel B, Pazdur M, Szeroczynska K, Wicik B (1993) Hight resolution lacustrine record of the late glacial/holocene transition in central Europe. Quat Sci Rev 12:287–294

Hughen KA, Overpeck JT, Peterson LC, Trumbore S (1996) Rapid climate changes in the tropical Atlantic region during the last deglaciation. Nature 380:51–54

Imbrie J, Boyle EA, Clemens SC, Duffy A, Howard WR, Kukla G, Kutzbach J, Martinson DG, McIntyre A, Mix AC, Molfino B, Morley JJ, Peterson LC, Pisias NG, Prell WL, Raymo ME, Shackleton NJ, Toggweiler JR (1992) On the structure and origin of major glaciation cycles, 1. Linear response to Milankovitch forcing. Paleoceanography 7:701–738

Jessen K (1935) Archaeological dating in the history of North Jutland's vegetation. Acta Archaeologica 5:185–214

Johnsen S, Dahl-Jensen D, Gundestrup N, Steffensen JP, Clausen HB, Miller H, Masson-Delmotte V, Sveinbjornsdottir AE, White J (2001) Oxygen isotope and palaeotemperature records from six Greenland ice-core stations: Camp Century, Dye-3, GRIP, GISP2, Renland and NorthGRIP. J Quat Sci 16:299–307

Keigwin LD, Jones GA (1990) Deglacial climatic oscillations in the Gulf of California. Paleoceanography 5:1009–1023

Latałowa M, Borówka K (2006) The Allerød/Younger Dryas transition in Wolin Island, northwest Poland, as reflected by pollen, macrofossils, and chemical content of an organic layer separating two aeolian series. Veg Hist Archaeobot 15:321–331

Lea DW, Pak DK, Peterson LC, Hughen KA (2003) Synchroneity of tropical and high-latitude Atlantic temperatures over the last glacial termination. Sci 301:1361–1364

Lehman SJ, Keigwin LD (1992) Sudden changes in North Atlantic circulation during the last deglaciation. Nature 356:757–762

Levesque AJ, Mayle FE, Walker IR, Cwynar LC (1993) The Amphi-Atlantic Oscillation: A proposed Late-Glacial climatic event. Quat Sci Rev 12:629–643

Limondin-Lozouet N, Bridault A, Leroyer C, Ponel P, Antoine P, Chausse C, Munaut AV, Pastre JF (2002) Evolution des ecosystemes de fond de vallee en France septentrionale au cours du Tardiglaciaire: l'apport des indicateurs biologiques. In: Bravard JP, Magny M (eds) Les fleuves ont une histoire. Paleoenvironnement des rivieres et des lacs français depuis 15 000 ans. Errance, Paris, pp 45–62

Lotter AF, Eicher U, Siegenthaler U, Birks HJB (1992) Late-glacial climatic oscillations as recorded in Swiss lake sediments. J Quat Sci 7:187–204

Loureiro JJ, Machado ML, Macedo ME, Nunes MN, Botelho OF, Sousa ML, Almeida MC, Martins JC (1986) Monografias hidrológicas dos principias cursos de água de Portugal continental. Direcção Geral dos Serviços Hidráulicos, Lisbon, 569 pp

Lowe JJ, Hoek WZ, INTIMATE group (2001) Inter-regional correlation of palaeoclimatic records for the Last Glacial–Interglacial Transition: A protocol for improved precision recommended by the INTIMATE project group. Quat Sci Rev 20:1175–1187

Lowe JJ, Rasmussen SO, Björck S, Hoek WZ, Steffensen JP, Walker MJC, Yu ZC, the INTIMATE group (2008) Synchronisation of palaeoenvironmental events in the North Atlantic region during the Last Termination: A revised protocol recommended by the INTIMATE group. Quat Sci Rev 27:6–17

Magny M, Bégeot C (2004) Hydrological changes in the European midlatitudes associated with freshwater outbursts from Lake Agassiz during the Younger Dryas event and the early Holocene. Quat Res 61:181–192

Magny M, Aalbersbergb G, Bégeot C, Benoit-Ruffaldia P, Bossueta G, Jean-Robert Disnar J-R, Heiri O, Laggoun-Defarge F, Mazier F, Millet L, Peyron O, Boris V, Walter-Simonnet A-V (2006) Environmental and climatic changes in the Jura mountains (eastern France) during the Lateglacial–Holocene transition: A multi-proxy record from Lake Lautrey. Quat Sci Rev 25:414–445

Maher LJ Jr (1981) Statistics for microfossil concentration measurements employing samples spiked with marker grains. Rev Palaeobot Palynol 32:153–191

Mangerud J, Andersen ST, Berglund BE, Donner JJ (1974) Quaternary stratigraphy of Norden, a proposal for terminology and classification. Boreas 3:109–128

Mathewes R, Heusser L, Patterson R (1993) Evidence for a Younger Dryas-like cooling event on the British Columbia Coast. Geology 21:101–104

Mayewski PA, Rohling E, Stager C, Karlén W, Maasch K, Meeker LD, Meyerson E, Gasse F, van Kreveld S, Holmgren K, Lee-Thorp J, Rosqvist G, Rack F, Staubwasser M, Schneider R (2004) Holocene climate variability. Quat Res 62:243–255

McManus JF, Francois R, Gherardi J-M, Keigwin LD, Brown-Leger S (2004) Collapse and rapid resumption of Atlantic meridional circulation linked to deglacial climate changes. Nature 428:834–837

Meese DA, Gow AJ, Alley RB, Zielinski GA, Grootes PM, Ram K, Taylor KC, Mayewski PA, Bolzan JF (1997) The Greenland Ice Sheet Project 2 depth-age scale: Methods and results. J Geophys Res 102:26,411–26,423

Mott RJ, Grant DR, Stea R, Occhietti S (1986) Lake-glacial climatic oscillation in Atlantic Canada equivalent to the Allerød/Younger Dryas event. Nature 323:247–250

Muñoz Sobrino C, Ramil-Rego P, Gomez-Orellana L (2004) Vegetation of the Lago Sanabria area (NW Iberia) since the end of the Pleistocene: A palaeoecological reconstruction on the basis of two new pollen sequences. Veg Hist Archeobot 13:1–22

Naughton F (2007) As variações climáticas dos últimos 30 000 anos e sua influência na evolução dos sistemas costeiros do norte de Portugal/Les variations climatiques des derniers 30 000 ans et leur influence sur l'évolution des systèmes côtiers du nord de Portugal. PhD thesis in cotutership, Bordeaux 1 and Lisbon Universities, Lisbon (Portugal), 303 pp

Naughton F, Sanchez Goni MF, Desprat S, Turon JL, Duprat J, Malaize B, Joli C, Cortijo E, Drago T, Freitas MC (2007a) Present-day and past (last 25 000 years) marine pollen signal off western Iberia. Mar Micropaleontol 62:91–114

Naughton AF, Sanchez Goni MF, Drago T, Freitas MC, Oliveira A (2007b) Holocene geomorphological changes in the Douro estuary (NW Iberia). J Coast Res 23:711–720

Naughton F, Bourillet J-F, Sánchez Goñi MF, Turon J-L, Jouanneau J-M (2007c) Long-term and millennial-scale climate variability in north-western France during the last 8 850 years. Holocene 17:939–953

Naughton F, Sánchez Goñi MF, Kageyama M, Bard E, Cortijo E, Desprat S, Duprat J, Malaizé B, Joli C, Rostek F, Turon J-L (2009) Wet to dry climatic trend in north western Iberia within Heinrich events. Earth Planet Sci Lett 284:329–342

O'Brien SR, Mayewski PA, Meeker LD, Meese DA, Twickler MS, Whitlow SI (1995) Complexity of Holocene climate as reconstructed from a Greenland ice core. Science 270:1962–1964

Pastre JF, Leroyer C, Limondin-Lozouet N, Chausse C, Fontugne M, Gebhardt A, Hatte C, Krier V (2000) Le Tardiglaciaire des fonds de vallée du Bassin Parisien (France). Quaternaire 11:107–122

Pastre JF, Limondin-Lozouet N, Leroyer C, Ponel Ph, Fontugne M (2003) River system evolution and environmental changes during the Lateglacial in the Paris Basin (France). Quat Sci Rev 22:2177–2188

Peñalba MC, Arnold M, Guiot J, Duplessy J-C, de Beaulieu J-L (1997) Termination of the Last Glaciation in the Iberian Peninsula inferred from the pollen sequence of Quintanar de la Sierra. Quat Res 48:205–214

Peteet DM, Vogel JS, Nelson DE, Southon JR, Nickmann RJ, Heusser LE (1990) Younger Dryas climatic reversal in northeastern USA? AMS ages for an old problem. Quat Res 33:219–230

Peyron O, Bégeot C, Brewer S, Heiri O, Magny M, Millet L, Ruffaldi P, Van Campo E, Yu G (2005) Lateglacial climatic changes in Eastern France (Lake Lautrey) from pollen, lake-levels, and chironomids. Quat Res 64:197–211

Pina Manique, Albuquerque (1957). Zones écologiques Portugaises. Publications of the institute of applied Biology. Tomo XXVI:19–26

Rahmstorf S (1995) Bifurcations of the Atlantic thermohaline circulation in response to changes in the hydrological cycle. Nature 378:145–149

Rasmussen TL, Thomsen E, van Weering TCE, Labeyrie L (1996) Rapid changes in surface and deep water conditions at the Faeroe Islands Margin during the last 58 ka. Paleoceanography 11:757–771

Reille M (1992) Pollen et spores d'Europe et d'Afrique du Nord. Laboratoire de botanique historique et palynologie, Marseille, 520 pp

Renssen H, van Geel B, van der Plicht J, Magny M (2000) Reduced solar activity as a trigger for the start of the Younger Dryas? Quat Int 68:373–383

Roucoux KH, de Abreu L, Shackleton NJ, Tzedakis PC (2005) The response of NW Iberian vegetation to North Atlantic climate oscillations during the last 65 kyr. Quat Sci Rev 24:1637–1653

Rull V (1987) A note on pollen counting in paleoecology. Pollen Spores 29:471–480

Sanchez Goñi MF (1996) The Older Dryas of northern France in a west European context. Revue de Paéobiologie 15:519–531

Sánchez Goñi MF, Loutre MF, Crucifix M, Peyron O, Santos L, Duprat J, Malaizé B, Turon J-L, Peypouquet J-P (2005) Increasing vegetation and climate gradient in Western Europe over the Last Glacial Inception (122–110 ka): Data-model comparison. Earth Planet Sci Lett 231:111–130

Santos L, Sanchez Goñi MF (2003) Lateglacial and Holocene environmental changes in Portuguese coastal lagoons 3: Vegetation history of the Santo Andre coastal area. Holocene 13:461–466

Shennan I, Hamilton SL, Hillier C, Woodroffe SA (2005) 16 000-year record of near-field relative sea-level changes, northwest Scotland, United Kingdom. Quat Int 133–134:95–106

Sikes EL, Keigwin LD (1996) A reexamination of northeast Atlantic sea surface temperature and salinity over the last 16 kyr. Paleoceanography 11:327–342

Stuiver M, Reimer P (1993) Extended ^{14}C database and revised CALIB radiocarbon calibration program. Radiocarbon 35:215–230

Stuiver M, Reimer PJ, Reimer RW (2005) CALIB 5.0. (WWW program and documentation)

Telford RJ, Heegaard E, Birks HJB (2004) The intercept is a poor estimate of a calibrated radiocarbon age. Holocene 14:296–298

Teller JT (1990) Volume and routing of late glacial runoff from the southern Laurentide Ice Sheet. Quat R 34:12–23

Teller JT, Leverington DW, Mann JD (2002) Freshwater outbursts to the oceans from glacial Lake Agassiz and their role in climate change during the last deglaciation. Quat Sci Rev 21:879–887

Thompson LG, Davis ME, Mosley-Thompson E, Sowers TA, Henderson KA, Zagorodnv VS, Lin P-N, Mikhalenko VN, Campen RK, Bolzan JF, Cole-Dai J, Francou B (1998) A 25,000-year tropical climate history from Bolivian Ice Cores. Science 282:1858–1864

Timmermann A, An S-I, Krebs U, Goosse H (2005) ENSO suppression due to weakening of the North Atlantic Thermohaline Circulation. J Clim 18:3122–3139

Turon J-L, Lézine A-M, Denèfle M (2003) Land-sea correlations for the last glaciation inferred from a pollen and dinocyst record from the Portuguese margin. Quat Res 59:88–96

Van de Knaap WO, Van Leewen JFN (1997) Late Glacial and early Holocene vegetation succession, altitudinal vegetation zonation, and climatic change in the Serra da Estrela, Portugal. Rev Palaeobot Palynol 97:239–285

Van Geel B, Van der Hammen T (1973) Upper Quaternary vegetational and climatic sequence of the Fuquene area (Eastern Cordillera, Colombia). Palaeogeogr Palaeoclimatol Palaeoecol 14:9–92

Vellinga M, Wood RA (2002) Global climatic impacts of a collapse of the Atlantic thermohaline circulation. Clim Change 54:251–267

von Grafenstein U, Erlenkeuser H, Brauer A, Jouzel J, Johnsen S (1999) A mid-European decadal isotope-climate record from 15,500 to 5,000 years B.P. Science 284:1654–1657

Walker MJC, Björck S, Lowe JJ, Cwynar L, Johnsen S, Knudsen K-L, Wohlfarth B, INTIMATE group (1999) Isotopic 'events' in the GRIP ice core: A stratotype for the Late Pleistocene. Quat Sci Rev 18:1143–1150

Wiersma AP, Renssen H (2005) Model-data comparison for the 8.2 ka BP event: Confirmation of a forcing mechanism by catastrophic drainage of Laurentide Lakes. Quat Sci Rev 25:63–88

Willard DA, Bernhardt CE, Korejwo DA, Meyers SR (2005) Impact of millennial-scale Holocene climate variability on eastern North American terrestrial ecosystems: Pollen-based climatic reconstruction. Glob Planet Change 47:17–35

Willard DA, Bernhardt CE, Brooks GR, Cronin TM, Edgar T, Larson R (2007) Deglacial climate variability in central Florida, USA. Palaeogeogr Palaeoclimatol Palaeoecol 251:366–382

Zazo C, Dabrio CJ, Goy JL, Lario J, Cabero A, Silva PG, Bardají T, Mercier N, Borja F, Roquero E (2008) The coastal archives of the last 15 ka in the Atlantic–Mediterranean Spanish linkage area: Sea level and climate changes. Quat Int 181:72–87

Chapter 2
Impact of Oporto Metropolitan Area Carbon Dioxide Emissions over the Adjacent Coastal Zone

Rogério Carvalho, Nelson Barros, and Pedro Duarte

Abstract Concerns about global warming over the last years have stimulated a large number of studies regarding atmospheric and oceanic carbon dioxide (CO_2) concentration and its consequences. In spite of the available data on global atmospheric CO_2, there is only limited knowledge on CO_2 variability at regional scales. Moreover, there is an important gap in our understanding of the contribution of high CO_2 emission regions, such as metropolitan areas, to CO_2 concentrations over nearby coastal areas–considered by several authors as an important CO_2 sink. A possible working hypothesis is that, large littoral metropolitan areas may have a significant influence on CO_2 atmospheric concentrations over those areas and exert an important influence on sea-air CO_2 exchanges. Therefore, the main objective of this study is to estimate CO_2 concentration at a regional scale, under the influence of Oporto Metropolitan Area (OMA) emissions as a first test of this hypothesis. To fulfil this objective, an emission database was built and used to force, together with meteorological synoptic data, a mesoscale atmospheric dispersion model. The model was used to simulate several weather scenarios and estimate CO_2 concentrations along a ca. 90 km stretch of the Portuguese northern shore. The results obtained suggest that emissions from OMA have an important influence on CO_2 atmospheric concentrations up to 6–12 km offshore, particularly in autumn and winter. However, this CO_2 increase does not seem to have the potential to significantly affect sea-air CO_2 exchanges, although this is just a preliminary conclusion that has to be tested by field work.

Keywords Carbon dioxide • Global warming • Coastal zone • Metropolitan area • Atmosphere • Ocean • Regional scale • Emission • Air–sea exchange • Model

R. Carvalho (✉), N. Barros, and P. Duarte
CIAGEB – Global Change, Energy, Environment and Bioengineering R&D Unit,
University Fernando Pessoa, Praça 9 de Abril, 349, 4249-004 Porto, Portugal
e-mail: carvalho@ufp.edu.pt; nelson@ufp.edu.pt; pduarte@ufp.edu.pt

P. Duarte and J.M. Santana-Casiano (eds.), *Oceans and the Atmospheric Carbon Content*,
DOI 10.1007/978-90-481-9821-4_2,

2.1 Introduction

Environmental issues began to be studied, with greater emphasis, at the end of the 1970s, because the scientific community, society and some governments felt the need to intensify the development of research in this area. In recent decades, concerns about global warming led to a large number of studies on emissions and concentrations of greenhouse gases, especially CO_2, and their consequences. Climate has changed in the past due to cyclic variations in the eccentricity of Earth's orbit around the sun, Earth's precessional motion and axis tilt, and in periods of intense volcanic activity (Jahn 2005). However, it is concern about the potential contribution of mankind to climate change that is stimulating much of the current debate on global warming.

In 1988, the UNEP (United Nations Environment Programme) created the IPCC (Intergovernmental Panel on Climate Change) (United Nations 1998). The first IPCC report (IPCC 1990) pointed out the need to reduce anthropogenic emissions of greenhouse gases to the atmosphere in order to decrease global warming trends. This first recommendation was confirmed in subsequent IPCC reports (IPCC 1995, 2001, 2007). The Kyoto Protocol was created, in 1997, within the United Nations Framework on Climate Change (UNFCC), leading to a commitment, between 2008 and 2012, of many governments to reduce greenhouse gas emissions to values below 1990, and drawing more attention to the role of carbon dioxide in the atmosphere (Baliunas 2002). In spite of IPCC claims through their assessment reports and the apparent political willingness of many governments to reduce carbon dioxide emissions, the links between the so-called "greenhouse gases" and climate change is still a matter of debate (e.g. Gerlich and Tscheuschner 2007).

CO_2 emissions increased throughout the twentieth century and continue to increase, mostly as a result of energy production followed by changes in land use, especially deforestation (IPCC 2007). Beginning in the 1950s, an increasing number of CO_2 monitoring stations were established worldwide (http://www.esrl.noaa.gov). However, the average distance between these stations is on the order of thousands of kilometres, making it difficult to have a clear picture of regional CO_2 variability. Without this degree of detail, it is hardly possible to access the influence of important emission areas, such as highly industrialized and urbanized regions, over nearby coastal zones, considered to be important CO_2 sinks according to the "continental shelf pump hypothesis" (Tsunogai et al. 1999; Thomas et al. 2004). Several papers have dealt with the evaluation of global air–sea CO_2 fluxes in coastal environments, such as Borges (2005), Borges et al. (2005, 2006), Cai et al. (2006), Chen and Borges (2009). Presumably, this role may be influenced by local CO_2 concentrations, since its partial pressure in the atmosphere will partly determine its exchanges across the sea-air interface. There are several papers that have shown that there is a local influence of land masses in atmospheric CO_2 measured at sea: Bakker et al. (1996), Borges and Frankignoulle (2001, 2003). Working on Dutch Coastal waters, the first of these authors found that existence of atmospheric CO_2 over the sea was influenced by the nearby land areas, with a high and variable CO_2 concentration in off shore winds.

From the above reasoning, a possible working hypothesis is that metropolitan areas can have a significant influence on atmospheric concentrations of CO_2 over adjacent coastal zones and thus exert a significant influence on CO_2 ocean -atmosphere exchanges in those zones. Therefore, the main objective of this study was to test this hypothesis for the Oporto Metropolitan Area (OMA), as a starting point to development of a more general test.

2.2 Methodology

The first step of this work was to implement a CO_2 emission database, linked to a Geographic Information System (GIS). Data was obtained from the National Inventory of Anthropogenic Emissions by Sources and Removals by Sinks of Air Pollutants (INERPA) of the Portuguese Environment Agency (APA) (IA2007), from the European Pollutant Emission Register (EPER) (http://eper.eea.europa.eu/eper) (current E-PRTR – www.prtr.ec.europa.eu) and from the most recent demographic survey conducted in Portugal-Census 2001 (http://www.ine.pt). APA is responsible for conducting annual inventories of national emissions of air pollutants. Under the European and other international commitments regarding the United Nations Framework Convention on Climate Change (UNFCCC), Convention on Long-range Transboundary Air Pollution (UNECE) and the directive on National Emission Ceilings (EU), participating countries have to update, on a yearly basis, their inventories of greenhouse gases (GHG) and other air pollutants.

The results of the database and larger-scale meteorology provided by synoptic analyses information, representing different seasons, were used to force the atmospheric model "The Air Pollution Model" (TAPM) (Hurley 2005a) to simulate CO_2 dispersion from the OMA towards the nearby coastal area.

2.2.1 Study Area: Oporto Metropolitan Area

The OMA is formed by 14 municipalities (Fig. 2.1). Currently, OMA occupies an area of 1,575 km^2, counting today, with a population of approximately 1,550,000 residents (http://www.amp.pt).

The coast line of the study area has a length of about 90 km and width of c.a. 60 km. The municipalities along the coast line are: Póvoa de Varzim, Vila do Conde, Matosinhos, Oporto, Vila Nova de Gaia and Espinho. There are three major rivers and estuaries along this coast line: Ave, Leça and Douro. Table 2.1 shows population and area of each municipality, its relative contribution to the total area and population density.

Within the OMA there are industries of particular significance to the country's economy, such as a refinery, a power plant, a steel factory, manufacturing industries, an international airport, a large seaport infrastructure, a large co-generation and an

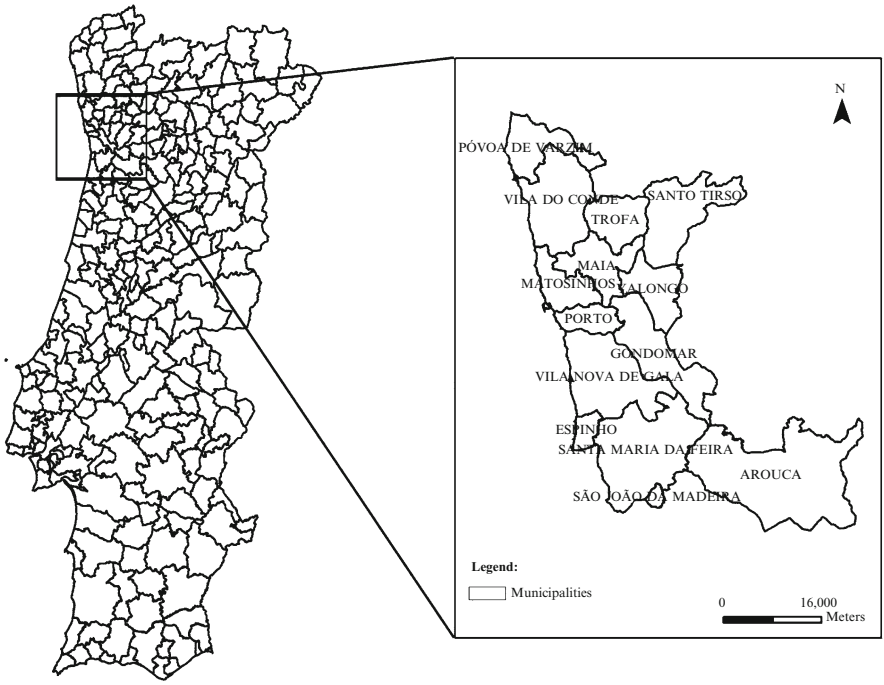

Fig. 2.1 Map of Portugal and Oporto Metropolitan Area

Table 2.1 OMA characterization in area and population (Census 2001)

Municipality	Area (km^2)	(%)	Population	Population density (inhab/km^2)
Espinho	21.1	1.3	33,701	1,596.6
Gondomar	131.9	8.4	164,096	1,244.4
Maia	83.1	5.3	120,111	1,444.7
Matosinhos	62.2	4.0	167,026	2,683.5
Porto	41.3	2.6	256,574	6,214.2
Póvoa de Varzim	82.1	5.2	63,470	773.5
Valongo	75.1	4.8	86,005	1,144.8
Vila do Conde	149.0	9.5	74,391	499.4
Vila Nova de Gaia	168.7	10.7	288,749	1,712.0
Arouca	329.1	20.9	24,227	73.6
Santo Tirso	136.5	8.7	72,396	530.4
São João da Madeira	7.9	0.5	21,102	2,659.4
Santa Maria da Feira	215.1	13.7	135,964	632.0
Trofa	71.9	4.6	37,581	522.8
Total	1,575		1,545,393	981.2

urban solid waste incineration facility. The major point sources in OMA are the Petrogal's Refinery, power plant Turbogás–Central da Tapada do Outeiro, the Solid Waste Treatment Facility (LIPOR II), the National Steel Factory of Maia and the company RAR–Cogeneration (Fig. 2.2).

In this area, apart from seasonal variations in air temperature, there are important variations in wind regime with predominance from northwest in spring (a) and summer (b), from southeast in autumn (c) and from northeast/east in winter (Fig. 2.3).

2.2.2 *Emission's Database*

The emission's database that was implemented contains carbon dioxide and carbon monoxide (CO) data, but in the study area there are no CO_2 monitoring stations. Therefore, CO data was used to validate the Air Pollution Model (TAPM) (cf. –2.3). As mentioned previously, the database was developed taking into account the public inventory available from APA, submitted to the UNFCCC in 2007, covering the period 1990–2005. The inventory contains information about the total national sources and sinks of several greenhouse gases and other pollutants, grouped in several categories. These categories were regrouped according to the following activity sectors: "Commercial and Institutional", "Residential", "Agriculture, Forestry and

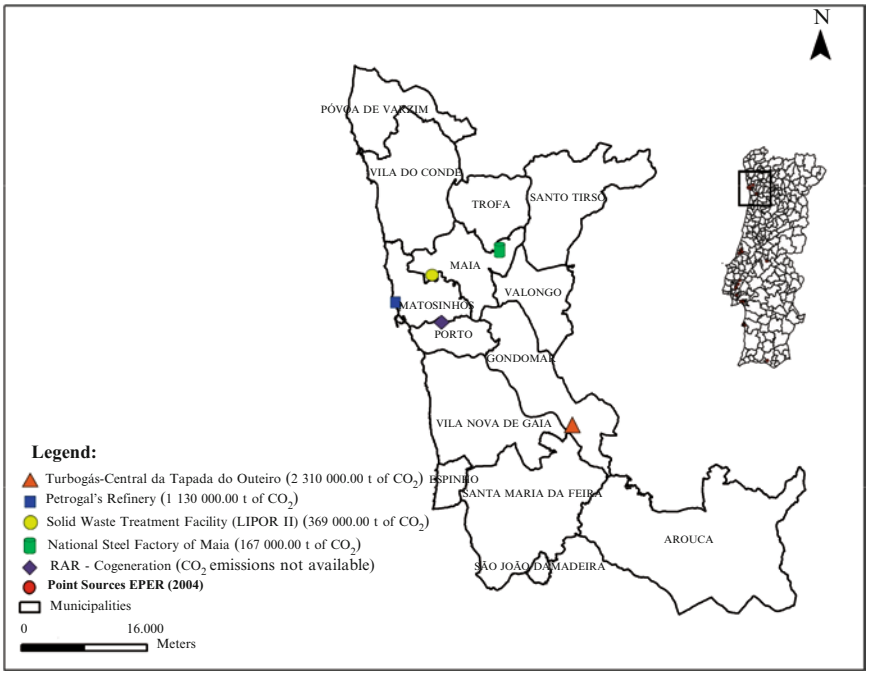

Fig. 2.2 Location and emissions of CO_2 point sources

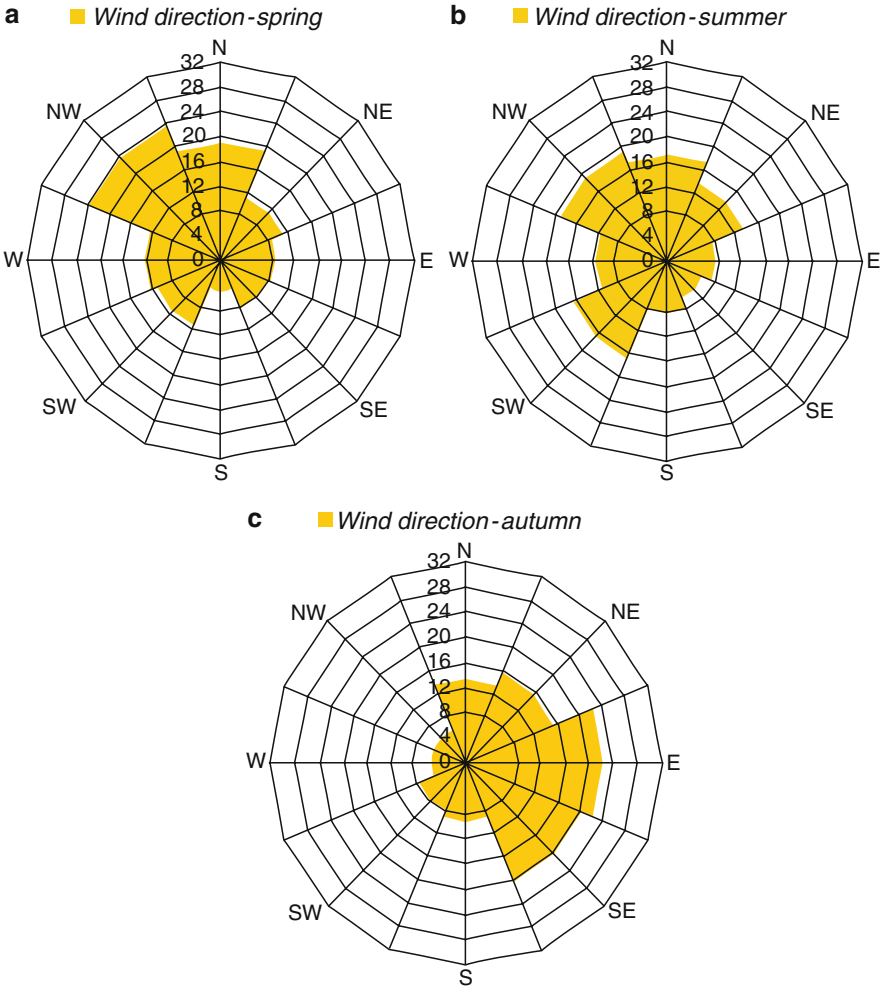

Fig. 2.3 Prevailing wind direction in (**a**) Spring, (**b**) Summer, (**c**) Autumn

Fisheries", "Transport", "Energy Industries" and "Manufacturing industries and construction". The reason for this regrouping was the need to disaggregate the results to different spatial scales according to demographic and other variables.

The emissions database includes only the area emissions. Point source emissions were treated in a different way. Area emissions included the relatively diffuse homogeneous sources that are difficult to identify separately such as: small industries, roads located within the urban perimeter, natural sources, etc.

The APA inventory does not distinguish between these area emissions and point sources. However, EPER has a national registry of industries with the greatest amount of emissions to the atmosphere, considered as point sources in this work. Therefore, large point sources (EPER emissions) were subtracted from the national

Table 2.2 The breakdown of atmospheric emissions in the study area according to sectors and dates

Activity sector	Municipality	Parish
Energy industries	Consumption of fuel oil and natural gas (2004)	Population (2001)
Manufacturing industries and construction	Number of enterprises and companies linked to extractive industry, manufacturing and construction (2004)	Population (2001)
Transport	Staff serving in societies (2004)	Population (2001)
Commercial and Institutional	–	Number of buildings (2001)
Residential	–	Population (2001)
Agriculture, forestry and fisheries	–	Utilized agricultural area (1999)

emission's inventory and allocated to their exact location in the emission's database and respective GIS files. The sectors of activity covered by this operation were "Industries of energy" and "Manufacturing and construction".

The breakdown (Table 2.2) of national emissions to different activity sectors and to the parish level was based on variables contained in the demographic Census survey conducted in 2001 (http://www.ine.pt). However, in some activity sectors ("Energy industries", "Manufacturing industries and construction" and "Transport") it was not possible to disaggregate national emissions directly to the parish level. The breakdown was made taking into account the proportionality between the variables at the national level and the variables at the municipality and/or parish. For example, the breakdown of the "Commercial and Institutional" sector was made directly to the parish level, taking into account the variable "number of buildings". The total number of buildings of the country corresponds to the known total emissions of that sector. By proportionality, the number of buildings of a parish will have its share of emissions.

The "Energy industries" sector emissions were first disaggregated to municipalities based on oil consumption and natural gas and then to the parish level based on population. In both cases a proportionality rule was followed (Table 2.2).

2.2.3 Dispersion Model (TAPM)

The results of the database and larger-scale meteorology provided by synoptic analyses information, representing different seasons (spring, summer, autumn and winter), were used to force the atmospheric model TAPM.

The TAPM uses the followings approaches: it solves approximations to the fundamental fluid dynamics and scalar transport equations to predict meteorology

and pollutant concentrations for a range of pollutants important for air pollution applications. It consists of coupled prognostic meteorological and air pollution concentration components, eliminating the need to have site-specific meteorological observations. Instead, the model predicts the flows important to local-scale air pollution, such as sea breezes and terrain-induced flows, against a background of larger-scale meteorology provided by synoptic analyses. The TAPM is a model of air quality that allows a realistic assessment of the dispersion of pollutants and their environmental impact. The model is a versatile tool that can be applied to any location in the world. It predicts all of the required local meteorology, using global terrain and land-use data as well as global synoptic analyses. It can be used to predict meteorological and air pollution parameters at inter-regional, city, or local scales, for simulation periods from a day to a year or more (Hurley 2005b). The diagram depicted in Fig. 2.4 synthesizes TAPM functioning.

The grid used in the model was the 3,000 × 3,000 m^2 (31 × 31 cells) grid (Fig. 2.5). Vertically, the model considers a domain of 8,000 m, spread across 25 levels of uneven spacing, being closer near the ground, with the first level at a height of 10 m. This was the level considered in this work, the objective being to assess the significance of the

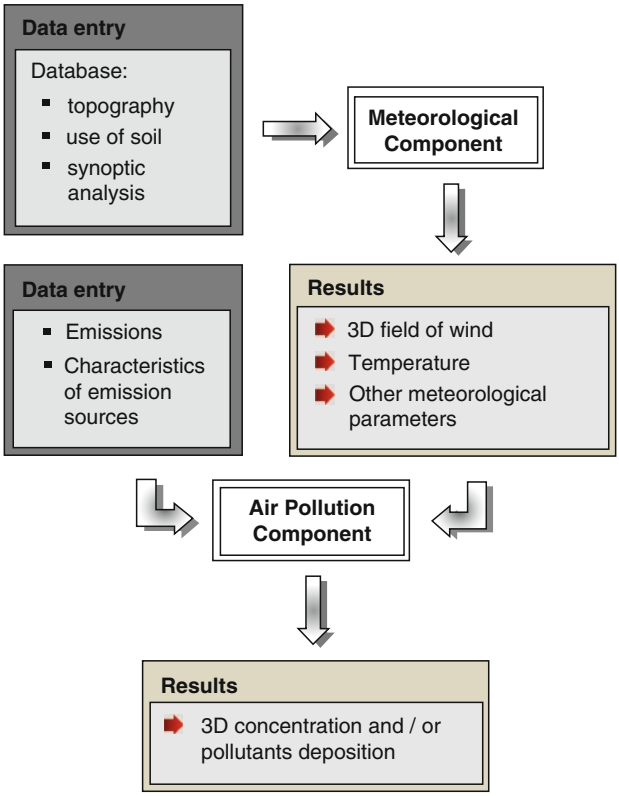

Fig. 2.4 Schematic representation of the Model TAPM (Adapted from Coutinho et al. 2007)

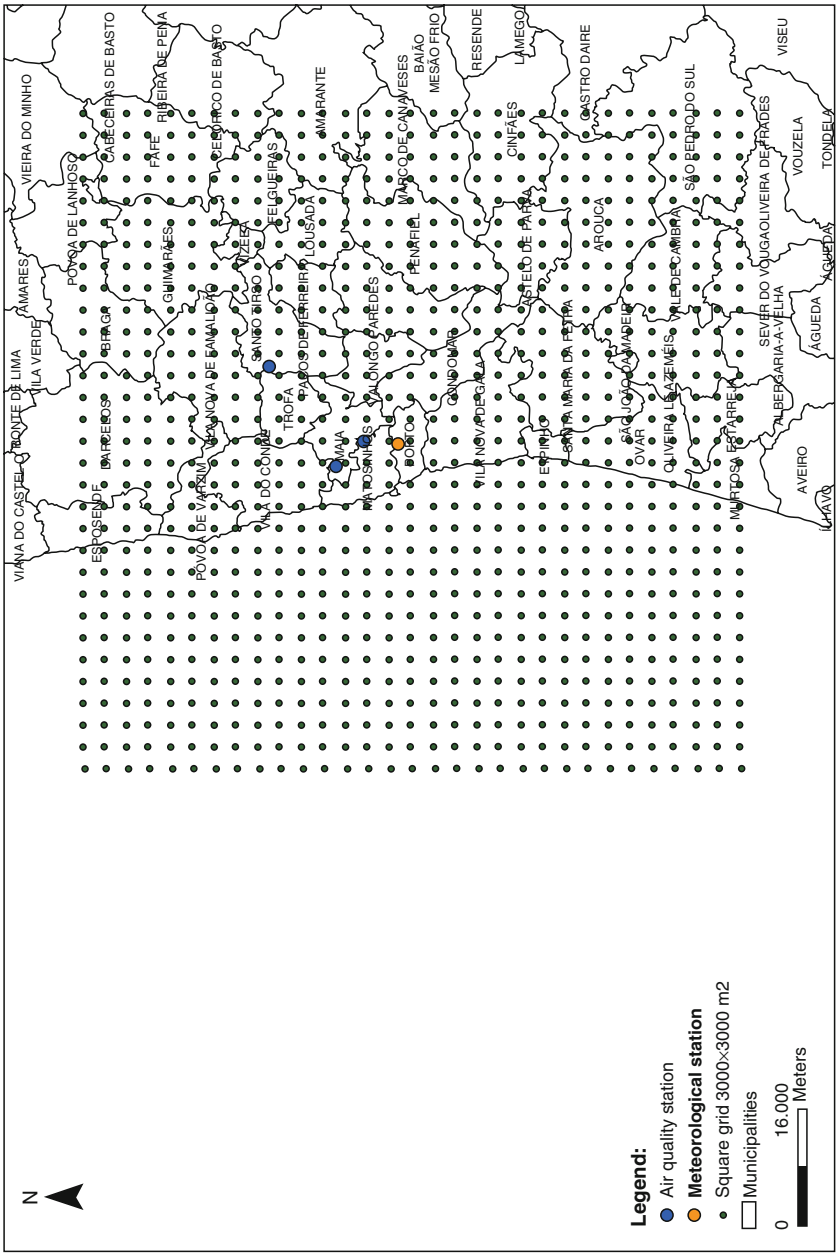

Fig. 2.5 Square grid 3,000 × 3,000 m^2 (186 × 186 cells) and location of the air quality stations and meteorological station

Table 2.3 Simulated periods

Seasonal period	Time period	Predominant wind direction
Spring	02/05/04 to 09/05/04	North (24.7%)/*Northwest* (30.0%)
Summer	15/08/04 to 22/08/04	North (21.3%)/*Northwest* (23.6%)
Autumn	21/11/04 to 28/11/04	Northeast (21.4%)/*Southeast* (28.1%)
Winter	01/02/04 to 29/02/04	Northeast/East/Southeast

increase in CO_2 concentrations on the coastal zone and the CO_2 flows between the ocean and atmosphere.

2.2.3.1 Modelling Scenarios

The modelling scenarios considered in this study included all four seasons with corresponding synoptic forcing for 2004, as depicted in Table 2.3. The start and end dates for each simulation were selected, taking into account the percentage of the prevailing wind direction. For example, the prevailing wind direction in spring is northwest (30.0%). Therefore, the chosen simulation dates corresponded to a time period with predominantly northwest wind. The meteorological data, such as wind speed and wind direction, were taken from a meteorological station located in VCI (Via de Cintura Interna) (Fig. 2.5).

Forcing data corresponds to year 2004, due to data availability constraints. In order to represent these data spatially, it was necessary to use demographic and administrative data from 2001–the most recent census done in Portugal.

2.2.3.2 Model Validation

The validation statistic model BOOT (Chang and Hanna 2005) has been used, mainly, to assess the performance of air dispersion models. However, the same procedures and approaches implemented in BOOT also apply to other types of models. In this validation model the following performance statistics are recommended: fractional bias (FB), geometric mean bias (MG), normalized mean square error (NMSE), geometric variance (VG), correlation coefficient (R) and the fraction of predictions within a factor of two of the observations (FAC2):

$$FB = \frac{\left(\overline{C_0} - \overline{C_p}\right)}{0.5\left(\overline{C_0} + \overline{C_p}\right)};$$

$$MG = \exp\left(\overline{\ln C_0} - \overline{\ln C_p}\right);$$

$$NMSE = \frac{\overline{\left(C_0 - C_p\right)^2}}{\overline{C_0}\,\overline{C_p}};$$

$$VG = \exp\left[\overline{\left(\ln C_0 - \ln C_P\right)^2}\right];$$

$$R = \frac{\overline{\left(C_0 - \overline{C_0}\right)\left(C_P - \overline{C_P}\right)}}{\sigma_{C_P}\sigma_{C_0}};$$

$$FAC2 = \text{fraction of data that satisfy } 0.5 \le \frac{C_P}{C_0} \le 2.0;$$

where:

C_P : predictions of the model

C_0 : observations

$\overline{C}$: average over the data

σ_C : standard derivation of data.

Park and Seok(2007) proposed ranges of values for these parameters, to allow classifying model performance as "Good", "Fair" and "Poor".

The model was validated with meteorological and carbon monoxide (CO) data. CO was used in the absence of CO_2 data because it is a relatively stable pollutant at the time scale of the simulations and, regarding the available data, the most conservative approximation at the present time (Table 2.3).

CO data used in the validation can be accessed at the Internet site of the Portuguese Agency for Environment, Qualar-Database Online on Air Quality (http://www.qualar.org). There are three types of stations, according to the type of influence: traffic, background and industries. The aim of this study is to evaluate the concentrations of CO without direct influence from industry and traffic. Accordingly, stations selected were: Vila Nova da Telha, Santo Tirso and Leça do Balio (Table 2.4).

Wind speed, wind direction and temperature data were taken from a meteorological station located in VCI. Figure 2.5 shows the stations used to validate the results of TAPM.

2.2.3.3 Approaches for Analysing the Significance of Model Predicted CO_2 Changes

The low spatial resolution of CO_2 monitoring turns the evaluation of significance of local and regional scale CO_2 variability into a difficult task. Therefore, in order to evaluate the significance of model predicted CO_2 increments over the coastal area under study, three approaches were followed: (i) Compare predicted spatial concentration gradients across the land-ocean boundary in the study area, with spatial gradients for

Table 2.4 Description of CO stations (http://www.qualar.org 2008) and meteorological station

Name/Parish/ Municipality	Start date	Type of environment/ Influence	Zone	Coordinate X[a] (m)	Coordinate Y[a] (m)	Altitude (m)
Leça do Balio/ Matosinhos	01/01/2000	Suburban/background	Porto Littoral (agglomeration)	158,043	472,397	40
Santo Tirso/ Santo Tirso	01/06/2003	Urban/background	Vale do Ave	171,307	486,432	–
Vila Nova da Telha/ Maia	01/01/1999	Suburban/background	Porto Littoral (agglomeration)	155,690	476,206	88
VCI/Porto	02/04/2004	–	Porto Littoral	158,906	467,238	10

[a]Military coordinates (Gauss)

monitoring stations located at approximately the same latitude; (ii) Compare differences between predicted CO_2 levels over the coastal zone and background concentrations with inter-annual and seasonal variability trends in these concentrations; (iii) Compare differences between predicted CO_2 levels over the coastal zone and background concentrations with the accuracy of CO_2 sensors.

In the first approach, stations located in Azores, Hungary and Romania were selected for calculating spatial gradients (Table 2.5).

In December 2003, the world average CO_2 concentration was around 375.7 ppmv (http://cdiac.ornl.gov). Measurements of CO_2 concentrations were effectively begun in the year of 1958 in Mauna Loa, Hawaii (NOAA1997). The concentration of this gas, in that year, was 315.98 ppmv. The average annual increase in this concentration has been around 0.41%, which means an annual increase of about 1.44 ppm (http://cdiac.ornl.gov).

Data for CO_2 monitoring stations were obtained from the Internet site of the Earth System Research Laboratory – National Oceanic & Atmospheric Administration (http://www.esrl.noaa.gov).

In order to perform the above comparisons, two areas were analysed separately: coastal waters and territorial waters (Fig. 2.6). The former is limited to 1 and the latter to 12 nautical miles offshore.

2.3 Results

2.3.1 Oporto Metropolitan Area–Emissions Characterization

As mentioned in Section 2.2.2, CO_2 emissions were grouped into six activity sectors. Figure 2.7 shows emissions of these activity sectors in 2001 and 2004.

The emissions databases for 2001 and 2004 (Fig. 2.7), suggest that the sectors with the greatest impact on emissions are “Energy industries”, “Transport” and “Manufacturing industries and construction”, mainly located in the municipalities of Gondomar, Maia and Matosinhos. From 2001 to 2004, the emissions of CO_2 decreased slightly in some sectors, as well as in some municipalities (Fig. 2.7).

Figure 2.8 shows areas, particularly in Gondomar, Maia, Matosinhos and Oporto, with a larger amount of emissions, explained by the location of large point sources such as Petrogal’s refinery, Turbogás power plant – Central da Tapada do Outeiro, the Solid Waste Treatment Facility (LIPOR II) and the National Steel Factory of Maia, as mentioned in subchapter 2.1.

2.3.2 Validation of the Results from TAPM

As mentioned in Section 2.2.3.2, the BOOT model was chosen to perform the validation process. The evaluation of statistical parameters regarding CO

Table 2.5 CO_2 stations description (http://www.esrl.noaa.gov)

Station	Type	Longitude	Latitude	Altitude (m)	First measure	Last measure
Terceira Island – Azores	Surface	27.38° O	38.77° N	40	31/12/1979	11/09/2008
Canary Islands – Tenerife	Surface	14.48° O	28.30° N	2,360	16/11/1991	03/10/2008
Mace Head – County Galway – Ireland	Surface	9.90° O	53.33° N	25	03/06/1991	01/09/2008
Black Sea – Constanta	Surface	28.68° E	44.17° N	3	19/10/1994	22/09/2008
Hegyhatsal – Hungary	Surface	16.65° E	46.95° N	248	02/03/1993	30/07/2008
Mauna Loa – Hawaii	Observatory	155.58° O	19.54° N	3	1958	18/11/2008

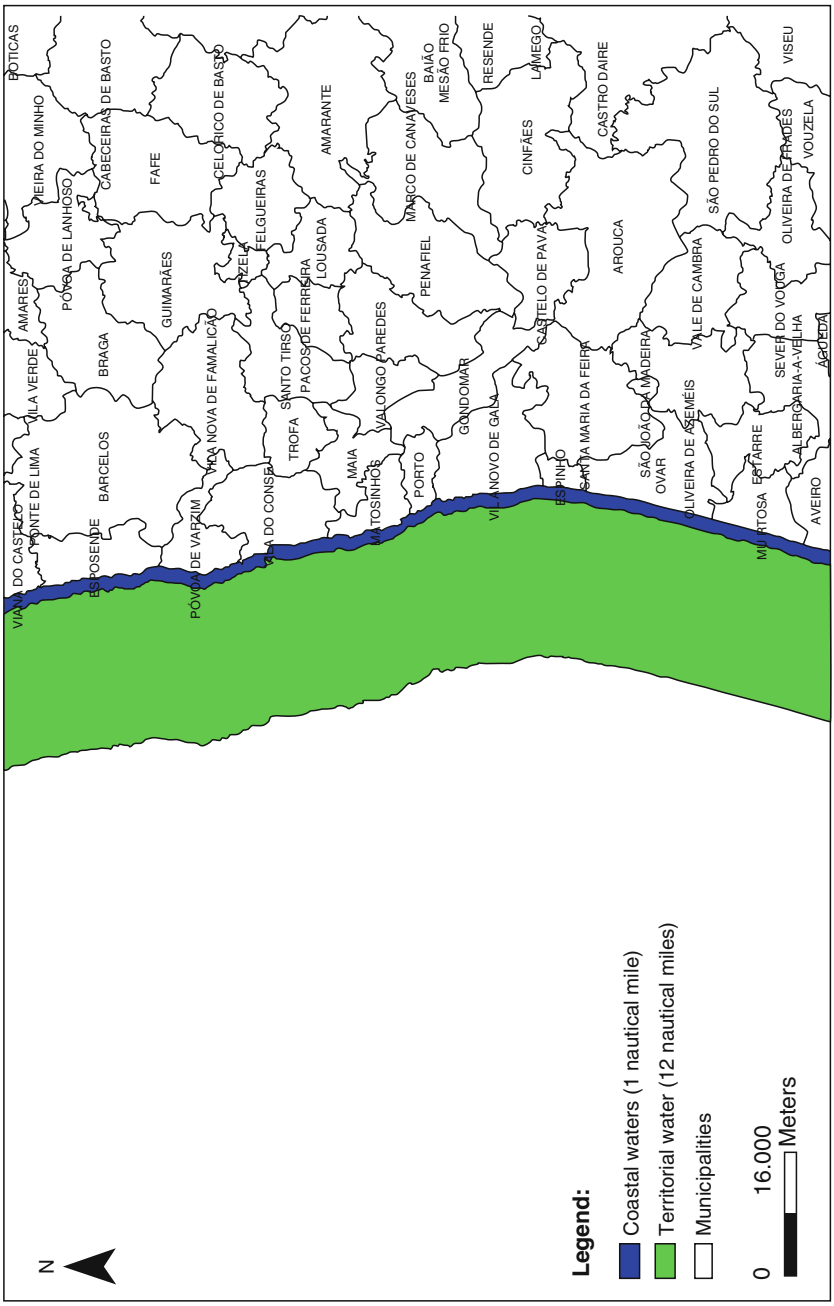

Fig. 2.6 Coastal waters (1 nautical mile – blue area) and territorial waters (12 nautical miles – green area)

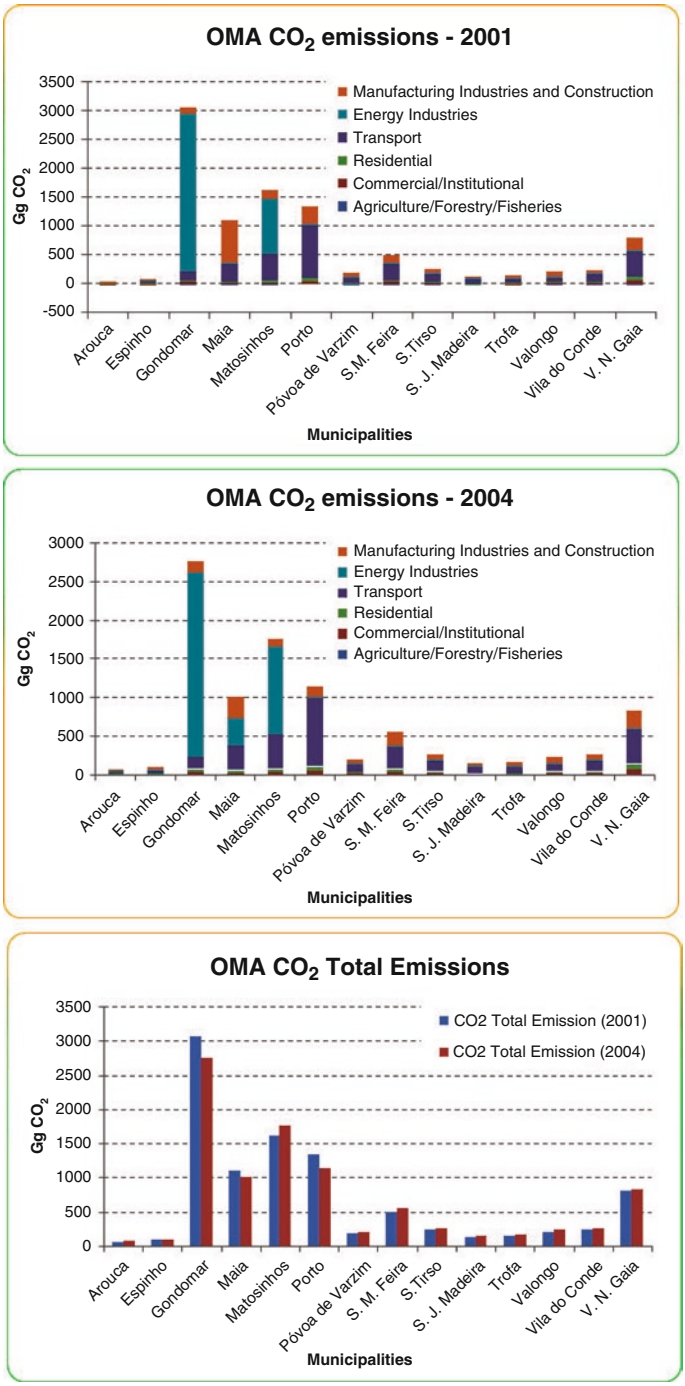

Fig. 2.7 CO_2 emissions (Gg) by activity sectors in 2001 (upper formed) and 2004 (middle formed); CO_2 total emissions (Gg) in 2001 and 2004 (lower formed)

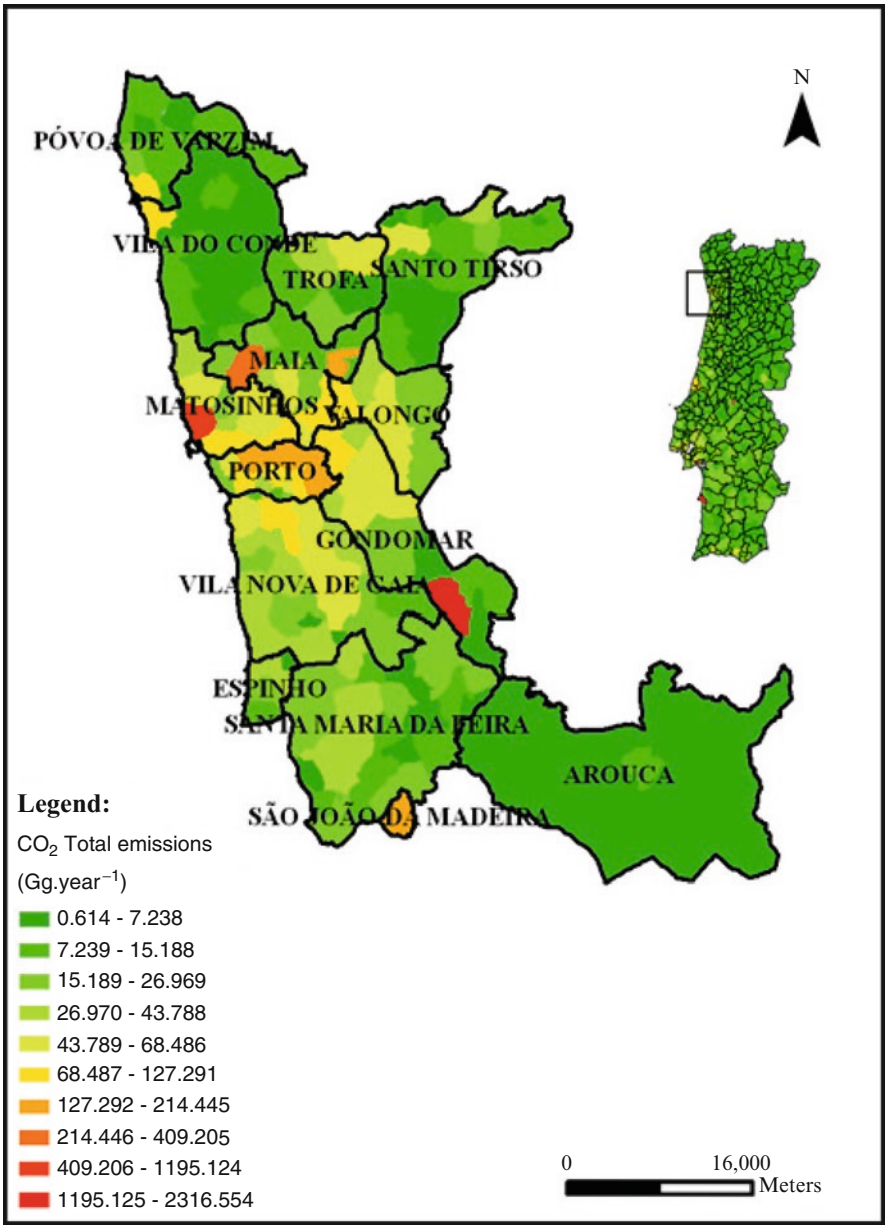

Fig. 2.8 CO_2 total annual emissions from OMA municipalities

concentrations and meteorological parameters simulated for the periods reported in Table 2.3, were good for the former and fair for the latter, according to the BOOT classification scheme (cf. 2.3.2). Figures 2.9 and 2.10 show some examples of observed and simulated data for CO concentration and meteorological parameters respectively.

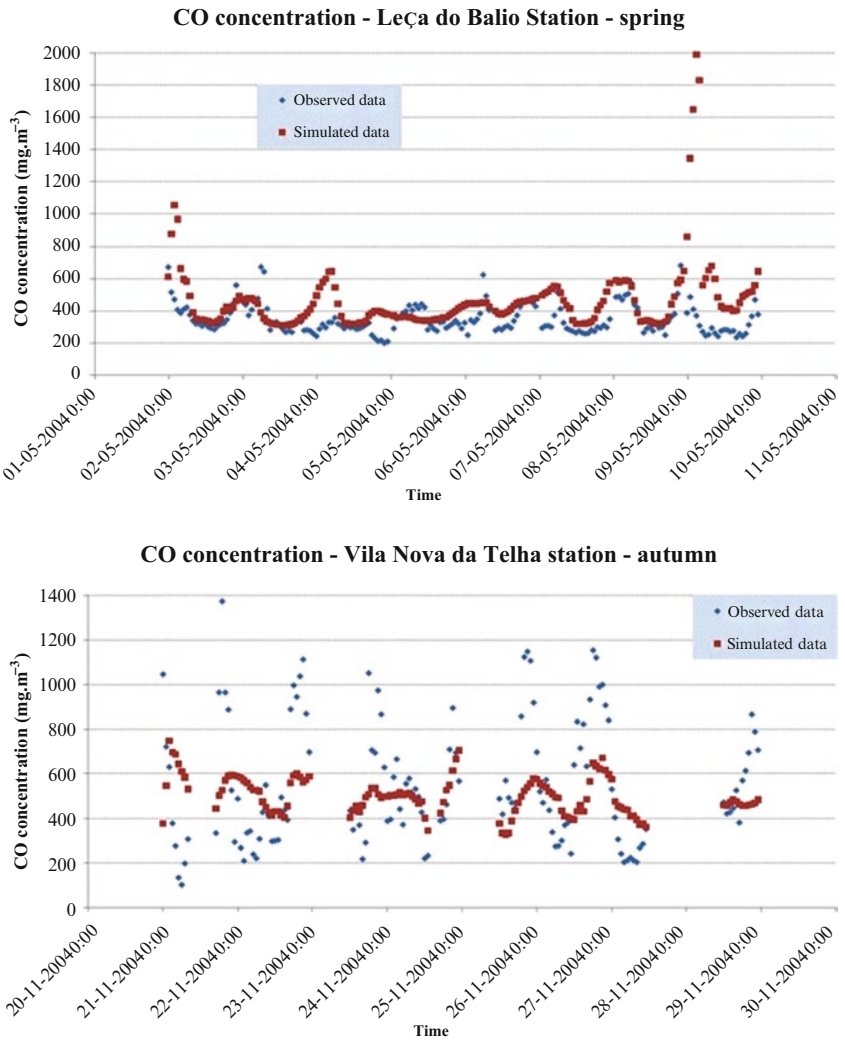

Fig. 2.9 Evaluation's examples between observed and simulated data for CO concentration

2.3.3 TAPM Simulations

Figure 2.11 shows time integrated results from TAPM simulations for different seasons. From these results, it is apparent that the spring and summer concentration plumes, influenced mostly by northwest winds, tend to spread more inland than offshore. However, a weaker southeast wind component explains some offshore transport and dispersion. In autumn and winter, the predominant southeast and east winds are responsible for an important offshore CO_2 transport and dispersion.

It is no surprise that OMA emissions have some influence over the nearby coastal zone, as shown in Fig. 2.11.

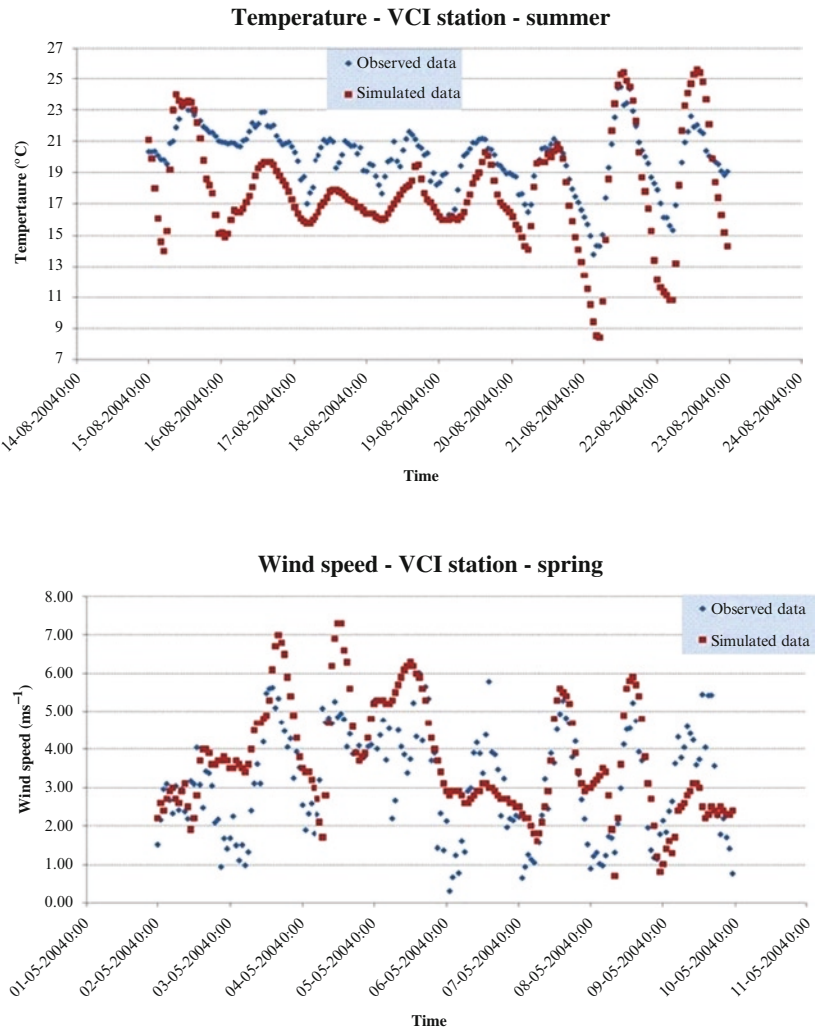

Fig. 2.10 Evaluation's examples between observed and simulated data for meteorological parameters

However, the important issue is to evaluate whether or not this influence is significant. In item 2.3.3, three approaches were mentioned to evaluate the significance of increases in CO_2 concentrations compared to the background concentration.

(i) Spatial gradients

Comparing the concentration gradient between stations (Table 2.6) (order of magnitude 10^{-3} ppm km^{-1}) with gradients of concentrations generated by TAPM (Table 2.7) (order of magnitude 10^{-1}–10^{-3} ppm km^{-1}), it appears that the latter are considerably higher than the former, regardless of the seasonal period, with only a few exceptions (Table 2.7). In the autumn, model predicted gradient is much higher for the seasons. As expected, the predicted gradient decreases offshore.

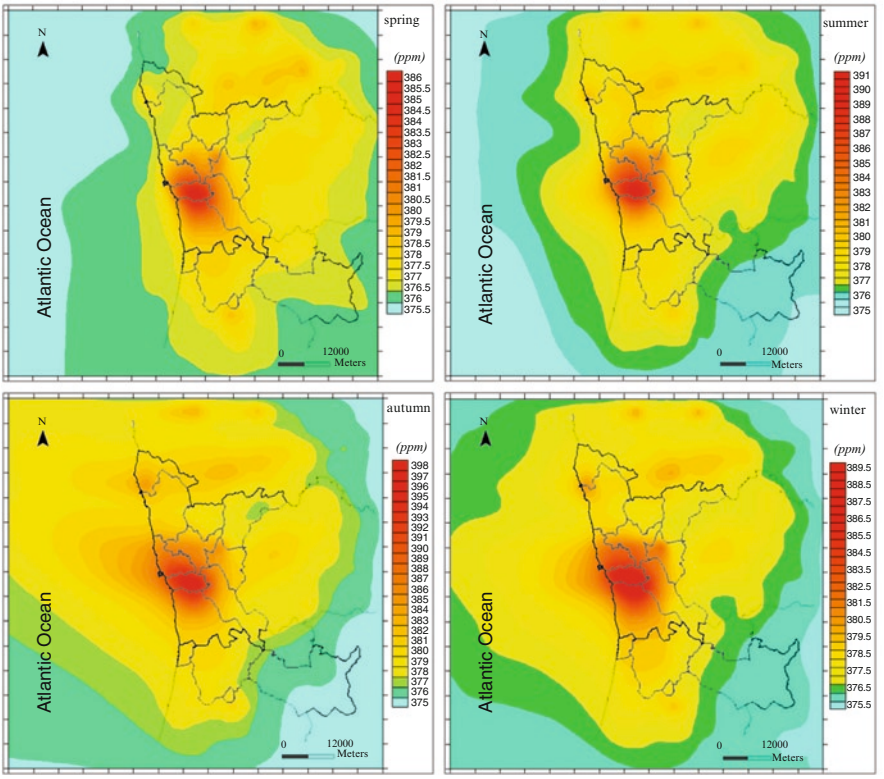

Fig. 2.11 CO_2 concentrations in the atmosphere in the study area

Table 2.6 Concentrations gradients between some stations (http://www.esrl.noaa.gov)

Stations	Distance (km)	Spatial concentrations gradient (ppm km^{-1})
Azores – Romania	4,618.60	2.40×10^{-3}
Hungary – Romania	922.11	6.99×10^{-3}

(ii) Predicted CO_2 levels and temporal variability

Table 2.8 shows the average concentrations and increased average suffered on the average tropospheric concentration in 2003, on "coastal waters" and "territorial waters", during the season's winter, spring, summer and autumn.

The inter-annual atmospheric CO_2 increase is around 1.74 ppm, corresponding to approximately a 0.41% increase. Model results suggest a potential CO_2 increase over the studied area that, on several occasions is larger than those figures, in winter, summer and autumn, within the 12 mile limit.

However, when the percent increases predicted by the model are compared to CO_2 seasonal coefficient variation, it is clear that the latter are much higher (Table 2.9).

Table 2.7 Concentrations gradient of TAPM between areas

		Seasonal period			
		Winter	Spring	Summer	Autumn
Zone		Spatial concentrations gradient (ppm km^{-1})			
Territorial waters	Between the shore to 3 miles offshore	2.32×10^{-1}	1.21×10^{-1}	2.58×10^{-1}	3.13×10^{-1}
	Between 3 and 6 miles offshore	8.77×10^{-3}	3.02×10^{-2}	7.76×10^{-2}	1.25×10^{-1}
	Between 6 and 12 miles offshore	4.59×10^{-3}	1.75×10^{-2}	5.01×10^{-2}	8.11×10^{-2}
Outside the territorial waters	Between 12 and 26 miles offshore	2.48×10^{-3}	6.89×10^{-3}	1.95×10^{-2}	5.37×10^{-2}

Table 2.8 Increasing concentrations of CO_2 in the zone "coastal waters", "territorial waters" and beyond that zone

		Seasonal period			
		Winter	Spring	Summer	Autumn
Zone		Average concentration (ppm)/percentage (%)			
Coastal waters	Between the shore to 1 mile offshore	379.01/0.88	376.71/0.27	378.22/0.67	381.47/1.56
Territorial waters	Between the shore to 3 miles offshore	378.40/0.72	–	377.60/0.50	380.57/1.30
	Between 3 and 6 miles offshore	377.74/0.54	–	376.91/0.32	379.67/1.06
	Between 6 and 12 miles offshore	377.23/0.41	–	376.41/0.19	378.89/0.85
Outside the territorial waters	Between 12 and 26 miles offshore	376.80/0.29	–	375.96/0.07	377.81/0.56

Table 2.9 Temporal variability of CO_2 concentrations in the stations in 2004 and seasonal variation coefficient (winter vs. summer) of CO_2 concentrations in the stations since the beginning of its activity

	Stations				
	Terceira Island Azores	Canary Islands Tenerife	Mace Head County Galway Ireland	Black Sea Constanta Romania	Hegyhatsal Hungary
	Concentration (ppm)				
Winter (February)	380.34	378.63	381.74	390.01	392.47
Spring (May)	380.49	379.36	381.21	382.61	376.79
Summer (August)	371.89	373.59	369.48	384.29	368.09
Autumn (November)	376.66	376.75	377.69	396.34	393.79
Seasonal variability	8.45	5.04	12.26	5.72	24.38
Seasonal variation of concentrations coefficient (%)	2.61	1.77	3.57	4.87	7.61

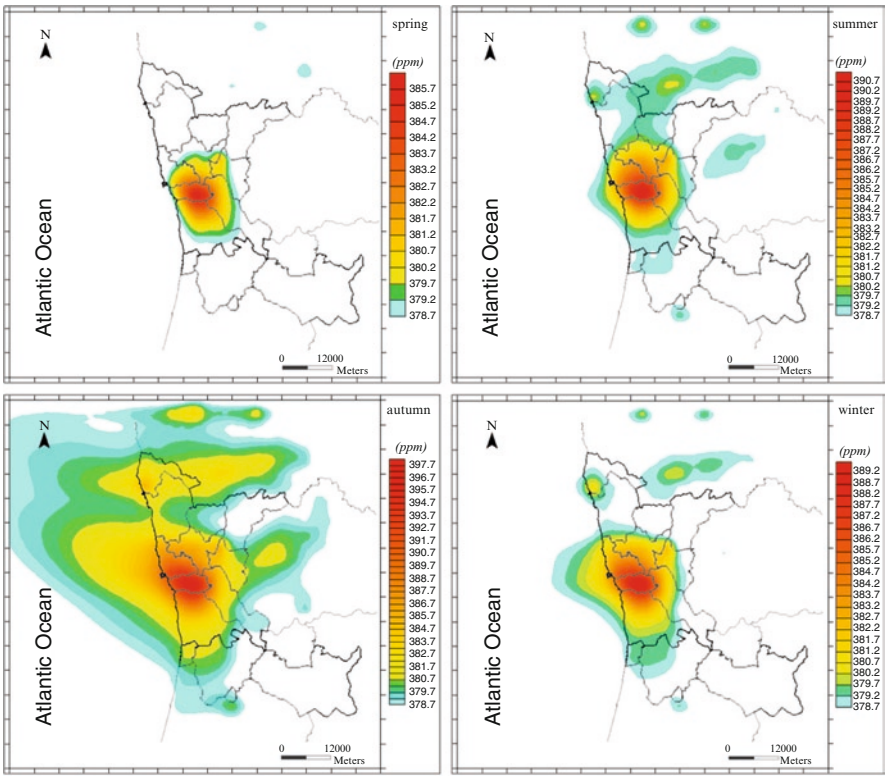

Fig. 2.12 Differences between expected concentrations and the average tropospheric concentration of atmospheric CO_2, higher than the sensitivity of the measuring CO_2 apparatus

(iii) Predicted CO_2 changes and accuracy CO_2 probe sensitivity

The measurement error of currently available CO_2 probe sensitivity is between ±0.5 and ±1 ppm. Figure 2.12 shows the locations where predicted concentrations are above the indicated accuracy.

This figure suggests that in spring and summer the model predicted influence of emissions from OMA on the adjacent coastal zone is hardly detected with present day technology. However, the same figure suggests the opposite for autumn and winter. Particularly in autumn, the "measurable" influence is over most of the model domain.

2.4 Discussion

Model simulations results presented before suggest that the CO_2 plume produced over the OMA may have an important offshore shift in winter and autumn as a result of the dominant wind offshore component. However, the main challenge here is trying to evaluate the significance of this effect over

tropospheric CO_2 concentrations. In the absence of nearby CO_2 monitoring stations, comparisons between CO_2 model predicted increases at various distances offshore, on one hand, and spatial and temporal CO_2 variability data, on the other hand, suggest that OMA may produce a local "bump" on CO_2 levels with increases over the sea, within the 12 miles limit, that are above inter-annual CO_2 variability but below CO_2 seasonal variability. Furthermore, in winter and, specially, in autumn the predicted concentration changes are detectable by current CO_2 measuring technology. Therefore, it is practicable to empirically test these model results.

From the above reasoning, it seems likely that the OMA may exert, at least, a measureable change on CO_2 concentrations over nearby coastal areas within a limited distance offshore (<12 miles). The next logical step is trying to anticipate the potential that these CO_2 increases may have in influencing CO_2 air–sea exchanges and the sink-source CO_2 rate of the coastal area under study.

2.5 Conclusions

Obtained results, based on the atmospheric mesoscale model (TAPM), suggest that the OMA has a significant impact on atmospheric CO_2 concentrations over the adjacent coastal zone up to c.a. 12 miles offshore. Consequently, a similar result may be expected for other metropolitan areas.

Therefore, obtained results support the initial hypothesis, stressing the need for further studies about their potential implications on CO_2 sinking capacity of coastal zones. A natural follow-up to this study would be an empirical assessment of CO_2 concentrations over the adjacent coastal area under different seasonal and synoptic forcing and their consequences on CO_2 air–sea exchanges.

References

Bakker DCE, De Baar HJW, de Wilde HPJ (1996) Dissolved carbon dioxide in Dutch coastal waters. Mar Chem 55:247–263

Baliunas S (2002). The Kyoto Protocol and global warming. The Lavoisier Group, Melbourne, Australia

Borges, AV, Frankignoulle M (2001) Short-term variations of the partial pressure of CO_2 in surface waters of the Galician upwelling system, Prog Oceanogr 50:283–302

Borges AV, Frankignoulle M (2003) Distribution of surface carbon dioxide and air-sea exchange in the English Channel and adjacent areas. J Geophys Res 108(C5):3140

Borges AV (2005) Do we have enough pieces of the jigsaw to integrate CO_2 fluxes in the Coastal Ocean? Estuaries 28(1):3–27

Borges AV, Delille B, Frankignoulle M (2005) Budgeting sinks and sources of CO2 in the coastal ocean: Diversity of ecosystems counts, Geophys Res Lett 32:L14601. doi:10.1029/2005GL023053

Borges AV, Schiettecatte L-S, Abril G, Delille B, Gazeau F (2006) Carbon dioxide in European coastal waters. Estuar Coast Shelf Sci 70(3):375–387

Cai W-J, Dai MH, Wang YC (2006) Air-sea exchange of carbon dioxide in ocean margins: A province-based synthesis. Geophys Res Lett 33:L12603. doi:10.1029/2006GL026219

Chang JC, Hanna SR (2005) Technical descriptions and user's guide for the BOOT statistical model evaluation software package, version 2.0. Harmonisation within atmospheric dispersion modelling for regulatory purposes

Chen CTA, Borges AV (2009) Reconciling opposing views on carbon cycling in the coastal ocean: Continental shelves as sinks and near-shore ecosystems as sources of atmospheric CO_2. Deep Sea Res II 56(8–10):578–590

Coutinho M, Ribeiro C, Borrego C (2007) Avaliação dos episódios de ozono de Julho e Agosto de 2003 na Região Sul de Portugal Continental. 9ª Conferência Nacional do Ambiente, Universidade de Aveiro

Gerlich G, Tscheuschner RD (2007) Falsification of the CO_2 greenhouse effects within the frame of physics. Institut fur Mathematische Physik, Technische Universität Carolo Wilhelmina, July 24

Hurley P (2005a) The Air Pollution Model (TAPM) version 3. User manual, CSIRO Atmospheric Research, Internal Paper No. 31

Hurley P (2005b) The Air Pollution Model (TAPM) version 3. Part 1: Technical description, CSIRO Atmospheric Research, Paper No. 71

IA (2007) Instituto do Ambiente. Portuguese National Inventory Report on Greenhouse Gases, 1990–2005. Ministério do Ambiente, Ordenamento do Território e do Desenvolvimento Regional

IPCC (1990) Intergovernmental panel on climate change, Reports prepared for IPCC by Working Groups I, II and III, United Nations Environmental Program and World Meteorological Organization, Cambridge University Press

IPCC (1995) Intergovernmental panel on climate change, Contributions of Working Groups I, II and III to the IPCC Second Assessment Report, Cambridge University Press

IPCC (2001) Intergovernmental panel on climate change, Contributions of Working Groups I, II and III to the IPCC Third Assessment Report, Cambridge University Press

IPCC (2007) Intergovernmental panel on climate change, Contributions of Working Groups I, II and III to the IPCC Fourth Assessment Report, Cambridge University Press

Jahn A (2005) Theories and modeling of glacial–interglacial cycles and glacial inception. Department of Atmospheric and Oceanic Sciences McGill University, Montreal, Canada

NOAA (1997) National oceanic and atmospheric administration, Mauna Loa Observatory: Where it all began. US Department of Commerce

Park O, Seok M (2007) Selection of an appropriate model to predict plume dispersion in coastal areas. Atmos Environ 41(2007):6095–6101

Thomas H, Bozec Y, Elkalay K, de Baar HJW (2004) Enhanced open ocean storage of CO_2 from shelf sea pumping. Science 304:1005–1008

Tsunogai S, Watanabe S, Sato T (1999) Is there a ''continental shelf pump'' for the absorption of atmospheric CO2? Tellus Ser B 51:701–712

United Nations (1998) Kyoto Protocol to the United Nations Framework Convention on climate change. Kyoto, Japan

Chapter 3
Present Day Carbon Dioxide Fluxes in the Coastal Ocean and Possible Feedbacks Under Global Change

Alberto V. Borges

Abstract The present day contemporary CO_2 fluxes in shelf seas could be significant for the global carbon cycle, since available estimates converge to a sink of ~0.3 PgC yr^{-1} corresponding to 21% of most recent estimate of contemporary sink of atmospheric CO_2 in open oceans of 1.4 PgC yr^{-1}. These estimates are prone to large uncertainty mainly due to inadequate representation of the spatial variability and need to be improved based on more data, requiring a concerted global observational effort. The potential feedbacks on increasing atmospheric CO_2 from changes in carbon flows in the coastal ocean could be disproportionately higher than in the open ocean. The changes in carbon flows and related potential feedbacks in the coastal ocean could be driven by 3 main processes: i) changes in coastal physics; ii) changes in land-used, waste water inputs, agricultural fertilizers and changes in hydrological cycle; iii) changes in seawater carbonate chemistry (ocean acidification). These potential feedbacks remain largely unquantified due to a poor understanding of the underlying mechanisms, or lack of modelling to quantify them. Based on reported evaluations and back of the envelop calculations, it is suggested that changes of biological activity due the increased nutrient delivery by rivers would provide by 2100 a negative feedback on increasing atmospheric CO_2 of the order of magnitude of the present day sink for atmospheric CO_2. This negative feedback on increasing atmospheric CO_2 would be one order of magnitude higher than negative feedback due to the decrease of either pelagic or benthic calcification related to ocean acidification, and than the negative feedback related to dissolution of $CaCO_3$ in sediments. The increase of export production could also provide a significant feedback to increasing atmospheric CO_2, although based on the conclusions from a single perturbation experiment. Feedbacks on increasing atmospheric CO_2 due to effects of C cycling in continental shelf seas related to changes in circulation or stratification could be important but remain to be quantified.

A.V. Borges (✉)
Chemical Oceanography Unit, University of Liège, Belgium
e-mail: alberto.borges@ulg.ac.be

P. Duarte and J.M. Santana-Casiano (eds.), *Oceans and the Atmospheric Carbon Content*,
DOI 10.1007/978-90-481-9821-4_3,

Keywords Carbon dioxide fluxes • Green house gases • Global change • Coastal ocean • Coastal environments • Feedbacks • Land use • Waste water inputs • Agricultural fertilizers • Hydrological cycle • Atmospheric deposition • Ocean acidification

Warming of the climate system is unequivocal based on observational evidence from all continents and most oceans (increases in global average air and ocean temperatures, melting of snow and ice, and increasing global average sea level) (IPCC 2007a). The observed increase in global average temperatures since the industrial revolution is very likely due to increasing concentrations in the atmosphere of anthropogenic green house gases (GHG). Global GHG emissions are expected to continue to grow over the next few decades, and warming and climate change in the near and long term will have a variety of negative impacts such as: changes in terrestrial and marine ecosystems (increased risk of species extinction, changes in ecosystem structure and function, loss of biodiversity, loss of ecosystem goods and services,…), changes in crop productivity, increasing risks on coasts (coastal erosion, floods,…), increasing exposure to extreme weather events (heat waves, heavy precipitation events, incidence of extreme high sea level,…), effects on health status of millions of people (increases in malnutrition, diseases, injury due to extreme weather events,…), exacerbate current stresses on water resources,… (IPCC 2007b).

Carbon dioxide (CO_2) is the most important anthropogenic GHG accounting for 77% of total anthropogenic GHG emissions in 2004 (IPCC 2007a). For the 2000–2006 period, 9.1 PgC $year^{-1}$ (PgC = 10^{15} gC) of CO_2 were emitted to the atmosphere mainly from fossil fuel combustion and cement production (7.6 PgC $year^{-1}$) and land use change (1.5 PgC $year^{-1}$). About 4.1 PgC $year^{-1}$ accumulated in the atmosphere, the land biosphere is supposed to have absorbed 2.8 PgC $year^{-1}$, and the oceans have absorbed the remaining 2.2 PgC $year^{-1}$ (Canadell et al. 2007). Hence, oceans are a major component of the global CO_2 cycle. However, the oceans are also vulnerable to climate change with potential changes in their capacity to absorb anthropogenic CO_2. These vulnerabilities include surface warming and related changes in circulation that will impact directly the chemical and physical oceanic CO_2 pumps. Changes in ocean physics are also expected to modify the vertical inputs of inorganic nutrients and light availability (increasing stratification), hence, affecting primary production and ecosystem structure, and modifying the biological CO_2 pump. The latter is also expected to respond to changes of seawater carbonate chemistry (ocean acidification) that could modify the rates and fates of primary production and calcification of numerous organisms.

Coastal environments only represent 7% of the total oceanic surface area, however, they are biogeochemically more dynamic, and probably more vulnerable to climate changes than the open ocean. Whatever the responses of the open ocean to climate changes, they will propagate on the coastal ocean. Superimposed on this "background open oceanic forcing", the coastal ocean will also respond to changes of fluxes from the land biosphere through rivers, ground waters and atmospheric deposition of major biogeochemical elements (carbon, nitrogen, phosphorous, silica) in organic and inorganic forms. Physical settings specific to the coastal ocean (coastal

upwelling, sea-ice,…) are also expected to respond to climate change probably leading to unique and local changes in carbon cycling. Finally, due to the shallowness of the coastal ocean, the benthic compartment will respond to changes of carbon cycling in surface waters on much shorter time scales than in the open ocean.

This chapter focuses on CO_2 cycling in the coastal ocean, briefly summarizing the current knowledge on the present day fluxes, and focussing more in depth on the possible evolution and feedbacks under global change.

3.1 Present Day Carbon Dioxide Fluxes in the Coastal Ocean

Continental shelf seas receive massive inputs of organic matter and nutrients from land, exchange large amounts of matter and energy with the open ocean across continental slopes and constitute one of the most biogeochemically active areas of the biosphere. The coastal ocean hosts between ~15% and ~30% of oceanic primary production and ~80% of oceanic organic matter burial (e.g. Gattuso et al. 1998a). It also hosts most of the benthic oceanic calcium carbonate ($CaCO_3$) production, ~20% of surface pelagic oceanic $CaCO_3$ stock (Balch et al. 2005), and ~50% of oceanic $CaCO_3$ deposition (Gattuso et al. 1998a). Hence, carbon (C) flows in the coastal ocean are disproportionately high in comparison with its surface area (~7% of total oceanic surface area). Intense air–water carbon dioxide (CO_2) exchanges can then be expected in the coastal ocean and could be significant for CO_2 flux budgets at regional (Frankignoulle and Borges 2001; Borges et al. 2006) and global scales (Table 3.1).

The contemporary flux of CO_2 between the coastal ocean and the atmosphere has been evaluated by several authors based on the global extrapolation of a flux value from a single shelf sea or from the compilation of literature data in several shelf seas (Table 3.1). The most recent evaluations converge towards a sink of atmospheric CO_2 of about 0.3 PgC year^{-1}. This CO_2 sink would be highly significant, corresponding to 21% of the most recent estimate of contemporary sink of atmospheric CO_2 in open oceans of 1.4 PgC year^{-1} (Takahashi et al. 2009).

Yet, these estimates based on literature compilations suffer from several caveats, one of the most important being the lack of data to adequately cover the full spatial extent of the coastal ocean and the diversity of biogeochemical C cycling related to extremely contrasted physical and biogeochemical settings. Indeed, the distribution of CO_2 flux data in shelf seas reported in literature is biased towards the mid-latitudes of the Northern Hemisphere. Data are lacking in large portions of the coastal ocean such as the Russian Arctic coast, the Eastern South America coast, the Eastern Africa coast, large sections of the Western Africa coast and large sections of the Antarctic coast.

Further, due to the high dynamic range of seasonal and spatial variations of the partial pressure of CO_2 (pCO_2) in coastal environments (Fig. 3.1), reported air–sea CO_2 fluxes can be biased by inadequate spatial or temporal coverage. For instance, in the Southern Bight of the North Sea where Thomas et al. (2004) reported a

Table 3.1 Reported estimates of the sink for atmospheric CO_2 in the coastal ocean (excluding near-shore environments)

CO_2 sink ($PgC\ year^{-1}$)	Reference	Comment
–1.0	Tsunogai et al. (1999)	Based on the global extrapolation of the average air–sea CO_2 flux in the East China Sea computed from five cruises (February 1993, October 1993, August 1993, November 1995 and September 1996). The annual air–sea CO_2 flux of Tsunogai et al. (1999) (2.9 $molC\ m^{-2}\ year^{-1}$) has been revised to a lower value (1.2 $molC\ m^{-2}\ year^{-1}$, Wang et al. 2000) based on a better coverage of the seasonal cycle and use of gas transfer velocities computed from wind speed rather than a constant value.
–0.40	Thomas et al. (2004)	Based on the global extrapolation of the average air–sea CO_2 flux in the North Sea (1.4 $molC\ m^{-2}\ year^{-1}$) computed from four cruises (September 2001, November 2001, February 2002, May 2002).
–0.37	Borges (2005)	Based on the compilation of annually integrated air–sea CO_2 fluxes in 15 shelf seas as reported in literature using partial pressure of CO_2 (pCO_2) measurements, scaled by latitudinal bands of 30° based on surface areas reported by Walsh (1988). Surface areas between 30°S and 30°N are under-estimated.
–0.45	Borges et al. (2005)	Based on the compilation of annually integrated air–sea CO_2 fluxes in 17 shelf seas as reported in literature using pCO_2 measurements, scaled by latitudinal bands of 30° based on surface areas reported by Walsh (1988). Air–sea CO_2 fluxes were recomputed to an uniform gas transfer velocity parameterization. Surface areas between 30°S and 30°N are under-estimated.
–0.22	Cai et al. (2006)	Based on the compilation of air–sea CO_2 fluxes in 29 shelf seas, scaled by 7 shelf provinces using classification and surface areas reported by Walsh (1988). Not all the air–sea CO_2 fluxes have a full annual coverage, and some of the fluxes are derived from C mass balance and not pCO_2 measurements.
–0.33 to –0.35	Chen and Borges (2009)	Based on the compilation of air–sea CO_2 fluxes in 58 shelf seas, scaled using a global average or by shelf provinces using classification and surface areas reported by Jahnke (2009). Not all the air–sea CO_2 fluxes have a full annual coverage and some of the fluxes are derived from C mass balance and not pCO_2 measurements.

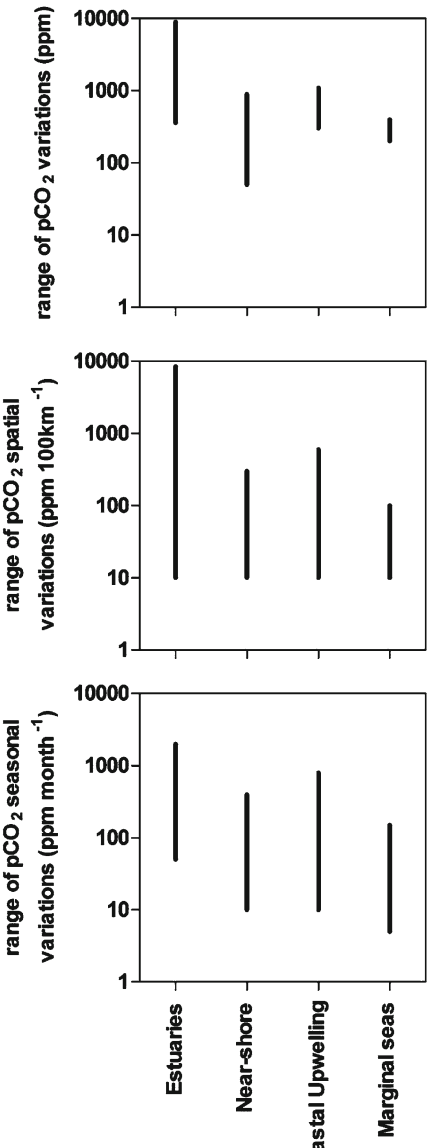

Fig. 3.1 Dynamic range of the partial pressure of CO_2 (pCO_2) variations across coastal ecosystems, of pCO_2 spatial gradients and of pCO_2 seasonal changes in estuaries (based on Frankignoulle et al. 1998; Bouillon et al. 2003), in near-shore ecosystems (based on Borges and Frankignoulle 2002a; Cai et al. 2003), and coastal upwelling systems (based on Friedrich et al. 2002, 2008; Goyet et al. 1998; Borges and Frankignoulle 2002b)

source of CO_2 based on a data-set with a lower temporal coverage than the one of Schiettecatte et al. (2007) who reported a sink of atmospheric CO_2. Another example is in the US South Atlantic Bight, where Cai et al. (2003) reported a source of CO_2 based on a data-set with a lower spatial resolution than the one of Jiang et al. (2008a) who reported a sink of atmospheric CO_2.

Inter-annual variations of air–sea CO_2 fluxes in the coastal ocean can be significant although they have been seldom investigated due to the lack of adequate data-sets. In continental shelf seas, these inter-annual variations can be due to large scale climate oscillations such as the El Niño Southern Oscillation (ENSO) (Ianson and Allen 2002; Friederich et al. 2002) or such as the Southern Annular Mode (SAM) (Borges et al. 2008a). In the case of the California current, the change of ENSO phases can lead to a reversal of the direction of annual air–sea CO_2 fluxes (Friederich et al. 2002). In near-shore ecosystems, inter-annual variations of air–sea CO_2 fluxes can be due to variable river influence (Borges and Frankignoulle 1999; Gypens et al. 2004; Borges et al. 2008b; Salisbury et al. 2009).

Contemporary air–sea CO_2 fluxes deduced from field measurements of pCO_2 are the combination of natural (pre-industrial) air–sea CO_2 flux signal and a perturbation air–sea CO_2 flux signal related to the anthropogenic increase of atmospheric CO_2. The pre-industrial air–sea CO_2 fluxes can be roughly evaluated by the mass balance of carbon inputs and outputs for the whole ocean (open and coastal) at global scale (e.g. Sarmiento and Sundquist 1992). In the open ocean, the inventory of anthropogenic dissolved inorganic carbon (DIC) can be evaluated by several back-calculation techniques (e.g. Vázquez-Rodríguez et al. 2009) that allow deriving a pre-formed DIC value that is removed from the observed DIC value, the difference corresponding to the anthropogenic DIC signal. The evaluation of a pre-formed DIC value relies on the analysis of chemical variables in water masses that are assumed to be devoid of anthropogenic DIC (deep waters). Due to the shallowness of the coastal ocean, it is impossible to evaluate pre-formed DIC values. Further, in the coastal ocean the anthropogenic air–sea CO_2 flux signal is expected to be influenced by other perturbations besides the increase of atmospheric CO_2, such as changes in nutrient inputs by atmospheric deposition or by rivers. The only attempts to evaluate the anthropogenic CO_2 sink in the coastal ocean have been made with two modelling studies. Mackenzie et al. (2004) used a single box model of the coastal ocean and evaluated the sink of anthropogenic CO_2 to 0.17 PgC $year^{-1}$. Bopp et al. (2008) used a high resolution ocean model (0.5° × 0.5°) and evaluated the sink of anthropogenic CO_2 in the coastal ocean to 0.13 PgC $year^{-1}$. Hence, the coastal ocean presently contributes between 6% and 11% of the sink of anthropogenic CO_2 in the open ocean, ranging between 1.5 and 2.2 PgC $year^{-1}$ (Sarmiento et al. 2000; Gloor et al. 2003; Quay et al. 2003; Gurney et al. 2004; Sabine et al. 2004; Patra et al. 2005; Gruber et al. 2009).

The proximal coastal ocean (estuaries, bays, salt-marshes, mangroves, and other near-shore ecosystems) is directly influenced by terrestrial inputs of DIC, nutrients and organic carbon. At ecosystem level, the aquatic compartment of these environments is net heterotrophic, consuming more organic carbon than the autochtonous gross primary production (GPP) (Odum and Hoskin 1958; Odum and Wilson 1962;

Heip et al. 1995; Kemp et al. 1997; Gattuso et al. 1998a; Gazeau et al. 2004; Hopkinson and Smith 2005). Accordingly, the aquatic compartment of these ecosystems is a source of CO_2 to the atmosphere (Frankignoulle et al. 1998, Borges et al. 2003; Abril and Borges 2004; Wang and Cai 2004). The contribution of CO_2 inputs by rivers to the overall estuarine emission is generally low (Borges et al. 2006; Jiang et al. 2008b). The overall source of CO_2 from near-shore ecosystems has been evaluated to ~0.50 PgC year^{-1}, mainly related to the emission of CO_2 to the atmosphere from estuaries (~0.36 PgC year^{-1}) (e.g. Chen and Borges 2009). These estimations also suffer from the same caveats as those for continental shelf seas. Data distribution is biased towards the temperate regions of the Northern Hemisphere, and most estuaries where CO_2 fluxes have been evaluated are macrotidal estuaries, while data in other types of estuarine environments (fjords, fjards, lagoons, micro-tidal estuaries,…) are scarce. Further, the dynamic range of pCO_2 variations in estuaries is very marked (Fig. 3.1) and issues of adequate spatial and temporal coverage are even more critical. Also, there is a large uncertainty related to value of estuarine surface area used to scale the CO_2 flux data as discussed by Abril and Borges (2004) and Borges (2005). Yet, the estimate of the emission of CO_2 from estuaries based on the scaled CO_2 flux data is in reasonable agreement with the estimate based on the input of river CO_2 and the degradation during estuarine transit of particulate (POC) and dissolved organic carbon (DOC) as discussed by Abril and Borges (2004), Borges (2005) and Chen and Borges (2009).

3.2 Possible Evolution and Feedbacks Under Global Change

Figure 3.2 depicts a conceptual diagram of the different anthropogenic forcings on the coastal ocean that can modify the sources and sinks of carbon and ultimately provide a feedback on increasing atmospheric CO_2. Hereafter, the impact of these forcings and potential associated feedbacks will be discussed in relation to air–sea CO_2 fluxes in the coastal ocean, when documented, and roughly quantified, when possible (Table 3.2).

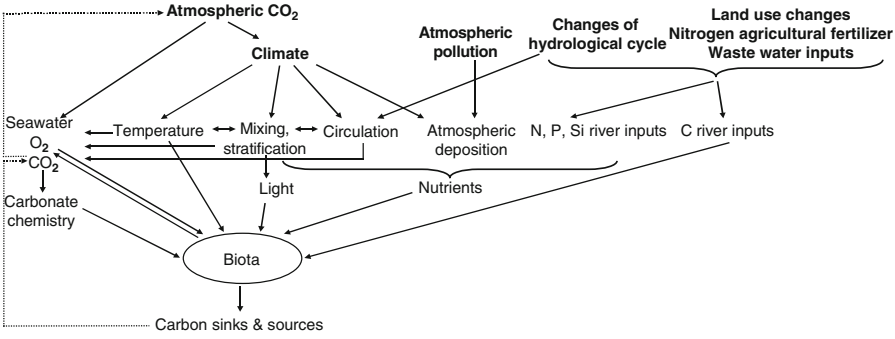

Fig. 3.2 Conceptual diagram of global change forcings on C cycling of the coastal ocean (*bold*), and feedbacks on increasing atmospheric CO_2 (Adapated from Riebesell 2007)

Table 3.2 Global change forcings on carbon cycling of the coastal ocean and associated feedback on increasing atmospheric CO_2 by year 2100. Refer to text for details on evaluation of sign and quantification of feedbacks

Global change forcings	Feedback	PgC year^{-1}	Comment
Changes in coastal physics			
Enhanced stratification	– ?	?	1
Enhanced (?) coastal upwelling	+ ?	?	2
Impact of expanding OMZ in coastal upwelling regions	+	?	3
Enhancement of air–sea CO_2 fluxes related to Arctic sea-ice retreat	–	0.002	4
Changes in land-used, waste water inputs, agricultural fertilizers and changes in hydrological cycle			
Increase of river organic carbon delivery to the Arctic Ocean	+	?	
Increase of river nutrients delivery to the Arctic Ocean	–	?	
Global increase in river nutrient and organic matter delivery	–	0.200	5
Global increase in nutrient atmospheric deposition	–	?	6
Expanding hypoxic and anoxic zones	+	?	3
Changes in seawater carbonate chemistry (ocean acidification)			
Decrease of benthic calcification			
Coral reefs	–	0.015–0.026	
Other benthic environments	–	0.025–0.046	
Decrease of pelagic calcification			
Coccolithophorids	–	0.013–0.019	
Other pelagic calcifiers	–	?	
Dissolution of metastable $CaCO_3$ in sediment porewaters	–	0.022	7
Enhancement of primary production and export production due increasing $[CO_2]$	–	0.108–0.216	8

1. Negative feedback only reported in Tasman shelf assuming pCO_2 behaviour during warm years is representative of response to global warming, if extrapolated globally would produce a negative feed-back of the order of ~0.1 PgC year^{-1}.
2. Assuming exact opposite response of model output with decreasing upwelling favourable winds.
3. Assuming enhanced denitrification leading to decreased primary production.
4. Feedback computed for the next decade and not until 2100.
5. The enhancement of primary production by nutrient inputs balances the additional CO_2 production by organic matter inputs.
6. Not taking into account enhancement of acidification of surface waters by sulphur atmospheric deposition.
7. Based on Andersson et al. (2003).
8. Based on a single mesocosm experiment with mixed diatom and coccolithophorid assemblage.

Several changes in coastal ocean physics are expected with global warming that can change C cycling and air–sea CO_2 fluxes, such as increasing stratification, enhanced coastal upwelling, expanding oxygen minimum zones, retreat of sea-ice and changes in freshwater delivery (Section 3.2.1).

Changes in land use, waste water inputs, agricultural fertilizers, hydrological cycle and atmospheric deposition increase the delivery of inorganic and organic carbon, and nutrients to the coastal ocean, and modify C flows (enhanced primary production and hypoxia/anoxia) and air–sea CO_2 fluxes in the coastal ocean with potential feedbacks on increasing atmospheric CO_2 (Section 3.2.2).

Changes in seawater carbonate chemistry in response to increasing atmospheric CO_2 content can change the rates and fates of primary production and calcification at organism and ecosystem community levels, modifying C flows and air–sea CO_2 fluxes in the coastal ocean with potential feedbacks on increasing atmospheric CO_2 (Section 3.2.3).

Finally, anthropogenic impacts on specific near-shore coastal ecosystems (coral reefs, seagrass meadows and mangroves) can alter C flows in these ecosystems (Section 3.2.4).

3.2.1 Changes in Coastal Ocean Physics

It has been hypothesized (Bakun 1990) and modelled (Snyder et al. 2003; Diffenbaugh et al. 2004) that the intensity and duration of coastal upwelling will increase in future due to climate change. Increasing land–sea thermal contrasts will increase alongshore winds driving Ekman upwelling. Locally, other factors such as decadal fluctuations in surface heat fluxes can modulate the response to increasing upwelling favorable winds and lead to increased stratification and surface ocean warming, as evidenced in the California Current in relation to the Pacific Decadal Oscillation (Di Lorenzo et al. 2005; Field et al. 2006). Yet, there is observational evidence in several coastal upwelling systems that suggest a general increasing trend in upwelling with global warming (Anderson et al. 2002; Mendelssohn and Schwing 2002; Goes et al. 2005; Santos et al. 2005; McGregor et al. 2007).

The response of air–sea CO_2 fluxes to increased upwelling is difficult to predict and can go both ways. Stronger vertical inputs of DIC would drive the system to emit more CO_2 to the atmosphere, while enhanced nutrient inputs would drive higher primary production, export production and a sink for atmospheric CO_2. Plattner et al. (2004) modelled the impact of decreasing upwelling favorable winds on C flows in the California Current system. Model results show that a 50% reduction of wind stress induces a ~50% decrease in net primary production and in export production; yet, the source of CO_2 to the atmosphere also decreases by about ~50% due to the decrease of vertical inputs of DIC and the decrease of the gas transfer velocity, providing a negative feedback on increasing atmospheric CO_2. However, the increase of upwelling favorable winds does not necessarily imply that the

ecosystem will respond by an increase of primary production. Increased upwelling winds can also lead to a reduction of light exposure due to deeper mixed layers and to an increase offshore advection of phytoplankton (Largier et al. 2006). Nevertheless, a time series in Monterey Bay (California) shows since 1993 an increasing trend in pCO_2 that is faster than the one expected from the equilibration with increasing atmospheric CO_2, in parallel with a decreasing trend in sea surface temperature (SST) and an increasing trend in chlorophyll-a (Francisco Chavez and Gernot Friederich, 2009, personal communication). This would suggest an increasing trend in upwelling and primary production with an increase in pCO_2 values, leading to an overall positive feedback on increasing atmospheric CO_2.

Climate change is expected to lead to a decrease of oxygen (O_2) content in the oceans due to the slowing down of the thermohaline circulation and decreasing solubility of O_2 (due to surface warming) of the source waters of intermediate and deep layers (Bopp et al. 2002; Matear and Hirst 2003). This will lead to the expansion of oxygen minimum zones (OMZ) as confirmed by historical observations (Bograd et al. 2008; Stramma et al. 2008). OMZ are associated to major coastal upwelling regions such as the Humbolt current, the Benguela current, the Canary current and the Arabian Sea. The upwelling source waters in coastal upwelling areas associated to OMZ are sources of CO_2 to the atmosphere because denitrification leads to lower concentrations of nitrate and excess of DIC relative to nitrogen (Fig. 3.3). Hence, coastal upwelling areas associated to OMZ are sources of atmospheric CO_2 such as the Arabian Sea (Goyet et al. 1998) and the Peruvian and Chilean coasts (Friederich et al. 2008; Paulmier et al. 2008). Coastal upwelling areas devoid of OMZ such as the Iberian coastal upwelling system (Borges and Frankignoulle 2002a) or with deep OMZ such as the Oregon coast (Hales et al. 2005) are sinks for atmospheric CO_2. The future horizontal and vertical expansion of OMZ is then expected to provide a positive feedback on increasing atmospheric CO_2 due to enhanced CO_2 emissions from coastal upwelling systems.

Sarmiento et al. (1998) showed that future increase in stratification reduces the thermohaline circulation and open oceanic uptake of anthropogenic CO_2. Yet, the ocean will also respond to increased stratification by changes in export production (Sarmiento et al. 1998; Bopp et al. 2001; Le Quéré et al. 2002, 2003) and in the vertical input of DIC, which potentially can provide feedbacks on increasing atmospheric CO_2. The comparison of negative and positive SST anomaly phases of the large scale climatic oscillations (ENSO, SAM,…) can be used as a natural laboratory to determine how marine biogeochemistry could respond to future increase in SST and stratification in the oceans (Le Quéré et al. 2002, 2003). However, time-series of pCO_2 with the adequate temporal resolution and duration to work out seasonal and inter-annual variations are extremely scarce in continental shelf seas. Borges et al. (2008a) constructed a time-series of pCO_2 and air–sea CO_2 fluxes in the Tasman continental shelf based on the analysis of anomalies of pCO_2 and SST from a data-set of 22 cruises spanning from 1991 to 2003. Over the Tasman continental shelf, during positive phases of SAM, there is a decrease of wind speed that leads to increasing SST and stratification (Fig. 3.4). The increase of stratification leads to a decrease of vertical inputs of DIC and overall decrease in pCO_2 and

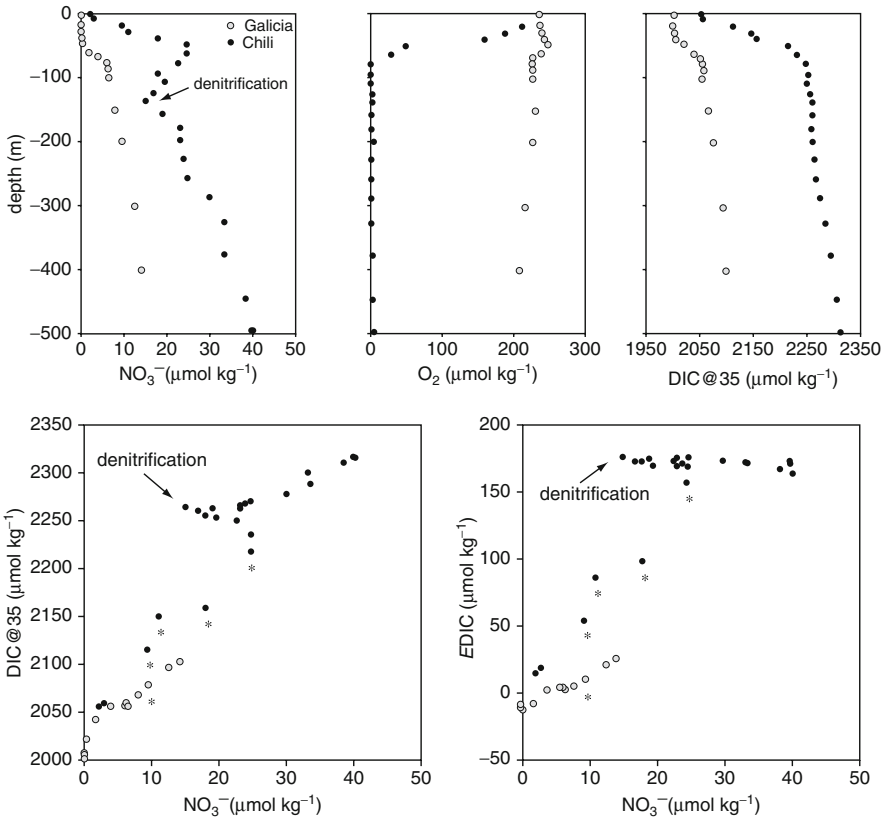

Fig. 3.3 Vertical profiles in the top 500 m of nitrate (NO_3^-), dissolved oxygen (O_2), dissolved inorganic carbon normalized to a salinity of 35 (DIC@35), DIC@35 vs NO_3^-, excess DIC (*E*DIC) vs NO_3^- at the continental shelf break of the Galician (–9.54°E 42.15°N) and Chilean (–77.59°E –12.45°N) upwelling systems. Chilean data were extracted from the Global Ocean Data Analysis Project (Key et al. 2004), Galician data are from the OMEX-II project (Borges and Frankignoulle 2002a). EDIC was computed as the difference between observed DIC and DIC computed from total alkalinity and atmospheric CO_2, and provides an estimate of CO_2 outgassing if the water mass is upwelled. Asterisks indicate the depths from which water can be upwelled (10–50 m in the Chilean upwelling system based on Paulmier et al. (2008) and 200 m in the Galician upwelling system based on Borges and Frankignoulle (2002a)). For a given NO_3^- value (indicative of potential primary production), DIC@35 and *E*DIC (indicative of potential CO_2 outgassing) are higher in the Chilean upwelling system than in the Galician upwelling, probably in relation to denitrification associated to the marked oxygen minimum zone in the Chilean upwelling system. This could explain that the Chilean upwelling system behaves as a source of CO_2 (Friederich et al. 2008) and the Galician upwelling system as a sink of CO_2 (Borges and Frankignoulle 2002a)

increase in the sink for atmospheric CO_2 (Fig. 3.4). Hirst (1999) modelled an increase of SST at the latitude of the Tasman continental shelf of about 2°C by 2100. If we assume that the response of air–sea CO_2 fluxes to inter-annual positive anomalies of SST are representative of the response of air–sea CO_2 fluxes under global warming, this would lead to an enhancement of the sink of atmospheric CO_2

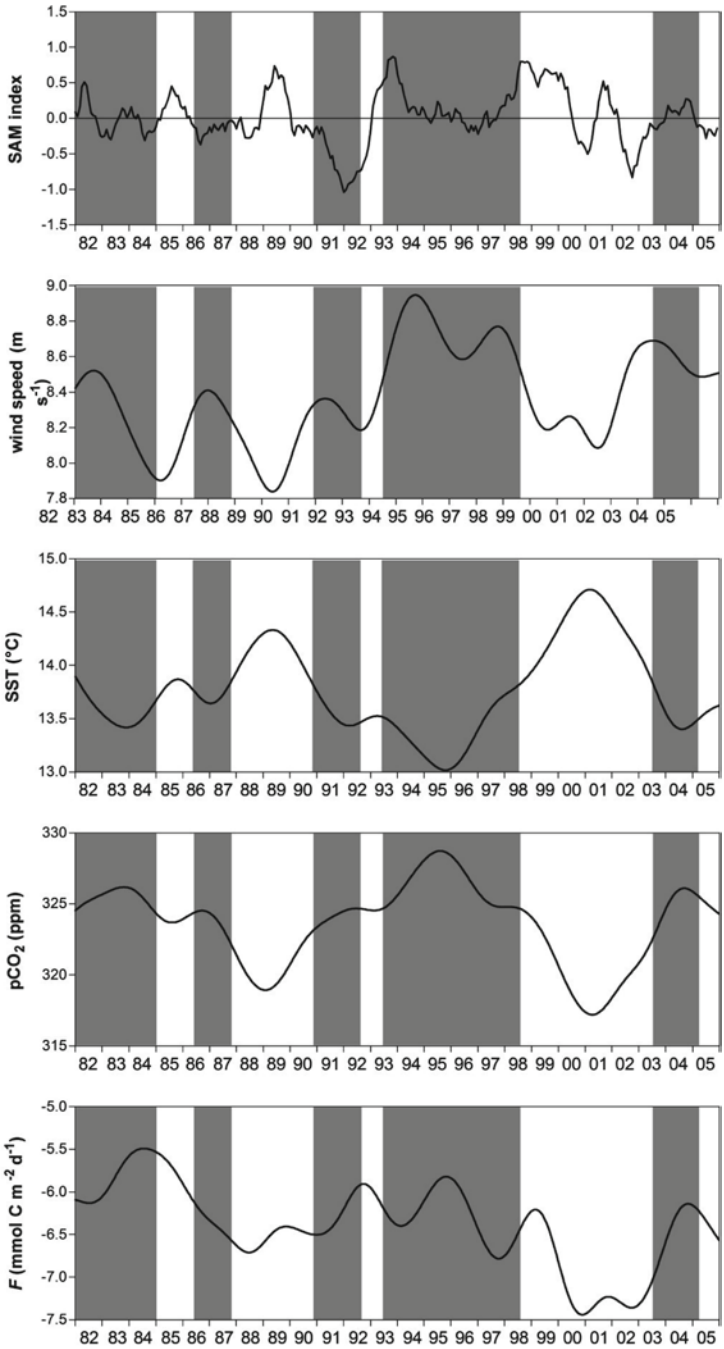

Fig. 3.4 Time-series from 1982 to 2005 of Southern Annular Mode (SAM) index and of deseasonalized sea surface temperature (SST), partial pressure of CO_2 (pCO_2) and air–sea CO_2 fluxes (F) in the Tasman continental shelf (adapted from Borges et al. 2008a). Grey areas correspond to periods of sustained negative SST anomalies

in the Tasman continental shelf of about 36%. Assuming all continental shelves respond similarly this would lead to a major feedback on increasing atmospheric CO_2 from a present day sink of 0.3–0.4 PgC year^{-1} by 2100. However, it is extremely unlikely that all continental shelves will respond by an increase in the sink of atmospheric CO_2 with increasing stratification. More data acquisition and analysis are required to characterize the possible responses of air–sea CO_2 fluxes to changes in stratification in continental shelf seas.

Climate changes will probably strongly affect C cycling and air–sea CO_2 fluxes in the Arctic Ocean that at present time has been evaluated as a sink for atmospheric CO_2 (Pipko et al. 2002; Murata and Takizawa 2003; Bates 2006; Bates et al. 2005; 2006; Else et al. 2008; Murata et al. 2008). Bates et al. (2006) found a positive relationship between air–sea CO_2 fluxes and the ice–sea cover in the Chukchi Sea. Assuming that this relationship could be used to predict the evolution of air–sea CO_2 fluxes with the future predicted sea-ice retreat, these authors estimated that the sink of atmospheric CO_2 in the Arctic Ocean would increase in the coming decade by 0.002 PgC year^{-1} compounded each year. However, it is also expected that future changes in temperature will modulate air–sea CO_2 fluxes directly through the thermodynamic change of pCO_2. Future changes in temperature will indirectly modulate air–sea CO_2 fluxes through changes in circulation (combined with salinity changes due to sea-ice retreat and changes in fresh-water delivery) that will affect DIC transport (horizontally and vertically) and will also affect biological activity and C flows.

3.2.2 Changes in Land Use, Waste Water Inputs, Agricultural Fertilizers, Hydrological Cycle and Atmospheric Deposition

A major change in C flows and air–sea CO_2 fluxes can be expected from the mobilization of terrestrial matter and transport by rivers to the Arctic Ocean. The Arctic Ocean receives almost 10% of global river discharge and about 0.025 PgC year^{-1} of terrestrial DOC (Opshal et al. 1999). Arctic river basins may store up to ~50% of the global soil organic carbon (Macdonald et al. 2006), with permafrost soils storing about 400 PgC (Davidson and Janssens 2006). An increase of fresh water discharge to the Arctic during the last 60 years has been reported (Peterson et al. 2002) and could continue to increase in future (McClelland et al. 2004). This could enhance organic carbon delivery by rivers to the Arctic Ocean that could be further increased by mobilization of soil organic carbon with permafrost thawing (Frey and Smith 2005). The DOC delivered during ice-out is mostly young (Benner et al. 2004; Raymond et al. 2007) and labile (Holmes et al. 2008). Hence, the degradation of the additional organic carbon delivered by rivers to the Arctic Ocean with climate changes would provide a positive feedback on increasing atmospheric CO_2 that could be significant but yet unquantified (Frey and McClelland 2009). On the other hand, the river delivery of dissolved inorganic nutrients (McClelland et al. 2007) and possibly dissolved organic nutrients (Frey and McClelland 2009) to the Arctic

Ocean could also increase with climate change. This could stimulate primary production and provide a negative feedback on increasing atmospheric CO_2 that could also be significant and is yet unquantified.

Changes in land use and waste water inputs have increased river nutrient contents (Green et al. 2004; Seitzinger et al. 2005) and are expected to continue to increase in future (Seitzinger et al. 2002; Galloway et al. 2004). The delivery of nutrients to the coastal ocean will also be modified by predicted future increasing global freshwater flow due to changes in the hydrological cycle (Douville et al. 2002; Labat et al. 2004; Milly et al. 2005; Aerts et al. 2006; Huntington 2006). However, future changes in freshwater flow will show regional differences, in general with an increase at high-latitudes and tropical latitudes and a decrease at mid-latitudes (Milly et al. 2005). The freshwater delivery to the coastal ocean will be further modulated by damming and other water diversion activities (Vörösmarty and Sahagian 2000; Vörösmarty et al. 2003).

It is established that nutrient delivery by rivers to the coastal ocean has increased during the past century and is expected to continue to increase in the future. This could lead to an enhancement of primary production and a negative feedback on increasing atmospheric CO_2. On the other hand, increased organic matter river loadings are expected to fuel heterotrophic activity in the coastal ocean and provide a positive feedback on increasing atmospheric CO_2. Yet, the balance between these two processes seems to be a negative feedback on increasing atmospheric CO_2 due to the enhancement of net ecosystem production (NEP). Based on a simple one-box model of the coastal ocean, Mackenzie et al. (2004) have evaluated the negative feedback on increasing atmospheric CO_2 by 2100 at ~0.20 PgC $year^{-1}$. Moreover, it has been recently reported that the impact of anthropogenic nitrogen atmospheric deposition on primary production has been under-estimated (Duce et al. 2008), hence the future increase in NEP and related negative feedback on increasing atmospheric CO_2 could be stronger. Based on a coupled general circulation model, da Cunha et al. (2007) have shown that variable river inputs of nutrients have little impact on C cycling in the open ocean, hence, this impact seems to be confined to the coastal ocean. Gypens et al. (2009) have shown, based on a regional model, that nutrient reduction policies can lead to a strong decrease of primary production and NEP and a positive feedback increasing atmospheric CO_2. However, at a global scale, the anthropogenic delivery of nutrients to the coastal zone and concomitant enhancement of NEP and sink of atmospheric CO_2 is expected to continue to increase. The environmental policies actually implemented in watersheds of developed countries are not expected to be implemented for decades in emergent countries.

Changes in land use on watersheds and in freshwater flow can also alter the delivery of bicarbonate (and total alkalinity (TA)) from rivers to the coastal ocean (Cai 2003; Raymond and Cole 2003; Raymond et al. 2008; Cai et al. 2008; Gislason et al. 2009). This in itself constitutes a sink for atmospheric CO_2 on the watershed if related to enhanced $CaCO_3$ weathering. However, it is unclear how this could affect the coastal ocean CO_2 sink, although an increase of the seawater buffering capacity can be expected. This will also be probably modulated by the changes in

DIC:TA ratio in river water (Cai et al. 2008). Also, it has been suggested that TA generation in near-shore environments (Cai and Wang 1998) could contribute to enhance the seawater buffering capacity and enhance the sink for atmospheric CO_2 in the coastal ocean (Fennel et al. 2008; Thomas et al. 2009).

An important consequence of eutrophication is the development of hypoxic or anoxic regions in coastal ecosystems (Diaz and Rosenberg 2008). In semi-enclosed seas permanently stratified, hypoxia is a perennial feature (Baltic Sea and Black Sea), while in seasonally stratified systems hypoxia is a seasonal feature, occurring usually in summer when temperature (and stratification) and organic matter availability are highest (Gulf of Mexico and East China Sea). In permanently well-mixed continental shelf seas, even highly eutrophicated such as the Southern Bight of the North Sea, hypoxia does not occur. However, in well-mixed (macro-tidal) estuaries, low oxygen levels and even hypoxia can occur mainly in maximum turbidity zones (e.g. Herman and Heip 1999), such as in the Scheldt estuary in the 1970s when eutrophication was highest (e.g. Soetaert et al. 2006). In estuaries, hypoxia can occur seasonally but also at daily time-scales (during the night) (Tyler et al. 2009). Hypoxia and anoxia have important consequences on benthic biomass and biodiversity with potential impacts on fisheries (Diaz and Rosenberg 2008). The impact on air–sea CO_2 fluxes is difficult to evaluate, yet, by analogy with OMZ (Section 3.2.2) it is expected that the enhancement of denitrification at low oxygen levels will lead to a net CO_2 production due to removal of nitrate and production of CO_2. Denitrification will also increase TA and increase the buffering capacity of seawater and decrease the seawater pCO_2 (Fennel et al. 2008; Thomas et al. 2009). This can lead to a negative feedback on increasing atmospheric CO_2. Yet, the model of Fennel et al. (2008) in the northwest North Atlantic continental shelf shows that the contribution of TA generation by benthic denitrification to the enhancement of the CO_2 sink (0.07 mmolC m^{-2} $year^{-1}$) is one order of magnitude lower than the decrease of the CO_2 sink due to lower primary production related to the removal of nitrate (0.17 mmolC m^{-2} $year^{-1}$). Hence, the expansion of hypoxic or anoxic zones in coastal environments that has been observed since the 1960s (Diaz and Rosenberg 2008) and could increase in future with sustained eutrophication, can be expected to lead to a positive feedback on increasing atmospheric CO_2 due to denitrification.

3.2.3 Changes in Seawater Carbonate Chemistry

Ocean acidification of surface waters corresponds to the increase of $[CO_2]$ and of $[H^+]$, the decrease of pH, of $[CO_3^{2-}]$, and of the saturation state (Ω) of calcite (Ω_{ca}) and aragonite (Ω_{ar}), all related to shifts in thermodynamic equilibria in response to the input of anthropogenic CO_2 from the atmosphere. The $CaCO_3$ production of benthic and planktonic calcifiers is expected to decrease with decreasing Ω due to ocean acidification (refer to reviews by Raven et al. (2005), Kleypas et al. (2006),

Fabry et al. (2008), Doney et al. (2009)). This is expected to provide a negative feedback on increasing atmospheric CO_2 since calcification leads to a shift from the bicarbonate to the CO_2 pool according to

$$Ca^{2+}+2\ HCO_3^- \rightarrow CaCO_3+CO_2+H_2O$$

Furthermore, ocean acidification is expected to lead to an enhancement of shallow-water $CaCO_3$ dissolution in the porewaters within sediments (Andersson et al. 2003), also providing a negative feedback on increasing atmospheric CO_2.

On the other hand, primary production of some pelagic (e.g. Riebesell et al. 1993; Qiu and Gao 2002) and benthic (e.g. Gao et al. 1993; Zimmerman et al. 1997) non-calcifying autotrophs could increase with $[CO_2]$. An increase in primary production associated to efficient organic carbon export would induce a negative feedback on increasing atmospheric CO_2, according to

$$CO_2+H_2O \rightarrow CH_2O+O_2$$

Besides changes in primary production and calcification, marine organisms and communities can also respond to ocean acidification through changes in N_2 fixation (e.g. Hutchins et al. 2007), shift in natural assemblages (e.g. Boyd and Doney 2002; Tortell et al. 2002; Engel et al. 2008) and an increase of export of organic matter to depth due to enhanced aggregation (e.g. Engel et al. 2004; Delille et al. 2005; Riebesell et al. 2007). All these processes could also provide a negative feedback on increasing atmospheric CO_2.

Since the coastal ocean hosts a disproportionately more important biological activity than the open ocean, the potential feedbacks on increasing atmospheric CO_2 related to the response of marine organisms and communities to the acidification of surface waters are expected to be disproportionately much more important in the coastal ocean than in the open ocean. Further, in coastal environments the acidification of surface waters could be enhanced compared to the open ocean due to anthropogenic atmospheric nitrogen and sulfur deposition (Doney et al. 2007), influence of river discharge (Gledhill et al. 2008; Salisbury et al. 2008) or related to upwelling of DIC rich waters (Feely et al. 2008).

During high-runoff, near-shore coastal environments influenced by estuaries can be exposed seasonally to low Ω values. Salisbury et al. (2008) showed that during high-runoff the plume of Kennebec river (Gulf of Maine) shows very low Ω values down to 0.4 associated to salinities down to 8. However, most rivers show Ω values above 1 for salinities above 10 (Salisbury et al. 2008), hence, river plumes under-saturated in $CaCO_3$ are not the common feature. Yet, in Arctic rivers Ω values are lower ($\Omega > 1$ for salinities > 25). Hence, the increase of Arctic river runoff under global warming (Section 3.2.2) could lead to an extension of river plumes with low Ω values in the Arctic Ocean. However, river plumes are also typically eutrophicated, leading to an increase in primary production with an effect on carbonate chemistry (Gypens et al. 2009; Borges and Gypens 2010). Figure 3.5 shows the decadal changes of carbonate chemistry in the Southern North Sea. From the 1950s to the mid 1980s when GPP

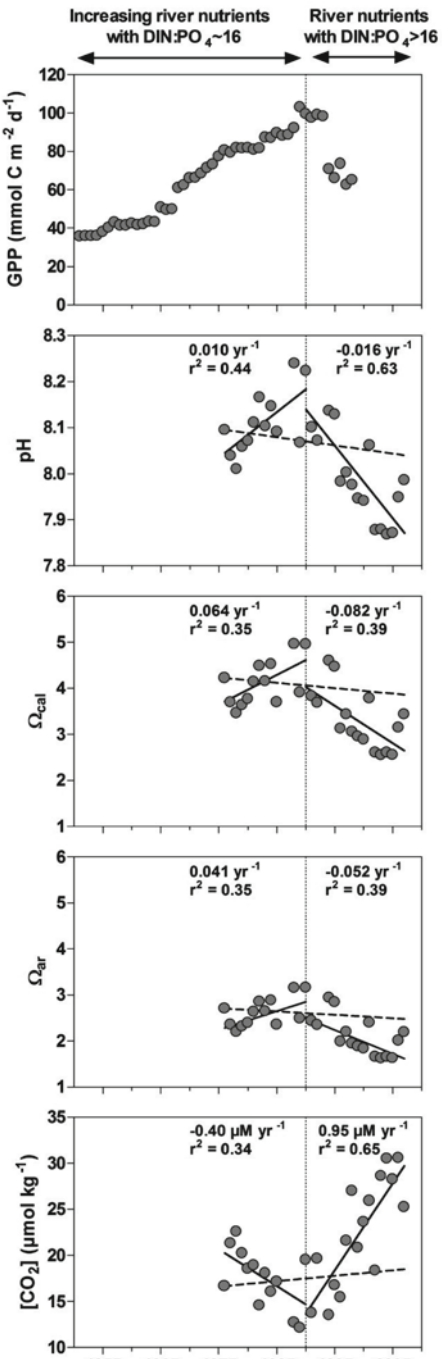

Fig. 3.5 Time series in the Southern North Sea of annual means of modelled gross primary production (GPP) by Gypens et al. (2009) and measured pH at a fixed station (3.2206°E 51.6586°N) from the Rijkswaterstaat database (measurements every 15 days from 1976 to 1987, and every month from 1988 to 2007; due to low seasonal coverage, years 1986, 1987 and 1993 were excluded from analysis). pH was converted from the National Bureau of Standards Scale to the Total Hydrogen Ion Scale. [CO_2], saturation state of calcite (Ω_{cal}) and of aragonite (Ω_{ar}) were computed from measured pH, salinity and temperature, calculated total alkalinity (from salinity based on the climatological relationship given by Borges et al. (2008b)), the carbonic acid dissociation constants of Mehrbach et al. (1973) refitted by Dickson and Millero (1987), the calcite and aragonite solubility of Mucci (1983). Solid lines correspond to linear regressions prior and after 1990, dotted line corresponds to the theoretical evolution of variables in surface waters had followed the increase of atmospheric CO_2 from the conditions of 1976. Periods prior and after 1990 can be distinguished based on the ratio of dissolved inorganic nitrogen (DIN) to phosphate (PO_4) of nutrient river delivery

increased due to eutrophication, there is an increasing trend in pH, in Ω_{ca} and in Ω_{ar} and a decreasing trend in [CO_2], while the equilibration of surface waters with increasing atmospheric CO_2 would have lead to the opposite trends. After the mid 1980s when phosphorus removal policies were implemented, primary production in the Southern Bight of the North Sea became increasingly limited by phosphorus availability, GPP decreased and the ecosystem shifted from net autotrophy to net heterotrophy (Gypens et al. 2009). The decrease of pH, Ω_{ca} and Ω_{ar} and the increase of [CO_2] were actually faster then those expected from the equilibration of surface waters with increasing atmospheric CO_2 (Fig. 3.5). Hence, the effect of eutrophication on carbon cycling that counter-acts the effect of ocean acidification could maintain carbonate chemistry conditions that remain favorable for benthic and pelagic calcification in near-shore coastal environments. Also, the application of nutrient delivery regulation policies can lead to transient changes of carbonate chemistry that are faster than those related solely to ocean acidification. Such regulation policies have been mainly implemented in industrialized countries, while in emerging economy countries, eutrophication can be supposed to continue to increase unregulated in coming decades.

The response of calcifiers to ocean acidification has been to some extent relatively well documented. Based on the upper bound value global calcification rate from coral reefs of 0.11 PgC $year^{-1}$ (Milliman and Droxler 1996) and assuming a decrease by 2100 of calcification ranging from 22% (Gattuso et al. 1998b) to 40% (Andersson et al. 2005), and using a molar ratio of CO_2 production to calcification (Ψ) of 0.6 (Frankigoulle et al. 1994), the negative feedback on increasing atmospheric can be roughly evaluated to range between 0.015 and 0.026 PgC $year^{-1}$. Benthic calcification in other coastal environments than coral reefs has been evaluated to 0.19 PgC $year^{-1}$ (Milliman and Droxler 1996), and assuming a similar range of decrease of calcification (22–40%) by 2100, the negative feedback on increasing atmospheric can be roughly evaluated to range between 0.025 and 0.046 PgC $year^{-1}$ (using a Ψ of 0.6).

Balch et al. (2007) recently estimated global pelagic calcification to 1.6 ± 0.3 Pg C $year^{-1}$, based on remote sensing data. This implies that coccolithophorids would be the single most important pelagic calcifier in the oceans, as other estimates of global pelagic calcification range between 0.7 PgC $year^{-1}$ based on historical accumulation rates and sediment trap data (Milliman et al. 1999) and 1.4 PgC $year^{-1}$, based on seasonal cycle of TA in the euphotic zone (Lee 2001). A global estimate of pelagic calcification is unavailable for the coastal ocean, but on first approximation, it can be evaluated to 0.38 ± 0.1 Pg C $year^{-1}$ scaled based on a fraction of the total $CaCO_3$ standing stock in the coastal ocean of 23% compared to the open ocean, based on remote sensing data (Balch et al. 2005). The decrease of global pelagic calcification for a doubling of atmospheric CO_2 has been evaluated to 7% using a general circulation ocean model (Gehlen et al. 2007). If we assume that this decrease also occurs in the coastal ocean, the negative feedback on increasing atmospheric CO_2 can be roughly evaluated to range between 0.013 and 0.019 PgC $year^{-1}$ (using a Ψ of 0.6).

The carboxylating enzyme Ribulose-1,5 bisphosphate-carboxylase/oxygenase (RUBISCO) relies exclusively on CO_2 as substrate and has a half saturation constant ranging between 20 and 70 μmol kg^{-1} (Badger et al. 1998). This can cause a rate limitation of phytoplankton photosynthesis, since [CO_2] in seawater at

Table 3.3 Minimum values of the partial pressure of CO_2 (pCO_2), pH, [CO_2] reported in various continental shelf seas

	pCO_2 (ppm)	pH(THIS)	[CO_2] (μmol kg^{-1})	Comment
Gotland Sea (Baltic)	160	8.413	6.2	1
Northern North Sea	225	8.261	10.9	2
Southern North Sea	125	8.459	5.7	2
English Channel	320	8.127	13.5	3
Celtic Sea	295	8.160	11.6	4
Bay of Angels (Mediterranean)	330	8.144	12.5	5
East China Sea	280	8.173	12.3	6
Chukchi Sea	70	8.647	4.7	7
US Middle Atlantic Bight	200	8.285	6.1	8

1. Based on Schneider et al. (2003) and Kuss et al. (2004)
2. Based on Omar et al. (2010)
3. Based on Borges and Frankignoulle (2003)
4. Based on Borges et al. (2006)
5. Based on Copin-Montégut et al. (2004)
6. Based on Wang et al. (2000)
7. Based on Bates (2006)
8. Based on DeGrandpre et al. (2002)

atmospheric equilibrium is typically ~10 μmol kg^{-1}. This can be a significant issue in near-shore environments where very low [CO_2] values can occur during the peak of the phytoplankton bloom. For instance, in Belgian coastal waters, at the peak of the *Phaeocystis* bloom extreme values of pCO_2 (72 ppm), pH (8.673 in the total hydrogen ion scale (THIS)) and [CO_2] (3 μmol kg^{-1}) were reported in May 1999 (Borges and Frankignoulle 2002b). However, in continental shelf seas with lesser influence from nutrient rich estuarine waters, values of the variables of carbonate system during phytoplankton blooms are not as extreme (Table 3.3).

Phytoplankton species have developed several carbon concentration mechanisms (CCMs) to overcome the potential CO_2 limitation of primary production (Raven 1991), leading to a specific sensitivity to CO_2 availability. Hence, photosynthesis by diatoms and the prymnesiophyte *Phaeocystis* (Burkhardt et al. 1999, 2001; Rost et al. 2003) is at or close to CO_2 saturation at typical actual marine CO_2 levels. On the other hand, photosynthesis of coccolithophorids is well below CO_2 saturation at typical actual marine CO_2 levels (Rost et al. 2003). However, these findings are mainly based on laboratory cultures with optimal light and nutrient conditions. In the real ocean, at the peak of phytoplankton bloom, nutrients are exhausted, and since CCMs rely in one way or another on enzymes, low nitrogen availability can lead to a down-regulation of CCMs. Since CO_2 levels are also low at the peak of the phytoplankton bloom, increasing levels of seawater CO_2 with global change could reduce the limitation of photosynthesis by CO_2 availability. In nutrient exhausted conditions, if light conditions remain favorable, phytoplankton continues to photosynthesize, and extracellular release of organic carbon allows regulation of the internal C:N:P ratios. This can lead to the formation of transparent

exopolymer particles that have strong aggregative properties and can enhance organic carbon export from surface to depth (Engel et al. 2004). Hence, increasing CO_2 levels with global change could lead to enhanced carbon export related to extracellular release of organic carbon in peak phytoplankton bloom conditions. Riebesell et al. (2007) have estimated that an increase of 27% of C export from mixed diatom and coccolithophorid assemblages would occur at an atmospheric pCO_2 of 750 ppm. Based on the present day estimates of export production from the coastal ocean ranging from 0.4 (Wollast 1998) to 0.8 PgC year^{-1} (Chen 2004), the potential negative feedback on increasing atmospheric CO_2 would range from 0.108 to 0.216 PgC year^{-1}.

Ocean acidification can also lead to changes in phytoplankton composition (Boyd and Doney 2002; Tortell et al. 2002), with potential impacts on C cycling and export, and ultimately on air–sea CO_2 fluxes. Further, the impact of ocean acidification will be modulated by the combined effect of other climate change impacts such as temperature increase and increased stratification. Temperature increase will directly impact metabolic rates of biota, while increased stratification will modulate vertical inputs of DIC and nutrients, and light conditions. The combined impact of temperature increase and acidification seems to lead to non-linear responses from phytoplankton (Feng et al. 2008). Temperature increase could also potentially modulate the response of coral reefs to ocean acidification (McNeil et al. 2004), although this has been strongly debated (Kleypas et al. 2005). Finally, increased stratification will favour phytoplankton communities that have a strong requirement for light availability and low inorganic nutrient requirements. Tyrrell and Merico (2004) reviewed the factors that favor the blooming of coccolithophorids and concluded that stratified and shallow mixed layers (inducing high light availability conditions) were one of the requisites for coccolithophorid blooming. Temperature increase and stratification could explain the appearance of not previously documented coccolithophorid blooms in some high latitude areas such as the Bering Sea (Merico et al. 2003) and the Barrents Sea (Smyth et al. 2004), the possible shift in the North Atlantic of phytoplankton communities towards coccolithophorids at the expense of diatoms based on the opal:$CaCO_3$ ratio of sedimenting particles (Antia et al. 2001), and the trend since the 1950s towards increasing pelagic calcification based on mass of $CaCO_3$ per coccolith from sediment cores (Iglesias-Rodriguez et al. 2008), in agreement with a global increase in stratification with strong impacts on marine productivity (Behrenfeld et al. 2006).

3.2.4 Anthropogenic Impacts on Specific Near-Shore Coastal Ecosystems

Specific near-shore coastal ecosystems are in most cases threatened by direct and indirect human impacts. For instance, losses in seagrass (Short and Neckles 1999;

Duarte 2002) and coral reef ecosystems (Hughes et al. 2003) are observed and predicted to continue due to mechanical damage (dredging and anchoring), eutrophication and siltation, the latter two leading in particular to light limitation. Negative indirect human impacts on seagrass and coral ecosystems include increases of erosion by the rise of sea level, frequency and intensity of extreme weather events, ultraviolet irradiance and water temperature. Other coastal ecosystems such as mangrove forests or salt-marshes are relatively resilient to the present and future alteration of hydrology, pollution or global warming, but in some parts of the world they are being cleared for urban development and aquaculture (Alongi 2002). Furthermore, some coastal habitats are predicted to adapt and survive with shifts in species composition, as coral reef ecosystems (Hughes et al. 2003; Baker et al. 2004) but with probable loss of biodiversity and modifications of carbon flows. It is unclear how these changes will affect carbon flows and ultimately air-sea CO_2 fluxes.

3.3 Conclusions

The present day contemporary CO_2 fluxes in shelf seas could be significant for the global carbon cycle, since available estimates converge to a value of 0.3 PgC $year^{-1}$ (Table 3.1) corresponding to 21% of the most recent estimate of contemporary sink of atmospheric CO_2 in open oceans of 1.4 PgC $year^{-1}$. However, these estimates are prone to large uncertainty, mainly due to inadequate representation of the spatial variability, and need to be improved based on more data, requiring a concerted global observational effort (Borges et al. 2009).

The potential feedbacks on increasing atmospheric CO_2 from changes in carbon flows in the coastal ocean could be disproportionately higher than in the open ocean. Yet, these potential feedbacks remain largely unquantified (Table 3.2) due to a poor understanding of the mechanisms, or lack of modelling to quantify them. Based on reported evaluations and back of the envelope calculations, it is suggested that changes of biological activity due to the increased nutrient delivery by rivers would provide by 2100 a negative feedback on increasing atmospheric CO_2 of the order of magnitude of the present day sink for atmospheric CO_2. This negative feedback on increasing atmospheric CO_2 would be one order of magnitude higher than negative feedback due to the decrease of either pelagic or benthic calcification related to ocean acidification, and than the negative feedback related to dissolution of $CaCO_3$ in sediments (Table 3.2). The increase of export production could also provide a significant feedback to increasing atmospheric CO_2, although based on the conclusions from a single perturbation experiment. Feedbacks on increasing atmospheric CO_2 due to effects of C cycling in continental shelf seas related to changes in circulation or stratification could be important but remain to be quantified.

Acknowledgments I'm grateful to Frédéric Gazeau for pointing out the availability of long pH time series in the Southern North Sea, to Nathalie Gypens for providing the GPP model outputs, and to Pedro Duarte for comments during manuscript elaboration. This is a contribution to Belgian Federal Science Policy Office PEACE project (SD/CS/03), EU IP CARBOOCEAN (511176), EU CSA COCOS (212196). The author is a research associate at the F.R.S.-F.N.R.S.

References

Abril G, Borges AV (2004) Carbon dioxide and methane emissions from estuaries. In: Tremblay A, Varfalvy L, Roehm C, Garneau M (eds) Greenhouse gases emissions from natural environments and hydroelectric reservoirs: Fluxes and processes. Springer, Berlin/Heidelberg, Germany/New York, pp 187–207

Aerts JCJH, Renssen H, Ward PJ, de Moel H, Odada E, Bouwer LM, Goosse H (2006) Sensitivity of global river discharges under Holocene and future climate conditions. Geophys Res Lett 33:LI9401. doi:10.1029/2006GL027493

Alongi DM (2002) Present state and future of the world's mangrove forests. Environ Conserv 29(3):331–349

Anderson DM, Overpeck JT, Gupta AK (2002) Increase in the Asian southwest monsoon during the past four centuries. Science 297:596–599

Andersson AJ, Mackenzie FT, Ver LM (2003) Solution of shallow-water carbonates: An insignificant buffer against rising atmospheric CO_2. Geology 31:513–516

Andersson AJ, Mackenzie FT, Lerman A (2005) Coastal ocean and carbonate systems in the high CO2 world of the Anthropocene. Am J Sc 305:875–918

Antia AN, Koeve W, Fischer G, Blanz T, Schulz-Bull D, Scholten J, Neuer S, Kremling K, Kuss J, Peinert R, Hebbeln D, Bathmann U, Conte M, Fehner U, ZeitzschelB (2001) Basin-wide particulate carbon flux in the Atlantic Ocean: Regional export patterns and potential for atmospheric CO2 sequestration. Global Biogeochem Cycles 15:845–862

Badger MR, Andrews TJ, Whitney SM, Ludwig M, Yellowlees CD, Leggat W, Price GD (1998) The diversity and coevolution of RUBISCO, plastids, pyrenoids, and chloroplastbased CO2-concentrating mechanisms in algae. Can J Bot 76:1052–1071

Baker AC, Starger CJ, McClanahan TR, Glynn PW (2004) Coral reefs: Corals' adaptive response to climate change. Nature 430(7001):741–741

Bakun A (1990) Global climate change and intensification of coastal ocean upwelling. Science 247(4939):198–201

Balch WM, Gordon HR, Bowler BC, Drapeau DT, Booth ES (2005) Calcium carbonate measurements in the surface global ocean based on Moderate-Resolution Imaging Spectroradiometer data. J Geophys Res 110:C07001. doi:10.1029/2004JC002560

Balch WM, Drapeau D, Bowler B, Booth E (2007) Prediction of pelagic calcification rates using satellite measurements. Deep Sea Res Part II 54:478–495

Bates NR (2006) Air-sea CO2 fluxes and the continental shelf pump of carbon in the Chukchi Sea adjacent to the Arctic Ocean. J Geophys Res 111:C10013. doi:10.1029/2005JC003083

Bates NR, Best MHP, Hansell DA (2005) Spatio-temporal distribution of dissolved inorganic carbon and net community production in the Chukchi and Beaufort Seas. Deep Sea Res II 52:3303–3323

Bates NR, Moran SB, Hansell DA, Mathis JT (2006) An increasing CO2 sink in the Arctic Ocean due to sea-ice loss. Geophys Res Lett 33:L23609. doi:10.1029/2006GL027028

Behrenfeld MJ, O'Malley RT, Siegel DA, McClain CR, Sarmiento JL, Feldman GC, Milligan AJ, Falkowski PG, Letelier RM, Boss ES (2006) Climate-driven trends in contemporary ocean productivity. Nature 444:752–755

Benner R, Benitez-Nelson B, Kaiser K, Amon RMW (2004) Export of young terrigenous dissolved organic carbon from rivers to the Arctic Ocean. Geophys Res Lett 31:L05305. doi:10.1029/2003GL019251

Bograd SJ, Castro CG, Di Lorenzo E, Palacios DM, Bailey H, Gilly W, Chavez FP (2008) Oxygen declines and the shoaling of the hypoxic boundary in the California Current. Geophys Res Lett 35:L12607. doi:10.1029/2008GL034185

Bopp L, Monfray P, Aumont O, Dufresne JL, Le Treut H, Madec G, Terray L, Orr JC (2001) Potential impact of climate change on marine export production. Global Biogeochem Cycles 15(1):81–99

Bopp L, Le Quéré C, Heimann M, Manning AC, Monfray P (2002) Climate-induced oceanic oxygen fluxes: Implications for the contemporary carbon budget. Global Biogeochem Cycles 16(2):1022. doi:10.1029/2001GB001445

Bopp L, Borges AV, Aumont O, Ethe C, Ciais P (2008) Integrating CO2 fluxes in the coastal ocean: Simulating natural variability and anthropogenic uptake with a global model of 0.5½b0 horizontal resolution, 2008 Ocean Sciences Meeting (ASLO AGU, TOS), March 2–7, 2008, Olando, FL

Borges AV (2005) Do we have enough pieces of the jigsaw to integrate CO2 fluxes in the Coastal Ocean ? Estuaries 28(1):3–27

Borges AV, Frankignoulle M (1999) Daily and seasonal variations of the partial pressure of CO_2 in surface seawater along Belgian and southern Dutch coastal areas. J Mar Syst 19:251–266

Borges AV, Frankignoulle M (2002a) Distribution of surface carbon dioxide and air-sea exchange in the upwelling system off the Galician coast. Global Biogeochem Cycles 16(2):1020. doi:10.1029/2000GB001385

Borges AV, Frankignoulle M (2002b) Distribution and air-water exchange of carbon dioxide in the Scheldt plume off the Belgian coast. Biogeochemistry 59(1–2):41–67

Borges AV, Frankignoulle M (2003) Distribution of surface carbon dioxide and air-sea exchange in the English Channel and adjacent areas. J Geophys Res 108(C8):3140. doi:10.1029/2000JC000571

Borges AV, Djenidi S, Lacroix G, Théate J, Delille B, Frankignoulle M (2003) Atmospheric CO_2 flux from mangrove surrounding waters. Geophys Res Lett 30(11):1558. doi:10.1029/2003GL017143

Borges AV, Delille B, Frankignoulle M (2005) Budgeting sinks and sources of CO_2 in the coastal ocean: Diversity of ecosystems counts. Geophys Res Lett 32:L14601. doi:10.1029/2005GL023053

Borges AV, Schiettecatte L-S, Abril G, Delille B, Gazeau F (2006) Carbon dioxide in European coastal waters, Estuarine. Coast Shelf Sci 70(3):375–387

Borges AV, Tilbrook B, Metzl N, Lenton A, Delille B (2008a) Inter-annual variability of the carbon dioxide oceanic sink south of Tasmania. Biogeosciences 5:141–155

Borges AV, Ruddick K, Schiettecatte L-S, Delille B (2008b) Net ecosystem production and carbon dioxide fluxes in the Scheldt estuarine plume. BMC Ecology 8:15. doi:10.1186/1472-6785-8-15

Borges AV, Alin SR, Chavez FP, Vlahos P, Johnson KS, Holt JT, Balch WM, Bates N, Brainard R, Cai W-J, Chen CTA, Currie K, Dai M, Degrandpre M, Delille B, Dickson A, Feely RA, Friederich GE, Gong G-C, Hales B, Hardman-Mountford N, Hendee J, Hernandez-Ayon JM, Hood M, Huertas E, Hydes D, Ianson D (IOS, CA), Krasakopoulou E, Litt E, Luchetta A, Mathis J, McGillis WR, Murata A, Newton J, Ólafsson J, Omar A, Perez FF, Sabine C, Salisbury JE, Salm R, Sarma VVSS, Schneider B, Sigler M, Thomas H, Turk D, Vandemark D, Wanninkhof R, Ward B (2009) Global sea surface carbon observing system: Inorganic and organic carbon dynamics in coastal oceans. In: Hall J, Harrison DE, Stammer D (eds) Proceedings of OceanObs'09: Sustained ocean observations and information for society (vol 2), Venice, Italy, 21–25 September 2009. ESA Publication WPP-306

Borges A.V. & N. Gypens (2010) Carbonate chemistry in the coastal zone responds more strongly to eutrophication than to ocean acidification, Limnology and Oceanography, 55, 346–353

Bouillon S, Frankignoulle M, Dehairs F, Velimirov B, Eiler A, Abril G, Etcheber H, Borges AV (2003) Inorganic and organic carbon biogeochemistry in the Gautami Godavari estuary (Andhra Pradesh, India) during pre-monsoon: The local impact of extensive mangrove forests. Global Biogeochem Cycles 17(No. 4):1114. doi:10.1029/2002GB002026

Boyd PW, Doney SC (2002) Modelling regional responses by marine pelagic ecosystems to global change. Geophys Res Lett 29. doi:10.1029/2001GL014130

Burkhardt S, Zondervan I, Riebesell U (1999) Effect of CO2 concentration on the C:N:P ratio in marinephytoplankton: A species comparison. Limnol Oceanogr 44:683–690

Burkhardt S, Amoroso G, Riebesell U, Sültemeyer D (2001) CO2 and HCO3– uptake in marine diatomsacclimated to different CO2 concentrations. Limnol Oceanogr 46:1378–1391

Cai W-J (2003) Riverine inorganic carbon flux and rate of biological uptake in the Mississippi River plume. Geophys Res Lett 30(2):1032. doi:10.1029/2002GL016312

Cai W-J, Wang Y (1998) The chemistry, fluxes, and sources of carbon dioxide in the estuarine waters of the Satilla and Altamaha Rivers, Georgia. Limnol Oceanogr 43(4):657–668

Cai W-J, Wang ZA, Wang Y (2003) The role of marsh-dominated heterotrophic continental margins in transport of CO2 between the atmosphere, the land-sea interface and the ocean. Geophys Res Lett 30:1849. doi:10.1029/2003GL017633

Cai W-J, Dai MH, Wang YC (2006) Air-sea exchange of carbon dioxide in ocean margins: A province-based synthesis. Geophys Res Lett 33:L12603. doi:10.1029/2006GL026219

Cai W-J, Guo X, Chen CTA, Dai M, Zhang L, Zhai W, Lohrenz SE, Yin K, Harrison PJ, Wang Y (2008) A comparative overview of weathering intensity and HCO_3^- flux in the world's major rivers with emphasis on the Changjiang, Huanghe, Zhujiang (Pearl) and Mississippi Rivers. Cont Shelf Res 28(1–2):1538–1549

Canadell JG, Le Quéré C, Raupach MR, Field CB, Buitenhuis ET, Ciais P, Conway TJ, Gillett NP, Houghton RA, Marland G (2007) Contributions to accelerating atmospheric CO_2 growth from economic activity, carbon intensity, and efficiency of natural sinks. Proc Natl Acad Sci U S A 104:18353–18354

Chen CTA (2004) Exchange of carbon in the coastal seas. In: Field CB, Raupach MR (eds) The global carbon cycle: Integrating human, climate and the natural world. SCOPE, Washington, DC, pp 341–351

Chen CTA, Borges AV (2009) Reconciling opposing views on carbon cycling in the coastal ocean: Continental shelves as sinks and near-shore ecosystems as sources of atmospheric CO_2. Deep Sea Res II 56(8–10):578–590

Copin-Montégut C, Bégovic M, Merlivat L (2004) Variability of the partial pressure of CO_2 on diel to annual time scales in the Northwestern Mediterranean Sea. Mar Chem 85(3–4): 169–189

da Cunha LC, Buitenhuis ET, Le Quéré C, Giraud X, Ludwig W (2007) Potential impact of changes in river nutrient supply on global ocean biogeochemistry. Global Biogeochem Cycles 21:GB4007. doi:10.1029/2006GB002718

Davidson EA, Janssens IA (2006) Temperature sensitivity of soil carbon decomposition and feedbacks to climate change. Nature 440(7081):165–173

DeGrandpre MD, Olbu GJ, Beatty CM, Hammar TR (2002) Air-sea CO2 fluxes on the US Middle Atlantic Bight. Deep Sea Res Part II 49(20):4355–4367

Delille B, Harlay J, Zondervan I, Jacquet S, Chou L, Wollast R, Bellerby RGJ, Frankignoulle M, Borges AV, Riebesell U, Gattuso J-P (2005) Response of primary production and calcification to changes of pCO2 during experimental blooms of the coccolithophorid Emiliania huxleyi. Global Biogeochem Cycles 19:GB2023. doi:10.1029/2004GB002318

Diaz RJ, Rosenberg R (2008) Spreading dead zones and consequences for marine ecosystems. Science 321:926–929

Dickson AG, Millero FJ (1987) A comparison of the equilibrium constants for the dissociation of carbonic acid in seawater media. Deep Sea Res 34:1733–1743

Diffenbaugh NS, Snyder MA, Sloan LC (2004) Could CO_2-induced land-cover feedbacks alter near-shore upwelling regimes? Proc Natl Acad Sci U S A 101(1):27–32

Di Lorenzo E, Miller AJ, Schneider N, McWilliams JC (2005) The Warming of the California current system: Dynamics and ecosystem implications. J Phys Oceanogr 35(3):336–362

Doney SC, Mahowald N, Lima I, Feely RA, Mackenzie FT, Lamarque J-F, Rasch PJ (2007) Impact of anthropogenic atmospheric nitrogen and sulfur deposition on ocean acidification and the inorganic carbon system. Proc Natl Acad Sci 104(37):14580–14585

Doney SC, Fabry VJ, Feely RA, Kleypas JA (2009) Ocean acidification: The other CO2 problem. Annu Rev Mar Sci 1:169–192

Douville H, Chauvin F, Planton S, Royer JF, Salas-Melia D, Tyteca S (2002) Sensitivity of the hydrological cycle to increasing amounts of greenhouse gases and aerosols. Clim Dyn 20:45–68

Duarte CM (2002) The future of seagrass meadows. Environ Conserv 29(2):192–206

Duce RA, LaRoche J, Altieri K, Arrigo KR, Baker AR, Capone DG, Cornell S, Dentener F, Galloway J, Ganeshram RS, Geider RJ, Jickells T, Kuypers MM, Langlois R, Liss PS, Liu SM, Middelburg JJ, Moore CM, Nickovic S, Oschlies A, Pedersen T, Prospero J, Schlitzer R, Seitzinger S, Sorensen LL, Uematsu M, Ulloa O, Voss M, Ward B, Zamora L (2008) Impacts of atmospheric anthropogenic nitrogen on the open ocean. Science 320:893–997

Else BGT, Papakyriakou TN, Granskog MA, Yackel JJ (2008) Observations of sea surface fCO2 distributions and estimated air-sea CO2 fluxes in the Hudson Bay region (Canada) during the open-water season. J Geophys Res 113:C08026. doi:10.1029/2007JC004389

Engel A, Thoms U, Riebesell U, Rochelle-Newall E, Zondervan I (2004) Polysaccharide aggregation as a potential sink of marine dissolved organic carbon. Nature 428:929–932

Engel A, Schulz KG, Riebesell U, Bellerby R, Delille B, Schartau M (2008) Effects of CO2 on particle size distribution and phytoplankton abundance during a mesocosm bloom experiment (PeECE II). Biogeosciences 5:509–521

Fabry VJ, Seibel BA, Feely RA, Orr JC (2008) Impacts of ocean acidification on marine fauna and ecosystem processes. J Mar Sci 65:414–432

Feely RA, Sabine CL, Hernandez-Ayon JM, Ianson D, Hales B (2008) Evidence for upwelling of corrosive "acidified" water onto the continental shelf. Science 320:1490–1492

Feng Y, Warner ME, Zhang Y, Sun J, Fu FX, Rose JM, Hutchins DA (2008) Interactive effects of increased pCO2, temperature and irradiance on the marine coccolithophore Emiliania huxleyi (Prymnesiophyceae). Eur J Phycol 43(1):87–98

Fennel K, Wilkin J, Previdi M, Najjar R (2008) Denitrification effects on air-sea CO2 flux in the coastal ocean: Simulations for the northwest North Atlantic. Geophys Res Lett 35:L24608. doi:10.1029/2008GL036147

Field D Cayan, Chavez DF (2006) Secular warming in the California current and North Pacific, California cooperative oceanic fisheries investigations report 47: 92–110

Frankignoulle M, Borges AV (2001) European continental shelf as a significant sink for atmospheric carbon dioxide. Global Biogeochem Cycles 15(3):569–576

Frankignoulle M, Canon C, Gattuso JP (1994) Marine calcification as a source of carbon dioxide: Positive feedback of increasing atmospheric CO2. Limnol Oceanogr 39:458–462

Frankignoulle M, Abril G, Borges A, Bourge I, Canon C, Delille B, Libert E, Théate J-M (1998) Carbon dioxide emission from European estuaries. Science 282(5388):434–436

Frey KE, McClelland JW (2009) Impacts of permafrost degradation on arctic river biogeochemistry. Hydrol Process 23:169–182

Frey KE, Smith LC (2005) Amplified carbon release from vast West Siberian peatlands by 2100. Geophys Res Lett 32:L09401. doi:10.1029/2004GL022025

Friederich GE, Walz PM, Burczynski MG, Chavez FP (2002) Inorganic carbon in the central California upwelling system during the 1997–1999 El Niño-La Niña event. Prog Oceanogr 54(1–4):185–203

Friederich GE, Ledesma J, Ulloa O, Chavez FP (2008) Air–sea carbon dioxide fluxes in the coastal southeastern tropical Pacific. Prog Oceanogr 79(2–4) 156–166

Galloway JN, Dentener FJ, Capone DG, Boyer EW, Howarth RW, Seitzinger SP, Asner GP, Cleveland CC, Green PA, Holland EA, Karl DM, Michaels AF, Porter JH, Townsend AR, Vörösmarty CJ (2004) Nitrogen cycles: Past, present, and future. Biogeochemistry 70:153–226

Gao K, Aruga Y, Asada K, Kiyohara M (1993) Influence of enhanced CO2 on growth and photosynthesis of the red algae Gracilaria sp and G-chilensis. J Appl Phycol 5:563–571

Gattuso J-P, Frankignoulle M, Wollast R (1998a) Carbon and carbonate metabolism in coastal aquatic ecosystems. Annu Rev Ecol Syst 29:405–433

Gattuso J-P, Frankignoulle M, Bourge I, Romaine S, Buddemeier B (1998b) Effect of calcium carbonate saturation of seawater on coral calcification. Glob Planet Change 18(1–2):37–46

Gazeau F, Smith SV, Gentili B, Frankignoulle M, Gattuso J-P (2004) The European coastal zone: Characterization and first assessment of ecosystem metabolism. Estuar Coast Shelf Sci 60(4):673–694

Gehlen M, Gangstø R, Schneider B, Bopp L, Aumont O, Ethe C (2007) The fate of pelagic CaCO3 production in a high CO2 ocean: A model study. Biogeosciences 4:505–519

Gislason SR, Oelkers EH, Eiriksdottir ES, Kardjilov MI, Gisladottir G, Sigfusson B, Snorrason A, Elefsen S, Hardardottir J, Torssander P, Oskarsson N (2009) Direct evidence of the feedback between climate and weathering. Earth Planet Sci Lett 277:213–222

Gledhill DK, Wanninkhof R, Millero FJ, Eakin M (2008) Ocean acidification of the Greater Caribbean Region 1996–2006. J Geophys Res 113:C10031. doi:10.1029/2007JC004629

Gloor M, Gruber N, Sarmiento J, Sabine CL, Feely RA, Rodenbeck C (2003) A first estimate of present and preindustrial air-sea CO_2 flux patterns based on ocean interior carbon measurements and models. Geophys Res Lett 30. doi:10.1029/2002GL015594

Goes JI, Thoppil PG, do R Gomes H, Fasullo JT (2005) Warming of the Eurasian landmass is making the Arabian Sea more productive. Science 308(5721):545–547

Goyet C, Millero FJ, O'Sullivan DW, Eischeid G, McCue SJ, Bellerby RGJ (1998) Temporal variations of pCO_2 in surface seawater of the Arabian sea in 1995. Deep Sea Res Part I 45(4–5):609–623

Green PA, Vörösmarty CJ, Meybeck M, Galloway JN, Peterson BJ, Boyer EW (2004) Pre-industrial and contemporary fluxes of nitrogen through rivers: A global assessment based on typology. Biogeochemistry 68:71–105

Gruber N, Gloor M, Mikaloff Fletcher SE, Doney SC, Dutkiewicz S, Follows MJ, Gerber M, Jacobson AR, Joos F, Lindsay K, Menemenlis D, Mouchet A, Müller SA, Sarmiento JL, Takahashi T (2009) Oceanic sources, sinks, and transport of atmospheric CO_2. Global Biogeochem Cycles 23:GB1005. doi:10.1029/2008GB003349

Gurney KR, Law RM, Denning AS, Rayner PJ, Pak B, the TransCom-3L2 modelers (2004) Transcom-3 inversion intercomparison: Control results for the estimation of seasonal carbon sources and sinks. Global Biogeocehm Cycles 18: GB1010. doi:10.1029/2003GB002111

Gypens N, Lancelot C, Borges AV (2004) Carbon dynamics and CO_2 air-sea exchanges in the eutrophicated coastal waters of the Southern Bight of the North Sea: A modelling study. Biogeosciences 1(2):561–589

Gypens N, Borges AV, Lancelot C (2009) Effect of eutrophication on air-sea CO2 fluxes in the coastal Southern North Sea: A model study of the past 50 years. Glob Change Biol 15(4): 1040–1056

Hales B, Takahashi T, Bandstra L (2005) Atmospheric CO2 uptake by a coastal upwelling system. Global Biogeochem Cycles 19:GB1009. doi:10.1029/2004GB002295

Heip C, Goosen NK, Herman PMJ, Kromkamp J, Middelburg JJ, Soetaert K (1995) Production and consumption of biological particles in temperate tidal estuaries. Oceanogr Mar Biol 33:1–149

Herman PMJ, Heip CHR (1999) Biogeochemistry of the MAximum TURbidity Zone of Estuaries (MATURE): Some conclusions. J Mar Syst 22:89–104

Hirst AC (1999) The Southern Ocean response to global warming in the CSIRO coupled ocean-atmosphere model. Environ Modell Softw 14(4):227–241

Holmes RM, McClelland JW, Raymond PA, Frazer BB, Peterson BJ, Stieglitz M (2008) Lability of DOC transported by Alaskan rivers to the arctic ocean. Geophys Res Lett 35:L03402. doi:10.1029/2007GL032837

Hopkinson CSJ, Smith EM (2005) Estuarine respiration: An overview of benthic, pelagic and whole system respiration. In: del Giorgio PA, Williams PJL (eds) Respiration in aquatic ecosystems. Oxford University Press, Oxford, pp 123–147

Hughes TP, Baird AH, Bellwood DR, Card M, Connolly SR, Folke C, Grosberg R, Hoegh-Guldberg O, Jackson JBC, Kleypas J, Lough JM, Marshall P, Nystrom M, Palumbi SR, Pandolfi JM, Rosen B, Roughgarden J (2003) Climate change, human impacts, and the resilience of coral reefs. Science 301(5635):929–933

Huntington TG (2006) Evidence for intensification of the global water cycle: Review and synthesis. J Hydrol 319:83–95

Hutchins DA, Fu FX, Zhang Y, Warner ME, Feng Y, Portune K, Bernhardt PW, Mulholland MR (2007) CO2 control of Trichodesmium N2 fixation, photosynthesis, growth rates, and elemental ratios: Implications for past, present, and future ocean biogeochemistry. Limnol Oceanogr 52(4):1293–1304

Ianson D, Allen SE (2002) A two-dimensional nitrogen and carbon flux model in a coastal upwelling region. Global Biogeochem Cycles 16(1):1011 doi:10.1029/2001GB001451

Iglesias-Rodriguez MD, Halloran PR, Rickaby REM, Hall IR, Colmenero-Hidalgo E, Gittins JR, Green DRH, Tyrrell T, Gibbs SJ, von Dassow P, Rehm E, Armbrust EV, Boessenkool KP (2008) Phytoplankton Calcification in a High-CO2 World. Science 320:336–340

IPCC (2007a) Climate change 2007: The physical science basis. Contribution of working group I to the fourth assessment report of the intergovernmental panel on climate change. In: Solomon S, Qin D, Manning M, Chen Z, Marquis M, Averyt KB, Tignor M, Miller HL (eds). Cambridge University Press, Cambridge, UK/New York, 996 pp

IPCC (2007b) Climate change 2007: Impacts, adaptation and vulnerability. Contribution of working group II to the fourth assessment report of the intergovernmental panel on climate change. In: Parry ML, Canziani OF, Palutikof JP, van der Linden PJ, Hanson CE (eds). Cambridge University Press, Cambridge 976 pp

Jahnke RA (2009) Global synthesis. In: Liu KK, Atkinson L, Quinones R, Talaue-McManus L (eds) (2010) Carbon and nutrient fluxes in continental margins: A global synthesis. Springer, New York

Jiang L-Q, Cai W-J, Wang Y (2008a) Carbon dioxide degassing in river- and marine-dominated estuaries: Importance of freshwater runoff. Limnol Oceanogr 53(6):2603–2615

Jiang L-Q, Cai W-J, Wanninkhof R, Wang Y, Hüger H (2008b) Air-sea CO2 fluxes on the US South Atlantic Bight: Spatial and seasonal variability. J Geophys Res 113:C07019, 17 pp. doi:10.1029/2007JC004366

Kemp WM, Smith EM, Marvin-DiPasquale M, Boynton WR (1997) Organic carbon-balance and net ecosystem metabolism in Chesapeake Bay. Mar Ecol Prog Ser 150:229–248

Key RM, Kozyr A, Sabine CL, Lee K, Wanninkhof R, Bullister JL, Feely RA, Millero FJ, Mordy C, Peng T-H (2004) A global ocean carbon climatology: Results from Global Data Analysis Project (GLODAP). Global Biogeochem Cycles 18:GB4031. doi:10.1029/2004GB002247

Kleypas JA, Buddemeier RW, Eakin CM, Gattuso J-P, Guinotte J, Hoegh-Guldberg O, Iglesias-Prieto R, Jokiel PL, Langdon C, Skirving W, Strong AE (2005) Comment on "coral reef calcification and climate change: The effect of ocean warming". Geophys Res Lett 32:L08601. doi:10.1029/2004GL022329

Kleypas JA, Feely RA, Fabry VJ, Langdon C, Sabine CL, Robbins LL (2006) Impacts of ocean acidification on coral reefs and other marine calcifiers: A guide for future research, report of a workshop held 18–20 April 2005, St. Petersburg, FL, sponsored by NSF, NOAA, and the US Geological Survey, 88 pp

Kuss J, Nagel K, Schneider B (2004) Evidence from the Baltic Sea for an enhanced CO2 air-sea transfer velocity. Tellus Series B 56(2):175–182

Labat D, Godderis Y, Probst JL, Guyot JL (2004) Evidence for global runoff increase due to climate warming. Adv Water Resour 27:631–642

Largier JL, Lawrence CA, Roughan M, Kaplan DM, Dever EP, Dorman CE, Kudela RM, Bollens SM, Wilkerson FP, Dugdale RC, Botsford LW, Garfield N, Kuebel Cervantes B, Koračin D (2006) WEST: A northern California study of the role of wind-driven transport in the productivity of coastal plankton communities. Deep Sea Res II 53:2833–2849

Lee K-S (2001) Global net community production estimated from the annual cycle of surface water total dissolved inorganic carbon. Limnol Oceanogr 46:1287–1297

Le Quéré C, Bopp L, Tegen I (2002) Antarctic circumpolar wave impact on marine biology: A natural laboratory for climate change study. Geophys Res Lett 29(10):1407. doi: 10.1029/2001GL014585

Le Quéré C, Aumont O, Monfray P, Orr J (2003) Propagation of climatic events on ocean stratification, marine biology, and CO2: Case studies over the 1979–1999 period. J Geophys Res 108(C12):3375. doi:10.1029/2001JC000920

MacDonald GM, Beilman DW, Kremenetski KV, Sheng YW, Smith LC, Velichko AA (2006) Rapid early development of circumarctic peatlands and atmospheric CH4 and CO2 variations. Science 314(5797):285–288

Mackenzie FT, Lerman A, Andersson AJ (2004) Past and present of sediment and carbon biogeochemical cycling models. Biogeosciences 1(1):11–32

Matear RJ, Hirst AC (2003) Long-term changes in dissolved oxygen concentrations in the ocean caused by protracted global warming. Global Biogeochem Cycles 17(4):1125. doi:10.1029/2002GB001997

McClelland JW, Holmes RM, Peterson BJ, Stieglitz M (2004) Increasing river discharge in the Eurasian Arctic: Consideration of dams, permafrost thaw, and fires as potential agents of change. J Geophys Res 109:D18102. doi:10.1029/2004JD004583

McClelland JW, Stieglitz M, Pan F, Holmes RM, Peterson BJ (2007) Recent changes in nitrate and dissolved organic carbon export from the upper Kuparuk River, North Slope, Alaska. J Geophys Res-Biogeosci 112:G04S60. doi:10.1029/2006JG000371

McGregor HV, Dima M, Fischer HW, Mulitza S (2007) Rapid 20th-century increase in coastal upwelling off Northwest Africa. Science 315:637–639

McNeil BI, Matear RJ, Barnes DJ (2004) Coral reef calcification and climate change: The effect of ocean warming. Geophys Res Lett 31:L22309. doi:10.1029/2004GL021541

Mehrbach C, Culberson CH, Hawley JE, Pytkowicz RM (1973) Measurement of the apparent dissociation constants of carbonic acid in seawater at atmospheric pressure. Limnol Oceanogr 18:897–907

Mendelssohn R, Schwing FB (2002) Common and uncommon trends in SST and wind stress in the California and Peru–Chile current systems. Prog Oceanogr 53:141–162

Merico A, Tyrrell T, Brown CW, Groom SB, Miller PI (2003) Analysis of satellite imagery for Emiliania huxleyi blooms in the Bering Sea before 1997. Geophys Res Lett 30:1337

Milliman JD, Droxler AW (1996) Neritic and pelagic carbonate sedimentation in the marine environment: Ignorance is not bliss. Geol Rundsh 85:496–504

Milliman JD, Troy PJ, Balch WM, Adams AK, Li YH, Mackenzie FT (1999) Biologically mediated dissolution of calcium carbonate above the chemical lysocline? Deep Sea Res Part I: Oceanogr Res Papers 46:1653–1669

Milly PCD Dunne KA, Vecchia AV (2005) Global patterns or trends in streamflow and water availability in a changing climate. Nature 438:347–350

Mucci A (1983) The solubility of calcite and aragonite in seawater at various salinities, temperatures, and one atmosphere total pressure. Am J Sci 283:781–799

Murata A (2006) Increased surface seawater pCO2 in the eastern Bering Sea shelf: An effect of blooms of coccolithophorid Emiliania huxleyi? Global Biogeochem Cycles 20:GB4006. doi:10.1029/2005GB002615

Murata A, Takizawa T (2003) Summertime CO2 sinks in shelf and slope waters of the western Arctic Ocean. Cont Shelf Res 23:753–776. 2003

Murata A, Shimada K, Nishino S, Itoh M (2008) Distributions of surface water CO2 and air-sea flux of CO2 in coastal regions of the Canadian Beaufort Sea in late summer. Biogeosci Discuss 5:5093–5132

Odum HT, Hoskin CM (1958) Comparative studies of the metabolism of Texas Bays. Publications of the Institute of Marine Science, University of Texas, vol 5, pp 16–46

Odum HT, Wilson R (1962) Further studies on the reaeration and metabolism of Texas Bays. Publications of the Institute of Marine Science, University of Texas, vol 8, pp 23–55

Omar AM, Olsen A, Johannessen T, Hoppema M, Thomas H, Borges AV (2010) Spatiotemporal variations of fCO2 in the North Sea. Ocean Sci 6:77–89

Opsahl S, Benner R, Amon RW (1999) Major flux of terrigenous dissolved organic matter through the Arctic Ocean. Limnol Oceanogr 44:2017–2023

Patra PK, Maksyutov S, Ishizawa M, Nakazawa T, Takahashi T, Ukita J (2005) Interannual and decadal changes in the sea-air CO_2 flux from atmospheric CO_2 inverse modeling. Global Biogeochem Cycles 19:GB4013. doi:10.1029/2004GB002257

Paulmier A, Ruiz-Pino D, Garçon V (2008) The oxygen minimum zone (OMZ) off Chile as intense source of CO_2 and N_2O. Cont Shelf Res 28:2746–2756

Peterson BJ, Holmes RM, McClelland JW, Vörösmarty CJ, Lammers RB, Shiklomanov AI, Shiklomanov IA, Rahmstorf S (2002) Increasing river discharge to the Arctic Ocean. Science 298:2171–2173

Pipko II, Semiletov IP, Tishchenko P, Ya Pugach SP, Christensen JP (2002) Carbonate chemistry dynamics in Bering Strait and the Chukchi Sea. Prog Oceanogr 55:77–94

Plattner G-K, Frenzel H, Gruber N, Leinweber A, McWilliams JC (2004) Changing winds and coastal carbon cycle: A case study for an upwelling region, The ocean in a high-CO2 world, 10–12 May 2004, Unesco, Paris, France

Qiu BS, Gao KS (2002) Effects of CO2 enrichment on the bloomforming cyanobacterium Microcystis aeruginosa (Cyanophyceae): Physiological responses and relationships with the availability of dissolved inorganic carbon. J Phycol 38:721–729

Quay P, Sommerup R, Westby T, Sutsman J, McNichol A (2003) Changes in the $^{13}C/^{12}C$ of dissolved inorganic carbon in the ocean as a tracer of anthropogenic CO_2 uptake. Global Biogeochem Cycles 17:No. 1. doi:10.1029/2001GB001817

Raven J, Caldeira K, Elderfield H, Hoegh-Guldberg O, Liss P, Riebesell U, Shepherd J, Turley C, Watson A (2005) Ocean acidification due to increasing atmospheric carbon dioxide. The Royal Society, London

Raven JA (1991) Physiology of inorganic C acquisition and implications for resource use efficiency by marine phytoplankton: relation to increased CO2 and temperature. Plant Cell Environ 14:779–794

Raymond PA, Cole JJ (2003) Increase in the export of alkalinity from North America's largest river. Science 301(5629):88–91

Raymond PA, McClelland JW, Holmes RM, Zhulidov AV, Mull K, Peterson BJ, Striegl RG, Aiken GR, Gurtovaya TY (2007) Flux and age of dissolved organic carbon exported to the Arctic Ocean: A carbon isotopic study of the five largest arctic rivers. Global Biogeochem Cycles 21:GB4011. doi:10Ð1029/2007GB002934

Raymond PA, Oh NH, Turner RE, Broussard W (2008) Anthropogenically enhanced fluxes of water and carbon from the Mississippi River. Nature 451(7177):449–452

Riebesell U (2007) What are the maximum impacts of projected environmental changes on marine biology and the carbon cycle? Surface ocean CO2 variability and vulnerability workshop, IOC/UNESCO, Paris, France April 11–14

Riebesell U, Wolf-Gladrow DA, Smetacek V (1993) Carbon dioxide limitation of marine phytoplankton growth rates. Nature 361:249–251

Riebesell U, Schulz KG, Bellerby RGJ, Botros M, Fritsche P, Meyerhofer M, Neill C, Nondal G, Oschlies A, Wohlers J, Zollner E (2007) Enhanced biological carbon consumption in a high CO2 ocean. Nature 450:545–548

Rost B, Riebesell U, Burkhardt S, Sültemeyer D (2003) Carbon acquisition of bloom-forming marine phytoplankton. Limnol Oceanogr 48:55–67

Sabine CL, Feely RA, Gruber N, Key RM, Lee K, Bullister JL, Wanninkhof R, Wong CS, Wallace DWR, Tilbrook B, Peng T-H, Kozyr A, Ono T, Rios AF (2004) The oceanic sink for anthropogenic CO_2. Science 305:367–371

Salisbury J, Green M, Hunt C, Campbell J (2008) Coastal acidification by rivers: A new threat to shellfish? Eos Trans AGU 89(50):513

Salisbury J, Vandemark D, Hunt C, Campbell J, Jonsson B, Mahadevan A, McGillis W, Xue H (2009) Episodic riverine influence on surface DIC in the coastal Gulf of Maine. Estuar Coast Shelf Sci 82:108–118

Santos AMP, Kazmin AS, Peliz A (2005) Decadal changes in the Canary upwelling system as revealed by satellite observations: Their impact on productivity. J Mar Res 63(2): 359–379

Sarmiento JL, Sundquist ET (1992) Revised budget for the oceanic uptake of Anthropogenic carbon dioxide. Nature 356:589–593

Sarmiento JL, Hughes TMC, Stouffer RJ, Manabe S (1998) Simulated response of the ocean carbon cycle to anthropogenic climate warming. Nature 393(6682):245–249

Sarmiento JL, Monfray P, Maier-Reimer E, Aumont O, Murnane RJ, Orr JC (2000) Sea-air CO_2 fluxes and carbon transport: A comparison of three ocean general circulation models. Global Biogeochem Cycles 14:1267–1281

Schiettecatte L-S, Thomas H, Bozec Y, Borges AV (2007) High temporal coverage of carbon dioxide measurements in the Southern Bight of the North Sea. Mar Chem 106(1–2): 161–173

Schneider B, Nausch G, Nagel K, Wasmund N (2003) The surface water CO2 budget for the Baltic Proper: A new way to determine nitrogen fixation. J Mar Syst 42(1–2):53–64

Seitzinger SP, Kroeze C, Bouwman AF, Caraco N, Dentener F, Styles RV (2002) Global patterns of dissolved inorganic and particulate nitrogen inputs to coastal systems: Recent conditions and future projections. Estuaries 25(4b):640–655

Seitzinger SP, Harrison JA, Dumont E, Beusen AHW, Bouwman AF (2005) Sources and delivery of carbon, nitrogen, and phosphorus to the coastal zone: An overview of Global Nutrient Export from Watersheds (NEWS) models and their application. Global Biogeochem Cycles 19:GB4S01. doi:10.1029/2005GB002606

Short FT, Neckles HA (1999) The effects of global climate change on seagrasses. Aquat Bot 63(3–4):169–196

Smyth TJ, Tyrrell T, Tarrant B (2004) Time series of coccolithophore activity in the Barents Sea, from twenty years of satellite imagery. Geophys Res Lett 31:L11302. doi:10.1029/2004GL019735

Snyder MA, Sloan LC, Diffenbaugh NS, Bell JL (2003) Future climate change and upwelling in the California Current. Geophys Res Lett 30(15):1823. doi:10.1029/2003GL017647

Soetaert K, Middelburg JJ, Heip C, Meire P, Van Damme S, Maris T (2006) Long-term change in dissolved inorganic nutrients in the heterotrophic Scheldt estuary (Belgium, The Netherlands). Limnol Oceanogr 51(1):409–423

Stramma L, Johnson GC, Sprintall J, Mohrholz V (2008) Expanding oxygen-minimum zones in the tropical oceans. Science 320:655–658

Takahashi T, Sutherland SC, Wanninkhof R, Sweeney C, Feely RA, Chipman DW, Hales B, Friederich G, Chavez F, Sabine C, Watson A, Bakker DCE, Schuster U, Metzl N, Yoshikawa-Inoue Hi, Ishii M, Midorikawa T, Nojiri Y, Körtzinger A, Steinhoff T, Hoppema M, Olafsson J, Arnarson TS, Tilbrook B, Johannessen T, Olsen A, Bellerby R, Wong CS, Delille B, Bates NR, de Baar HJW (2009) Climatological mean and decadal change in surface ocean pCO2, and net sea-air CO2 flux over the global oceans. Deep Sea Res II 56(8–10):554–577

Thomas H, Bozec Y, Elkalay K, De Baar HJW (2004) Enhanced open ocean storage of CO_2 from shelf sea pumping. Science 304(5673):1005–1008

Thomas H, Schiettecatte L-S, Suykens K, Koné YJM, Shadwick EH, Prowe AEF, Bozec Y, de Baar HJW, Borges AV (2009) Enhanced ocean carbon storage from anaerobic alkalinity generation in coastal sediments. Biogeosciences 6:1–8

Tortell PD, DiTullio GR, Sigman DM, Morel FMM (2002) CO2 effects on taxonomic composition and nutrient utilization in an Equatorial Pacific phytoplankton assemblage. Mar Ecol-Prog Ser 236:37–43

Tsunogai S, Watanabe S, Sato T (1999) Is there a “continental shelf pump” for the absorption of atmospheric CO2? Tellus Ser B 51(3):701–712

Tyler RM, Brady DC, Targett TE (2009) Temporal and spatial dynamics of diel-cycling hypoxia in estuarine tributaries. Estuar Coast 32:123–145

Tyrrell T, Merico A (2004) Emiliania huxleyi: Bloom observations and the conditions that induce them in Coccolithophores. In: Thierstein HR, Young JR (eds) From molecular processes to global impact. Springer, Berlin, pp 75–97

Vázquez-Rodríguez M, Touratier F, Lo Monaco C, Waugh DW, Padin XA, Bellerby RGJ, Goyet C, Metzl N, Ríos AF, Pérez FF (2009) Anthropogenic carbon distributions in the Atlantic Ocean: Data-based estimates from the Arctic to the Antarctic. Biogeosciences 6:439–451

Vörösmarty CJ, Sahagian D (2000) Anthropogenic disturbance of the terrestrial water cycle. BioScience 50(9):753–765

Vörösmarty CJ, Meybeck M, Fekete B, Sharma K, Green P, Syvitski JPM (2003) Anthropogenic sediment retention: Major global impact from registered river impoundments. Glob Planet Change 39(1–2):169–190

Walsh JJ (1988) On the nature of continental shelves. Academic, San Diego, CA/New York/Berkeley CA/Boston, MA/London/Sydney/Tokyo/Toronto

Wang SL, Chen CTA, Hong G-H, Chung CS (2000) Carbon dioxide and related parameters in the East China Sea. Cont Shelf Res 20(4–5):525–544

Wang ZA, Cai W-J (2004) Carbon dioxide degassing and inorganic carbon export from a marsh-dominated estuary (the Duplin River): A marsh CO_2 pump. Limnol Oceanogr 49(2):341–354

Wollast R (1998) Evaluation and comparison of the global carbon cycle in the coastal zone and in the open ocean. In: Brink KH, Robinson AR (eds) The global coastal ocean. Wiley, New York, pp 213–252

Zimmerman RC, Kohrs DG, Steller DL, Alberte RS (1997) Impacts of CO2 enrichment on productivity and light requirements of eelgrass. Plant Physiol 115:599–607

Chapter 4
Aspects of Phytoplankton Communities Response to Climate Changes

Maria da Graça Cabeçadas, Maria José Brogueira, Maria Leonor Cabeçadas, Ana Paula Oliveira, and Marta Cristina Nogueira

Abstract Climate changes concerning shifts in seasonal dominant winds and increases in atmospheric CO_2 are underway. Thus, changes are occurring in coastal upwelling regimes as well as increases in CO_2 absorption by the ocean/acidification impacting phytoplankton communities in terms of abundance and diversity. In order to illustrate these apparent changes we present results obtained from coastal waters adjacent to the Tagus estuary under different hydrological conditions. Upwelling events prevailed in winter 1994, were absent in winter 2001 and were present in summer 2002. Chemical and biological properties are examined: in March 1994, a strong bloom of phytoplankton developed (chlorophyll *a* up to 40 mg m^{-3}) which was attributed to the combined effect of intense freshwater runoff and upwelling, leading to the establishment of a strong frontal boundary and a supply of a considerable amount of nutrients. In March 2001, under an extremely intense river discharge and absence of upwelling, only values up to 1.5 mg m^{-3} of chlorophyll *a* were measured. On the other hand, in June 2002, when Tagus river inflow was reduced and nutrient levels were quite low, chlorophyll *a* levels attained 5 mg m^{-3} despite the occurrence of upwelling.

Over the same study area, potential impacts of acidification on phytoplankton communities are discussed. Actually, blooms of calcifying organisms occur often in Iberian coastal waters linked to upwelling events. In June 2002, a bloom episode of the Coccolithophore, *Coccolithus braarudii*, developed attaining up to 60 cells mL^{-1}, being responsible for production of 11.2 mmol $CaCO_3$ m^{-2} d^{-1}. In the context of actual lowering of seawater pH, the expected calcification slow-down as well as the reduction of buffering seawater ability, a shift of such a phytoplankton group to other groups is likely to be induced. Thus, the maintenance of biogeochemical

M. da Graça Cabeçadas (✉), M.J. Brogueira, A.P. Oliveira, and M.C. Nogueira
Instituto Nacional de Recursos Biológicos, INRB/IPIMAR, Av. de Brasilia 1449-006, Portugal
e-mail: gc@ipimar.pt; mzb@ipimar.pt; aoliveira@ipimar.pt; mnog@ipimar.pt

M.L. Cabeçadas
Agência Portuguesa do Ambiente, APA, R. da Murgueira 9/9A-Zambujal Ap. 7585-Alfragide 2721-865, Amadora, Portugal
e-mail: leonor.cabecadas@iambiente.pt

P. Duarte and J.M. Santana-Casiano (eds.), *Oceans and the Atmospheric Carbon Content*,
DOI 10.1007/978-90-481-9821-4_4,

time-series is crucial for the detection of future changes in the structure and functioning of this marine ecosystem.

Keywords Carbon dioxide • Climate change • Phytoplankton • Chlorophyll *a* • Calcifying organisms • Coastal upwelling • Wind • Estuary • River • Ocean • Acidification • Nutrients • pH • Calcium carbonate • Marine ecosystem

4.1 Introduction

Climate changes, namely shifts in wind regime and increase in atmospheric CO_2 concentrations, impact ocean biota in many ways. In this work we have concentrated on aspects of phytoplankton responses to such climate perturbations.

Regarding the recurrence of coastal upwelling during summer, several changes in this pattern have been reported since the 1970s. While some authors found an increasing trend in upwelling intensity in response to the intensification and steadiness of favourable northerly winds (Dickson et al. 1988 ; Bakun 1990, 1992), others reported a decreasing one (Dias 1994; Dias et al. 1996, unpublished; Lavin et al. 2000). A more consistent change in patterns of coastal upwelling off Western Iberia was during the period of 1947–2001, the increase in frequency and intensity of northerly winds in winter, favouring upwelling (Dias et al. 1996, unpublished; Borges et al. 2003; Santos et al. 2005). Some evidence that these alterations are related to the North Atlantic Oscillation index have been reported (NAO) (Borges et al. 2003; Santos et al. 2005), and are part of large-scale patterns of the whole Canary Current Upwelling System (Santos et al. 2005). From the early 1940s until the early 1970s, NAO index dropped, but over the following 25 years the dominance of NAO positive phase occurred with unprecedented high values (Hurrell 1995; Hurrell and van Loon 1997; Jones et al. 1997). Further, it has been noticed that after 1970 changing wind trends were in phase with the NAO index during winter. In fact, Borges et al. (2003) found highly significant positive correlations between the NAO index and the frequency and intensity of upwelling favourable wind (northerlies) off Western Iberia during winter time.

Besides the upwelling, poleward slope currents carrying warm and saline waters as well as buoyant plumes from river discharges, are dominant oceanographic features along the Western Iberia coast in winter (e.g. Peliz et al. 2005; Relvas et al. 2007). Nogueira et al. (1997) show nutrients enrichment process off the Western coast to be related to the intensity and persistence of winds, which promote the transport of such elements to the euphotic zone, allowing phytoplankton growth. Moreover, the higher availability of nutrients originated from rivers and/or regenerated, contributes as well to the enhancement of phytoplankton productivity. Actually, the buoyant plumes induce the seaward transport of land-derived sediments and nutrients. Furthermore, highly stratified plumes lead to well-defined density fronts along their boundaries, where high chlorophyll *a* values are frequent in winter. Peliz and Fiuza (1999)

hypothesized that, in this period of the year, the stratification of shelf waters induced by river runoff and the slope circulation could, in part, drive high concentrations and significant gradients of chlorophyll *a* at the shelfbreak. Thus, the nutrients discharged by the rivers at the subsurface waters may be added to the upwelled nutrients, favouring the enhancement of biological productivity, which in turn contribute to local nutrients depletion. Nevertheless, under intense upwelling, the biota may not have a chance to grow before the nutrient-rich water is diverged from the upwelling center, making the biological production actually low near this zone.

As, in winter, some factors such as high nutrient inputs from the rivers and low surface temperatures may mask the signal of coastal upwelling, diverse indicators namely the Aging Upwelling Index (Takahaschi et al. 1986) can be used in expressing the aging status of upwelled waters.

Increasing levels of CO_2 in the atmosphere is a product of the industrial revolution and consumption of fossil fuels. Fifty years ago atmospheric CO_2 levels were roughly 280 μatm and have gradually increased to a level of about 370 μatm during the past 50 years. The ocean uptake of antrophogenic carbon led to alterations of biogeochemical properties and an average decrease in pH of 0.10 units has occurred since the pre-industrial era. Currently, the oceans are taking up CO_2 at a rate of ~7 Gt $year^{-1}$ giving rise to further acidification. Thus, the gradually increased CO_2 levels form the baseline of carbon concentrations in the ocean, producing acidification.

Several models predict that over the next centuries the ocean will, eventually, take up most of the CO_2 released to the atmosphere, with expectation of an average reduction in surface ocean pH between 0.14 and 0.35 units over the twenty-first century (IPCC 2007). This represents a change beyond the range of seasonal or spatial variability of environmental conditions that phytoplankton species usually encounter in the ocean. Further, upwelling events contribute to bringing CO_2 as well as nutrients from deeper to surface waters, triggering additional phytoplankton blooms that continue the process and put more CO_2 into the system, thus enhancing acidification. In addition, in eutrophic, highly productive shelf and coastal environments the biological demands on dissolved CO_2 coupled with the chemical dynamics of riverine inputs combine to produce variations of as much as one pH unit (Hinga 2002). The great and rapid changes in the carbonate chemistry of systems may affect plankton species composition, in particular, calcifying organisms such as coccolithophores, foraminifera and corals, owing to inhibition of calcification in waters with high CO_2 (Riebesell 2004; Engel et al. 2005; Orr et al. 2005; Royal Society 2005). The decline of carbonate saturation state leads to significant inhibition of the ability of such species to calcify (Riebesell et al. 2000). According to Engel et al. (2005), the coccolithophorid *Emiliania huxleyi*, which forms extensive blooms in large areas of temperate and subpolar latitudes, is indeed sensitive to changes in CO_2 concentrations, in terms of reduction of net specific growth rates and calcification of cells. Thus, if phytoplankton species composition is vulnerable to this type of perturbation, one may expect impacts on the higher trophic levels that have specific trophic links.

This article is organized as follows: in Section 1 we examine the variability of nutrients and chlorophyll patterns under different hydrological settings and analyse

the consequences of changes of upwelling patterns on phytoplankton biomass in Tagus adjacent coastal waters. In Section 2 we provide a view on the development and biogeochemistry of a bloom of the marine coccolithophorid C*occolithus braarudii*, a phytoplankton species vulnerable to CO_2-habitat, in the same area and discuss the potential impact of increasing seawater acidification on the Portuguese coastal phytoplankton communities.

4.2 Material and Methods

4.2.1 Study Area and Sampling Locations

The present work was carried out along the Portuguese coast between 38.28°–38.70°N and 9.10°–9.50°W, in March 1994, March 2001 and June 2002, mainly covering the continental shelf and shelfbreak of Tagus estuary (Fig. 4.1). The coastline of this region is interrupted by two capes (Raso and Espichel) and a pronounced embayment, and the bottom topography of the area is dominated by the Lisbon submarine canyon. The hydrogeomorphological features are deeply marked by the relatively intense discharge of the Tagus river which amounts to an annual mean flow of 350 m^3 s^{-1}. Wind-driven upwelling events occur seasonally in the area. All these features drive a complex water circulation pattern over the study area.

Sampling was carried out on board the RV *Mestre Costeiro* (March 1994 and June 2002) and RV *Noruega* (March 2001). Twenty one stations were sampled for water chemistry and chlorophyll analysis and as well for phytoplankton identification and quantification (Fig. 4.1).

4.2.2 Analytical Methods

Temperature and salinity profiles were obtained with a SeaBird SBE 19-CTD probe being salinities calibrated using an Autosal (Guildline4 Model 8400B) salinometer. Discrete water samples were taken using a Seabird rosette sampler (8 L Niskin bottles) for determination of nutrients (NO_3+NO_2 referred herein as NO_3, NH_4, PO_4 and $Si(OH)_4$), total phosphorus (TP), total nitrogen (TN), chlorophyll *a* (Chl *a*), pH and total alkalinity (TA). Nutrient samples were filtered through MSI Acetate Plus filters and analyses carried out on a TRAACs 2000 Autoanalyser, following methods of Tréguer and Le Corre (1975). Accuracy of nutrients data was maintained through the use of Sagami CSK standards (WAKO, Japan). The estimated precision was 0.8% for NO_3, 2% for NH_4, 1.9% for PO_4 and 2.5% for $Si(OH)_4$. To determine total phosphorus (TP) and total nitrogen (TN) concentrations persulphate oxidation was used (ISO methodology 1997) followed by a subsequent measurement of PO_4 and NO_3. Samples for Chl *a* determination were collected from surface to bottom at shallow stations and from surface to 50 m depth at deeper stations. Chl *a* was

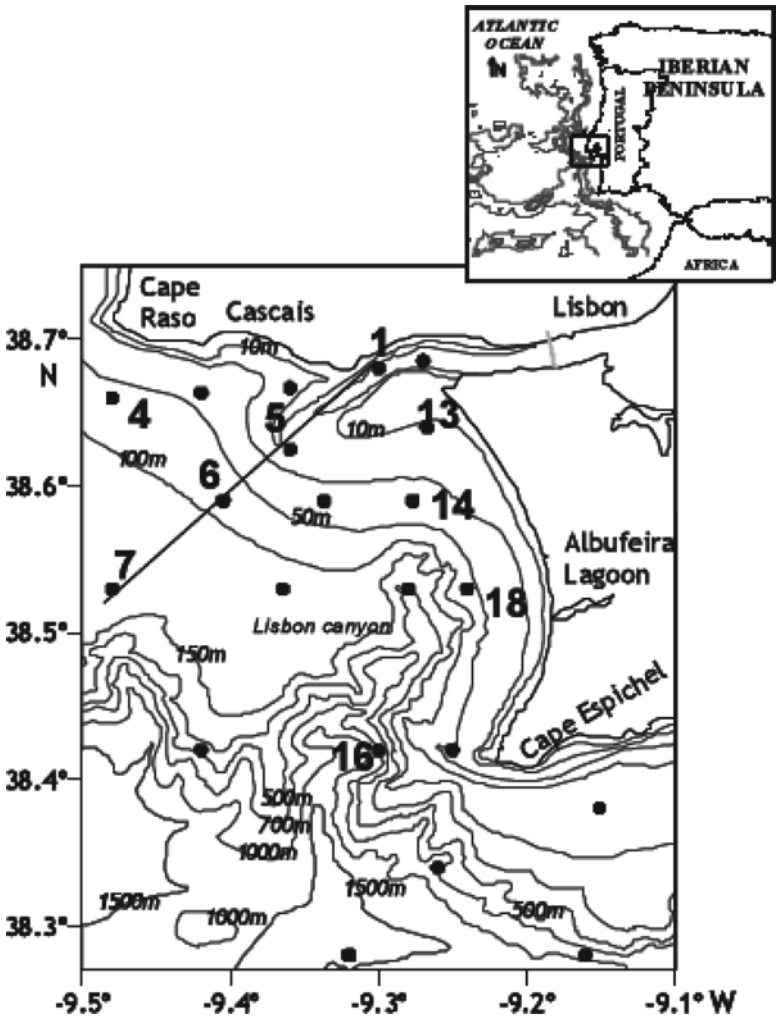

Fig. 4.1 Map of North Atlantic ocean showing the study region. The expanded view shows bathymetry of the study area as well as the distribution of sampling stations. Also shown transect St.1–7

measured by filtering aliquots of 50–100 mL water through Whatman GF/F filters. The filters were frozen and later extracted in 90% acetone for analysis in a Perkin Elmer Fluorometer, following Strickland and Parsons (1972). The precision was 1.8%. pH was measured using a Metrohm 704 m and a combination electrode calibrated against NBS buffers. Precision of pH measurements was 0.14%. TA was determined by potentiometric titration past the end-point of 4.5, according to Dickson and Goyet (1994), with a precision of 0.5%. The system was calibrated using certified reference material (CRM) from A.G. Dickson of Scripps Institution of Oceanography. Partial pressure of CO_2, pCO_2, was estimated from pH and TA data and calculations performed with the PROTALK program (Oliveira 1999).

Constants were taken from Roy et al. (1993) and Weiss (1974), and the errors estimated to be less than 5 μatm (Lee et al. 1997). Phytoplankton samples for coccolithophores identification were filtered through Millipore filters (0.45 μm) and examined with a Zeiss Standard Axioskop Mod-2 microscope.

4.2.3 Calculation of the Degree of Nutrient Consumption

In order to calculate the *Degree of Nutrient Consumption* DNC we have applied Chen et al. (2004) nomenclature, a modification of the Aging Upwelling Index proposed by Takahaschi et al. (1986). The index DNC was estimated taking into account the relative percentages of biological elements in their inorganic and organic forms. We used the degree of phosphorus consumption (DNC_p), following Chen's (2000) equation:

$$DNC_p = \frac{DOP + PP}{DIP + DOP + PP}$$

Where, DOP, PP and DIP are, respectively, dissolved organic phosphorus, particulate phosphorus and dissolved inorganic phosphorus. Concentration of dissolved organic P plus particulate P (DOP+PP), was calculated by subtracting dissolved inorganic P (DIP) from total P (TP).

As newly upwelled water contains high amounts of DIP and little amounts of organic P (DOP+PP), the DNC_p is small. By contrast, in old upwelled water a large portion of its dissolved inorganic fraction is converted to organic P, which means that DNC_p approaches one.

Phosphorus consumption was evaluated in 1994 at four specific sites: two located in the estuarine plume (Sts. 13 and 14) and two corresponding to maximum values of phytoplankton biomass, one at the limit of the plume (St. 7) and the other outside the plume (St. 16), in the vicinity of Lisbon canyon (Fig. 4.1). In 2002, phosphorus consumption was calculated in three sites, one right at the center of upwelling (St. 4), one at the frontal boundary (St. 6) and the other site outside the upwelling influence (St. 18).

4.3 Results and Discussion

4.3.1 Section 1

4.3.1.1 Hydrological, Chemical and Productivity Features

In March 1994 (winter), a moderately intense river discharge gave rise to a well-defined river plume showing marked spatial gradients in salinity (Fig. 4.2a) and nutrients. As a result, surface nutrients reached values up to 1.0 μM PO_4 (Fig. 4.2b),

17 μM NO_3, 15 μM $Si(OH)_4$, 6.5 μM TP and 36 μM TN nearby the estuary mouth. One week prior to sampling an upwelling event occurred, which was reflected in lower surface temperatures (13.7–13.8°C) detected close to the coast (Fig. 4.3a). Also nutrients rising from about 100 m depth to the surface waters were noticed in the cross-shelf section St.1–7 (Fig. 4.3b), although due to nutrient enriched fresh water input, upwelled nutrients were masked at surface. A strong boundary was established between the river plume and the upwelled waters, particularly in the northern part of Tagus bay as illustrated by the density structure, dominated by the effect of salinity (Fig. 4.4a). The interaction of water masses all over the area, estuarine water contribution ranging from 14% to 49% and upwelled water from 51% to 86%, apparently favoured the development of an early and very strong phytoplankton bloom, reaching values of Chl *a* up to 40 mg m^{-3} in the upper 10 m of the water column (Fig. 4.4b). Besides temperature and nutrient distributions, the Upwelling Aging Index (AUI=DNC_P) allowed us to define the center of upwelling and the outside region. DNC_P values (Table 4.1) indicate the presence of more recently outcropped water in stations 13 and 14 (0.88), the centers of upwelling, and more aged waters as far away at stations 7 and 16 (respectively 0.95 and 0.99). Regarding the uptake of nutrients, in particular phosphate (calculated taking into account the nutrient content of two main water-masses reaching the area), in those sites, the estimated values varied only between 11% and 15% at the center of upwelling and between 65% and 91% outside it (Table 4.1). As expected, the highest phosphate uptake occurred in the region where maxima values of phytoplankton biomass were attained.

The situation observed in March 2001 is in stark contrast to the one just described for March 1994, since upwelling was absent and the river discharge was

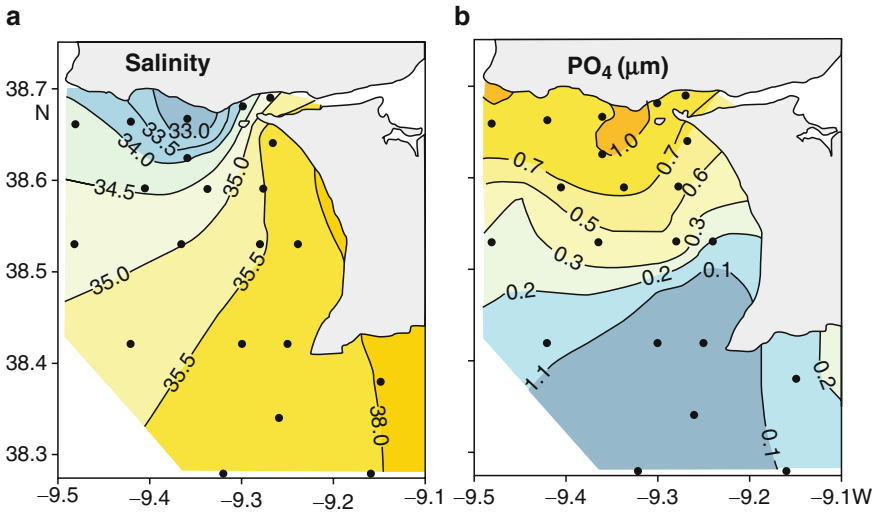

Fig. 4.2 Surface salinity distribution (**a**) and surface phosphate distribution (adapted from Cabeçadas et al. 1999) (**b**) in March 1994

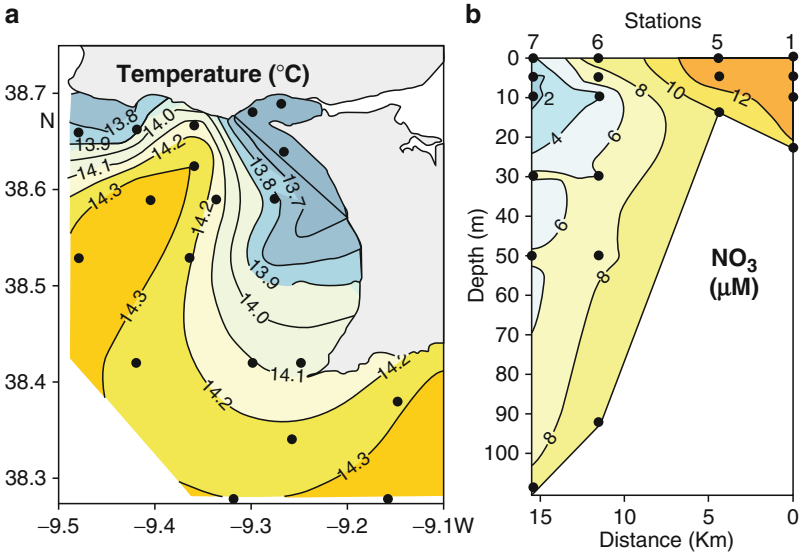

Fig. 4.3 Surface temperature distribution (**a**) and vertical nitrate distribution (**b**) in March 1994

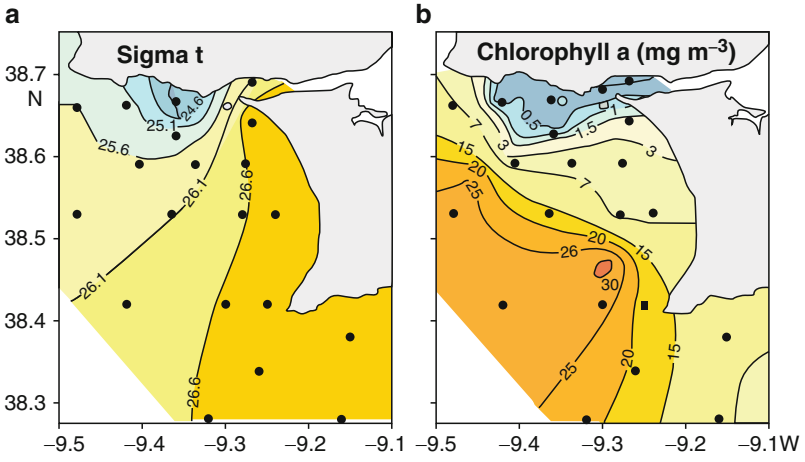

Fig. 4.4 Surface density distribution (**a**) and Chl *a* (integrated to 10 m depth) distribution (**b**) in March 1994

extremely high (1,800 m^3 s^{-1}). The estuarine plume extended quite offshore and relatively low salinity values (34.5) were found all over Tagus Bay (Fig. 4.5a). Nutrients reached at surface a maximum of 0.74 μM PO_4, 25 μM NO_3 and 27 μM $Si(OH)_4$, while Chl *a* did not surpass 1.9 mg m^{-3} in the estuarine plume boundary (Fig. 4.5b).

In June 2002, when river discharge was rather reduced (46 m^3 s^{-1}), the river plume was almost imperceptible and salinity was higher than 35. 5 all over the area (Fig. 4.6a).

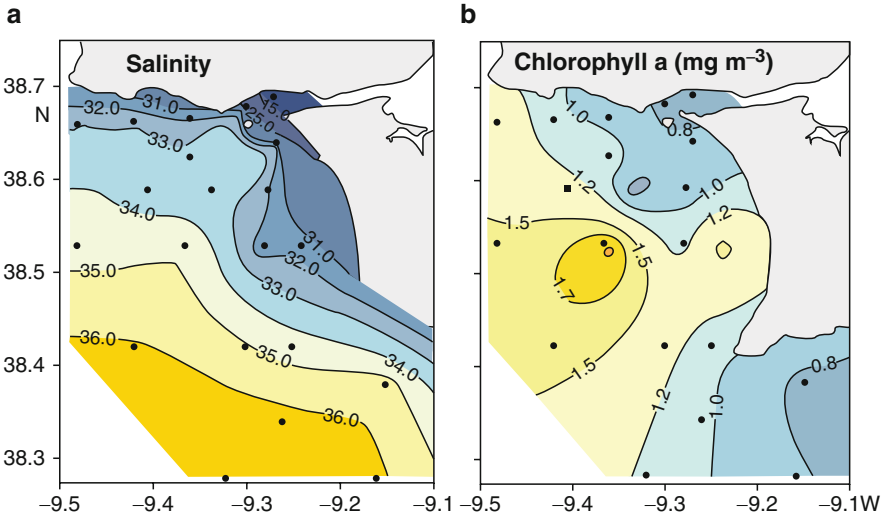

Fig. 4.5 Surface salinity distribution (**a**) and surface Chl *a* distribution (**b**) in March 2001

Table 4.1 Phosphate, total phosphorus, chlorophyll *a*, DNC_P and phosphate uptake in selected sampling stations, from Winter 1994 and Summer 2002

	Winter 1994				Summer 2002		
	St.13	St.14	St.7	St.16	St.4	St.6	St.18
PO_4 (μM)	0.64	0.58	0.28	0.06	0.42	0.09	0.21
TP (μM)	3.6	4.9	6.2	5.4	0.8	0.4	0.7
Chl*a* (mg m^{-3})	0.3	2.0	24.8	31.6	0.6	3.2	4.2
DNC_P	0.88	0.88	0.95	0.99	0.48	0.76	[a]
PO_4 uptake (%)	11	15	65	91	14	84	70

[a]Not estimated (located out of upwelling influence)

The signature of upwelling was clearly noticeable particularly at the northern margin (Fig. 4.6b) where cold water reached the surface (minimum temperature of 14.5°C). Nutrients displayed values up to 0.8 μM PO_4 (Fig. 4.7a), 9 μM NO_3, 3.2 μM $Si(OH)_4$, 1.68 μM TP and 49 μM TN at the estuary mouth, and Chl *a* reached maximum values up to 4.5 mg m^{-3} (Fig. 4.7b). Concerning the aging of upwelled waters, the calculated DNC_P (Table 4.1) attained a value of 0.48 at station 4 (center of upwelling) and 0.76 at station 6 which indicates younger upwelled waters at St.4. Calculated phosphate uptake varied between 14% at station 4 and 84% at station 6 (Table 4.1). Precisely in this last site, a higher amount of phytoplankton biomass developed, attaining chlorophyll *a* a value of 3.2 mg m^{-3}. Moreover, further outside the upwelling influence (St.18), a relatively high proportion of dissolved inorganic phosphorus uptake (70%) occurred, being likely responsible for the development of moderately high phytoplankton biomass, as Chl *a* reached values up to 5.0 mg m^{-3}.

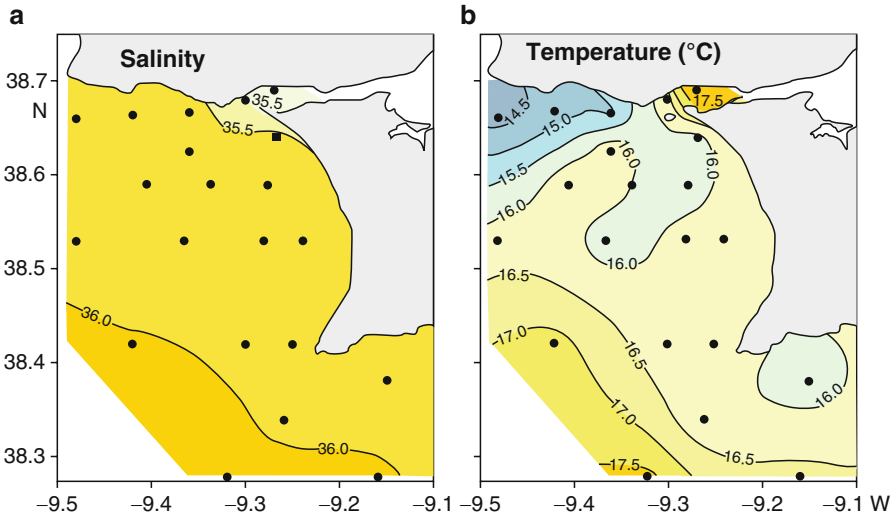

Fig. 4.6 Surface temperature distribution (**a**) and surface salinity distribution (**b**) in June 2002

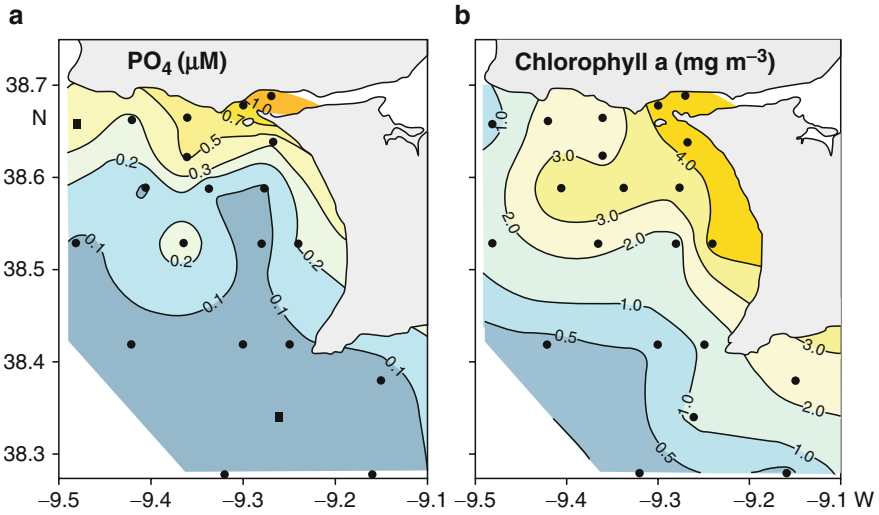

Fig. 4.7 Surface phosphate distribution (**a**) and surface Chl *a* distribution (**b**) in June 2002

Our results reveal the biogeochemical implications of distinct hydrological conditions over Tagus coastal waters, specifically in winter 1994, winter 2001 and summer 2002. In winter 1994 (March included), an extremely high positive NAO index was attained and upwelling developed in the study area. River discharge was considerable and a strong physical boundary was generated between the stratified river plume and the upwelled waters. The supply of nutrients carried by upwelled water from deeper layers and transported from the Tagus estuary, contributed to

maintain an exceptionally high phytoplankton blooming, favoured by the water column stability along the established front. Also, values of DNC_P index determined outside the center of upwelling, corresponding to more aged waters, were consistent with the considerable amounts of phytoplankton biomass developed. By contrast, the lower index values determined in the center of upwelling corresponded to more recently outcropped waters and were reflected in reduced phytoplankton biomass.

In winter 2001, following a shift in the NAO pattern from positive to negative, and under an extremely intense river discharge, the development of phytoplankton was quite reduced.

Furthermore, in June 2002, when an upwelling event occurred simultaneously with a reduced river flow, much lower phytoplankton biomass developed than in winter 1994. Apparently, during this sampling period, more recently upwelled waters than in 1994, as revealed by the lower index DNC_P in the upwelling center (Table 4.1), occupied the study area, which is in accordance with the moderately low amounts of phytoplankton biomass attained.

Finally, from our results, it can be concluded that DNC index can be used as a reasonably good indicator of upwelling events over the study area, even under changing upwelling regime.

4.3.2 Section 2

4.3.2.1 Phytoplankton and Ocean CO_2 Uptake

Increasing CO_2 concentration and continued acidification of surface seawater result in deterioration of ocean chemical conditions. Such changes, as already mentioned, are likely to affect the physiology of marine organisms, in particular the shell-forming and the coccolithophores, this oceanic primary producers group being an important carbonate producer.

Coccolithophores have been found in upwelling regions of both the northern and southern Atlantic (Blasco et al. 1980; Girandeau and Rogers 1994). There are frequent records of the Coccolithophorid species, in particular *Coccolithus pelagicus* (= *coccolithus braarudii*), in the Portuguese shelf associated with the Iberian upwelling season (Cachão and Moita 2000). Here we report the presence of a bloom of *C. braarudii* which developed in June 2002 in coastal waters adjacent to the Tagus estuary under the mentioned hydrographic conditions – upwelling and reduced Tagus river discharge. The phytoplankton bloom extended over the study area but maximum abundances of *C. braarudii* (Fig. 4.8a and b) were detected along the strong frontal region between upwelled and non-upwelled waters. Densities up to 60 cells mL^{-1} were reached at 30–50 m depth (Fig. 4.8b). Regarding pCO_2, values varied from 750 to 1,650 μatm (Fig. 4.9), the saturation of CO_2 with respect to atmospheric equilibrium being close to 460% saturation. Maximum oversaturation of pCO_2 corresponded to the upwelled waters (Fig. 4.6b) which transport high amounts of inorganic C from deeper layers (Figs. 4.6b and 4.9). It is

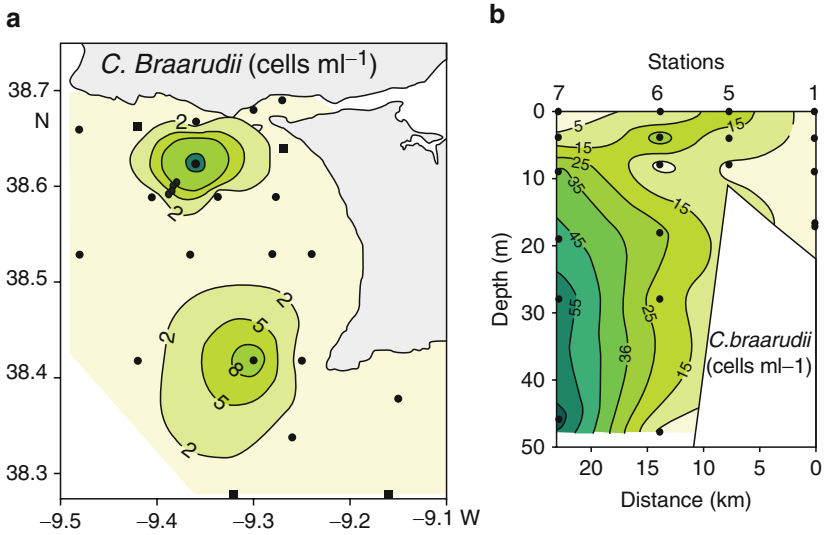

Fig. 4.8 Vertical *Coccolithus braarudii* distribution along transect St.1–7 (**a**) and surface *Coccolithus braarudii* distribution (**b**) in June 2002 (Adapted from Cabeçadas and Oliveira 2005)

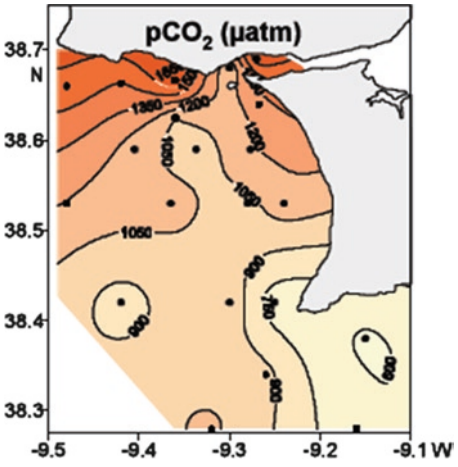

Fig. 4.9 Surface pCO_2 distribution in June 2002 (Adapted from Cabeçadas and Oliveira 2005)

worth noting that while the main phytoplankton group, the diatoms, proliferated throughout turbulent waters, coccolithophores developed under more stable conditions not directly affected by anthropogenic inputs and associated with relatively low nutrient levels. Apparently, the species *C. braarudii* found optimal

growing conditions close to the frontal zone between the upwelled mixed water and the thermally stratified one which occupied Tagus bay. Actually, based on the inorganic carbon content of *C. braarudii*, ~5 t of calcite were produced along the referred cross-shelf transect in the upper 30 m of the water column, which confirms that a significant deposition of calcium carbonate ($CaCO_3$) can occur in this coastal ecosystem (Cabeçadas and Oliveira 2005). Also, a value of 7.4 mmol CO_2 m^{-2} d^{-1} was calculated to be released by the total population of *C. braarudii* present, indicating that the calcification process constitutes an additional source of CO_2 to the water and, eventually, to the atmosphere in this area.

The present rise in atmospheric CO_2 levels and consequent changes in surface ocean pH and carbonate chemistry may, nevertheless, induce the slow-down of calcium carbonate production in the ocean surface. This decline of calcium carbonate production, as predicted by previous studies, will persist for hundreds of years even when surface waters remain supersaturated with respect to $CaCO_3$ (Kleypas et al. 1999; Feely et al. 2004). As a matter of fact, laboratory experiments with monospecific cultures of coccolithophorids *Emiliania huxleyi* and *Geophyrocapse oceanica* have shown that the ratio of particulate inorganic carbon (PIC) to particulate organic carbon (POC) decreased with increasing CO_2 concentrations. Such change in PIC/POC ratios is attributed to a decrease in calcification rates as well as to an increase in organic carbon production (Riebesell et al. 2000; Zondervan et al. 2001, 2002). Although, at present, it is not clear whether the reaction of other coccolithophorid species is similar to that of *E. huxleyi*, still coccolithophores are likely to change in the foreseeable future under a changing climate. In fact, the response of unicellular microalga, particularly coccolithophores, to the change of CO_2 chemistry in seawater, might be a shift towards noncalcifying phytoplankton species.

4.4 Final Remarks

Our findings highlight how diverse and complex effects of climate changes can be detected through various indicators in Tagus bay.

The results presented show that shifts of upwelling regime to winter, to a large extent attributable to changes in the NAO, lead to short-term effects on the biological patterns. Simultaneous intense river discharges can be considered an important driver to the increment of phytoplankton productivity in the coastal waters adjacent to the Tagus estuary. The excess of nutrients (inorganic and organic forms) supplied simultaneously by upwelled and Tagus river waters, stimulates, as well, phytoplankton growth. Further, physical settings consisting of a strong front established between the stratified plume waters and the mixed upwelled waters, favour the development of phytoplankton.

On the other hand, changes in seawater chemistry already emerging and trends predicted by the end of the century, might well cause shifts in current algal communities and alter the structure and biodiversity of coastal ecosystems. In particular, in Portuguese coastal waters, decreasing pH may have detrimental effects on coccolithophores and

influence competition among main phytoplankton taxa, being expected impacts at multiple trophic levels.

Although our findings illustrate the sensitivity of the shelf system under study to climate variations, knowledge about trophic relationships is scarce in the ocean around Iberia and the direction and magnitude of changes in the algal community are still not very well understood, predictions therefore being difficult to make.

References

Bakun A (1990) Global climate change and intensification of coastal ocean upwelling. Science 247:198–201

Bakun A (1992) Global greenhouse effects, multi-decadal wind trends and potential impacts on coastal pelagic fish populations. ICES Mar Sci Symp 195:316–325

Blasco D, Estrada M, Jones B (1980) Relationships between the phytoplankton distribution and composition and the hydrography in the Northwest African upwelling region near Cabo Corbeiro. Deep Sea Res 27:799–821

Borges MF, Santos AMP, Crato N, Mendes H, Mota B (2003) Sardine regime shifts off Portugal: A time series analysis of catches and wind conditions. Sci Mar 67:235–244

Cabeçadas G, Brogueira MJ, Cabeçadas L (1999) Tagus and Sado adjacent coastal waters (Portugal). In: Sheppard CRC (ed) Seas at the Millenium: An experimental evaluation. Elsevier, Kidlington, Oxford, UK, pp 151–165

Cabeçadas L, Oliveira AP (2005) Impact of a *Coccolithus braarudii* bloom on the carbonate system of Portuguese coastal waters. J Nannoplankton Res 27(2):141–147

Cachão M, Moita MT (2000) *Coccolithus pelagicus*, a productivity proxy related to moderate fronts off Western Iberia. Mar Micropaleontol 39:131–155

Chen ST (2000) The study of aging index of upwelling by the contents of several species of phosphorus. Acta Oceanol Sin 22:51–59 (in Chinese with English abstract)

Chen ST, Hsing LY, Liu CL, Wang SL (2004) Degree of nutrient consumption of upwelled water in the Taiwan Strait based on dissolved phosphorus or nitrogen. Mar Chem 87:73–86

Dias CA (1994) Notas sobre o hidroclima costeiro de Portugal Continental (Notes on the coastal hydroclimate of the Portuguese Mainland coast). IPIMAR Technical Report, unpublished

Dickson AG, Goyet C (1994) Handbook of methods for the analysis of the various parameters of the carbon dioxide system in seawater, version 2. US Department of Energy, Washington, DC

Dickson RR, Kelly PM, Colebrook JM, Wooster WS, Cushing DH (1988) North winds and production in the eastern North Atlantic. J Plankton Res 10(1):151–169

Engel A, Zondervan I, Aerts K, Beaufort L, Benthien A, Chou L, Delille B, Gattuso JP, Harlay J, Heemann C, Hoffmann L, Jacquet S, Nejstgaard J, Pizay MD, Rochelle-Newall E, Schneider U, Terbrueggen A, Riebesell U (2005) Testing the direct effect of CO_2 concentration on a bloom of the coccolithophorid *Emiliania huxleyi* in mesocosm experiments. Limnol Oceanogr 50:493–507

Feely RA, Sabine CL, Lee K, Berelson W, Kleypas J, Fabry VJ, Millero FJ (2004) Impact of anthropogenic CO_2 on the $CaCO_3$ system in the oceans. Science 305:362–366

Girandeau J, Rogers J (1994) Phytoplankton biomass and sea-surface temperature estimates from sea-bed distribution of nannofossils and planktonic foraminifera in the Benguela upwelling system. Micropaleontology 40(3):275–285

Hinga KR (2002) Effects of pH on coastal marine phytoplankton. Mar Ecol Prog Ser 238:281–300

Hurrell JW (1995) Decadal trends in the North Atlantic oscillation regional temperatures and precipitation. Science 269:676–679

Hurrell JW, van Loon H (1997) Decadal variations in climate associated with the North Atlantic oscillation. Clim Change 36:301–326

IPCC (2007) Climate change 2007: The physical science basis–Summary for policymakers contribution of working group I to the fourth assessment report of the intergovernmental panel on climate change. Intergovernmental Panel on Climate Change, Geneva, Switzerland

ISO (1997) Water quality–Determination of nitrogen, ISO, 11905-1, 13 p

Jones PD, Jonsson T, Wheeler D (1997) Extension of the North Atlantic oscillation using early instrumental pressure observations from Gibraltar and south-west Iceland. Int J Climatol 17:1433–1450

Kleypas JA, Buddemeier RR, Archer D, Gattuso JP, Lansdon C, Opdyke BN (1999) Geochemical consequences of increased atmospheric carbon dioxide on coral reefs. Science 284:118–120

Lavin A, Diaz del Rio G, Casas G, Cabanas JM (2000) Afloramiento en el noroeste de la Peninsula Ibérica. Índices de afloramiento para el punto 43ºN, 11ºO, Periodo 1990–1999 (Upwelling in the NW of the Iberian Peninsula. Upwelling indexes at 43ºN, 11ºW between 1990 and 1999). Datos y Resúmenes Instituto Espanol de Oceanografia (15)

Lee K, Millero FJ, Wanninkhof R (1997) The carbon dioxide system in the Atlantic Ocean. J Geophys Res 102(C7):15693–15707

Nogueira E, Pérez FF, Rios AF (1997) Seasonal patterns and long-term trends in an estuarine upwelling ecosystem (Ria de Vigo, NW Spain). Estuar Coast Shelf Sci 44:285–300

Oliveira AP (1999) PROTALK–Potentiometric titration for determination of total alkalinity – a program developed for CO_2 system calculation. Rel IPIMAR, 73 pp

Orr JC, Fabry VJ, Aumont O, Bopp L, Doney SC, Feely RA, Gnanadesikan A, Gruber N, Ishida A, Joos F, Key RM, Lindsay K, Maier-Reimer E, Matear R, Monfray P, Mouchet A, Najjar RG, Plattner G, Rodgers KB, Sabine CL, Sarmiento JL, Schlitzer R, Slater RD, Totterdell IJ, Weirig MF, Yamanaka Y, Yool A (2005) Anthropogenic ocean acidification over the twenty-first century and its impact on calcifying organisms. Nature 437:681–686

Peliz A, Dubert J, Santos AMP, Oliveira PB, Le Cann B (2005) Winter upper ocean circulation in the Western Iberia Basin–fronts, eddies and poleward flows: An overview. Deep Sea Res I 52:621–646

Peliz AJ, Fiuza AFG (1999) Temporal and spatial variability of CZCS-derived phytoplankton pigment concentrations off the western Iberia Peninsula. Int J Remote Sens 20:14197–14207

Relvas P, Barton ED, Dubert J, Oliveira PB, Peliz A, da Silva JCB, Santos AMP (2007) Physical oceanography of the Western Iberia, ecosystems: Latest views and challenges. Prog Oceanogr 74(2–3):149–173

Riebesell U (2004) Effects of CO_2 enrichment on marine phytoplankton. J Oceanogr 60:19–729

Riebesell U, Zondervan I, Rost B, Tortell PD, Zeebe RE, Morel FMM (2000) Reduced calcification on marine plankton in response to increased atmospheric CO_2. Nature 407:364–367

Roy RN, Roy LN, Vogel KM, Porter-Moore C, Pearson T, Good CE, Millero F, Campbell DM (1993) The dissociation constants of carbonic acid in seawater at salinities 5 to 45 and temperatures 0 to 45ºC. Mar Chem 44:249–267 (Erratum, 1994. Mar Chem 45:337. Erratum, 1996. Mar Chem 52:183)

Royal Society (2005) Ocean acidification due to increasing atmospheric carbon dioxide. Policy Document 12/05, The Royal Society

Santos AMP, Kazmin AS, Peliz A (2005) Decadal changes in the Canary upwelling system as revealed by satellite observations: Their impact on productivity. J Mar Res 63:359–379

Strickland JDH, Parsons TR (1972) A practical handbook of seawater analysis. Bull Fish Res Board Can 167:201

Takahaschi M, Ishimaru T, Atkinson LP, Lee TN, Yamaguchi Y, Fujita Y, Ichimura S (1986) Temporal change in nutrient concentrations and phytoplankton biomass in short time scale local upwelling around the Izu Peninsula, Japan. J Plankton Res 8:1039–1049

Tréguer P, Le Corre P (1975) Manuel d'analyse des sels nutritifs dans l´éau de mer. Utilisation de l'auto-analyzer II: Technicon. LOC-UBO, Brest. 2ème Edition, 110 pp

Weiss RF (1974) Carbon dioxide in water and seawater; the solubility of a non-ideal gas. Mar Chem 2:203–215

Zondervan I, Zeebe RE, Rost B, Riebesell U (2001) Decreasing marine biogencalcification: A negative feedback on rising atmospheric pCO_2. Global Biogeochem Cycles 15(2):507–516

Zondervan I, Rost B, Riebesell U (2002) Effect of CO_2 concentration on the PIC/POC ratio in the coccolithophore *Emiliania huxleyi* grown under light-limiting conditions and different day lengths. J Exp Mar Biol Ecol 272:55–70

Chapter 5
pH Decrease and Effects on the Chemistry of Seawater

Juana Magdalena Santana-Casiano and Melchor González-Dávila

Abstract Variation in seawater pH is just one response to the increased CO_2 concentration in the atmosphere due to anthropogenic activities. The decrease in pH has a significant effect on the carbonate chemistry of the ocean and causes a decrease in the calcium carbonate saturation state (Ω). Ten years of experimental pH measurements at the ESTOC station show a progressive reduction on pH in the ocean (-0.0017 ± 0.0002 year^{-1}) and its effects on its carbonate chemistry. The calcium carbonate saturation state decreases by 0.018 ± 0.006 unit year^{-1} for calcite and 0.012 ± 0.004 unit year^{-1} for aragonite. The direct consequences of the pH decrease are a decrease in the buffer capacity (-1.99 ± 0.25 μmol kg^{-1} year^{-1}) and an increase in the Revelle factor (0.02 ± 0.002 year^{-1}) of the surface seawater.

Keywords Carbon dioxide • pH • Alkalinity • Total inorganic carbon • Carbonate • Seawater • Atmosphere • Borate • Saturation state • Calcite • Aragonite • ESTOC • Time series station • Buffer capacity • Revelle factor

5.1 Introduction

Distribution of the different components of the CO_2 system in the oceans has been studied by many workers. An extensive review has been recently presented by Millero (2007) about the marine carbon cycle and the effects of excess CO_2 in the atmosphere on the carbonate system. Reduction of pH due to anthropogenic

J.M. Santana-Casiano (✉) and M. González-Dávila
Faculty of Marine Science, Department of Chemistry,
University of Las Palmas de Gran Canaria, 35017 Las Palmas, Spain
e-mail: jmsantana@dqui.ulpgc.es; mgonzalez@dqui.ulpgc.es

P. Duarte and J.M. Santana-Casiano (eds.), *Oceans and the Atmospheric Carbon Content*,
DOI 10.1007/978-90-481-9821-4_5,

activities (Orr et al. 2005; Raven et al. 2005) is one of the most important features of the increased concentration of carbon dioxide in the atmosphere. Calculations, based on measurements of the ocean surface and coupled with existing knowledge of the ocean's chemistry, indicate that the uptake of CO_2 after pre-industrial time has led to a reduction of the surface seawater pH of 0.1 units over its pre-industrial values. This is equivalent to a 30% increase in the concentration of hydrogen ions (Caldeira and Wickett 2003). By the end of the century, the models predict that pH will decrease another 0.3–0.4 units (Haugan and Drange 1996), the dissolved inorganic carbon, C_T, may increase by over 12%, and the carbonate ion concentration may decrease by 60% (Kleypas et al. 1999).

In the last years, the term "ocean acidification" has been used to describe the decreasing pH of the ocean. However, as pointed out by Kleypas et al. (2006), this terminology must be used to describe the process rather than a chemical state because the ocean pH is not expected to be lower than 7.

Variation in pH is not an isolated problem. Change in pH has important consequences for most of the biogeochemical processes occurring in the ocean, including biological activity, toxicity of metals, bioavailability, making it more difficult for marine calcifying organisms to form biogenic calcium carbonate. A lower ocean pH has an impact, not only on the carbonate biochemistry, but also on the chemistry of the other compounds present in seawater, mainly those relating to biological activity, such as trace metals, which are modified in speciation (Santana-Casiano et al. 2006). A decrease in pH may affect the solubility of some minerals (Stumm and Morgan 1981; Liu and Millero 2002) and also the distribution of chemical species, favouring the free dissolved forms of metals, and exerting significant physiological, ecological and toxicological effects on organisms.

In this chapter we study step by step the different consequences that the reduction of pH has had in the surface inorganic carbon chemistry and in its buffer capacity in the ocean during the decade 1995–2005. To achieve this fCO_2 (μatm), pH_T total alkalinity (A_T) and total inorganic carbon (C_T) over 10 years at the ESTOC site have been examined.

5.2 The Oceanic Time Series Station ESTOC

The ESTOC site (29°10′N, 15°30′W) is located at approximately 100 km north of the islands of Gran Canaria and Tenerife, and has a depth of 3,600 m (Fig. 5.1). The time series station was inaugurated in February, 1994 and has continued its monthly operations through the year 2004. After 2004, the ESTOC site has been visited seasonally. This station is intended to be representative of the eastern boundary of the northeast Atlantic Ocean.

During the first 10 years, samples were taken monthly at the station and were supplemented by current meters and sediment trap moorings, attended by

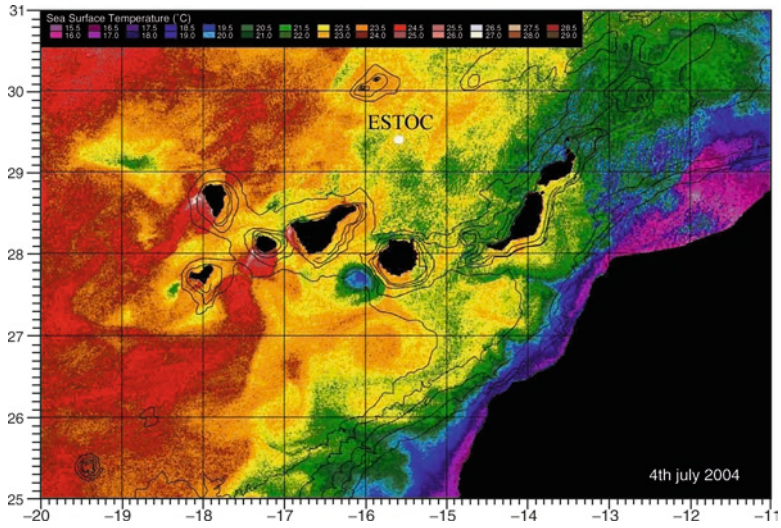

Fig. 5.1 Location of the ESTOC site (29°10′N, 15°30′W) in the Eastern North Atlantic Ocean. (AVHRR Image was provided by SeaS Canarias-Departamento de Biología ULPGC-Viceconsejería de Pesca)

German research groups from the Institut für Meereskunde, Kiel, and the Fachbereich Geowissenschaften, at the University of Bremen. Monthly cruises were conducted by the Instituto Canario de Ciencias Marinas. Additional validation cruises (2 year^{-1}), on board the German vessels, resolved the spatial variability of the biogeochemical parameters near the ESTOC. From September 1995, registers of the carbon dioxide system variables, including pH in total scale at 25°C (pH_T), total alkalinity (A_T), the fugacity of CO_2 in the atmosphere (fCO_2 air) and surface seawater (fCO_{2sw}) were added to the monthly determinations for oxygen, nutrients and chlorophyll concentration. During 2004, direct determination of the total dissolved inorganic carbon concentration (C_T) was also included in the sampling strategy. From 2005 to 2008 the fugacity of CO_2 in the atmosphere (fCO_2 air) and surface seawater (fCO_{2sw}) have been registered inside the CARBOOCEAN Project using a voluntary observing ship in the QUIMA-VOS line.

The hydrograph properties present a seasonal variation that can be observed in Fig. 5.2. The temperature varies from 18°C to 24°C and the salinity from 36.6 to 37 and consequently the density changes from 25 to 26.4. Convective mixing in winter and stratification of the water column from May to October controls the seasonal change. As a consequence the depths of the mixed layer fluctuated from 25 to 200 m reaching maximum stratification in September–October. The deepest winter values of the mixed layer changed from 120 m in 1998, 2003 to 200 m in 1996, 1999 and 2000 (Santana-Casiano et al. 2007).

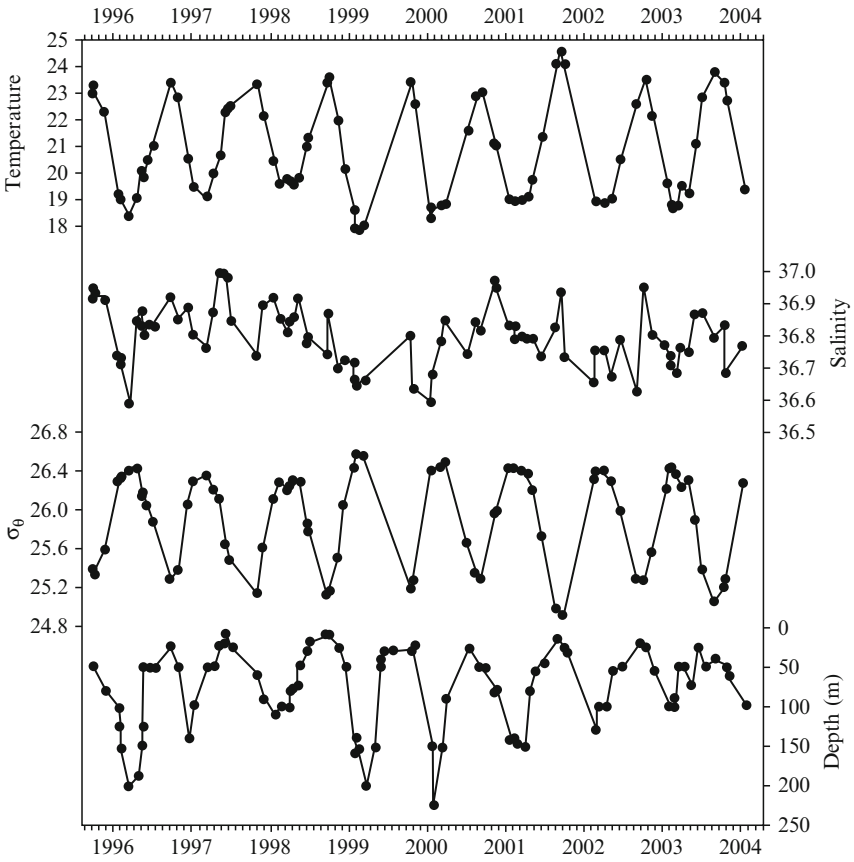

Fig. 5.2 Time series of hydrography properties at ESTOC station from 1995 to 2004. Temperature, Salinity, Potential density σ_θ, and mixed layer depth (MLD)

5.3 The Carbon Dioxide System at the ESTOC Site

The carbonate system regulates the pH of seawater and controls the circulation of CO_2 between the biosphere, the lithosphere, the atmosphere and the ocean. The CO_2 enters in the ocean across the air–sea interface and participates in the equilibrium processes outlined by Eqs. 5.1–5.4. The CO_2 dissolved in the ocean is also used by plants in primary production and this is taken into account considering Eq. 5.5.

$$CO_{2(g)} \leftrightarrow CO_{2(aq)} \tag{5.1}$$

$$CO_{2(aq)} + H_2O \leftrightarrow H^+ + HCO_3^- \tag{5.2}$$

$$HCO_3^- \leftrightarrow H^+ + CO_3^{2-} \tag{5.3}$$

$$Ca^{2+} + CO_3^{2-} \leftrightarrow CaCO_{3(s)} \quad (5.4)$$

$$CO_2 + H_2O \leftrightarrow CH_2O + O_2 \quad (5.5)$$

To characterize the components of the carbonate system, at least two of the four measurable parameters must be used: the fugacity of CO_2 (fCO_2), the pH, the total alkalinity (A_T) and the total inorganic carbon (C_T). A detailed description of carbonate system equilibrium, a definition of the components of the carbonate system and the use of different constant sets is given by Millero (2007).

5.3.1 fCO_2

5.3.1.1 fCO_2 Measurements

The fCO_2 in air and in surface seawater is determined using a flow system described by González-Dávila et al. (2003). A differential, non-dispersive infrared gas analyzer (LI-6262 CO_2/H_2O Analyzer) measures the concentration of CO_2 in the air and in the equilibrated air samples. The system is calibrated by measuring two different standard gases with mixed ratios of around 350 and 450 ppm CO_2 in the air (NOAA), traceable to the World Meteorology Organization Scale. The system has a precision of ±1 μatm and its accuracy compared to standard gases of ±2 μatm. The fugacity of CO_2 in seawater is calculated from the measured x_{CO2} following Dickson and Goyet (1994).

5.3.1.2 fCO_2 Results

Studies made at the ESTOC site showed that fCO_2 increased in seawater from 1995 to 2004, at an average rate of 1.55 ±0.43 μatm year^{-1}, (Santana-Casiano et al. 2007) similar to the increased uptake in the atmosphere (1.6 ± 0.7 μatm year^{-1}), obeying Henry´s law whereby the surface waters mix slowly with deeper waters inside subtropical areas. Seawater fCO_2 is strongly correlated with temperature with a seasonal variability of around 70 μatm, with minimum values (320–330 μatm) in Winter and the maximum ones (390–400 μatm) in Summer. The correlation with the temperature is defined by the equation

$$fCO_2 = -2924.72 + 1.546t + 9.535SST - 2.253\sin\left(2\pi\left(t - 1995\right)\right) \quad R^2 = 0.89. \quad (5.6)$$

The average annual increase of fCO_2 during the first 10 years was 1.55 ± 0.43 μatm year^{-1} and considering the values until today the increase reaches values of 1.75 μatm year^{-1}.

The atmospheric fCO_2 presents a seasonal variability of 7 μatm with an average annual increase of 1.6 ± 0.7 μatm year^{-1} and actually 1.8 μatm year^{-1}.

5.3.2 pH

5.3.2.1 pH Measurements

The pH is measured in total scale ($[H^+]_T = [H^+]_F + [HSO_4^-]$, where $[H^+]_F$ is the free proton concentration), pH_T. A potentiometric technique using a ROSS™ glass pH electrode and an Orion double junction Ag/AgCl reference electrode was initially used until June 1997 for the determination of pH_T at 25°C. The electrode was calibrated by using a Tris/HCl buffer in synthetic seawater with salinity 35 SOP 6 (Dickson and Goyet 1994). Repeated CRM (Certified Reference Material for CO_2 determinations) samples (n = 90, batch #34, #42) gave a standard deviation of 0.003 units.

After June 1997, an automated system based on the spectrophotometric technique of Clayton and Byrne (1993) with the m-cresol purple as indicator is used (González-Dávila et al. 2003). CRMs pH_T reading (batch #42) gave a standard deviation of 0.0015 (n = 59).

The pH in total scale at 25°C, $pH_{T,25}$, together with total alkalinity is used to compute the pH in total scale at in situ temperature conditions, $pH_{T,in\ situ}$ following Millero (2005) and the CO2sys program (Lewis and Wallace 1998).

5.3.2.2 pH Results

The ESTOC site is a long-time series station in the ocean with direct monthly determinations of pH as of October 1995, showing that the Eastern Atlantic Ocean has suffered a decrease in $pH_{T,25}$ (Fig. 5.3) at a rate of 0.0017 ± 0.0004 $year^{-1}$ (Santana-Casiano et al. 2007). pH has decreased 0.017 units over the last decade. If it is assumed that the pH is to continue decreasing at the same rate, a variation around 0.2 units in the next century is predicted, and this value should be considered as a minimum one. This variation confirms the model predictions with respect to pH changes in the next century (Caldeira and Wickett 2003). However, the prediction of a continuous exponential CO_2 emission along this century may increase the rate over longer periods and consequently the final effect.

5.3.3 A_T

5.3.3.1 A_T Measurements

Samples for A_T are potentiometrically titrated with standarized 0.25 M HCl (0.45M in NaCl) to the carbonic acid end point using two similar systems, described in detail by Mintrop et al. (2000). The titration of different CRMs (#32, #35, #42, #46) is used to test the performance of the titration system, given values that are within ±1.5 μmol kg^{-1} of the certified value. After 2004, a VINDTA 3C system (Mintrop

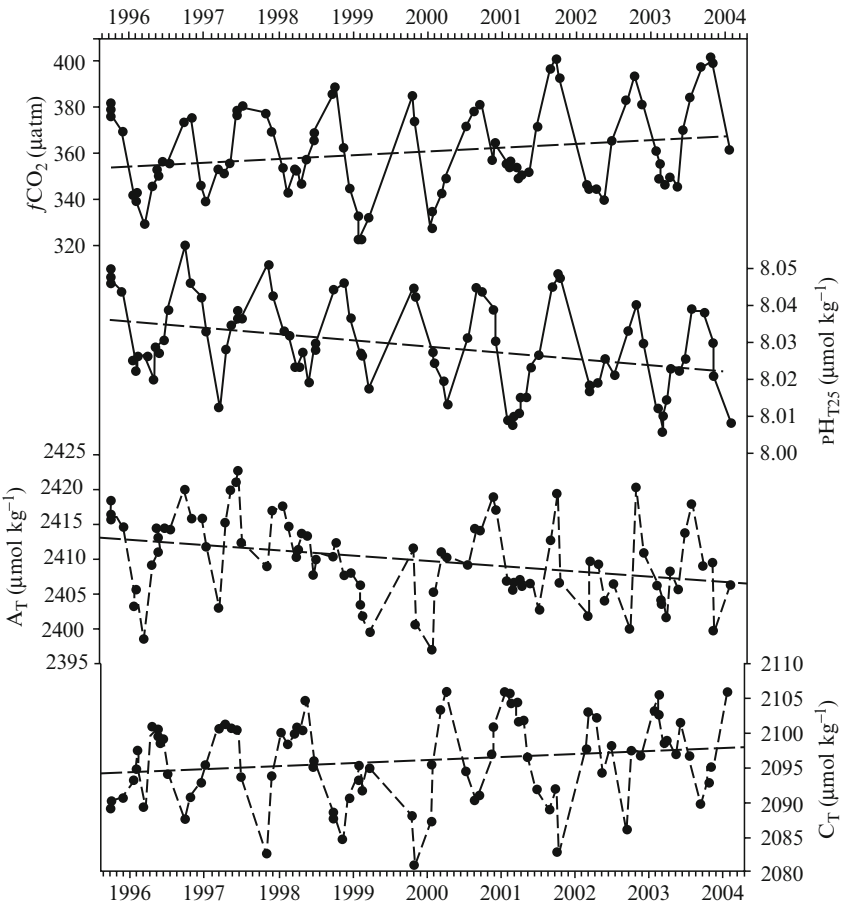

Fig. 5.3 Time series of inorganic carbon parameters at ESTOC station from 1995 to 2004. fCO_2, pH_T, A_T, C_T. Dotted line represents linear trend for the experimental data

et al. 2000) was used for alkalinity measurements with a precision of ±1.0 μmol kg^{-1} (www.MARIANDA.com).

5.3.3.2 A_T Results

The surface's total alkalinity shows a variability of 25 μmol kg^{-1} closely linked to the salinity cycle (r = 0.812) and when it is normalized to the mean salinity value at ESTOC of 36.8, a constant value of 2409.7 ± 2.4 μmol kg^{-1} is obtained.

When the total alkalinity is normalized to a constant salinity of 35, a value of 2291.8 ± 2.2 μmol kg^{-1} is obtained which coincides with the mean value for the North Atlantic Ocean given by Millero et al. (1998).

5.3.4 C_T

5.3.4.1 C_T Measurements

C_T is computed from experimental values of pH_T and A_T using the carbonic acid dissociation constants of Mehrbach et al. (1973) after Dickson and Millero (1987). On average, the $C_T(pH_T\text{-}A_T)$ values are 1 μmol kg^{-1} higher than certified CRMs values with a C_T residual of ±3 μmol kg^{-1} (n = 90). After 2004, a VINDTA 3C system (Mintrop et al. 2000) with coulometer determination was used with a substantially increased system precision of ±1.0 μmol kg^{-1} (www.MARIANDA.com).

5.3.4.2 C_T Results

The dissolved inorganic carbon in the surface presented a seasonal variability of 20–30 μmol kg^{-1} with the lowest values in October and maximum values in April and May.

C_T has increased 10 μmol kg^{-1} in a decade with a seasonal variability inversely related to SST changes (González-Dávila et al. 2007), changes in biological production and gas exchange processes in the area. NC_T has increased at a rate of 0.99 μmol kg^{-1}.

5.4 Inorganic Carbon and Boron Speciation

The pH is the chemical variable that controls the speciation of acid–base equilibrium of the carbonic and boric systems. The total inorganic carbon, defined by the sum of inorganic carbon species, $C_T = CO_{2(aq)}$ (+ H_2CO_3) + HCO_3^- + CO_3^{2-}, and the relative proportion of these carbon species mainly control the pH of surface seawater and to a lesser extent the borate –boric acid system. Both systems buffer the solution and restrict the capacity for changes in the pH. Boric acid together with the carbonate system significantly contribute to the A_T of seawater. The total boron is $B_T = H_3BO_3 + B(OH)_4^-$ and the concentration of $B(OH)_4^-$ to the total alkalinity is determined from $[B(OH)_4^-] = B_T K_B/([H^+] + K_B)$ where the total boric acid in seawater is assumed $B_T = 0.000412$ (S/35) following Dickson (1990).

From the measurements of fCO_2, pH_T, *in situ* A_T and S at the ESTOC site, the evolution of the different inorganic carbon species ($NC_{T,36.8}$, HCO_3^-, CO_3^{2-}) and borate ($B(OH)_4^-$) during the 10 years of study have been determined using the CO2sys program and the Mehrbach et al. (1973) after Dickson and Millero (1987) set of constants, and presented in Fig. 5.4. Taking into account that the total inorganic carbon concentration normalized to a constant salinity of 36.8, $NC_{T,36.8}$, has increased at a rate of 0.99 ± 0.12 μmol kg^{-1} $year^{-1}$ since 1995 (Santana-Casiano et al. 2007; González-Dávila et al. 2007), the net effect of the increased atmospheric CO_2 concentration in the seawater at the ESTOC site is the increase in the concentration of H^+ or the decrease of $pH_{T,in\ situ}$ (0.0017 ± 0.0002 $year^{-1}$), the increase in

the HCO_3^- concentration (1.24 ± 0.16 μmol kg^{-1} year^{-1}), the decrease of the CO_3^{2-} concentration (–0.89 ± 0.06 μmol kg^{-1} year^{-1}) and the decrease of the $B(OH)_4^-$ concentration (–0.31 ± 0.02 μmol kg^{-1} year^{-1}) (Fig. 5.4). The total alkalinity, normalized to a constant salinity of 35, kept constant during the study period to a value of 2291.8 ± 2.2 μmol kg^{-1} (Santana-Casiano et al. 2007). Figure 5.4 also shows the annual variation after removing the seasonal variability using the SPSS

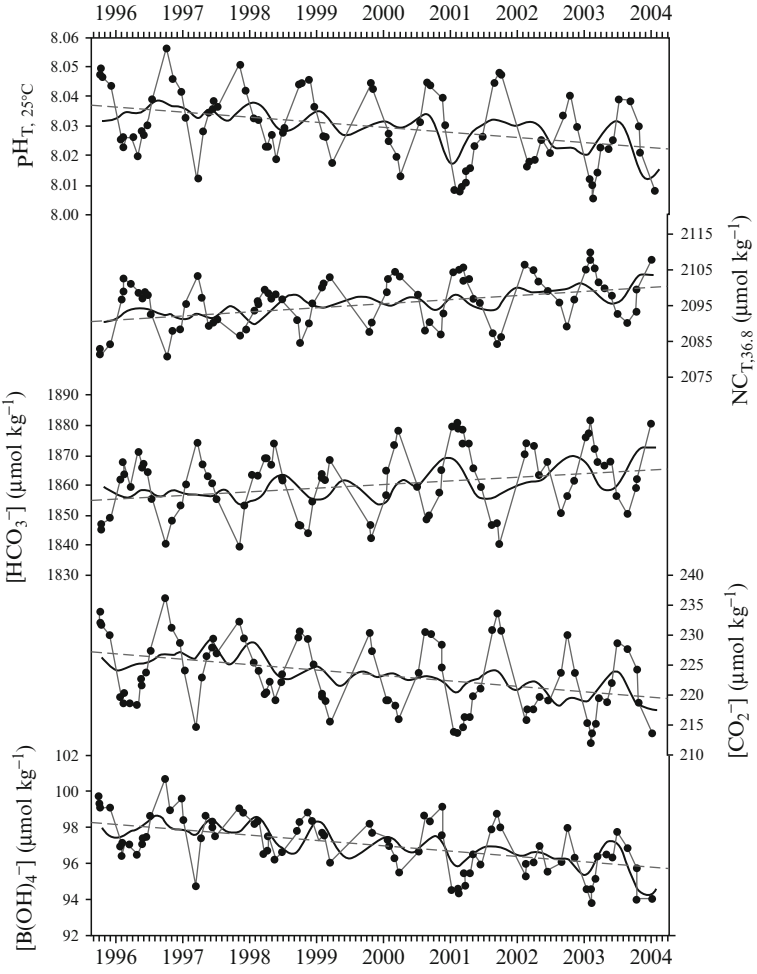

Fig. 5.4 Time series of pH in total scale at 25°C, total dissolved inorganic carbon normalized to an average salinity of 36.8, $NC_{T,36.8}$, inorganic carbon species HCO_3^-, CO_3^{2-} and borate, $B(OH)_4^-$ in the upper-ocean surface of the North East Atlantic Ocean, at the ESTOC site (29°10′ N, 15°30′ W). To highlight interannual variability, the mean seasonal cycle was removed by subtracting harmonics with 12-, 6- and 4-month periods from the data. The resulted values (*smoothing splines*) are the corresponding seasonal de-trended time series data and dotted lines are the linear regressions for de-trended data

program (version 13) and the routine trend cycle, to obtain what we know as "de-trended" data (González-Dávila et al. 2003).

5.5 Buffer Intensity

The ability of a solution to accommodate addition of acid or base without appreciable pH change (Stumm and Morgan 1981; Pankow 1991) is measured by the buffer intensity of the solution, β (μmol kg^{-1}). In open ocean waters, pH and buffer intensity are mainly controlled by the carbonate system, and to a lesser effect by the borate system (Fig. 5.5). An increase in fCO_2 in seawater produces a change in the pH which affects the buffer intensity of the ocean (Skirrow 1975). The buffer intensity is defined as a function of the C_T, pH and total boron in seawater and expressed by Eq. 5.7.

$$\beta = 2.303\ \{C_T K_1^* H\left(H^2 K_1^* K_2^* + 4K_2^* H\right)/\left(H^2 + K_1^* H + K_1^* K_2^*\right)^2 + B_T K_B^* H / \left(K_B^* + H\right)^2 + H + OH\} \tag{5.7}$$

where K^*_1 and K^*_2 are the first and second stoichiometric ionization constants of carbonic acid in seawater, and B_T and K^*_B are the total concentration and stoichiometric ionization constants of borate acid in seawater (Dickson 1990; Millero 2007).

Figure 5.5 shows two regions of high buffer intensity (around 1,200 μmol kg^{-1}) at the pH values corresponding with the pK* values of the carbonic acid. The presence

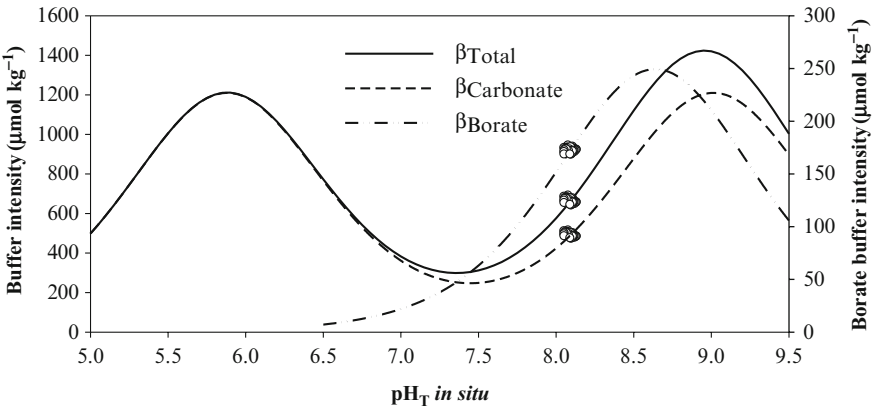

Fig. 5.5 Total buffer intensity in μmol kg^{-1} computed according to Eq. 5.7 as a function of pH_T at *in situ* conditions. Carbonate and Borate buffer intensity are also included together with experimental values (*open circles*) determined in surface waters at ESTOC site from 1995 to 2004

of boric acid in seawater with a pK^* value of 8.6 (20.7°C) significantly contributes to the total buffer intensity, reaching values of 250 μmol kg^{-1} in the maximum buffer intensity of the borate system. As a result of both contributions, the total buffer intensity (Eq. 5.7) follows a similar behaviour to the carbonate buffer intensity at pH below 7, being modified at higher pH by the boric contribution. It should also be pointed out that the pH_T in surface seawater (Fig. 5.5) and in the water column ranges from 8.1 to 7.4 which are located out of the region of maximum buffer intensity of natural seawater.

The average buffer intensity of surface seawater at ESTOC in the studied period is 662 ± 12 μmol kg^{-1}. The seasonal variability of the buffer intensity is affected by seasonal changes in C_T, pH and B_T. As a result, β presents maximum values in September–October over 670 μmol kg^{-1} and minimum ones in February–March with values below 650 μmol kg^{-1}. The buffer intensity values obtained for the ESTOC are in accordance with values reported for the global ocean (Zhang 2001). As the pH is decreasing and moving out of the maximum buffer capacity, the increased CO_2 levels in the atmosphere will produce higher changes in the pH of surface seawater. The buffer intensity of seawater has decreased at a rate of –1.99 ± 0.16 μmol kg^{-1}, thereby changing the ability of the surface seawater solution to accommodate addition of acids from β = 682 μmol kg^{-1} in autumn 1995, to β = 665 μmol kg^{-1} in 2003 (Fig. 5.6).

The buffer intensity is decreasing not only due to carbon chemistry, but also to the progressive lower contribution of borate (Fig. 5.6) to the buffer capacity of seawater as a result of pH reduction. The carbonate contribution presents a seasonal variability of 30 μmol kg^{-1} related to the seasonal change in C_T (Santana-Casiano et al. 2007) with decreasing values from $\beta_{Carbonate}$ = 507 μmol kg^{-1} in autumn 1995, to $\beta_{Carbonate}$ = 497 μmol kg^{-1} in 2003. The borate contribution follows a similar pattern with a seasonal variability of 6 μmol kg^{-1} and changing from β_{Borate} = 175 μmol kg^{-1} in autumn 1995, to β_{Borate} = 169 μmol kg^{-1} in 2003. The rate of change in both contributors in the period 1995–2004 was –1.33 ± 0.43 and –0.44 ± 0.07 μmol kg^{-1} $year^{-1}$ for carbonate and borate, respectively. In order to account for the observed changes, Fig. 5.7 shows the annual contribution in percentage of carbonate, borate, and OH^- + H^+ systems to the total buffer intensity. As $pH_{T,in\ situ}$ change seasonality (Fig. 5.6) with maximum values in February–March and minimum values in September–October, the contribution of the different systems is changing. However, the contribution of carbonate and borate systems presents an opposite trend. This behaviour can be explained following the rate of change as a function of pH from Fig. 5.5.

The consequences of increased CO_2 atmospheric concentration in surface waters at the ESTOC site during the decade can be observed in Fig. 5.8, where the buffer intensity is plotted vs the pH_T at the in situ temperature condition. In 1996, $pH_{T,in\ situ}$ was in the range from 8.08 (October) to 8.13 (March), while β moved from 690 to 665 μmol kg^{-1}, respectively. In 2003, the $pH_{T,in\ situ}$ decreased 0.02 units (8.055 in October to 8.11 in March), and β decreased 15 μmol kg^{-1} (675–640 μmol kg^{-1}). If this similar trend is sustained in the coming years, none of the values observed for both surface pH and buffer intensity in 1996 will be found after 25 years (around 2021). By the end of this century, the surface ocean pH is expected to be reduced in 0.3–0.4 units under the IS92a scenario (Haungan and Drange

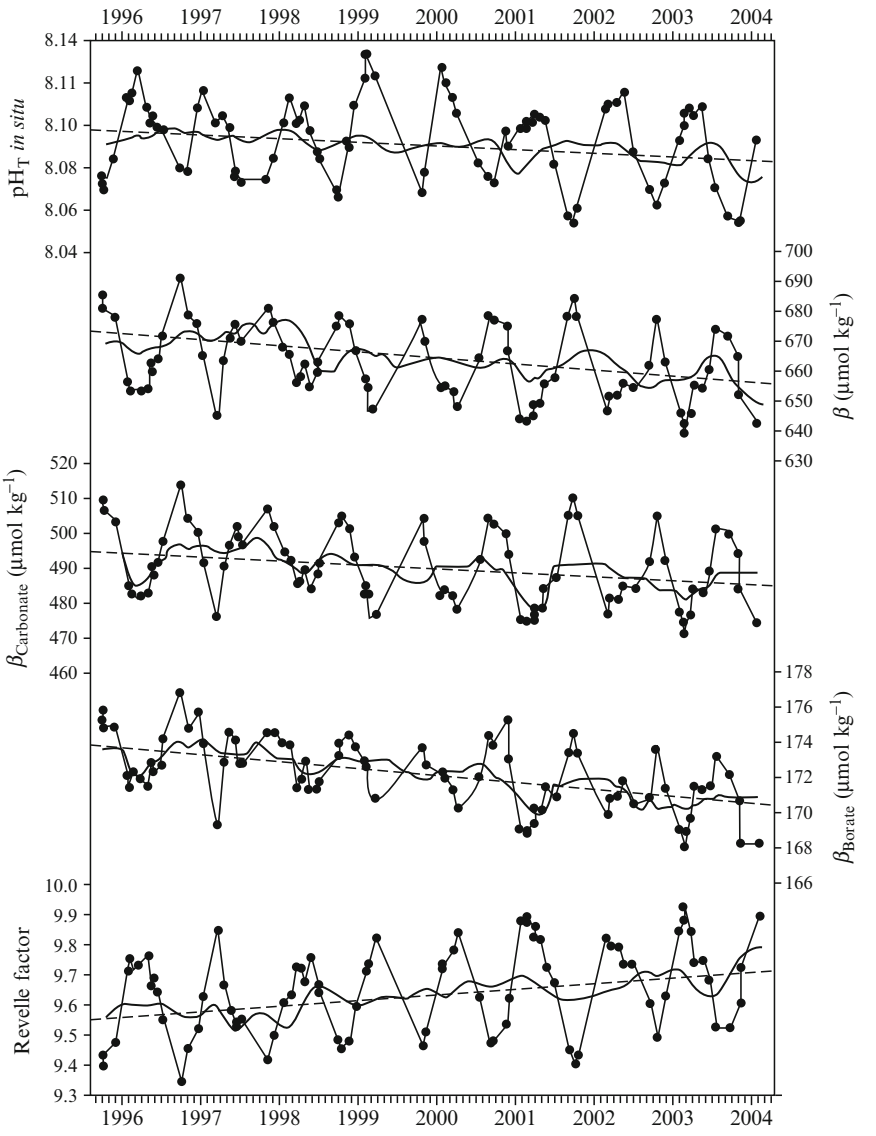

Fig. 5.6 Time series of pH in total scale at *in situ* conditions, total buffer intensity and carbonate and borate buffer intensities in µmol kg^{-1} together with Revelle factor *R* in the surface waters at the ESTOC site. Seasonal de-trended time series data (*splines*) are also included

1996; Brewer 1997). If only the change in pH is considered and the 1996 $pH_{T,in\ situ}$ at ESTOC (8.05) reduces by 0.3 units, β, $\beta_{Carbonate}$ and β_{Borate} will be reduced by 36%, 35% and 38%, respectively. However, as a decrease in pH occurs with an increase in C_T, if we assume a steady rate of increase in C_T of 0.99 µmol kg^{-1} year^{-1}

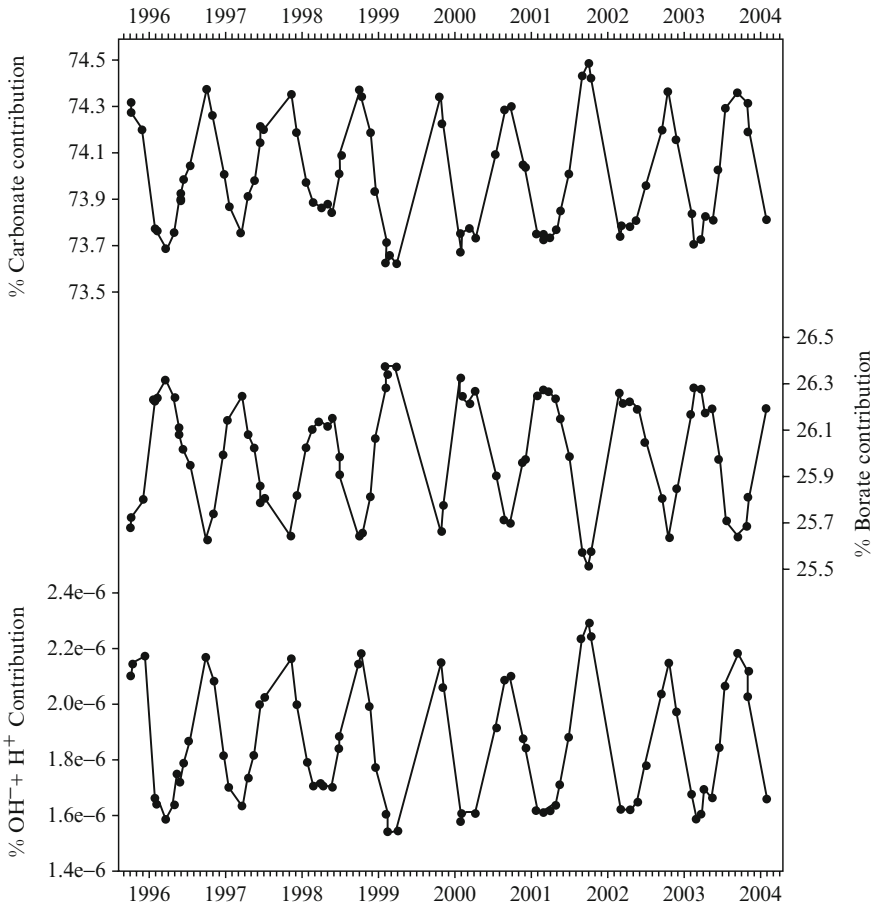

Fig. 5.7 Time series of data for the carbonate, borate and (OH^-+H^+) percentage of contribution to the total buffer intensity following Eq. 5.1 considering *in situ* conditions

determined in ESTOC, the buffer capacity will decrease by 33% instead of the above indicated 36%.

5.6 Revelle Factor

The reduction of pH also affects the efficiency of the ocean to take up CO_2. To compute this effect, is necessary to take into consideration the Revelle factor, *R*. This factor defines the relationship between the changes in the pCO_2 (ΔpCO_2) and the C_T (ΔC_T) in the ocean (Revelle and Suess 1957), and is given by

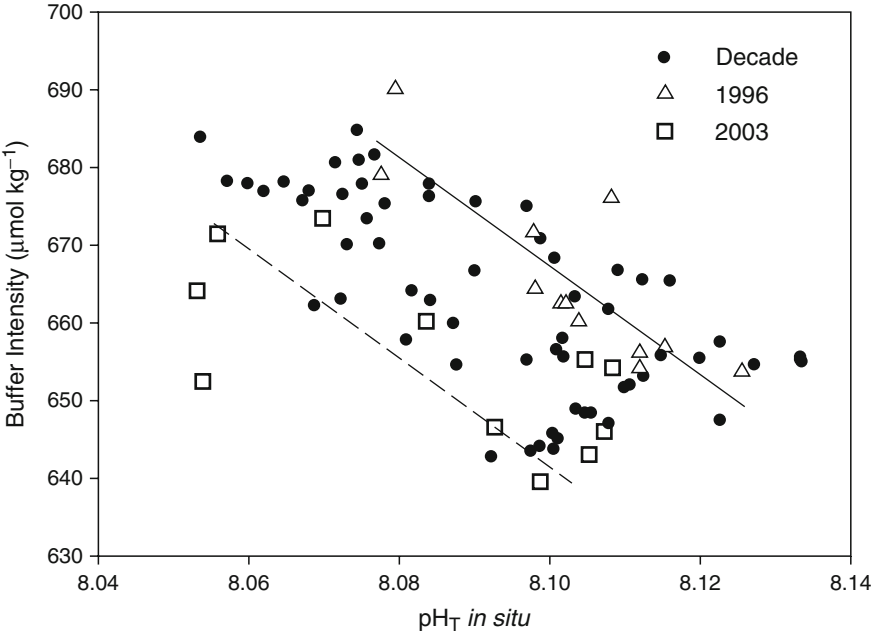

Fig. 5.8 Total Buffer intensity β as a function of pH_T at *in situ* conditions for 10 years at ESTOC site. Values and amplitude of the seasonal variability is shown for 1996 and 2003

$$R = \frac{d \ln pCO_2}{d \ln C_T} = \frac{\Delta pCO_2}{\Delta C_T} \tag{5.8}$$

The lower Revelle factor is, the better is the buffer capacity of the seawater. When atmospheric CO_2 dissolves in seawater, the pH decreases but, because of the carbonate buffer capacity, the solution is still slightly alkaline.

$$CO_2 + CO_3^{2-} + H_2O \Leftrightarrow 2HCO_3^- \tag{5.9}$$

An increase in oceanic fCO_2 produces an increase in the calcium carbonate dissolution (Eq. 5.9) and a decrease in the amount of CO_3^{2-} dissolved (Fig. 5.4). The interannual variability of the Revelle factor at the ESTOC site shows an increase of 0.02 ± 0.002 year^{-1} (Fig. 5.6). From the global estimate of the cumulative oceanic sink of anthropogenic CO_2 for the period 1800–1994 (Sabine et al. 2004), the current Revelle factors are about one unit higher than they were in the pre-industrial ocean. The ESTOC site data indicate that, in the Eastern Atlantic, the Revelle factor has increased by 0.2 units in the last decade alone. This increase in R means that a change in CO_2 is followed by a 0.02% increase in the total inorganic carbon per year. The capacity of the ocean to take up CO_2 from the atmosphere is inversely proportional to the value of R. The Revelle factor increases with CO_2 atmospheric partial pressure and decreases with rising seawater temperature. As the carbonate

ion concentration decreases, *R* increases, and the ability of the ocean to absorb more CO_2 from the atmosphere decreases, and the higher the atmospheric CO_2 partial pressure gets (positive feedback). For a given atmospheric perturbation of CO_2, an increase in the Revelle factor indicates that the oceanic equilibrium concentration of anthropogenic CO_2 will be lower than in previous times.

5.7 Calcium Carbonate Saturation State

Calcium carbonate plays a dual role in regulating carbon sequestration by the oceans. An increase in the dissolution of $CaCO_3$dissolution in the upper ocean will produce a more uniform alkalinity profile (Millero 2007). A decrease in carbonate precipitation in surface waters will increase CO_3^{2-}concentration in solution, will decrease the Revelle factor and will consequently increase the capacity of the oceans to take up CO_2 from the atmosphere. The data at ESTOC shows a reduction of 9 μmol kg^{-1} of , in the last decade, from 224 to 215 μmol kg^{-1} (Fig. 5.4). This follows the same trend as described for the global ocean, but with annual values slightly higher than the global figures and lower than the tropical figures reported (Orr et al. 2005).

The invasion of anthropogenic CO_2 has already reduced the present-day surface [CO_3^{2-}] by over 10% in relation to pre-industrial conditions. This is a reduction of 29 μmol kg^{-1} in the Tropics and 18 μmol kg^{-1} in the Southern Ocean (Orr et al. 2005). The predictions are that the average tropical surface [CO_3^{2-}] will decline to 149 ± 14 μmol kg^{-1} by the year 2100 according to the IPCC (International Panel for Climate Change) IS92a scenario (Hougton et al. 2001). This is a reduction of 45% relative to pre-industrial levels (Orr et al. 2005; Kleypas et al. 1999; Broecker and Peng 1979).

The increase in the Revelle factor and the decrease in buffer capacity of the seawater are also followed by an ocean response to excess CO_2 in order to avoid a greater pH change through calcium carbonate dissolution. This can be followed by studying the evolution of the state of calcite and aragonite saturation (Fig. 5.9). A decrease in the calcium carbonate saturation state is observed at the ESTOC site over the period studied. The $\Omega_{calcite}$ (Fig. 5.9) decreases at a rate of 0.018 ± 0.006 unit $year^{-1}$ (0.2 units in a decade). These results were related mathematically, after decomposing the series by trend, seasonal components and errors, using harmonic functions and fitted to

$$\begin{aligned}\Omega_{\text{calcite}} &= 41.84 - 1.8210^{-2}\,\text{date} - 0.1697\sin\left(2\pi\left(\text{date}-1995\right)\right) \\ &\quad - 4.08510^{-2}\cos\left(2\pi\left(\text{date}-1995\right)\right)\end{aligned} \tag{5.10}$$

(standard error of estimate 0.062).

Seasonal variability accounts for a 0.4 change in $\Omega_{calcite}$ while the interannual change makes the $\Omega_{calcite}$ decrease from 5.5 in autumn 1995 to 5.3 in 2003. The $\Omega_{aragonite}$ decreases at a rate of 0.012 ± 0.004 unit $year^{-1}$, following the equation.

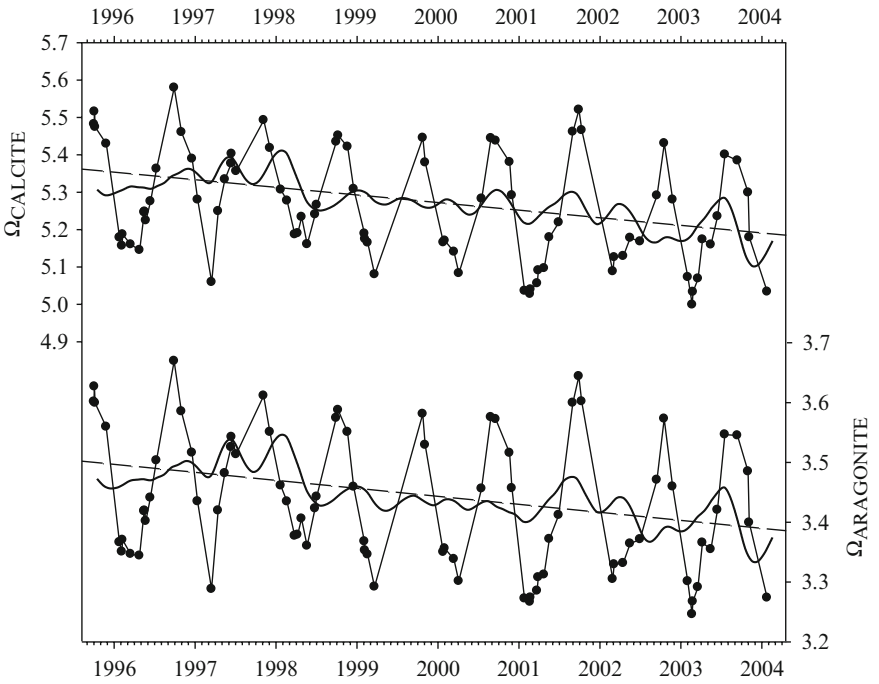

Fig. 5.9 Time series of calcite and aragonite saturation state in surface water at the North-East Atlantic Ocean. Seasonal de-trended time series data (*splines*) are also included

$$\Omega_{\text{aragonite}} = 27.75 - 1.21\,10^{-2}\,\text{date} - 0.131\sin\left(2\pi\left(\text{date} - 1995\right)\right) - 3.292\cdot 10^{-2}\,\text{con}\left(2\pi\left(\text{date} - 1995\right)\right) \tag{5.11}$$

(standard error of estimate 0.042).

Surface values of $\Omega_{\text{aragonite}}$ were 3.6 at the end of 1995 and 3.5 in 2003. A seasonal variability of 0.3 units is observed.

Most of the ocean's surface waters are saturated, at present, in their levels of calcite and aragonite, $\Omega > 1$, and carbonate chemistry was not a limiting factor in the biogenic calcification. Recent studies (Feely et al. 2004) show that the degree of super-saturation has an important effect on the rates of calcification of the various organisms, especially calcareous plankton (Broecker and Peng 1979) and coral reef communities (Caldeira and Wickett 2003; Feely et al. 2004; Urban-Rich et al. 2001). They show a decrease in the rate of calcification in response to the decreased $CaCO_3$, even when the system is saturated. The impact of ocean acidification on the marine ecosystem is unclear, but it will most probably be dependent on species adaptability, with the range of change of seawater pH relative to its natural variability. As it was shown above, around 25 years are needed to change the acid–basic characteristic of surface seawater to conditions never before presented in the seasonal cycle.

Experimental evidence indicates that calcifying rates will decrease in low latitude corals (Kleypas et al. 1999; Gattuso et al. 1998; Langdon et al. 2003) and in phytoplankton (Riebesell et al. 2000; Zondervan et al. 2001).

5.8 ESTOC Data Under Two IPCC Scenarios

To quantify futures changes in the ocean carbonate chemistry at ESTOC station two, atmospheric CO_2 scenarios from the Intergovernmental Panel on Climate Change (IPCC) were used: the IPCC IS92a, a continually increasing scenario (788 ppmv in the year 2100) and the IPCC S650, a stabilization scenario (563 ppmv in the year 2100).

The ESTOC data show that under an IS92a scenario $\Omega_{calcite}$ will reach values of 2.97 while $\Omega_{aragonite}$ will be 1.93, assuming constant alkalinity (Santana-Casiano et al. 2007) and negligible sea surface temperature change. In a more conservative stabilised scenario S650, $\Omega_{calcite}$ will be 3.81 and $\Omega_{aragonite}$, 2.48 (26% lower than the present values).

A recent study (Orr et al. 2005) suggests that the Southern Ocean surface waters will become more depleted of aragonite, probably within the next 50 years. In 100 years, this under-saturation may extend over the entire Southern Ocean and into the sub-Artic Pacific Ocean. The model predictions for low and intermediate latitudes seem to evolve at a slower rate for subtropical areas, however, the ESTOC data show that this variation is, effectively, taking place.

5.9 Environmental Consequences

The changes in the surface ocean pH are rapid when the CO_2 is absorbed from the atmosphere, but the CO_2 however is slowly transferred to the deep ocean and sediments by mixing, advection and through the biological pump. The time scales for mixing of surface waters downward into the deep ocean may amount to centuries. In the past, in the mid-Eocene, the levels of CO_2 were higher (Petit et al. 1999) and the oceans had the capacity to adapt to an increase in CO_2 levels, because the rate of change took place during periods that enabled sufficient mixing of deep waters and sediments. On a higher scale, the geological scale, balance has been reached through the geological reservoir over hundreds of thousands of years (Ridgwell and Zeebe 2005). The ocean has actually reached high levels of CO_2 over the last 200 years. As in the past, the ocean is reacting to this change. However, as opposed to the past, the period over which the change is now occurring is extremely short and insufficient for deep ocean participation to occur, meaning that most of the CO_2 is accumulated in surface water. The immediate oceanic response is the pH reduction of surface waters and the reduction of the state of saturation in the upper waters. These changes are so rapid that they are reducing the buffering capacity of the natural processes that have moderated changes in ocean chemistry over most of geological time. The pronounced shoaling observed for both aragonite and

calcite saturation in all oceans (Feely et al. 2004), mainly in the polar areas (Orr et al. 2005) and the results obtained in ESTOC station confirm this fact.

How this response may affect marine organisms and the biological pump is a question that remains to be solved. There is some evidence with respect to the impact on calcifying organisms (Orr et al. 2005; Feely et al. 2004). A reduction in CO_2 emissions and efficiency carbon sequestration technology look like the only solutions to avoid increasing a problem which is causing significant consequences in the physical, chemical and biological behaviour of the ocean, together with the development of marine calcifying organisms.

5.10 Conclusions

Uncontrolled increase of anthropogenic CO_2 in the atmosphere over the last 200 years, and future increases, will affect the buffer capacity and the saturation state of calcium carbonate in the surface ocean, as shown in this study from the ESTOC site. Considering actual rate of change, a decrease of pH in the upper waters of the ocean of 0.002 pH units per year will reduce the saturation state of calcite and aragonite by 0.018 and 0.012 per year. In the year 2100 with an expected atmospheric partial pressure of CO_2 of 788 ppmv, surface $\Omega_{calcite}$ will reach values of 2.97 while $\Omega_{aragonite}$ will be 1.93. The pH decrease will also affect the buffer capacity of the ocean (-1.99 ± 0.25 μmol kg^{-1} year^{-1}) and will increase the Revelle factor (0.02 ± 0.002 year^{-1}) of the surface seawater changing the efficiency of the ocean to accommodate acids and take up CO_2. These findings are the results of ESTOC site trends during 1995–2004. Similar trends for the positive rate of increase in both the fCO_2 and C_T and the corresponding decrease in the seawater pH have been determined in both Bermuda time series station BATS (Gruber et al. 2002) and Hawaii time series site HOT (Brix et al. 2004) indicating that the effects on the saturation state of calcite and aragonite, buffer capacity and Revelle factor in the Subtropical gyres move towards the same direction.

Acknowledgments This work has been supported by the European Commission, through the MAST III program, the CANIGO project (MAS3-CT96-0060), by the Ministerio de Ciencia y Tecnología, Proyecto FLUCAN (2002-01548) and by the European Project CARBOOCEAN 2005–2009, CN 511176-2. The authors thank all the participants in the ESTOC work during these 10 years, in special Dr. O. Llinás and M.J. Rueda from the ICCM-Gobierno de Canarias in charge of keeping the station work, Dr. E.F. González-Dávila for the statistical data treatment and the SeaS Canarias-Departamento de Biología ULPGC-Viceconsejería de Pesca (G.A.C) by to provide us the AVHRR image in Fig. 5.1. We thank Frank J. Millero for his helpful discussion and comments which improved the manuscript.

References

Brewer PG (1997) Ocean chemistry of the fossil fuel CO_2 signal: The haline signal of "business as usual". Geophys Res Lett 24:1367–1369

Brix H, Gruber N, Keeling CD (2004), Interannual variability of the upper ocean carbon cycle at station ALOHA near Hawaii, Global Biogeochem Cycles 18:GB4019, doi:10.1029/2004GB002245

Broecker WS, Peng TH (1979) Fate of fossil fuel carbon dioxide and the global carbon budget. Science 206:409–418

Caldeira K, Wickett ME (2003) Anthropogenic carbon and ocean pH. Nature 425:365

Clayton TD, Byrne RH (1993) Spectrophotometric seawater pH measurements: Total hydrogen ion concentration scale calibration of m-cresol purple and at-sea results. Deep Sea Res I 40:2115–2129

Dickson AG (1990) Thermodynamic of the dissociation of Boric acid in synthetic seawater from 273.15 to 298.15 K. Deep Sea Res 37:755–766

Dickson AG, Goyet C (eds) (1994) Handbook of methods for the analysis of the various parameters of the carbon-dioxide system in sea water, rep. ORNL/CDIAC-74, US Department of Energy, Washington, DC

Dickson AG, Millero FJ (1987) A comparison of the equilibrium constants for the dissociation of carbonic acid in seawater media. Deep Sea Res 34:1733–1743

Feely et al. (2004) Impact of anthropogenic CO_2 on the $CaCO_3$ system in the oceans. Science 305:362–366

Gattuso JP, Frankignoulle M, Borges I, Romaine S, Buddemeier RW (1998) Effect of calcium carbonate saturation of seawater on coral calcification. Glob Planet Change 18:37–46

González-Dávila M, Santana-Casiano JM, Rueda MJ, Llinás O, González-Dávila E (2003) Seasonal and interanual variability of sea-surface carbon dioxide species at the European station for Time Series in the Ocean at the Canary Islands (ESTOC) between 1996 and 2000. Global Biochem Cycles 17(3):1076. doi:10.1029/2002GB001993

González-Dávila M, Santana-Casiano, González-Dávila E (2007) Interannual variability of the upper ocean carbon cycle in the northeast Atlantic Ocean, Geophys Res Lett 34:L07608. doi:10.1029/2006GL028145

Gruber N, Keeling CD, Bates NR (2002) Interannual variability in the North Atlantic Ocean carbon sink, Science 298:2374–2378

Haugan P M, Drange H (1996) Effects of CO_2 on the ocean environment. Energy Convers Mgmt 37:1019–1022

Houghton JT, Ding Y, Griggs DJ, Noguer M, van der Linden PJ, Dai X, Maskell K, Johnson CA (eds.). IPCC, 2001: Climate Change 2001: The Scientific Basis. Contribution of Working Group I to the Third Assessment Report of the Intergovernmental Panel on Climate Change Cambridge University Press, Cambridge, United Kingdom and New York, NY, USA, pp 881

Kleypas JA et al. (1999) Geochemical consequences of increased atmospheric carbon dioxide on coral reefs. Science 284:118–120

Kleypas JA, Feely RA, Fabry VJ, Langdon C, Sabine CL, Robins LL (2006) Impacts on ocean acidification on coral reefs and other marine calcifiers: A guide for future research. Report of a workshop, 2005. NSF, NOA and US Geological Survey, St. Petersburg, FL

Langdon C et al. (2003) Effect of elevated CO_2 on the community metabolism of an experimental coral reef. Global Biogeochem Cycles 17:1011. doi:10.1029/2002GB001941

Lewis D, Wallace WR. (1998) CO_2 System. Program developed for CO_2 system calculation. Oak Ridge National Laboratory. ORNL/CDIA-105

Liu X, Millero FJ (2002) The solubility of Fe(III) in seawater. Mar Chem 77:43–54

Mehrbach C, Culberson CH, Hawley JE, Pytkowicz RN (1973) Measurements of the apparent dissociation constants of carbonic acid in seawater at atmospheric pressure. Limnol Oceanogr 18:897–907

Millero FJ (2005) Chemical oceanography, 3rd edn. CRC Press, Florida

Millero FJ (2007) The marine inorganic chemistry. Chem Rev 107:308–341

Mintrop L, Pérez FF, González-Dávila M, Santana-Casiano JM, Körtzinger A (2000) Alkalinity determination by potentiometry: Intercalibration using three different methods. Cienc Mar 26:23–37

Orr JC et al. (2005) Anthropogenic ocean acidification over the twenty-first century and its impact on calcifying organisms. Nature 437:681–686

Pankow FJ (1991) Aquatic chemistry concepts. Lewis, Chelsea, MI

Petit JR et al. (1999) Climate and atmospheric history of the past 420,000 years from the Vostok ice core, Antarctica. Nature 399:429–436

Raven J et al. (2005) Ocean acidification due to increasing atmospheric carbon dioxide. The Royal Society, UK

Revelle R, Suess HE (1957) Carbon dioxide exchange between the atmosphere and ocean and the question of an increase of atmospheric CO_2 during the past decades. Tellus 9:18–27

Ridgwell A, Zeebe RE (2005) The role of the global carbonate cycle in the regulation and evolution of the Earth system. Earth Planet Sci Lett 234:299–315

Riebesell U et al. (2000) Reduced calcification of marine plankton in response to increased atmospheric CO_2. Nature 407:364–367

Sabine CL et al. (2004) The oceanic sink for anthropogenic CO2. Science 305:367–371

Santana-Casiano J M, González-Davila M, Millero FJ (2006) The role of Fe(II) species on the oxidation of Fe(II) in natural waters in the presence of O2 and H2O2. Mar Chem 99:70–82

Santana-Casiano JM, González-Dávila M, Rueda MJ, Llinás O, González-Dávila EF (2007) Interannual variability of oceanic CO_2 parameters in the North East Atlantic subtropical gyre at the ESTOC site. Global Biogeochem Cycles 21:GB1015. doi:10.1029/2006GB002788

Skirrow G (1975) Chemical oceanography vol II. Riley P, Skirrow G (eds). Academic, London

Stumm W, Morgan JJ (1981) Aquatic chemistry, 2nd edn. Wiley, New York

Urban-Rich J, Daga M, Peterson J (2001) Copepod grazing on phytoplankton in the Pacific sector of the Antarctic Polar Front. Deep Sea Res II 48:4223–4246

Zhang J-Z (2001) The use of pH and buffer intensity to quantify the carbon cycle in the ocean. Mar Chem 70:121–131

Zondervan I, Zeebe R, Rost B, Riebesell U (2001) Decreasing marine biogenic calcification: A negative feedback on rising atmospheric pCO_2. Global Biogeochem Cycles 15:507–516

Chapter 6
Effects of Sediment Acidification on the Bioaccumulation of Zn in *R. Philippinarum*

Inmaculada Riba, Enrique García-Luque, Judit Kalman, Julián Blasco, and Carlos Vale

Abstract Acidification resulting from the increase of carbon dioxide in the ocean is one of the main effects of global warming. Models predict that a decrease of pH in surface sediments results in higher mobility of metals in sediment pore water and overlying water. This hypothesis has been tested in an exposure sediment bioassay using the clam *R. philippinarum*. Different sediment samples (toxic mud from a mining spill; estuarine samples from the Ria de Huelva and Guadalquivir rivers, and sediments located in the Bay of Cadiz, all in Spain) were used to address the

I. Riba (✉)
Instituto de Ciencias Marinas de Andalucía, CSIC, Avda, República Saharaui s/n, 11510 Puerto Real, Cádiz
and
UNESCO Chair UnitWin-WiCoP, Faculty of Marine and Environmental Sciencies, Physical-Chemistry Department, University of Cadiz, Cadiz, Spain
and
IPIMAR, Avenida Brasilia 1449-016, Lisboa Portugal
e-mail: inmaculada.riba@uca.es

E. García-Luque
UNESCO Chair UnitWin-WiCoP, Faculty of Marine and Environmental Sciencies, Physical-Chemistry Department, University of Cadiz, Cadiz, Spain
e-mail: Enrique.luque@uca.es

J. Kalman
Instituto de Ciencias Marinas de Andalucía, CSIC, Avda, República Saharaui s/n, 11510 Puerto Real, Cádiz
and
UNESCO Chair UnitWin-WiCoP, Faculty of Marine and Environmental Sciencies, Physical-Chemistry Department, University of Cadiz, Cadiz, Spain
e-mail: judit.kalman@uca.es

J. Blasco
Instituto de Ciencias Marinas de Andalucía CSIC Avda República Saharaui s/n, 11510 Puerto Real Cádiz Spain
e-mail: julian.blasco@icman.csic.es

C. Vale
IPIMAR, Avenida Brasilia 1449-016, Lisboa Portugal
e-mail: cvale@ipimar.pt

P. Duarte and J.M. Santana-Casiano (eds.), *Oceans and the Atmospheric Carbon Content*,
DOI 10.1007/978-90-481-9821-4_6,

influence of pH values (6.5–8.5) in bioaccumulation of the metal Zn. Results show that there is a significant ($p < 0.05$) increase in bioaccumulation of this metal at lower values of pH (6.5 and 7.5) compared to the 8.5 value. These results indicate that modification of one unit in pH produces a significant effect in Zn bioavailability, which is also associated with adverse biological effects such us mortality. The results point out the importance of addressing the influence of sediment acidification and their implications in risk assessment in estuarine sediments or in special areas selected for carbon dioxide capture in marine environments.

Keywords Ocean acidification • Bioaccumulation • Metals • Zn • Carbon dioxide • Global warming • Estuarine sediments • Bioavailability • Clams • Carbon dioxide capture • Sediment quality

6.1 Introduction

The urgent need to reduce greenhouse emissions to the atmosphere has led researchers to study new systems for capture and storage of carbon dioxide (CCS). The sequestration of CO_2 in marine geological formations is one of these systems, proposed at an international level, to effectively reduce the concentration of atmospheric CO_2 (IPCC 2005). Although permanent containment is intended, it is necessary to determine the risk of leakage to the marine environment. In particular, we need to establish the magnitude of risk associated with potential leakages in the area of injection and storage, including their surrounding areas. One of the main impacts expected in this scenario is a limitation on pH values that provoke acidification of the sediments located in the area. In this sense, different international conventions, associated with the CCS (OSPAR Convention 2005, 2007; London Convention and Protocol 2006; London Protocol 2007) have agreed on the principle and recommended different approaches to determining the mechanism of these potential leakages and other related risks. Monitoring is one of the key enabling technologies for CO_2 storage (Benson 2006). It is necessary to define the precision and detection levels that the chosen technology should provide to not only guarantee safety of the environment and maintenance of human health, but in order to assure proper accounting for inventory and trading of carbon credits. In this sense, it is necessary a correct monitoring measurement to control injection and storage of CO_2.

The UNESCO Intergovernmental Panel on Climate Change (IPCC 2007) stressed our limited experience with processes of monitoring, verification and information of the rates of leakages and uncertainties associated with storage of CO_2. In order to monitor the effects of storage in the marine environment, it is necessary to properly understand the processes and mechanisms that control leakages in different types of geological formations in which it is possible to store CO_2. Besides, it is necessary to understand the behaviour of the environment, species and ecosystems when they are exposed to CO_2 and the incidental associated substances. One of the deficiencies to be addressed (among other lines of evidence to address environmental degradation

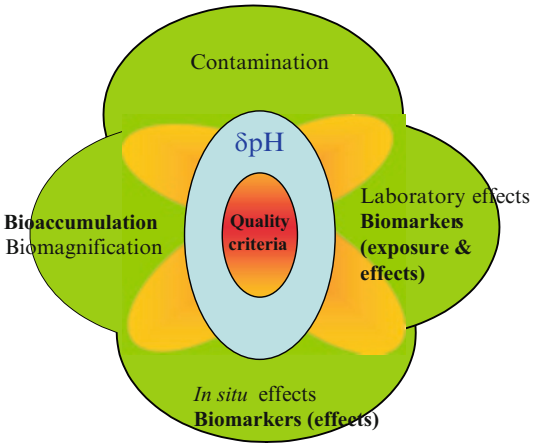

Fig. 6.1 Synoptic representation of a weight-of-evidence method to address the environmental degradation associated with the potential leakages of carbon dioxide in sediments located in areas for injection and storage of this gas. The different lines of evidence, including bioaccumulation must be adapted to the new conditions of variable pH and acidification

effects) is the influence of sediment acidification produced by these leakages on the bioaccumulation of contaminants such as metals (Fig. 6.1).

Anthropogenic inputs of various trace metals to aquatic systems have been increasing in recent years. Marine sediments represent the final repository of most contaminants, such as trace metals, because metals are mainly transported to the marine environment by rivers through estuaries and can be deposited and incorporated into the sediments. As estuaries are among the most ecologically sensitive ecosystems in the world, assessments of estuarine sediments are strongly recommended (Chapman and Wang 2001). Besides, estuarine and coastal sediments with high contents of organic matter producing CO_2 and pH values of 6.5 or below are commonly registered in organically rich coastal sediments. If those sediments are contaminated by metals, the ecosystem will have a combined effect of low pH and high metal availability. Furthermore, sediments influenced by the discharge of mining activities also presented low pH.

The bioavailability of trace metals bound to sediments depends on the physical and chemical forms of the metal (Luoma 1983). Dissolved or weakly adsorbed contaminants are more bioavailable to aquatic biota compared to more structurally complex mineral and/or organic-bound contaminants. In aqueous systems, bioavailability is often correlated with free metal concentration, because the free ions have been considered as the most bioavailable forms of dissolved metals (Chapman et al. 2003). It is generally believed that an increase of free ion concentration will increase bioavailability and thus increase metal accumulation and toxicity (Blackmore and Wang 2003). As H^+ may compete with trace metals for aquatic ligands, at low pH value metals tend to be found as free ionic species (Rensing and Maier 2003) (Fig. 6.2). However, although it is known that the pH has significant influence on the partitioning and bioavailability of contaminants, few studies have reported on the effects of pH changes on metal toxicity and bioaccumulation to aquatic organisms (Riba et al. 2003a, 2004).

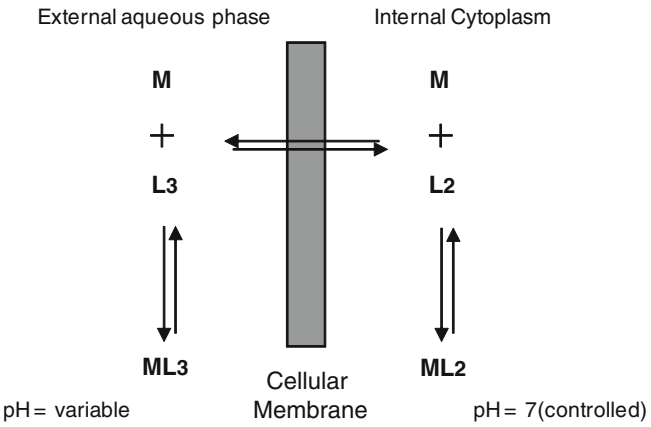

Fig. 6.2 Equilibrium between a metallic ion inside and outside an organism cell

Fig. 6.3 Photograph for *R. philippinarum* (http://www.fao.org/fishery/culturedspecies/Ruditapes_philippinarum/es#tcN9003F)

Most of the species commonly used in marine and freshwater sediment toxicity/bioaccumulation assays are inadequate for testing estuarine sediment quality because they have a narrow pH tolerance or are not indigenous estuarine species. Estuarine sediment toxicity/bioaccumulation tests should incorporate estuarine organisms tolerant to changes of abiotic factors, such as pH. The commonly used clam, *Ruditapes philippinarum* (Fig. 6.3) allows a more complete and realistic assessment of metal contaminants in estuarine environments (DelValls and Conradi 2000). These estuarine organisms are able to adapt to the wide range of estuarine salinity and pH values. Moreover, clams are filter-feeder bivalves and, therefore, may accumulate metals in their tissues (Shin et al. 2002; Lee et al.2005).

The acidification resulting from an increase of carbon dioxide in the ocean is one of the main effects of global warming. Models predict that decrease of pH in surface sediments results in higher mobility of metals in sediment pore water and overlying water. This hypothesis has been tested in an exposure sediment bioassay

using juveniles of the clam *R. philippinarum*. Different sediment samples (contaminated material from a mining spill; estuarine samples from the Ria de Huelva, Guadalquivir river and the Bay of Cádiz, Spain) were used to address the influence of pH values (6.5–8.5) in bioaccumulation of the metal Zn.

6.2 Material and Methods

6.2.1 Approach

In order to test the influence of sediment acidification on the bioaccumulation of Zn, sediment samples were collected in estuarine areas of the Guadalquivir estuary (GR) that was impacted by an acute mining spill (April, 1998) caused by the breakage of a tailing pond in a pyrite mine located in 'Aznalcóllar' (Gómez-Parra et al. 2000; Riba et al. 2003b), of the Ria de Huelva (H), which is a heavily industrialized area located at the mouth of two estuaries defined by the rivers Tinto and Odiel, and of the Gulf of Cádiz (Ca), an area with a low contamination (Fig. 6.4).

The area of Huelva receives acidic fluvial water discharges with high concentrations of metals from the Roman Empire times, several centuries ago (Cabrera et al. 1992; García-Luque et al. 2003). Samples were prepared from different dilutions of contaminated sediment collected in the proximity of the mine (Riba et al. 2003b) and using clean sediment from the Bay of Cádiz (0.3% and 5% of contaminated versus 99.7% and 95% of clean sediment). These two samples were named DIL0.3 and DIL5 respectively. Dilutions were selected based on previous experiences with these sediments and organisms (Riba et al. 2003a, 2004).

Sediments were collected with a 0.025 m^2 Van Veen grab and transferred to the cooler. When sufficient sediment was collected from a particular station, the cooler was transported to the laboratory. The contents of the cooler were homogenized with a Teflon spoon until no colour or textural differences could be detected. The sediments were sub-sampled for chemical quantification (1.5 L aliquots). Then the sediment samples were kept in the cooler at 4°C in the dark until they were used for sediment toxicity assays, but in no case for longer than 2 weeks. Prior to sample collection and storage, all beakers were thoroughly cleaned with acid (10% HNO_3), and rinsed in double-deionized (Milli-Q) water.

6.2.2 Bioassay

Juveniles of clams (*Ruditapes philippinarum*; shell length about 1 cm, average weight about 0.42 g) were obtained from an aquaculture farm (AMALTHEA, S.L., Cádiz, Spain) and kept in our laboratory for 1 month before being acclimated to the

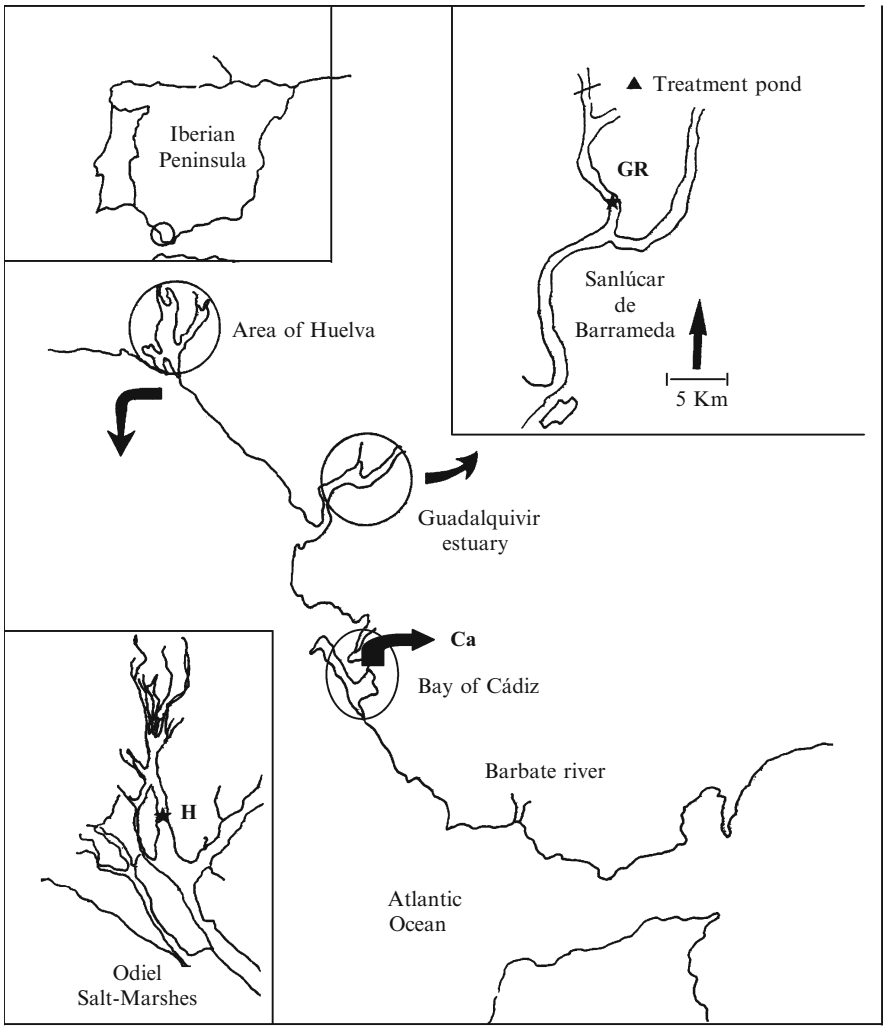

Fig. 6.4 A schematic map of the studied area in the south of Spain showing the locations of the environmental sampling stations selected in the three estuarine ecosystems, Bay of Cádiz (Ca) Ría de Huelva (H) and Guadalquivir estuary (GR). It also shows the location in the mining area at which the contaminated sediment was collected

pH values selected for the assays. During this period, clams were fed on a mixture of micro algae (*Tetraselmis chuii*, *Isocrhysis galbana*, *Chaetoceros gracilis*).

Different values of pH (6.5, 7.5 and 8.5) were spiked in overlying water prior to exposure of the organisms to the sediment samples. Sea water salinity was used in the bioassays (S = 36). The overlying sea water used in the pH dependent assays was set up to permit a pH control using the buffer capacity of the carbonate system in oceanic waters as reported by Mount and Mount (1992). Briefly, we manipulate

the carbon dioxide concentration in the atmosphere over the assay solutions, as well as adding about 10 mM of HCO^-_3 to increase the buffer capacity of sea water. The pH was adjusted using HCl and NaOH (Merck, Darmstadt, Germany). Once the various pH values selected for each assay treatment had been separately fixed, this sea water was used during the acclimation period (15 days) of the organisms prior to performing the assays. During this period, the animals were maintained in tanks of about 20 L capacity, fed on a mixture of micro algae as described above, the water was continuously aerated and replaced (80% v/v) every 3 days with fresh sea water of pH values adjusted to those required. The pH, salinity (36), temperature (20°C) and the concentration of dissolved oxygen (>5 mg L^{-1}, 60% saturation) were measured and controlled every day.

After the acclimation period the bioassays were performed in replicate using different values of pH. The assays were performed in whole sediment (2L per assay) using a water to sediment ratio of 1:4 v/v, at constant temperature (20°C), as reported by DelValls et al. (2002) using vessels of 15 L capacity. Briefly, 40 organisms previously acclimated to each particular set of pH values were added to each vessel and exposed for 28 days (Fig. 6.5). The percentage of mortality at the end of the experiment was recorded together with the metal concentration in the clams. Individuals were dissected and analysed at day 0 to control the bioaccumulation of metals during the different treatments.

Water replacement (80%) was performed on day 5 of the experiment, except for those assays where mortality was measured, in which it was performed on the same day as the mortality detection (DelValls et al. 2002).

6.2.3 Chemical Analyses in Organism Tissues: Bioaccumulation

Laboratory-exposed organisms were depurated for 48 h before processing to avoid any sediment contamination. Then, organisms were dissected and damped out.

Fig. 6.5 Photographs of the clams *R. philippinarum* used in the bioaccumulation assay. On the left, the juveniles of the clams used. On the right, the aquarium with the clams and the sediments contaminated by metals

The samples of the juveniles *Ruditapes phillipinarum* correspond to soft body organisms. Organisms were divided, in general, into three pools of five to ten specimens and then lyophilized in a VIRTIS lyophilizer (Casado-Martínez et al. 2006).

The concentration of Zn was determined on lyophilized samples that were crushed and homogenized to a fine powder in an agate bowl with a Planetary Mono mill (Pulverisette 6, Fristch). Then, samples were digested with nitric acid (Suprapur) and hydrogen peroxide (Suprapur) for 1 h at 95°C. The total volume was raised to 5 mL by adding distilled water and analyzed by inductively coupled plasma mass spectrometry (ICP-MS) (Amiard et al. 1987). The analyzed concentrations were validated by performing metal analyses on reference material NRCC-TORT-2 lobster hepatopancreas (National Research Council of Canada, Ottawa, ON, Canada). Agreement between the chemical concentration and the standards was approximately 90%. Metal concentrations in soft tissues are expressed as micrograms per kilogram dry weight.

6.2.4 Sediment Analysis

For sediment grain size, an aliquot of wet sediment was analyzed using a laser particle-size Fristch analyser (model Analysette 22, Laval lab, Lavel, PQ, Canada) by following the method reported by DelValls and Chapman (1998) and DelValls et al. (1998). The remaining sediment was dried at 40°C prior to chemical analysis. Dried sediments were gently homogenized. The organic carbon content was determined following the method reported by El-Rayis (1985). For Zn analysis, the sediments were digested as described by Loring and Rantala (1992). Zn concentrations in the extracts were determined with a Perkin-Elmer 2100 Flame Atomic Absorption Spectrophotometer. Results are expressed as milligrams per kilogram dry sediment. The analytical procedures were checked using reference material (MESS-1 NRC and CRM 277 BCR) and present agreement to more than 90% with the certified values.

6.2.5 Water Analysis

The pH (SWS or sea water scale) was measured with a potentiometric analyzer (Metrohm, 670, Berchem, Belgium) with a glass combination electrode (Metrohm, ref. 6.0210.100). Salinity and oxygen concentration were measured as reported by Gómez-Parra and Forja (1994).

6.2.6 Data Calculation and Statistical Analysis

The metal and metalloid concentration in the clams from the replicated assays and the controls were compared using ANOVA and Tukey's ***F*** tests to identify significant differences in sensitivity between media ($p < 0.05$ and $p < 0.1$).

Adequate quality assurance/quality control (QA/QC) measures were followed in all aspects of the study, from field sampling through to laboratory and data entry as described by Chapman (1988), Luoma and Ho(1992)and the ASTM (1991a, b).

6.3 Results and Discussion

6.3.1 Sediment Chemistry

The summarized concentrations of Zn, Fe, Mn, organic carbon and percentages of fine sediments analyzed in the five sediments used in the bioaccumulation test are given in Table 6.1. The amount of organic carbon, Fe and Mn are in the normal range of estuarine and littoral ecosystems in the area of study (Casado-Martínez 2006; Campana et al. 2005). The organic carbon concentration is lower in the dilution treatments and at the station located in the Bay of Cadiz than those from the Ria de Huelva and the Guadalquivir river.

Sediments from the Bay of Cádiz (Ca) showed the lowest concentration of Zn. The concentrations of Zinc in sediments located in Huelva (2,551 mg kg^{-1}) were the highest. The station located at the Guadalquivir estuary showed intermediate concentrations of metals between Huelva and the area located in the Bay of Cádiz.

6.3.2 Sediment Bioassay Bioaccumulation

Significant mortality ($p < 0.1$) was recorded only in the highest dilution of contaminated material (about 5% of contaminated material and 95% of clean sediment) for pH values 7.5 (28% – average mortality recorded) and 6.5 (55% – average mortality recorded). The rest of the treatment shows no significant mortality compared to that at the control station, although higher values were measured at the Huelva station.

Figure 6.6 shows the metal concentrations in the total body of the clams exposed to the five different sediments and the tissue concentrations in pre-exposure conditions (horizontal line, day 0, clams maintained in flowing sea water and fed with a mixture

Table 6.1 Summarized results for sediment physico-chemical characteristics used in the bioaccumulation test. All concentrations expressed as mg kg^{-1} dry weight, except the organic carbon content (OC), fines and Fe in %

Station	Zn	Fe	Mn	OC	Fines
Ca	6.28	0.5	163	1.07	49
DIL5	1,700	3.9	166	1.06	48
DIL0.3	100	5.6	155	0.97	49
H	2,551	4.1	354	3.20	85
GR	152	3.2	812	2.10	90

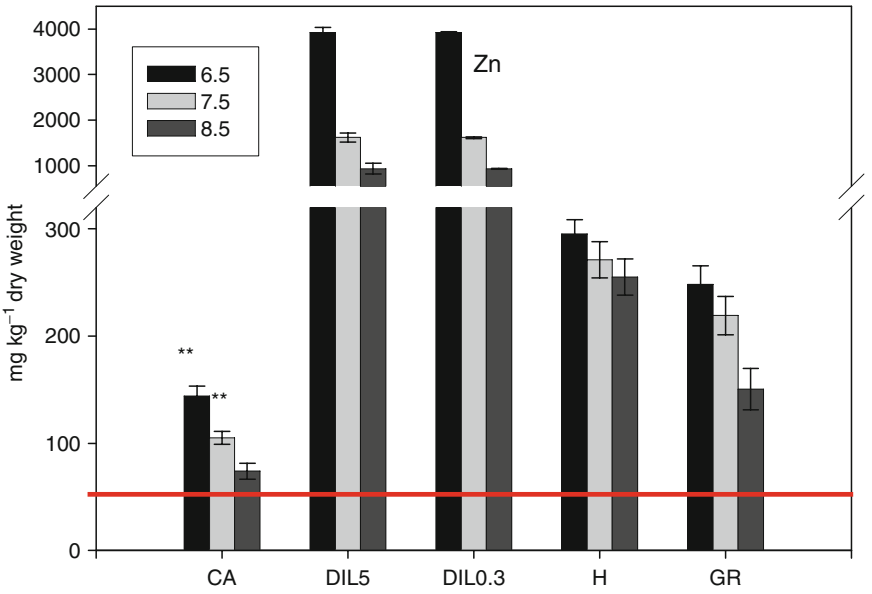

Fig. 6.6 Zn concentrations analyzed in this study in clam tissue for the bioaccumulation test of individuals exposed to sediments sampled in the Gulf of Cadiz (Ca, H, GR) and dilution of contaminated mining sediments (DIL0.3 and DIL5) at the three pH values selected to address the effect of acidification in the bioaccumulation of metals. The horizontal red line shows the background concentration of metals measured in the clams on day 0 before the start of the bioassay

of microalgae). The metal background concentration in the pre-exposure conditions shows high levels although lower than the concentrations measured in the bioassay. The background level could be related to potential sources of low contamination associated with aquaculture activities and related to food or water conditions. In any case, they show a kind of background conditions for the clams used in the bioassay. In this sense, comparison to the concentration of metals measured in the clams exposed to the sediments showed, independently of its contamination, an increase in all metal concentrations. In all the treatments a significant ($p < 0.05$) enrichment of metals in the juvenile clams was measured.

In general, the highest concentration of Zn was measured in clams exposed to the highest dilution of contaminated sediment (DIL5), the lowest measured in the sediments being located in the Bay of Cádiz. The comparison of metal bioaccumulation among the sediments collected in estuaries along the Gulf of Cadiz with different origins of contamination (GR and H) shows that Zn bound to sediments impacted by an accidental mining spill (GR) are more bioavailable than the same metal from sediments located at Huelva affected by low, albeit continuous spills.

The proportions of metal that organisms accumulated from different exposure routes (e.g., ingestion versus water for aquatic organisms) are variable, probably depending on the degree of contamination of those different exposure routes. Metal-accumulation tends to be both organism- and situation-specific (Chapman

et al. 2003; Riba et al. 2005a, b). In this sense, the highest concentration of Zn measured in sediments (Ria de Huelva, H) was not reflected in bioaccumulation by clams. This fact could be related to the easier mobility of Zn bound to the contaminated sediment dilutions (DIL0.3 and DIL5) compared to Zn bound to sediments from the Gulf of Cadiz, namely the area of Huelva in which concentration of metals in sediments are significantly higher than in the dilution of contaminated sediments. These results are, in accordance with previous findings, obtained using this kind of material suggesting a higher mobility of metals for this kind of sediments (Riba et al. 2003a, 2004).

The concentration of Zn analyzed in juveniles of the clam exposed to no contaminated sediments (Bay of Cadiz, Ca and lower dilution, DIL0.3) are in agreement with the baseline accumulation observed in this kind of study for uncontaminated/low-contaminated sediments reported in previous studies (Casado-Martínez 2006). Furthermore, they are generally in agreement with the values available in the literature for adults (Ji et al. 2006; Martin-Díaz et al. 2008) for those sediment samples collected in estuarine areas (Guadalquivir estuary, GR and Huelva, H). However, tissue concentrations of Zn obtained in this study for the highest dilution of contaminated material considered (DIL5) are in the highest range of values available in the literature (Ji et al. 2006).

When determining the contribution of sediments as sources of metals, in this case Zn, the bioavailability of this metal is an important tool to understand the bioaccumulation that can occur in exposed organisms. There are, however, several biotic and abiotic parameters that affect metal bioavailability and accumulation in the soft tissue of organisms. It is therefore more appropriate to evaluate bioavailability by direct measures of bioaccumulation of specific compounds within organisms. Such bioavailability studies have been conducted in several countries for sediment assessment (Catsiki et al. 1994), and relationships between bioavailability and bioaccumulation for sediment toxicity assessment have been developed by many authors (Campana et al. 2005; Otero et al. 2005; Martín-Díaz et al. 2006). When a contaminant is bioavailable and accumulated in biological tissues, it may produce toxicity or not. Toxicity occurs when the rate of metal uptake from all resources exceeds the combined rates of detoxification and excretion (if present) of Zn (and other metals, e.g., Wang and Rainbow 2005). In this sense, it has been demonstrated that juveniles of the clam *R. phillipinarum* are adequate organisms to address bioaccumulation of Zn without a significant toxicity measured (except a moderate mortality in one of the treatments, $p < 0.1$) even using high-contaminated sediments, either contaminated from a mining spill or those collected in estuaries along the Gulf of Cadiz.

The bioaccumulation can provoke the uptake of metals in the trophic chain and consequently associates a risk to the environment and potentially for humans by consumption of contaminated species. The bioaccumulation of Zn and other metals in estuarine and marine species has been demonstrated in previous studies, two examples of it are: (a) Marinduque, Philippines. In 1996, a severe spill occurred from a tailings pond at Marcopper Mine, Marinduque. Coastal sediments near the river outflow contain high amounts of copper, manganese, lead and zinc and there

are concerns that the toxic metals are persisting and may be taken up into bottom dwelling organisms and hence into the food chain (David 2002). (b) Aznalcóllar mining spill (Spain, 1998). The spill affected the Guadalquivir estuary and part of the coastal area surrounding the National Park of Doñana (Gómez-Parra et al. 2000; Riba et al. 2002).

6.3.3 *Influence of Acidification in Zn Bioaccumulation*

The concentration of Zn in clams exposed to sediments at the three different values of pH tested in this study (6.5, 7.5 and 8.5) is shown in Fig. 6.6. The concentrations of Zn measured in tissues were affected by the change in pH. A negative trend was recorded for Zn as a decrease in pH value resulted in higher concentration of this metal in the organisms. To address the influence of the pH values, the statistical differences among all the treatments using different 'p' values are shown in Fig. 6.7 ($p < 0.05$ and $p < 0.1$).

The results confirm that acidification significantly increase the bioaccumulation of metals bound to the sediments utilized in the juveniles of *R. phillipinarum*. For most of the treatments, the variation in one unit of pH produces a significant ($p < 0.1$, 0.05) effect in the increase of Zn bioaccumulation in clams. The variation of two units in the value of pH produce an influence in the bioaccumulation of metals significantly higher ($p < 0.05$, 0.1). In general, the influence of pH values is lower in field collected samples than in the dilution of contaminated material using sediments from the Bay of Cadiz.

Fig. 6.7 Summary of the statistical results obtained in sediment bioaccumulation assays at different pH values. Treatments not underlined by the same line are significantly different at $p < 0.05$ and/or $p < 0.1$ (Tukey's F tests)

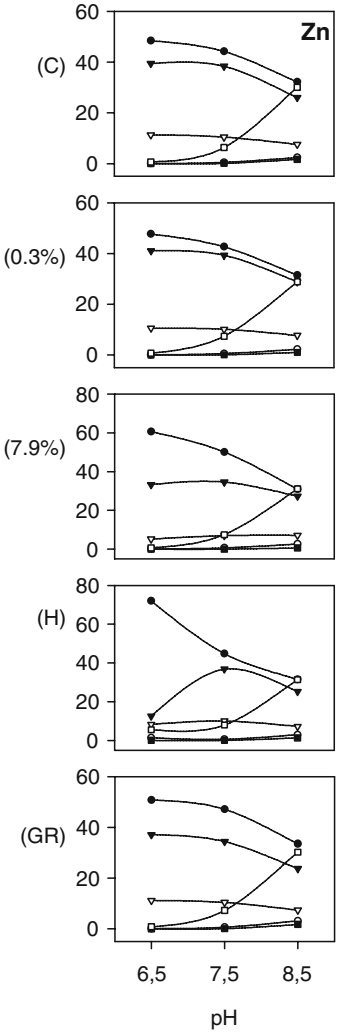

Fig. 6.8 Diagrams of chemical speciation of metal Zn bound to sediments studied, Bay of Cádiz (C), toxic mud dilution (0.3% and 7.9%), Ría of Huelva (H) and Guadalquivir estuary (GR) as a function of pH values. Chemical species (● Free metal, ○ ∑MOH, ▼ ∑MCl, ▼∑MSO_4, ■∑MCO_3, ↑ $Cu(OH)_2^{2+}$ and ZnOHCl) are expressed as percentage of the total dissolved concentration of the metals mobilized from the sediments assayed (Adapted from Riba et al. 2003a)

Data obtained from the pH dependent bioassay demonstrate that the acidification of samples has been associated with the mobilization of Zn. In acidic pH, Zn exists as free ions, but at alkaline pH the ions precipitate as insoluble oxides or hydroxides (Fig. 6.8). Therefore, the availability depends upon the pH; at lowest values metals bound to sediments are often more bioavailable and thus toxic for test organisms (Chapman et al. 2003; Riba et al. 2003a, 2004). The clams in acidified environments are exposed not only to high concentration of hydrogen ions themselves, but also to elevated concentrations of more than one metal.

Some authors have proposed that the bioavailability of a dissolved metal is related to its free ion activity (e.g., Morel 1983). The first step in the uptake of metals by an organism comprises the transport of the cation through the plasmatic membrane (Fig. 6.2). For many dissolved metals, including Zn, entry into mollusks

involves passive diffusion, perhaps facilitated by carrier molecules, and passage along a gradient maintained by intracellular ligands of increasing binding strength (Langston et al. 1998). Nevertheless, changes in the composition and conditions of the medium may modify the structure of the plasmatic membrane and the number of available ligand groups present in the carrier proteins, hence affecting their chemical speciation and their bioavailability (Van Ginneken et al. 1999).

The bioaccumulation of Zn by the clam *R. philippinarum* in estuarine areas is of particular concern due to their permanent interaction with sediments. If their assimilation efficiency is high, metals are accumulated and toxicity can be produced. Once assimilated, metals represent an obvious risk not only of contamination transference to predatory species or even to human populations, but also, a risk to the ecosystem structure. The results obtained pointed out that Zn and potentially other metals bound to contaminated sediment samples, located in areas of the estuary in which the pH values are determined by marine influence (higher than 7.5) and that are not uptaken by clams or are toxic, can became toxic, or be accumulated by clams, if pH values decrease and reach values of around seven or lower. These increases in the bioaccumulation of metals can be associated with the potential leakages in sediment above carbon dioxide storage in sub-seabed geological formations. For this case, the acidification of the sediments associated with leakages of CO_2 can produce the uptake of metals that were safely stored in sediments. In this sense, the results obtained in this study point to the importance in conducting bioaccumulation studies of addressing the potential risk associated with these leakages. Risk assessment during the selection of sites for carbon capture storage in sub-seabed geological formations must consider this kind of studies to address potential impacts, not only to the surrounding benthic and pelagic ecosystems, but also to the marine/aquatic food chain, possibly causing long term health effects on marine life and potential risk to human health by consumption of contaminated species.

6.4 Conclusion

This study presents results of the acidification of sediments on the bioaccumulation of Zn under laboratory conditions, using both contaminated material from a mining spill and field collected sediments in three estuarine areas located along the Gulf of Cadiz. It is a snapshot to determine the influence of variation of pH using environmental samples in the bioaccumulation of that metal. Also, the implications of this bioaccumulation are considered in relation to the variation of pH provoked by mitigation techniques such us CCS or natural variability such as that associated with estuaries. The conclusions are summarized below, based on the utilization of three different pH values of 6.5, 7.5 and 8.5 that can be measured in estuarine natural waters and that can be expected under potential low and/or moderate leakages in sediments above carbon dioxide storage in sub-seabed geological formations:

1. Sediment acidification increases bioaccumulation of Zn in all the stations. It can increase the adverse effects to the biota associated with an originally not toxic

sediment area, either natural (estuaries) or artificial (sediments above CO_2 storage in sub-seabed geological formations).

2. The metal Zn from the mining spill bound to the dilution of the contaminated material (DIL0.3 and DIL5) show more bioaccumulation at low pH values than metals bound to sediments collected in the estuaries located in Gulf of Cadiz (H, GR and Ca). Although the concentrations of metals in the dilutions of contaminated material are much lower than those monitored in the Ría de Huelva, they produce lethal toxicity. This gives an interesting indication of the fundamental difference between the long-term effects of continuous metal discharge over centuries and the effect of an isolated, albeit very large, single discharge.

It has been demonstrated that the acidification of sediments produce changes in the biological availability of contaminants such as Zn, considered in this study. Besides, the increase in the bioaccumulation of Zn associated with the acidification of sediments can have implications not only on the ecosystem health but also potentially in human health by consumption of contaminated species such as the commercial clam considered in this study.

Acknowledgments The authors want to thank IPIMAR staff for their help during the setup of the manuscript. The described work was partially supported by grants funded by the Spanish Ministry of Science and Innovation (CTM2008-06344-C03-02/TECNO and CTM2008-06344-C03-03/TECNO) and by grant RNM P08-RNM-3924 funded by Junta de Andalucia Dra. Inmaculada Riba thanks the Spanish Science and Innovation program 'Jose Castillejo' for supporting her stay at IPIMAR. Judit Kalman also thanks the I3P program for funding her research at ICMAN/CSIC.

References

American Society for Testing and Materials (1991a) Standard guide for conducting 10 days static sediment toxicity test with marine and estuarine amphipods. In: 1991 Annual Book of ASTM Standards. E 1367-90. Philadelphia, PA, pp 310–390

American Society for Testing and Materials (1991b) Standard guide for collection, storage, characterization and manipulation of sediments for toxicological testing. In: Annual Book of ASTM Standards. E 1391-90. Philadelphia, PA

Amiard JC, Pineau A, Boiteau HL, Metayer C, Amiard-Triquet C (1987) Application of atomic absorption spectrophotometry using Zeeman effect, to the determination of eight trace elements (Ag, Cd, Cr, Cu, Mn, Ni, Pb and Se) in biological materials. Water Res 21:693–697

Benson SM (2006) Monitoring carbon dioxide sequestration in deep geological formations for inventory verification and carbon credits. SPE International 102833

Blackmore G, Wang W-X (2003) Inter-population differences in Cd, Cr, Se, and Zn accumulation by the green mussel *Perna viridis* acclimated at different salinities. Aquat Toxicol 62:205–218

Cabrera F, Conde B, Flores V (1992) Heavy metals in the surface sediments of the tidal river Tinto (SW Spain). Fres Environ Bull 1:400–405

Campana O, Rodríguez A, Blasco J (2005) Bioavailability of heavy metals in the Guadalete River Estuary (SW Iberian Peninsula). Cienc Mar 31:135–147

Casado-Martínez MC (2006) Caracterización de material de dragado optimizando un método integrado de evaluación de la calidad ambiental. Tesis Doctoral. Universidad de Cádiz, 344 pp

Casado-Martínez MC, Blasco J, González-Castromil MA, Riba I, DelValls TA (2006) Inter-laboratory assessment of marine bioassays to evaluate environmental quality of coastal sediments in Spain: V. The whole sediment toxicity test using the juvenile bivalve *Ruditapes philipinarum* (Reeves 1864). Cienc Mar 32:159–166

Catsiki VA, Bei F, Nicolaidou A (1994) Size dependent metal concentrations in two marine gastropod species. Neth J Aquat Ecol 28(2):157–165

Chapman PM (1988) Marine sediment toxicity tests. In: Lichtenberg JJ, Winter FA, Weber CI, Frakin L (eds) Chemical and biological characterization of sludges, sediments, dredge spoils, and drilling. STP 976. American Society for Testing and Materials, Philadelphia, PA, pp 391–402

Chapman PM, Wang F (2001) Assessing sediment contamination in estuaries. Environ Toxicol Chem 20:3–22

Chapman PM, Wang F, Janssen CR, Goulet RR, Collins Kamunde N (2003) Conducting ecological risk assessments of inorganic metals and metalloids: Current status. Human Ecol Risk Assess 9:641–697

David CP (2002) Heavy metal concentrations in marine sediments impacted by a mine-tailings spill Marinduque Island, Philippines. Environ Geol 42:955–965

DelValls TA, Chapman PM (1998) Site-specific sediment quality values for the Gulf of Cádiz (Spain) and San Francisco Bay (USA), using the sediment quality triad and multivariate analysis. Cienc Mar 24(3):313–336

DelValls TA, Conradi M (2000) Advances in marine ecotoxicology: Laboratory tests versus field assessment data on sediment quality studies. Cienc Mar 26(1):39–64

DelValls TA, Forja JM, González-Mazo E, Blasco J, Gómez-Parra A (1998) Determining contamination sources in marine sediments using multivariate analysis. TRAC-Trend in Anal Chem 17(4):181–192

DelValls TA, Forja JM, Gómez-Parra A (2002) Seasonality of contamination, toxicity, and quality values in sediments from littoral ecosystems in the Gulf of Cadiz (SW Spain). Chemosphere 46:1033–1043

El Rayis OA (1985) Re-assessment of the titration method for determination of organic carbon in recent sediments. Rapp Comm Int Mer Medit 29:45–47

García-Luque I, Sáenz I, Riba I, DelValls TA, Forja JM, Gómez-Parra A (2003) Heavy metals at the Guadalquivir estuary. Cienc Mar 29(4):457–468

Gómez-Parra A, Forja JM (1994) An operative definition of alkalinity in interstitial water. Mar Chem 45:53–65

Gómez-Parra A, Forja JM, DelValls TA, Saénz I, Riba I (2000) Early contamination by heavy metals of the Guadalquivir Estuary after the Aznalcóllar mining spill (SW Spain). Mar Poll Bull 40:1115–1123

IPCC (2005) Special report on carbon dioxide capture and storage. Prepared by working group III of the United Nations Intergovernmental Panel on Climate Change (IPCC). Bert Metz, Ogunlade Davison, Heleen de Coninck, Manuela Loos and Leo Meyer (eds). Cambridge University Press, Cambridge, UK, p 431

IPCC (2007) Climate change 2007: Synthesis report. Contribution of working groups I, II and III to the fourth assessment report of the United Nations Intergovernmental Panel on Climate Change. Core Writing Team, Pachauri RK, Reisinger A (eds). IPCC, Geneva, Switzerland, 104 pp

Ji J, Choi HJ, Ahn IY (2006) Evaluation of Manila clam *Ruditapes philippinarum* as a sentinel species for metal pollution monitoring in estuarine tidal flats of Korea: Effects of size, sex, and spawning on baseline accumulation. Mar Poll Bull 52:447–453

Langston WJ, Bebianno MJ, Burt GR (1998) Metal handling strategies in molluscs. In: Langston WJ, Bebianno MJ (eds) Metal metabolism in aquatic environments. Chapman and Hall, London, pp 219–283

Lee BG, Yu XL, Jung SK, Yang SY, Lee IT, Lee JS (2005) A radiotracer study on the chronic effects and subcellular partitioning of metals in the Manila clam *Ruditapes philippinarum*. Proceedings of International Symposium on Research Reactor and Neutron Science: In Commemoration of the 10th Anniversary of HANARO

London Convention and Protocol (2006) Risk assessment and management framework for CO2 sequestration in sub-seabed geological formations. London Convention on the prevention of Marine Pollution by Dumping of Wastes and Other Matter 1972 and 1996 Protocol Thereto

London Protocol (2007) Specific guidelines for the assessment of carbon dioxide streams for disposal into sub-seabed geological formations. 1996 London Protocol on the prevention of Marine Pollution by Dumping of Wastes and Other Matter

Loring DH, Rantala RTT (1992) Methods for the geochemical analyses of marine sediments and suspended particulate matter. Earth Sci Rev 32:235–283

Luoma SN (1983) Bioavailability of trace metals to aquatic organisms-A review. Sci Total Environ 28:1–22

Luoma SN, Davis JA (1983) Requirements for modelling trace metal partitioning in oxidized estuarine sediments. Mar Chem 12:159–181

Luoma SN, Ho KT (1992) The appropriate uses of marine and estuarine sediment bioassays. In: Calow P (ed) The handbook of ecotoxicology, vol 1. Blackwell Scientific, Cambridge, MA, pp 193–226

Martín-Díaz ML, Riba I, Casado-Martínez MC, DelValls TA (2006) Bioavailability of metals in sediments from Spanish estuaries using *Carcinus maenas*. Cien Mar 32(2B):412–420

Martín-Díaz ML, Jiménez-Tenorio N, Sales D, DelValls TA (2008) Accumulation and histopathological damage in the clam *Ruditapes philippinarum* and the crab *Carcinus maenas* to assess sediment toxicity in Spanish ports. Chemosphere 71:1916–1927

Morel FMM (1983) Principles of aquatic chemistry. Wiley, New York

Mount DR, Mount DI (1992) A simple method of pH control for static and static-renewal aquatic toxicity tests. Environ Toxicol Chem 11:609–614

OSPAR (2005) The Royal Society of the United Kingdom. Ocean acidification due to increasing atmospheric carbon dioxide. The Royal Policy Document 2005. OSPAR Convention for the Protection of the Marine Environment of the North-East Atlantic

OSPAR (2007) Guidelines for risk assessment and management of storage of carbon dioxide streams in sub-seabed geological formations. OSPAR Convention for the Protection of the Marine Environment of the North-East Atlantic

Otero XL, Vidal-Torrado P, Calvo de Anta MR, Macías F (2005) Trace elements in biodeposits and sediments from mussel culture in the R´ıa de Arousa (Galicia, NW Spain). Eviron Pollut 136:119–134

Rensing C, Maier RN (2003) Issues underlying use of biosensors to measure bioavailability. Ecotoxicol Environ Saf 56:140–147

Riba I, DelValls TA, Forja JM, Gómez-Parra A (2002) Influence of the Aznalcóllar mining spill on the vertical distribution of heavy metals in sediments from the Guadalquivir estuary (SW Spain). Mar Poll Bull 44:39–47

Riba I, García-Luque E, Blasco J, DelValls TA (2003a) Bioavailability of heavy metals bound to estuarine sediments as a function of pH and salinity values. Chem Spec Bioavailab 15(4):101–114

Riba I, Zitko V, Forja JM, DelValls TA (2003b) Deriving sediment quality guidelines in the Guadalquivir estuary associated with the Aznalcóllar mining spill: A comparison of different approaches. Cienc Mar 29(3):261–274

Riba I, DelValls TA, Forja JM, Gómez-Parra A (2004) The influence of pH and Salinity values in the toxicity of heavy metals in sediments to the estuarine clam 'Ruditapes phillipinarum'. Environ Toxicol Chem 23(5):1100–1107

Riba I, Blasco J, Jiménez-Tenorio N, DelValls TA (2005a) Heavy metal bioavailability and effects: I. Bioaccumulation caused by mining activities in the Gulf of Cádiz (SW, Spain). Chemosphere 58:659–669

Riba I, Blasco J, Jiménez-Tenorio N, González de Canales ML, DelValls TA (2005b) Heavy metal bioavailability and effects: II. Histopathology-bioaccumulation relationship caused by mining activities in the Gulf of C adiz (SW, Spain). Chemosphere 58:671–682

Shin PKS, Ng AWM, Cheung RYH (2002) Burrowing responses of the short-neck clam *Ruditapes philippinarum* to sediment contaminants. Mar Pollut Bull 45:133–139

Van Ginneken L, Chowdhury MJ, Blust R (1999) Bioavailability of cadmium and zinc to the common carp, *Cyprinus carpio*, in complexing environments: A test for the validity of the free ion activity model. Environ Toxicol Chem 18:2295–2304

Wang W, Rainbow PS (2005) Influence of metal exposure history on trace metal uptake and accumulation by marine invertebrates. Ecotox Environ Saf 61:145–159

Chapter 7
Contaminant Cycling Under Climate Change: Evidences and Scenarios

Carlos Vale, João Canário, Miguel Caetano, Laurier Poissant, and Ana Maria Ferreira

Abstract Marine ecosystems are influenced by many factors related with human activity, such as eutrophication, chemical contamination, selective overfishing, bottom trawling and blast fishing. However, various regions have shown at least some changes that were likely to be attributable to recent climate change. Although various works have pointed to repercussions of climate change on ocean processes at physical and biological levels, a few thoughts were highlighted on contaminant pathways in concert with the predicted and confirmed climate changes. Human activities released during the last century a cocktail of contaminants that are stored in soil, coastal sediments and ice. Predicted alterations under climatic changes raise pertinent questions on this topic. Are hazardous substances stored in those compartments released to cycling within the ecosystem under climate changes? To what extent are quantities injected in the ecosystems toxic to marine organisms? Does it affect ecosystem functioning?

This article reviews relevant aspects of contaminant cycling under climate changes and gives examples of evidences and scenarios. The selected examples are: melting of ice in the Arctic and the already observed increase of trace metals availability in water; temperature increase and the enhanced production of methyl mercury, a potent neurotoxin; prolonged periods of UV radiation and mercury release from soils and air-exposed sediments; sea-level rise and coastal erosion and the release of metals and organic pollutants from salt marshes; heavy rainfall events and abrupt input of historical and present contaminants from agriculture fields, obsolete industrial and urbanised areas.

Keywords Climate change • Temperature • Contaminant • Metals • Mercury • Particulate metals • Sea level • Salt marshes • Polycyclic Aromatic Hydrocarbons • Polychlorinated biphenyls

C. Vale (✉), J. Canário, M. Caetano, and A.M. Ferreira
IPIMAR, National Institute of Biological Resources, Avenida Brasília, 1449-006, Lisbon, Portugal
e-mail: cvale@ipimar.pt; j.canario@ipimar.pt; mcaetano@ipimar.pt; amfer@ipimar.pt

L. Poissant
Environment Canada, Science and Technology Branch, 105 Rue McGill 7e étage (Youville), Montreal,Québec, H2Y2E7, Canada
e-mail: laurier.poissant@ec.gc.ca

P. Duarte and J.M. Santana-Casiano (eds.), *Oceans and the Atmospheric Carbon Content*,
DOI 10.1007/978-90-481-9821-4_7,

7.1 Introduction

Natural processes, such as solar variability and volcanic outgassing, are the dominant forces that produce long-term climate changes (Hambrey and Harland 1981). However, there is now convincing evidence that recent human activities, resulting in increasing concentrations of greenhouse gases, have become a major agent of climate change (Philippart 2007). Greenhouse gases affect the global climate by retaining heat in the troposphere, thus raising the average temperature of the planet and altering global atmospheric circulation and precipitation patterns. A great concern emerged that climate change may rapidly and extensively modify the equilibrium of the most sensitive ecosystems with unknown consequences. Research has shown that the Northern Hemisphere has been warmer since 1980 than at any other time during the last 2000 years (Philippart 2007). Evidences of increasing temperature have been registered both in air (Tett et al. 1999) and in water (Barnett et al. 2005).

Climate change influences the oceans and coasts in various ways (Philippart 2007). The observed increase of temperature under climatic change resulted in acceleration of the melting of glaciers and the Greenland ice cap (Teng et al. 2006). Coupled ocean-atmosphere models pointed out that sea levels rise and seas become stormier, increasing the risk of coastal flooding, including large cities and industrial zones. Hurricane intensity appears to be greater. Precipitation is more variable with more frequent intense rainfall events leading to extensive flooding (Frei et al. 2006). Springtime is occurring earlier. Duration and severity of droughts has increased, leading to the migration of humans to cities in undeveloped regions. There is a poleward shift in the distribution of many species (Beaugrand et al. 2002; Brander et al. 2003). The number of harmful algal blooms in coastal regions appears to have increased. Many of these events are thought to be a consequence of predominantly human-induced climate change.

Although marine ecosystems are influenced by many factors related with human activity such as eutrophication (Goolsby 2000), chemical contamination (Libes 1992), selective overfishing (Myers and Worm 2003), and destructive practices like bottom trawling and blast fishing (Meysman et al. 2006; Morton and Blackmore, 2001), various regions have shown at least some changes that were likely to be attributable to recent climate change (Philippart 2007). For the most northern seas, such as the Arctic Sea, the most obvious temperature-related change is the decline in sea-ice cover and a decrease in surface salinity. For most open seas there is evidence of geographic displacement of species populations northwards. The enclosed seas have noticeably undergone dramatic changes as a consequence of changes in the frequency of inflow (e.g. Baltic Sea) or in temperature (e.g. Mediterranean Sea).

In an overview of the research needs and future scientific challenges of climate change, a panel of experts (Philippart 2007) conjectured physical responses and impacts, including alterations to the Artic-sea cover, near-surface stratification related to elevated summer temperatures, and loss of coastal habitats as a

consequence of coastal flooding. Biological responses and impacts predicted by current models point to progressive increase of primary production with possible influences on recruitment processes, changes in geographic distribution of marine species, local alterations on the interaction between species and its competitors, predators, prey or pathogens. Few works highlighted the anthropogenic impacts, e.g. contaminant pathways, acting in concert with the predicted and confirmed changes mentioned above (MacDonald et al. 2005; Schiedek et al. 2007).

During the last century, human activities caused the release of a cocktail of contaminants to the soil that via rivers and atmosphere reached the ocean, where they have accumulated and recycled through water, sediments and organisms. Many of these contaminants are referred to as hazardous substances, as they accumulate in the marine food web to levels that are toxic to organisms, including fisheries populations and therefore affecting humans. Whether climate changes affect major factors that influence the availability of contaminants in excess of threshold levels somewhere in the marine ecosystem, is a matter of future research. This paper reviews relevant aspects of contaminant cycling under climate changes and gives examples of evidences and scenarios.

7.2 The Effect of Temperature

One of the most evident aspects of climate change is the rising of temperature. The number of "tropical nights" (nights with minimum temperatures above 20°C) in southern European regions is one of the temperature indices that presented a larger variation since 1976, the start of the warming period. In Lisbon, Portugal, the number of tropical nights has increased from an average value of 7 days, in the 1970s, to around 20 days by the end of the twentieth century. This increase is clearly related to the positive trend of minimum temperatures registered from 1976 (Miranda et al. 2002).

Temperature has long been known to modify the chemistry of a number of chemical pollutants resulting in significant alterations in their toxicities, e.g. for fish. It is also generally accepted that a higher temperature increases the rate of uptake of pollutants via changes in ventilation rate in response to an increased metabolic rate and decrease in oxygen solubility (Kennedy and Walsh 1997; Schiedek et al. 2007). For a variety of freshwater fish species it has been shown that the upper temperature tolerance limits are decreased in the presence of certain organic chemicals (Cossins and Bowler 1987; Patra et al. 2007; Schiedek et al. 2007). Additionally, contaminant pathways that will become altered by climate change include volatilisation, adsorption, hydrolysis, biodegradation, photodegradation, photo-enhanced toxicity, uptake and metabolism. Whilst rates of some of these processes are increased with increasing temperature, quantitative predictions and assessments of interactions are complex (Schiedek et al. 2007).

7.2.1 The Arctic and Mercury Cycling

The Arctic epitomizes the globe's sensitivity to climate change and, due at least partly to albedo feedback, it is projected that temperature rise within the Arctic will be double that of the global average (Schiedek et al. 2007). Therefore, we may expect all of the same issues with thermal thresholds to pertain in the Arctic. The Arctic (and probably the Antarctic) is not only in the vanguard of global change (ACIA 2005), it is also in the vanguard of model-interactions between ecosystem change and contaminants imported from other parts of the world (AMAP 1998; Macdonald et al. 2000; Schiedek et al. 2007). However, it is not temperature, per se, but the 0° isotherm that forms the tipping point–basically the difference between liquid and solid water (Schiedek et al. 2007). This phase boundary offers a variety of opportunities to alter the transport of contaminants to, and within the Arctic (Macdonald et al. 2005). For example, the exchange of gases between air and water is controlled by ice cover, particulate deposition to the ocean is impeded by ice, and materials that deposit on ice are transported with the ice drift and become deposited only when the ice melts. Often this occurs in productive marine regions (Schiedek et al. 2007).

Among the contaminants, mercury is a special case. Mercury has a natural cycle that has been overloaded by human activities over the past two centuries (Mason et al. 1994). As a consequence, fluxes and burdens of mercury in air and surface water have generally risen, perhaps by a factor of two to three, and one may infer that the global risk from mercury has risen (e.g. MacDonald et al. 2000, 2005). While Hg sources are often localized in industrial and urban regions, dispersion of Hg through the atmosphere or through the hydrological cycle has resulted in the contamination of ecosystems that are remote from point source inputs (Moreno et al. 2005).

Mercury contamination in the Artic region has raised substantial concerns, especially since the first report of Atmospheric Mercury Depletion Events (AMDEs) in the Arctic (Schroeder et al. 1998). Indeed, the Arctic is believed to be an important global sink for atmospheric Hg, especially during the AMDEs that occur in spring time (Schroeder et al. 1998; Lindberg et al. 2002; Poissant et al. 2002; Ariya et al. 2004). During AMDEs, deposited Hg may enter the ecosystem, resulting in elevated Hg levels in Artic food chains. Moreover, some evidence has been accumulating during the past decade to indicate that global change may alter exposure risks to contaminants, such as Hg, delivered in the Arctic. It is estimated that 90–450 t of Hg are deposited annually in the Arctic due to AMDEs (Ariya et al. 2004; Skov et al. 2004). This deposition term is generally well accepted, but the fate and processes of deposited Hg are strongly debated (Lindberg et al. 2002; Outridge et al. 2007; Douglas et al. 2008). Douglas et al. (2008) pointed out the importance of the formation and post-deposition crystallographic history of snow and ice crystals in determining the fate and concentration of mercury in the cryosphere in addition to AMDEs. Data from Ellesmere

Island shows that total Hg concentrations of surface snow samples were 5–22 ng L^{-1} and increased to 121–182 ng L^{-1} following AMDEs (Steffen et al. 2002). The same trend has been observed at Barrow where total Hg snow concentrations increased from the typical background level of 1–90 ng L^{-1} following AMDEs (Lindberg et al. 2002; Brooks et al. 2006). AMDEs recorder at Ny-Ålesund, Svalbard (Norway) showed an increase also in total Hg snow concentration from the background concentration of 1 ng L^{-1} to levels of 30 ng L^{-1} (Berg et al. 2003) and in Kuujjuarapik and Churchill (Canada), where total Hg concentrations increased from 1–5 to 60–80 ng L^{-1} following AMDEs (Poissant 2000; Kirk et al. 2006).

One of the most environmentally troubling aspects of mercury cycling is its methylation to produce methylmercury (MeHg), a strong neurotoxin that tends to accumulate in aquatic organisms. Methylmercury toxicity is mainly related to its high mobility in living organisms due to the formation of a complex with the amino acid cysteine. The structure of this complex resembles that of a large neutral amino acid, methionine, and thereby gains entry into cells on the large neutral amino acid carrier (Clarkson and Magos 2006).

Since AMDEs add bioavailable Hg to the snow cover of Polar Regions, investigations have been conducted to detect the presence of MeHg in the snowpack. Indeed, the analysis of MeHg concentration in snowmelt water discharges on Ellesmere Island revealed that snowmelt water was the most important source of MeHg for the Arctic ecosystems (Loseto et al. 2004a, b). Further investigations showed that MeHg detected in the snow represented up to 7.5% of the total Hg (Ferrari et al. 2004; Lahoutifard et al. 2005; St. Louis et al. 2005; Constant et al. 2007). On Cornwallis Bay snow, MeHg concentrations were between <10 and 140 pg L^{-1} (Lahoutifard et al. 2005), while levels of up to 280 pg L^{-1} have been reported for samples collected on Ellesmere Island (St. Louis et al. 2005, 2007). At Station Nord, Greenland, MeHg concentrations between <10 and 113 pg L^{-1} have been detected in the snow cover (Ferrari et al. 2004). Interestingly, snow samples collected at Kuujjuarapik (Canada) revealed a significant rise of MeHg concentration during the snow melting period, with the detection of concentrations as high as 700 pg L^{-1} (Constant et al. 2007).

An enhancement of contaminant concentrations was also found in ice cores collected at Kuujjuarapik (Canada) compared to the concentrations determined in water. In a field campaign performed in April 2008 concentrations of As, Cd, Cr, Cu, Ni, Pb and U were found to be up to two orders of magnitude higher in snow than in the underlying water (Fig. 7.1) in four stations along Great Whale River and Hudson Bay (Canário and Poissant unpublished). The results obtained in Kuujjuarapik ice were similar to those observed in the frozen Saint-Louis Lake near Montréal (Canada), a heavy industrial zone, and we may estimate that, a similar pattern should be observed in the ice covering the Arctic. An environmental concerning question is what happens during ice melt, but an increase of the contaminant concentrations in the water is expected with direct consequences to the aquatic biota, especially on coastal zones where most of the biota are living. It is

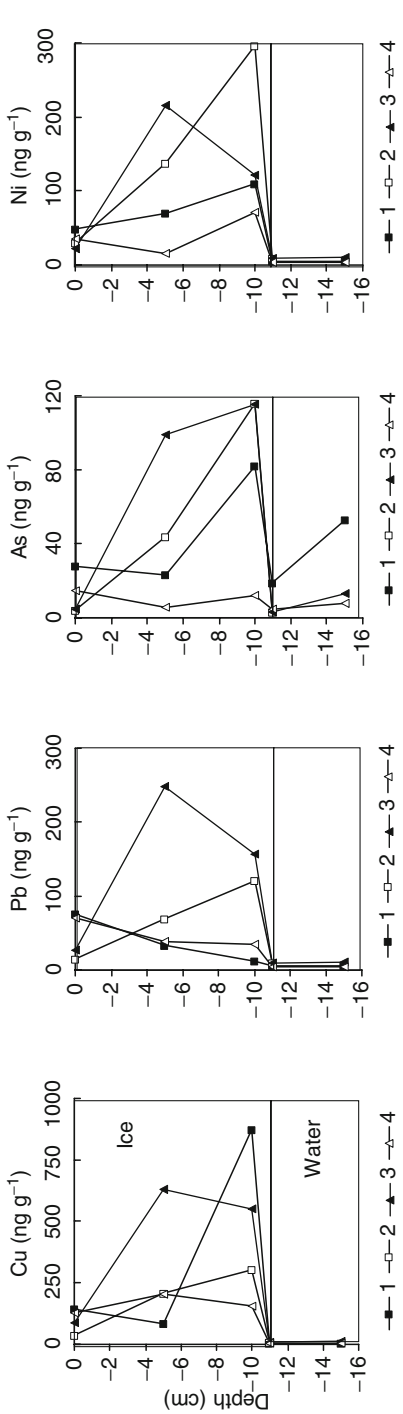

Fig. 7.1 Depth profiles of Cu, Pb, As and Ni (ng g^{-1}) concentrations in suspended particulate matter in ice cores and water column collected in four stations at Great Whale River (St. 1, 2 and 3) and Hudson Bay (St. 4). Depths ate only indicative

well known that marine environment is far more productive in the Arctic. Ice edges and associated waters are key areas of productivity in all regions of the Arctic (UNEP 1997). Hence fauna associated with the ice edge form an important pathway for contaminants, especially mercury (Hg) to enter the food web between primary producers and fish, sea birds, and mammals (UNEP 1997), they are very fragile to climate changes.

In a climate change scenario with an increase of temperature and the consequent melting of ice and snow a release of contaminants to the aquatic environment is expected.

Another consequence of a warming climate is related to melting of permafrost. There is an increasing concern about the effects of climate change on the melting of permafrost at high latitudes and the movement of carbon, nutrients, and metals within and from watersheds underlain by permafrost. Rising temperatures are beginning to melt the Arctic permafrost as potential driving factors for releasing contaminants and carbon into water and air. For example, permafrost contains mercury and as it melts some portion of the mercury could migrate into the aquatic system and be transformed into methylmercury (AMAP 2006; IPCC 2007). As a result, the permafrost melting can promote an additional input of contaminants that could have serious consequences for marine and aquatic life and to further accelerate global warming in the North.

7.2.2 The Effect of Increasing Temperatures in Mercury Methylation

The conversion of inorganic Hg into MeHg is a critical step in its pathway and toxicity. The net MeHg concentrations result from the balance between methylation and demethylation processes, which are not completely understood (Mason and Benoit 2003). The most important factors influencing biological methylation are the availability of inorganic mercury and the nature of the microbial community (Mauro et al. 1999), although influenced by physical and chemical parameters such as temperature, pH, salinity, organic carbon, and redox potential (Gilmour and Henry 1991; Barkay et al. 1997; Mason and Benoit 2003). Despite the paucity of information concerning sources, in situ production, biogeochemistry and bioaccumulation of MeHg in marine organisms and sediments appear as potentially significant sources of MeHg to food webs in the coastal zone (Mason et al. 1999; Gill et al. 1999; Covelli et al. 1999; Langer et al. 2001; Hammerschmidt et al. 2004) and possibly to the open ocean via hydrological or biological transport.

Climate change scenarios predict strong alterations in estuaries, particularly related to the physical–chemical factors that affect methylation. Increases of air and water temperature which may turn the microbiological community more active and the increase of salinity within the estuaries enhancing the availability

of Hg are possible scenarios for predicting an increase of Hg methylation in contaminated areas.

Two confined areas of the Tagus Estuary are historically contaminated by mercury from industrial sources (Figuères et al. 1985). High levels of mercury (Figuères et al. 1985; Canário et al. 2003a, b) and of MeHg (Canário et al. 2005) have been reported in surface sediments from the two hot spots. In order to compare the MeHg budgets in estuarine sediments at different temperatures, 40 surface sediments were collected in the Tagus Estuary in July and December 2004 and analysed for MeHg (Canário et al. 2007). Although MeHg levels ranged within similar intervals, significant differences were found between July and December (Fig. 7.2). In 86% of the samples, both MeHg concentrations and proportions to total Hg were higher in July, including the most contaminated area. On the basis of these values and considering an area of 320 km^2 (estuary total area) one may estimate that approximately 7 kg of MeHg increased in the first 2-cm of surface sediments of the entire estuary (26 kg in July minus 19 kg in December). This corresponds to a 37% increase. The results of this work suggest that methylation processes were more efficient in July (up to 20°C warmer) than in December. Although the full explanation of the MeHg variation was not found in this study one may conclude a possible seasonal fluctuation of Hg methylation rate in other temperate ecosystems. Interestingly, the process tends to occur either in contaminated sediments or in lower contaminated areas, which gives it more relevance in environmental terms, because benthic invertebrates may increase the uptake of MeHg in summer. These results are consistent with the effect of climate change scenarios (e.g. Heugens et al. 2001).

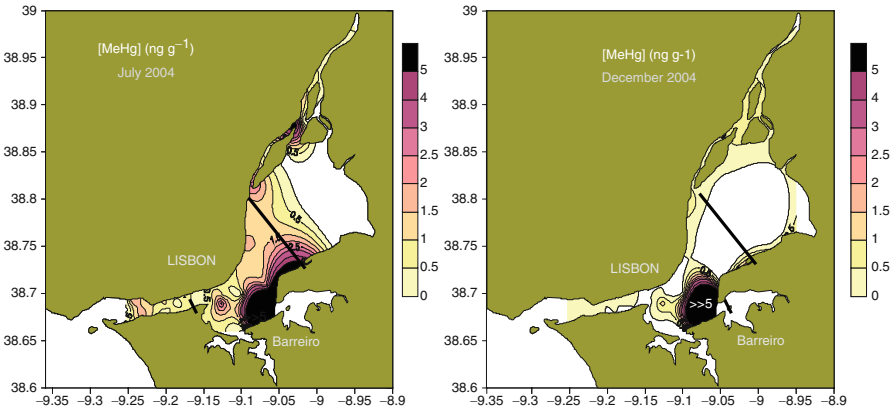

Fig. 7.2 Methylmercury distribution in surface sediments of the Tagus Estuary determined in July and December 2004 (Adapted from Canário et al. 2007)

7.3 The Sea Level Rising

The sea-level rise is a consequence of oceanic thermal expansion and melting of Antarctic and Artic glaciers (Carlson et al. 2008). There is great uncertainty about the global sea level rising. Estimates made by several authors range from 9 to 88 cm in global sea level by 2100 (Titus et al. 1991). The uncertainty appears to result from difficulties in predicting the rates of temperature increase and melting of glaciers and small ice caps (Simas et al. 2001; Philippart 2007). Recent forecasts report that sea level rise from greenhouse-induced warming of the Greenland ice sheet could double or triple the estimates of IPCC over the next century. A study on a long-melted ice sheet pointed out that the sea levels could rise more than 1 m per century (Carlson et al. 2008). The foreseen consequences of sea level rising could be increasing of storms, coastline erosion and habitats destruction, and impacts in urban areas surrounding estuaries and coastal lagoons.

7.3.1 The Effect on the Dynamic of Salt Marshes

Salt marshes are coastal ecosystems occupied by halophytic vegetation and exposed to low hydrodynamic conditions and tidal flooding. These ecosystems are characterised by their high biological productivity (Mitsch and Gosselink 2000). In addition, they serve as nurseries for fishes and crustaceans, and feeding and nesting sites for waterfowl and shorebirds. Tidal amplitude, flooding regime, topography and wind are factors determining marsh development. These characteristics are particularly vulnerable to climate change, since as sea level rises the outer salt marsh boundary tends to erode and new marsh areas form inland (Simas et al. 2001). The ecosystem response to the sea-level rise depends upon their ability to maintain their relative elevation through sedimentation. In cases where the sedimentation rate exceeds sea-level rise a positive balance is expected, while the opposite situation would result in erosion (Hackney and Cleary 1987; Reed 1990; Reed and Foote 1997). The loss of salt marsh areas may have implications for the decomposition rate of organic matter, litter quality, sediment properties, and bacterial and fungal populations (Nyman et al. 1993, 1994; Caldwell et al. 2006).

7.3.2 The Predicted Effects on Metal Cycling

An elevated plant biomass in salt marshes leads to the retention of large quantities of contaminants uptaken from sediments and water (Windham et al. 2003). Plant biomass reaches high values during the growing season and subsequently degrades in the fall and winter. Decomposing plant tissues may be either a source of metals that are released through leaching and mineralization, or sink through adsorption

on litter (Weis and Weis 2004; Pereira et al. 2007). The consequence of losing salt marsh areas as sea level rises (Simas et al. 2001) may result in additional quantities of dead biomass. Since metals are likely to persist within tissues after plants die, metal leaching in decaying litter over time may be an additional contribution to the metal budgets at the estuarine ecosystem level (Banus et al. 1974; Dorgelo et al. 1995; Zawislanski et al. 2001; Du Laing et al. 2006). Metal-containing litter from aboveground biomass will be retained and/or exported from the marsh according to the flooding regime, elevation gradient and topography of the marsh and wind (Halupa and Howes 2004; Neckles and Neill 2004). A large majority of salt marsh ecosystems exports energy-rich substances (reduced nitrogen compounds, dissolved and particulate organic matter) to deeper waters (Mitsch and Gosselink 2000; Valiela et al. 2004). Several authors have highlighted that a substantial export of metals associated with litter from halophytes are removed by tides from the marsh surfaces (Banus et al. 1974, 1975; Burke et al. 2000; Valiela et al. 2004). In particular, Caçador et al. (2009) estimated that over a growing season 68 kg of Zn, 8.2 kg of Cu, 13 kg of Co and 0.35 kg of Cd were washed out from a 200 ha marsh area of the Tagus estuary, Portugal, which is daily inundated by tides. These results suggest that, as salt marshes are destroyed under climate changes, the amount of metals associated to leaves and stems that are exported to the adjoining areas increases. This effect may have a considerable magnitude in macro- and meso-estuaries containing extensive inter-tidal areas and salt marshes, like the Tagus estuary (2,000 ha of wetlands). Storms and sea level rising by increasing tidal energy will favour a wide dispersion of organic detritus through the branched system of channels and its export to the adjoining areas. Under these circumstances, the metal-containing litter acts as a source of metals before being buried in sediments since they are easily degraded by decomposers and weathering (Weis and Weis 2004; Du Laing et al. 2006). Moreover, these predicted alterations will lead to a reduction of the role of salt marshes in detoxifying the estuarine system.

In salt marshes of temperate regions, belowground biomass often exceeds the aboveground biomass, generating large amounts of litter in sediments (Zawislanski et al. 2001). It is well documented that belowground biomass contains higher metal concentrations (Fig. 7.3) than aboveground biomass (e.g. Weis and Weis 2004). The decay of the generated litter depends on a number of external factors, such as temperature, frequency of tidal inundation, chemical characteristics of sediments, litter composition, detritus-feeding animals and microorganisms (Wilson et al. 1986; Hemminga and Buth 1991; Foote and Reynolds 1997; Sundby et al. 2003). Litter degradation, which occurs over different rates, leaches out the most soluble fractions of the plant material including contaminants (Valiela et al. 1985; Wilson et al. 1986; Benner et al. 1991; Pereira et al. 2007). By varying the most important variables that control the degradation rates, climate changes may have direct consequences on the release of contaminants to the salt marsh area. The rise of sea level will influence the temperature of submerged sediments and the penetration of UV-radiation. Temperature has a direct effect on degradation of litter and therefore in the metal release, while UV-radiation has an indirect effect by changing species composition of microbial communities. Although sunlight scarcely penetrates the sediment surface, the supplemental UV-B radiation decreases mycorrhizae, fungi

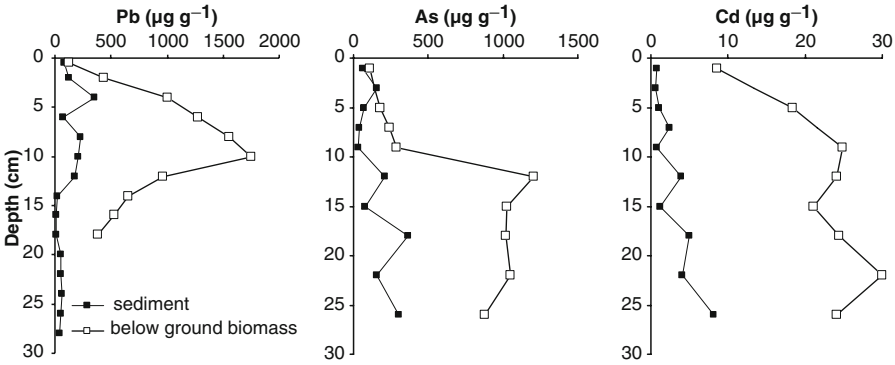

Fig. 7.3 Depth profiles of Pb, As and Cd (µg g^{-1}) concentrations in sediments colonised by *Spartina maritima* and in belowground biomass from Tagus salt marsh (SW Europe)

and bacteria associated with roots (Caldwell et al. 2007) affecting plant nutrition and metal cycling (Caldwell et al. 2007). Moreover, the migration of the salt marsh to inland as sea level raises results in additional amounts of litter and consequently increases the leaching out of metals to the ecosystem, making them available to the trophic web or entering the estuarine water (Breteler and Teal 1981; Larsen and Schierup 1981; Zawislanski et al. 2001; McFarlane et al. 2003).

7.3.3 The Predicted Effects on Polycyclic Aromatic Hydrocarbons

The few works on Polycyclic Aromatic Hydrocarbons (PAHs) in salt marshes have pointed to high retention of heavier PAHs in sediments colonised by halophyte plants, and lighter ones in aboveground parts of the plants (Martins et al. 2008a). As plants uptake water, dissolved solutes in pore water and overlying water migrate towards the roots. This pumping mechanism explains the retention of metals, PAHs and other organic contaminants in rooting sediments (Martins et al. 2008b). However, the smaller retention of lighter PAHs in rooting sediments appears to result from a faster degradation rate of these compounds by bacteria activities. The marshes have therefore been seen as a natural environment to decompose the most labile PAH compounds. Destruction of salt marshes by erosion or sea level rising will imply a reduction of that role in detoxifying the ecosystem.

7.4 The Rainfall Events

Classic works have pointed out the importance of river floods on the transport of suspended particulate matter to estuaries and adjoining coastal waters (e.g. Meade 1972; Avoine et al. 1981; Castaing et al. 1981; Bale et al. 1985; Vale et al. 1993).

In macro- and meso-tidal estuaries characterised by a turbidity maximum zone, the seaward substantial escape of suspended sediment occurs in short periods of exceptionally high river flows (Avoine et al. 1981). Under these circumstances, the turbidity maximum zone moves seaward and the suspended load that reaches the adjoining coastal zone does not return to the estuary.

The Tagus River, which drains an area of 86,000 km^2, is the principal source of freshwater to the Tagus estuary, Portugal. Tagus estuary is the largest meso-tidal estuary in Western Europe (320 km^2), with a residence time of freshwater ranging from 65 days, at a discharge of 100 $m^3\ s^{-1}$, to 6 days, at a discharge of 2,200 $m^3\ s^{-1}$ (Martins et al. 1984). Because of the construction of several reservoirs along the course of the river, the suspended sediment load was estimated at 4×10^5 t (Vale and Sundby 1987), one order of magnitude less than the suspended-sediment load of a comparable river, such as the Gironde (Allen et al. 1980). However, during a catastrophic flood in 1979 (average daily freshwater discharge estimated in 13,000 $m^3\ s^{-1}$), a large pulse of fluvial sediment amounting to about 1×10^6 t over a 10-day period was produced (Vale 1981). This amount is equivalent to several years of normal river sediment discharge. The increase in the frequency and intensity of rainfall events under climate changes will imply the transport of huge amounts of sediments to estuaries and adjacent coasts in short periods of time.

7.4.1 Transport of Particulate Metals

The elemental composition of the suspended load by the Tagus river under an exceptional flood pointed to concentrations (Vale 1981) only slightly above the pre-industrial values and comparable to the suspended load composition of the major world rivers (Martin and Meybeck 1979). Possibly, eroded particles from the extensive cultivated fields in the drainage river basin diluted metal-rich particles from industrial and urban areas. A similar situation was registered in the Guadiana estuary during a major flood in 2001 (Caetano et al. 2006). The Guadiana River, located in the south Iberian Peninsula with a drainage basin dominated by rural activities and forest, is a typical example of southern European systems highly influenced by short periods of runoff. In both fluvial systems, river floods caused a considerable discharge of metals to the estuary and adjoining coast. Increase of the frequency and intensity of these events under climate changes may represent, therefore, pulse inputs of large amounts of metals to the estuary and adjoining coastal area. However, the suspended load may contain relatively low metal concentrations in rivers crossing less industrialised areas due to the substantial erosion of rural areas.

7.4.2 Transport of Particulate Organic Pollutants

The situation of organic compounds used in agriculture may be rather different. Despite restrictions on the use of most toxic pesticides in the last decades

(e.g. DDT in Europe), they have been quantified in biota, suspended particles and sediments of estuarine and coastal environments (Lee et al. 2001; Olsen et al. 1993; Phillips 1986). The values registered in certain regions are still a matter of concern due to their toxicity. In fact, most of these compounds have short residence time in water, being rapidly adsorbed onto suspended particulate matter and accumulated organisms. The increasing frequency and intensity of runoff periods under climate change may result in additional amounts of contaminants derived from soil erosion to the estuarine and coastal ecosystems.

Estuarine systems receiving low freshwater discharges in most times of the year and abrupt inputs in short periods of heavy rain can be used as an ecosystem model. The Sado estuary, Portugal, is a good system to test the hypothesis of storms influencing the transport of organic contaminants to the coastal environments and the potential impact in target aquatic organisms. In favour of this choice is the seasonal and inter-annual variations of freshwater discharge, agriculture being practically the only human activity in the Sado river basin, and the presence of wild oyster grounds in the upper part of the estuary. The compound pp'-DDE, a metabolite of pp'-DDT, was used as a model contaminant used in agriculture (Ferreira and Vale 1995; Vale et al. 1993).

7.4.3 Example of a Historical Pollutant: pp'-DDE

Figure 7.4 shows the seasonal variation of river discharges and of pp'-DDE concentrations in suspended particulate matter (SPM) and in whole soft oyster tissues over

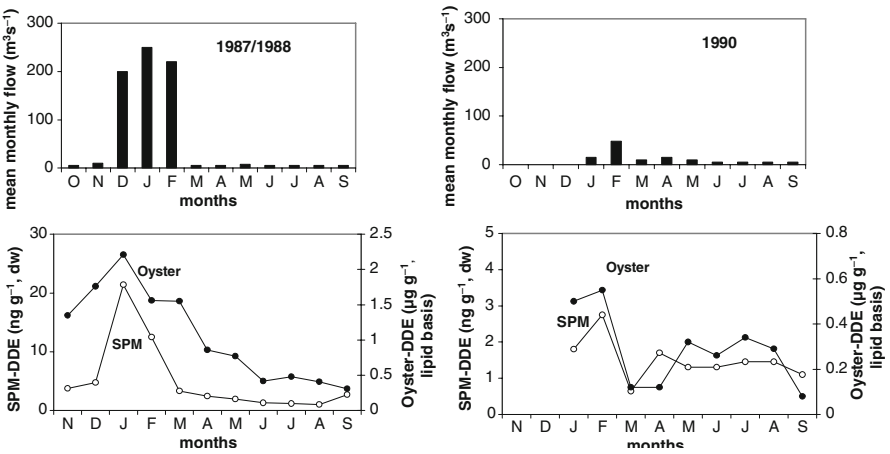

Fig. 7.4 Mean month flow ($m^3\ s^{-1}$) of Sado River between October 1987 and September of 1988 and from January to September of 1990. Concentrations of DDE (ng g^{-1}) in suspended particulate matter (SPM) and in oysters (µg g^{-1}) collected at the upper Sado estuary in the same periods

two annual periods with a contrasting hydrological cycle. In summer and autumn, river flows were lower than 2 $m^3 s^{-1}$, in winter 1990 a mean daily flow of 14 $m^3 s^{-1}$ (average year) was reached, but in winter 1989 it went up to 250 $m^3 s^{-1}$ (exceptional wet year). In periods of higher river flows the levels of pp'-DDE were elevated both in SPM and in oysters, reaching a maximum of 21.4 ng g^{-1} and 2.2 μg g^{-1},respectively (Ferreira and Vale 2001). These levels exceeded largely the values reported for the dry season of this year (max of 1.1 ng g^{-1}, and 0.3 μg g^{-1}, respectively) and the values found for the same period of the dry year (max of 1.3 ng g^{-1}, and 0.3 μg g^{-1}, respectively). Levels reported for oysters were normalised to lipids in order to minimise the physiological effect on the accumulated values. In fact, the accumulated levels of lipophilic compounds tend to increase in pre-spawning periods due to the enrichment of lipids in tissues. These results evidenced that, despite the prohibition of DDT use in agriculture, runoff appears as a major vehicle to transport this historical pollutant to the estuary. On the basis of these observations one may predict that an increase in the number of runoff episodes associated with storms under climate change will pulse several contaminants, retained in the river basin soil, to the coastal environments. Furthermore, the similar pattern in suspended particles composition and in oyster accumulated levels indicated the possible repercussion of these episodes on the wellbeing of wild target organisms.

7.4.4 Example of Polychlorinated Biphenyls Compounds

Restrictions placed internationally on manufacture and use of polychlorinated biphenyls (PCBs) implied that their discharges by industry became less common (Connell et al. 1998). However, trace quantities of these contaminants are still found in the coastal environment supplied through rivers (Van Zoest and Van Eck 1990), atmospheric deposition (Sanders et al. 1996) and dumping of dredged material (Tang and Myers 2002). Despite the high chemical stability of PCB congener molecules, it has been proved that chlorine might be replaced mainly in meta- and para-position in the rings by hydrogen (Bedard et al. 1996). This dechlorination process may occur with slow kinetics in particles by microbial activity (Chang et al. 2001) and by photodegradation with a faster rate (Chang et al. 2002).

The levels of PCB congeners in topmost sediments of the Guadiana River estuary before and after an exceptional river flood following a week of heavy rains differed significantly (Ferreira et al. 2003). Nevertheless, the largest differences were registered in the tri- and tetra-chlorinated congeners. Figure 7.5 compares the median values of tri+tetra-CB and hexa-chlorinated CB in topmost sediments. This study permitted us to conclude that flood material contains different CB compositions from near the PCB point sources, where higher chlorinated compounds tend to be predominant (Lee et al. 2001). The absence of industries in the drainage river basin suggests that the increase in the proportion of less chlorinated congeners resulted from inputs to the river by atmospheric deposition, directly or followed by runoff. In fact these compounds exhibit a higher mobility in the atmosphere and aquatic milieu

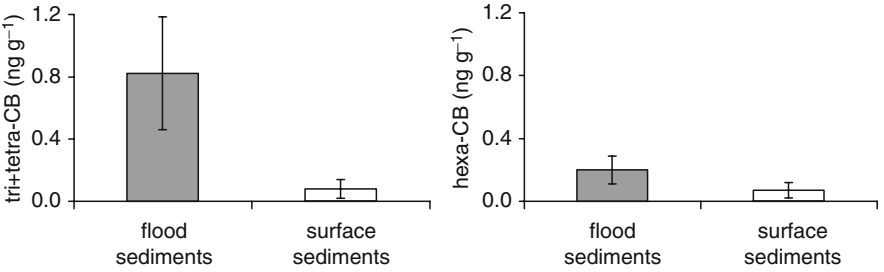

Fig. 7.5 Mean concentration of tri+tetra-CB and hexa-CB (ng g^{-1}) in flood sediments (*dashed bar*) and surface sediments (*open bar*) collected along Guadiana River-estuary, after a river flood

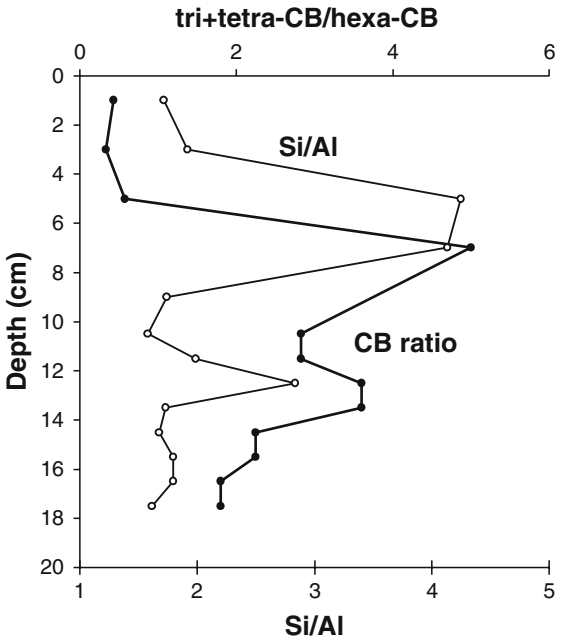

Fig. 7.6 Depth variation of Si/Al and tri+tetra-CB/hexa-CB ratios in a sediment core from adjoining coastal area of Guadiana estuary

(Dannenberger 1996). In addition, we should not exclude the possibility of higher chlorinated compounds incorporated in the soil being degraded to lower CB by photodegradation (Chang et al. 2002). On the basis of these results one may predict that increase of the number of episodic rainfall events under climate changes would result in additional river inputs of degraded compounds transported by the atmosphere from distant sources to estuaries. Depending on the intensity of these events, alterations may also occur in the adjoining coastal zone, as in the case of the Guadiana River estuary. Figure 7.6 presents the depth profile of Si/Al ratio and tri+tetra-CB/hexa-CB

ratio in the first 17-cm of a sediment core from the adjoining area to the Guadiana estuary (Ferreira et al. 2003; Martins et al. 2005). Maximum of Si/Al ratios (a proxy of coarser sediments) marks the episodic transport of coarser particles to the coast associated with river runoff. The parallelism between the depth profiles of tri+tetra-CB/hexa-CB ratio and Si/Al ratio indicated the extension of the runoff effect to the adjoining coastal zone. If intensity and frequency of these episodes tend to increase the compounds stored in soils will reach the coast more effectively.

7.5 Duration of Droughts (Effect of UV Radiation)

Conversely, the decrease of precipitation may also alter the transport, transfer, deposition and fate of contaminants. Climate change scenarios for the UK indicate annual average temperature increases from 2°C to 3.5°C by 2080s and, consequently, the existence of larger summer periods (DEFRA 2002). In southern European countries, this scenario could be more pronounced. The last 10 years were one of the driest decades in the last centuries with extended periods of drought. In 2003, during a big heat wave, summer temperatures in Portugal increased up to 5°C above average (Santos et al. 2006). One of the consequences of prolonged summers could be the duration of UV radiation on the ecosystems. The enhanced of UV radiation annual exposure results also from the depletion of ozone layer due to halogen-containing contaminants in the stratosphere, which has been especially worrisome in Polar Regions (Schiedek et al. 2007).

The alterations in UV radiation background could have a strong effect in the pathway and fate of contaminants. Macdonald et al. (2005) found growing evidence that certain PAHs may pose a greater hazard to aquatic organisms when exposed to ultraviolet light due to photo-enhanced toxicity (phototoxicity). Laboratory studies have also showed that the toxicity of anthracene, fluoranthene and pyrene to marine invertebrate larvae and embryos is significantly increased (Pelletier et al. 1997) in the presence of environmentally realistic levels of UV-radiation, compared with embryos exposed to PAH alone, at levels previously deemed to have little acute biological effect (Lyons et al. 2002).

Mercury is other contaminant extremely susceptive to UV radiation. Among the volatile forms of mercury, Hg^0 is the major constituent of the dissolved gaseous mercury in open ocean waters (Mason et al. 2001), and several works have shown its transference to the atmosphere (Hudson et al. 1995; Fitzgerald and Mason 1997; Beucher et al. 2002). In last decade there was an increasing evidence of the primary importance of photochemical reactions in the mercury reduction processes (Schroeder et al. 1991; Munthe and McEloy 1992; Xiao et al. 1994; Beucher et al. 2002). The ability of many Hg(II) compounds to absorb part of the solar radiation – mainly UVB radiation – (Lin et al. 1999; O'Driscoll et al. 2007) and the importance of Fe(III) in the reduction processes (Zhang and Lindberg 2001) are mechanisms proposed for the reduction of Hg(II). Even solid surfaces such as HgS can also be photochemically reduced (Nriagu 1994). Soils naturally

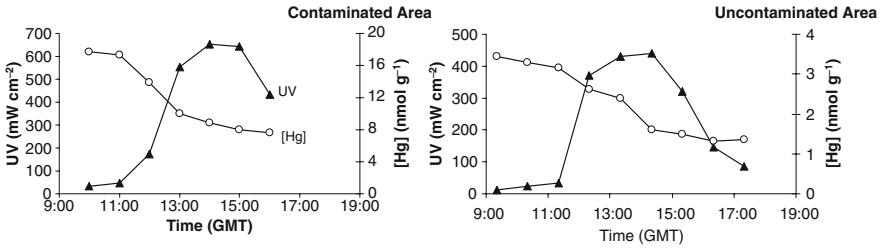

Fig. 7.7 Time course evolution of UV radiation intensity (mW cm^{-2}) and total mercury concentrations (nmol g^{-1}) in sediments exposed to solar radiation in contaminated and uncontaminated areas (Adapted from Canário and Vale 2004)

enriched in Hg have been considered important sources contributing to the atmospheric Hg load (e.g. Rasmussen 1994). Recent field investigations indicate that these natural sources may be comparable to the anthropogenic sources in their impacts on regional and global atmospheric Hg pools (Gustin et al. 1999). Several works have indeed proved that UV radiation is the key factor for understanding these processes.

In freshwater systems, Amyot et al. (1997) found that UVB radiation is particularly important for mercury photo-reduction in low DOC temperate lakes and other researchers have also identified UV radiation as the principal driver of DGM (dissolved Hg^0) production in freshwaters (Garcia et al. 2005; O'Driscoll et al. 2007).

In a recent work in the inter-tidal areas of the Tagus Estuary it was observed a rapidly decrease in Hg concentrations when sediments were exposed to the atmosphere and solar radiation (Canário and Vale 2004). Moreover this process was registered in both contaminated and non-contaminated sediments (Fig. 7.7). The transformations, which occurred in the short period of time that solar radiation was more intense (3–4 h), pointed out to the possibility of mercury escaping to the atmosphere when sediments are exposed to solar radiation. The escape may be quite substantial occurring in all intertidal areas independently of the degree of sediment contamination, as can be inferred from the high proportion (>50%) of mercury that escape from low- to high-contaminated sediments used in the field experiments. The authors suggested that the transfer of Hg^0 to the atmosphere can occur frequently in physically dominated estuaries and coastal lagoons with extensive inter-tidal areas. Strong tidal currents, winds or benthic organisms can renew the topmost layer of sediments, exposing fresh surface of inter-tidal sediments to solar radiation. This transfer of Hg to the atmosphere until Hg complexes susceptible of being destroyed by UV radiation are present.

In a climate change scenario with prolonged summer it is expected that these process tend to occur more frequently. For example, the predicted scenarios point to increase of almost 100% of the number of summer days in south-west of Portugal (Santos et al. 2006). This factor could contribute to the increase of Hg release to atmosphere from inter-tidal areas and the consequent input of this contaminant on a regional and global scale.

References

ACIA (2005) Arctic climate impact assessment, Cambridge University Press, New York, 1038 pp
Allen GP, Salomon JC, Bassoulet P, Du Penhoat Y, De Grandpre C (1980) Effects of tides on mixing and suspended sediment transport in macrotidal estuaries. Sediment Geol 26:69–90
AMAP (1998) AMAP assessment report: Arctic pollution issues, Arctic monitoring and assessment programme, Oslo, Norway
AMAP (2006) Arctic monitoring and assessment program. Acidifying pollutants, Arctic haze and acidification in the Arctic. Arctic Monitoring and Assessment Programme (AMAP), Oslo, Norway
Amyot M, Mierle G, Lean D, McQueen D (1997) Effect of solar radiation on the formation of dissolved gaseous mercury in temperate lakes. Geochem Cosmochem Acta 61:975–987
Ariya PA, Dastoor AP, Amyot M, Schroeder WH, Barrie L, Anlauf K, Raofie F, Ryzhkov A, Davignon D, Lalonde J, Steffen A (2004) The Arctic: A sink for mercury. Tellus 56B:397–403
Avoine J, Allen JP, Nichols M, Salomon JC, Larsonneur C (1981) Suspended-sediment transport in the Seine estuary, France : Effect of man-made modifications on estuary-shelf sedimentology. Mar Geol 40:119–137
Bale AJ, Morris AW, Howland RJM (1985) Seasonal sediment movement in the Tamar estuary. Oceanol Acta 8:1–6
Banus M, Valiela I, Teal J (1974) Export of lead from salt marshes. Mar Pollut Bull 5:6–9
Banus M, Valiela I, Teal J (1975) Lead, zinc and cadmium budgets in experimentally enriched salt marsh ecosystems. Estuar Coast Mar Sci 3:421–430
Barkay T, Gillman M, Turner RR (1997) Effects of dissolved organic carbon and salinity on bioavailability of mercury. Appl Environ Microbiol NOV:4267–4271
Barnett TP, Pierce DW, AchutaRao KM, Gleckler PL, Santer BD, Gregory JM, Washington WM (2005) Penetration of human induced warming into the world's oceans. Science 309:284–287
Beaugrand G, Reid PC, Ibanez F, Lindley JA, Edward M (2002). Reorganization of North Atlanctic marine copepod biodiversity and climate. Science 31(296):1692–1694
Bedard DL, Bunnell SC, Smullen LA (1996) Stimulation of microbial para-dechlorination of polychlorinated biphenyls that have persisted in Housatonic River sediments for decades. Environ Sci Technol 30:687–694
Benner R, Fogel ML, Sprague EK (1991) Diagenesis of belowground biomass of Spartina alterniflora in salt-marsh sediments. Limnol Oceanogr 36:1358–1374
Berg T, Sekkesæter S, Steinnes E, Valdal A-K, Wibetoe G (2003) Springtime depletion of mercury in the European Arctic as observed at Svalbard. Sci Total Environ 304(1–3):43–51
Beucher C, Wong-Wah-Chung P, Richard C, Mailhot G, Bolte M, Cossa D (2002) Dissolved gaseous mercury formation under UV irradiation of unamended tropical waters from French Guyana. Sci Total Environ 290:131–138
Brander KM, Dickson RR, Edwards M (2003). Use of continuous plankton recorder information in support of marine management applications in fisheries, environmental protection, and in the study of ecosystem response to environmental change. Prog. Oceanogr. 58:175–191
Breteler R, Teal JM (1981) Trace element enrichments in decomposing litter of Spartina alterniflora. Aquat Bot 11:111–120
Brooks SB, Saiz-Lopez A, Skov H, Lindberg SE, Plane JMC, Goodsite ME (2006) The mass balance of mercury in the springtime arctic environment. Geophys Res Lett 33:L13812. doi:10.1029/2005GL025525
Burke D, Weis J, Weis P (2000) Release of metals by the leaves of the salt marsh grasses Spartina alterniflora and Phragmites australis. Estuar Coast Shelf Sci 51:153–159
Caçador I, Caetano M, Duarte B, Vale C (2009) Stock and losses of trace elements from salt marsh plants. Mar Environ Res 67(2):75–82
Caetano M, Vale C, Falcão M (2006) Particulate metal distribution in Guadiana estuary punctuated by flood episodes. Estuar Coast Shelf Sci 70:109–116

Caldwell MM, Flint SD (2006) Use and evaluation of biological spectral UV weighting functions for the ozone reduction issue. In: Ghetti F, Checcucci G, Bornman JF (eds) Environmental UV radiation: Impact on ecosystems and human health and predictive models. Springer, The Netherlands, pp 71–84

Caldwell MM, Bornman JF, Ballaré CL, Flint SD, Kulandaivelu G (2007) Terrestrial ecosystems, increased solar ultraviolet radiation, and interactions with other climate change factors. Photochem Photobiol Sci 6:252–266

Canário J, Vale C (2004) Rapid release of mercury from intertidal sediments exposed to solar radiation: A field experiment. Environ Sci Technol 38:3901–3907

Canário J, Vale C, Caetano M (2003a) Mercury in contaminated sediments and pore waters at a contaminated site of the Tagus Estuary. Cienc Mar 29(4):535–545

Canário J, Vale C, Caetano M, Madureira MJ (2003b) Mercury in contaminated sediments and pore waters enriched in sulphate (Tagus Estuary, Portugal). Environ Poll 126(3):425–433

Canário J, Vale C, Caetano M (2005) Distribution of monomethylmercury and mercury in surface sediments of the Tagus Estuary (Portugal). Mar Poll Bull 50:1142–1145

Canário J, Branco V, Vale C (2007) Seasonal variation of monomethylmercury concentrations in surface sediments of the Tagus estuary (Portugal). Environ Poll 148:380–383

Carlson AE, LeGrande AN, Oppo DW, Came RE, Schmidt GA, Anslow FS, Licciardi JM, Obbink EA (2008) Rapid early Holocene deglaciation of the Laurentide ice sheet. Nat Geosci 1:620–624

Castaing P, Aleen GP (1981) Mechanisms controlling seaward escape of suspended sediment from the Gironde: A macrotidal estuary in France. Mar Geol 40:101–118

Chang BV, Liu WG, Yuan SY (2001) Microbial dechlorination of three PCB congeners in river sediment. Chemosphere 45:849–856

Chang FC, Yen J-H, Wang Y–S (2002) Dechlorination of PCBs by UV irradiation in water and their correlative of the charge distribution on carbon atom. Organohalogen Compd 58:13–16

Clarkson TW, Magos L (2006) The toxicity of mercury and its chemical compounds. Crit Rev Toxicol 36:609–662

Connell DW, Wu RSS, Richardson BJ, Leung K, Lam PSK, Connell PA (1998) Occurrence of persistent organic contaminants and related substances in Hong Kong marine areas: An overview. Mar Poll Bull 36:376–384

Constant P, Poissant L, Villemur R, Yumvihoze E, Lean D (2007) Fate of inorganic mercury and methyl mercury within the snow cover in the low arctic tundra on the shore of Hudson Bay (Québec, Canada). J Geophys Res 112:D08309. doi:10.1029/2006JD007961

Cossins AR, Bowler K (1987) Temperature biology of animals. Chapman and Hall, London

Covelli S, Faganeli J, Horvat M, Brambati A (1999) Pore water distribution and benthic flux measurements of mercury and methylmercury in the Gulf of Trieste. Estuar Coast Shelf Sci 48:415–428

Dannenberger D (1996) Chlorinated microcontaminants in surface sediments of the Baltic Sea: Investigations in the Belt Sea, the Arkona Sea and the Pomeranian Bight. Mar Pollut Bull 32:772–781

DEFRA (2002) Climate change scenarios for the UK

Dorgelo J, Meester H, Vanvelzen C (1995) Effects of diet and heavy metals on growth rate and fertility in deposit-feeding snail Potamopyrgus jenkinsi (Smith) (Gastropoda: Hydrobiidae). Hydrobiologia 316:199–210

Douglas TA, Sturm M, Simpson WR, Blum JD, Alvare-Aviles L, Keeler GJ, et al. (2008) Influence of snow and ice crystals formation and accumulation on mercury deposition to the Arctic. Environ Sci Technol 42:1542–1552

Du Laing G, Ryckegem G, Tack F, Verloo M (2006) Metal accumulation in intertidal litter through decomposing leaf blades, sheaths and stems of Phragmites australis. Chemosphere 63:1815–1823

Ferrari CP, Dommergue A, Boutron CF, Jitaru P, Adams FC (2004) Profiles of mercury in the snow pack at Station Nord, Greenland shortly after polar sunrise, Geophys Res Lett 31:L03401. doi:10.1029/2003GL018961

Ferreira AM, Vale C (1995) The importance of runoff to DDT and PCB inputs to the Sado estuary and Ria Formosa. Netherlands J Aquat Ecol 29:211–216
Ferreira AM, Vale C (2001) Seasonal and inter-annual variations of PCB and DDT contents in the oyster *Crassostrea angulata* from the Sado estuary (Portugal). Cienc Mar 27:255–268
Ferreira AM, Martins M, Vale C (2003) Influence of diffuse sources on levels and distribution of polychlorinated biphenyls in the Guadiana River estuary, Portugal. Mar Chem 83:175–184
Figuères G, Martin JM, Meybeck M, Seyler P (1985) A comparative study of mercury contamination in the Tagus Estuary (Portugal) and major French Estuaries (Gironde, Loire, Rhône). Estuar Coast Shelf Sci 20:183–203
Fitzgerald WF, Mason RP (1997) In mercury and its effects in the environment biology, Siegel A, Siegel H (eds). Marcel Decker, New York, pp 53–111
Foote AL, Reynolds KA (1997) Decomposition of saltmeadow cordgrass (Spartina patens) in Louisiana coastal marshes. Estuaries 90:579–588
Frei C, Scholl R, Fukutome S, Schmidli J, Vidale PL (2006). Future change of precipitation extremes in Europe: Intercomparision of scenarios from regional climate models. J Geophys Res 111:D0 6105, 22p
Garcia E, Amyot M, Ariya PA (2005) Relationship between DOC photochemistry and mercury redox transformations in temperatelakes and wetlands. Geochim Cosmochim Acta 69(8): 1917–1924
Gill GA, Bloom NS, Cappellino S, Driscoll CT, Mason RP, Rudd JWM (1999) Sediment-water fluxes of mercury in Lavaca Bay, Texas. Environ Sci Technol 33:747–756
Gilmour C, Henry EA (1991) Mercury methylation in aquatic systems affected by acid deposition. Environ Poll 71:131–169
Goolsby DA (2000) Mississippi Basin nitrogen flux believed to cause gulf hypoxia. Eos. Trans Am Geophys Union 81:321–326
Gustin MS, Lindberg SE, Marsik F, Casimir A, Ebinghaus R, Edwards G, Fitzgerald-Huble C, Kemp R, Koch H, Leonard T, London J, Majewski M, Owens J, Pilote M, Poissant L, Rasmussen P, Schneeberger D, Schroeder W, Sommar J, Turner R, Vette A, Wallschlaeger D, Xiao ZF, Zhang HJ (1999) Nevada STORMS project: Measurement of mercury emissions from naturally enriched surfaces. J Geophys Res 104(D17):21831–21844
Hackney CT, Cleary WJ (1987) Saltmarsh loss in Southeastern North Carolina Lagoons: Importance of sea-level rise and inlet dredging. J Coast Res 3(1):93–97
Halupa P, Howes B (2004) Effects of tidally mediated litter moisture contents on decomposition of Spartina alterniflora and S. patens. Mar Biol 123:379–391
Hambrey MJ, Harland WB (1981) The evolution of climates. In: Greenwood PH, Cocks LRM (eds) The evolving Earth.Cambridge University Press, UK, pp 137–154
Hammerschmidt CR, Fitzgerald WF, Lamborg CH, Balcom PH, Visscher PT (2004) Biogeochemistry of methylmercury in sediments of Long Island Sound. Mar Chem 90:31–52
Hemminga MA, Buth GJC (1991) Decomposition in salt marsh ecosystems of the SW Netherlands: The effects of biotic and abiotic factors. Vegetatio 92:73–83
Heugens EHW, Henriks AJ, Dekker T, van Straalen NM, Admiraal W (2001) A review on the effects of multiple stressors on aquatic organisms and analysis of uncertainty factors for use in risk assessment. Crit Rev Toxicol 31:247–284
Hudson RJM, Gherini SA, Fitzgerald WF, Porcella DB (1995) Anthropogenic influences on the global mercury cycle: A model-based analysis. Water Air Soil Pollut 80:265–272
IPCC (2007) The Intergovernmental Panel on Climate Change, IPCC report, http://www.ipcc.ch/
Kennedy CJ, Walsh PJ (1997) Effects of temperature on xenobiotic metabolism. In: Wood CM, McDonald DG (eds) Global warming – implications for freshwater and marine fish. Cambridge University Press, UK, pp 303–324
Kirk JL, St. Louis VL, Sharp ML (2006) Rapid reduction and reemission of mercury deposited into the snowpacks during atmospheric mercury depletion events at Churchill, Manitoba, Canada. Environ Sci Technol 40:7590–7596
Lahoutifard N, Sparling M, Lean D (2005) Total and methyl mercury patterns in Arctic snow during springtime at Resolute, Nunavut, Canada. Sci Total Environ 39:7597–7606

Langer CS, Fitzgerald WF, Visscher PT, Vandal GM (2001) Biogeochemical cycling of methylmercury at Barn Island salt marsch, Stonington, CT, USA. Wetlands Ecol Mang 9:295–310

Larsen VJ, Schierup H (1981) Macrophyte cycling of zinc, copper, lead, and cadmium in the littoral zone of a polluted area and a non-polluted lake: II. Seasonal changes in heavy metal content of above-ground biomass and decomposing leaves of Phragmites australis (Cav.) Trin Aquat Bot 11:211–230

Lee KT, Tanabe S, Koh CH (2001) Contamination of polychlorinated biphenyls (PCBs) in sediments from Kyeonggi Bay and nearby areas, Korea. Mar Poll Bull 42:273–279

Libes S (1992) An introduction to marine biogeochemistry. Wiley, New York, pp 734

Lin CJ, Pehkonen SO (1999) The chemistry of atmospheric mercury: A review. Atmos Environ 33:2067–2079

Lindberg S, Brook S, Lin C-J, Scott KJ, Landis MA, Stevens RK, Goodsite M, Richter A (2002) Dynamic oxidation of gaseous mercury in the Arctic troposphere at Polar Sunrise. Environ Sci Technol 36:1245–1256

Loseto L, Lean DRS, Siciliano SD (2004a) Snowmelt sources of methylmercury to high arctic ecosystems. Environ Sci Technol 38:3004–3010

Loseto LL, Siciliano SD, Lean DRS (2004b) Methylmercury production in high Arctic wetlands. Environ Toxicol Chem 23:17–23

Lyons BP, Pascoe CK, McFadzen IRB (2002) Phototoxicity of pyrene and benzo[a]pyrene to embryo-larval stages of the pacific oyster Crassostrea gigas, Mar Environ Res 54:627–631

Macdonald RW, Barrie LA, Bidleman TF, Diamond ML, Gregor DJ, Semkin RG, Strachan WJ, Li YF, Wania F, Alaee M, Alexeeva JB, Backus SM, Bailey R, Bewers JM, Gobeil C, Halsall CJ, Harner T, Hoff JY, Jantunen LMM, Lockhart WL, Mackay D, Muir DCG, Pudykiewicz J, Reimer KJ, Smith JN, Stern GA, Schroeder WH, Wagemann R, Yunker MB (2000) Contaminants in the Canadian Arctic: 5 years of progress in understanding sources, occurrence and pathways. Sci Total Environ 254:93–234

Macdonald RW, Harner T, Fyfe J (2005) Recent climate change in the Arctic and its impact on contaminant pathways and interpretation of temporal trend data. Sci Total Environ 342:5–86

Martin JM, Meybeck M (1979) Elemental mass-balance of material carried by major world rivers. Mar Chem 7:178–206

Martins M, Ferreira J, Calvão T, Figueiredo H (1984) Nutrientes no estuário do Tejo – comparação de situação em caudais médios e em cheia, com destaque para alterações na qualidade da água. Proceedings first Symposium Luso-Brasileiro de Eng. sanitária e Ambiental, pp 9

Martins M, Ferreira AM, Vale C (2005) PCB composition in flood material and sediments from the Guardiana River estuary. Cienc Mar 31:285–291

Martins M, Ferreira AM, Vale C (2008a) Retention and partitioning of polycyclic aromatic hydrocarbons in *Sarcocornia fruticosa* from two Portuguese salt marshes. Cienc Mar 34:373–380

Martins M, Ferreira AM, Vale C (2008b) The influence of *Sarcocornia fruticosa* on retention of PAHs in salt marsh sediments (Sado estuary, Portugal). Chemosphere 71:1599–1606

Mason RP, Benoit JM (2003) Organomercury compounds in the environment. In: Graig P (ed) Organometallic compounds in the environment. Wiley, West Sussex, UK, pp 57–99

Mason RP, Fitzgerald WF, Morel FMM (1994) The biogeochemical cycling of elemental mercury: Anthropogenic influence. Geochim Cosmochim Acta 58:3191–3198

Mason RP, Lawson NM, Lawrence AL, Leaner JJ, Lee JG, Sheu GR (1999) Mercury in Chesapeake Bay. Mar Chem 65:77–96

Mason RP, Lawson NM, Sheu G-R (2001) Mercury in the Atlantic Ocean: Factors controlling air–sea exchange of mercury and its distribution in the upper waters. Deep Sea Res II 48:829–2853

Mauro JBN, Guimarães JRD, Melamed R (1999) Mercury methylation in a tropical macrophyte: Influence of abiotic parameters. Appl Organometal Chem 13:631–636

McFarlane G, Pulkownik A, Burchet M (2003) Accumulation and distribution of heavy metals in grey mangrove, Avicennia marina (Forsk.) Vierh.: Biological indication potential. Environ Pollut 123:139–151

Meade R (1972) Transport and deposition of sediments in estuaries. In: Environmental framework of of coastl-plin estuaries. Geol Soc Am Memoirs 133:91–120

Meysman FJR, Middelburg JJ, Heip CHR (2006) Bioturbation: A fresh look at Darwin's last idea. Trends Ecol Evol 21:688–695
Miranda P, Coelho, Tomé A, Valente MA (2002) 20th century Portuguese climate and climate scenario. In: Santos FD, Forbes K, Moita (eds) Climate change in Portugal. Scenarios, impacts and adaptation measures. SIAM Project, Gradiva, pp 27–83
Mitsch W, Gosselink J (2000) Wetlands. Wiley, New York, pp 920
Moreno FN, Anderson CWN, Stewart RB, Robinson BH (2005) Mercury volatilization and phytoextraction from base-metal mine tailings. Environ Pollut 136:341–352
Morton B, Blackmore G (2001) South China Sea. Mar Pollut Bull 42:1236–1263
Munthe J, McElroy WJ (1992) Some aqueous reactions of potential importance in the atmospheric chemistry of mercury. Atmos Environ 26A:553–557
Myers R, Worm B (2003). Rapid worldwide depletion of predatory fish communities. Nature 423:280–283
Neckles H, Neill C (2004) Hydrologic control of litter decomposition in seasonally flooded prairie marshes. Hydrobiologia 286:155–165
Nriagu JO (1994) Mechanistic steps in the photoreduction of mercury in natural waters. Sci Total Environ 154:1–8
Nyman JA, DeLaune RD, Roberts HH, Patrick Jr, WH (1993) Relationship between vegetation and soil formation in a rapidly submerging coastal salt marsh. Mar Ecol Prog Ser 96:269–279
Nyman JA, Carloss M, DeLaune RD, Patrick Jr, WH (1994) Erosion rather than plant dieback as the mechanism of marsh loss in an estuarine marsh. Earth Surf Proc Landf 19:69–84
O'Driscoll NJ, Poissant L, Canário J, Ridal J, Lean D (2007) Continuous analysis of dissolved gaseous mercury and mercury volatilization in the upper St. Lawrence River; exploring temporal trends and UV attenuation. Environ Sci Technol 41:5342–5348
Olsen CL, Larsen PJ, Mulholland KL, Von Damm JM, Grebmeier LC, Schaffner RJ, Diaz RJ, Nichols MM (1993) The concept of an equilibrium surface applied to particles sources and contaminant distributions in estuarine sediments. Estuaries 16:683–696
Outridge PM, Sanei H, Stern GA, Hamilton PB, Goodarzi F (2007) Evidence for control of mercury accumulation rates in Canadian high Arctic lake sediments by variations of aquatic primary productivity. Environ Sci Technol 41:5259–5265
Patra RW, Chapman JC, Lim EP, Gehrke PC (2007) The effects of three organic chemicals on the upper thermal tolerances of four freshwater fishes. Environ Toxicol Chem 26:1454–1459
Pelletier MC, Burgess RM, Ho KT, Kuhn A, McKinney RA, Ryba SA (1997) Phototoxicity of individual polycyclic aromatic hydrocarbons and petroleum to marine invertebrate larvae and juveniles. Environ Toxicol Chem 16:2190–2199
Pereira P, Caçador I, Vale C, Caetano C, Costa A (2007) Decomposition of belowground biomass litter and metal dynamics in salt marshes (Tagus Portugal). Sci Total Environ 380:93–101
Philippart CJM (2007) Impact of climate change on the European marine and coastal environment. Marine Board Position Paper 9, European Science Foundation, France, pp 83
Phillips DJH (1986) Use of organisms to quantify PCBs in marine and estuarine environments. In: Waid JS (ed) PCBs and the environment, vol 2. CRC Press, Florida, pp 127–181
Poissant L (2000) Atmospheric mercury transport, oxidation and fallout in northern Québec (Nunavik): An important potential route of contamination. Northern Contaminants Program, synopsis of research 1999–2000. Montréal, Canada, Indian and Northern Affairs Canada, 0-662-29320-7, pp 132–136
Poissant L, Dommergue A, Ferrari CP (2002) Mercury as a global pollutant. J Phys IV France 12:143–160
Rasmussen PE (1994) Current methods of estimating atmospheric mercury fluxes in remote areas. Environ Sci Technol 28:2233–2241
Reed DJ (1990) The impact of sea-level rise on coastal salt marshes. Prog Phys Geog 14:465–481
Reed DJ, Foote AL (1997) Effect of hydrologic management on marsh surface sediment deposition in coastal Louisiana. Estuaries 20:301–311
Sanders G, Hamilton-Taylor J, Jones KC (1996) PCB and PAH dynamics in a small rural lake. Environ Sci Technol 30:2958–2966

Santos FD, Forbes K, Moita (2006) Climate change in Portugal. Scenarios, impacts and adaptation measures. SIAM Project, Gradiva, pp 454

Schiedek D, Sundelin B, Readman JW, MacDonald RW (2007) Interactions between climate change and contaminants. Mar Pollut Bull 54:1845–1856

Schroeder WH, Yarwood G, Niki H (1991) Transformation processes involving mercury species in the atmosphere — results from a literature survey. Water Air Soil Pollut 56:653–666

Schroeder WH, Anlauf KG, Barrie LA, Lu JY, Steffen A, Schneeberger DR, Berg T (1998) Arctic springtime depletion of mercury. Nature 394:331–332

Simas T, Nunes JP, Ferreira JG (2001) Effects of global climate change on coastal salt marshes. Ecological Modeling 139:1–15

Skov H, Christensen JH, Goodsite ME, Heidam NZ, Jensen B, Wahlin P, Geernaert G (2004) Fate of elemental mercury in the Arctic during atmospheric mercury depletion episodes and the load of atmospheric mercury to the Arctic. Environ Sci Technol 38(8):2373–2382

Steffen A, Schroeder W, Bottenheim J, Narayan J, Fuentes JD (2002) Atmospheric mercury concentrations: Measurements and profiles near snow and ice surfaces in the Canadian Arctic during Alert 2000. Atmos Environ 36:2653–2661

St. Louis VL, Sharp MJ, Steffen A, May A, Barker J, Kirk JL, Kelly DJA, Arnott SE, Keatley B, Smol JP (2005) Some sources and sinks of monomethyl and inorganic mercury on Ellesmere Island in the Canadian high Arctic. Environ Sci Technol 39(8):2686–2701

St. Louis VL, Hintelmann H, Graydon JA, Kirk JL, Barker J, Dimock B, Sharp MJ, Lehnherr I (2007) Methylated mercury species in Canadian high Arctic marine surface waters and snowpacks. Environ Sci Technol 41(18):6433–6441

Sundby B, Vale C, Caetano M, Luther G (2003) Redox chemistry in the root zone of a salt marsh sediment in the Tagus estuary, Portugal. Aquat Geochem 9:257–271

Tang NH, Myers TE (2002) PCB removal from contaminated dredge material. Chemosphere 46:477–484

Teng H, Washington WM, Meehl GA, Buja LE, Strand GW (2006) Twenty-first century Arctic climate change in the CCSM3 IPCC scenario simulations. Clim Dyn 26:601–616

Tett SFB, Stott PA, Allen MR, Ingram WJ, Mitchell JFB (1999) Causes of twentieth-century temperature change near the Earth's surface. Nature 339:569–572

Titus JG, Park RA, Leatherman SP, Weggel JR, Greene MS, Mausel PW, Brown S, Gaunt C, Trehan M, Yohe G (1991) Greenhouse effect and sea level rise: The cost of holding back the sea. Coast Manage 19:171–210

UNEP (1997) Global Environment Outlook-1. Global State of the Environment Report 1997 (www.unep.org/GEO////geo1/misc/about.htm)

Vale C (1981) Input of suspended particulate matter in the Tagus estuary during the flood of February 1979. Rec Hidric 2:37–45

Vale C, Sundby B (1987) Suspended sediment fluctuations in the Tagus Estuary on semi-diurnal and fortnightly time scales. Estuar Coast Shelf Sci 25:495–508

Vale C, Cortesão C, Castro O, Ferreira AM (1993) Suspended-sediment responses to pulses in river flow and semi-diurnal and fortnightly tidal in mesotidal estuary. Mar Chem 43:21–31

Valiela I, Teal J, Allen S, van Etten R, Goehringer D, Volkmann S (1985) Decomposition in salt marsh ecosystems: The phases and major factors affecting disappearance of aboveground organic matter. J Exp Mar Biol Ecol 89:29–54

Valiela I, Rutecki D, Fox S (2004) Salt marshes: Biological controls of food webs in a diminishing environment. J Exp Mar Biol Ecol 300:131–159

Van Dolah FM (2000) Marine algal toxins: Origins, health effects, and their increased occurrence. Environ Health Persp Suppl 108:S1, March 2000

Van Zoest R, Van Eck GTM (1990) Behaviour of particulate polychlorinated biphenyls and polycyclic aromatic hydrocarbons in the Sheldt estuary. Neth J Sea Res 26:89–96

Weis J, Weis P (2004) Metal uptake, transport and release by wetland plants: Implications for phytoremediation and restoration. Environ Int 30:685–700

Wilson JO, Buchsbaum R, Valiela I, Swain T (1986) Decomposition in salt marsh ecosystems: Phenolic dynamics during decay of litter of Spartina alterniflora. Mar Ecol Prog Ser 29:177–187

Windham L, Weis J, Weis P (2003) Uptake and distribution of metals in two dominant salt marsh macrophytes, Spartina alterniflora (cordgrass) and Phragmites australis (common reed). Estuar Coast Shelf Sci 56:63–72

Xiao ZF, Munthe J, Stromberg D, Lindqvist O (1994) In: Watras CJ, Huckabee JW (eds) Mercury pollution: Integration and synthesis;. Lewis, Boca Raton, FL, pp 581–592

Zawislanski P, Chau S, Mountford H, Wong H, Sears T (2001) Accumulation of selenium and trace metals on plant litter in a tidal marsh. Estuar Coast Shelf Sci 52:589–603

Zhang H, Lindberg SE (2001) Sunlight and iron(III)-induced photochemical production of dissolved gaseous mercury in freshwater. Environ Sci Technol 35:928–935

Chapter 8
The Use of Weight of Evidence for Environmental Quality Assessment in Sediments Above Sub-Seabed Geological Formations for the Storage of Carbon Dioxide

Tomás-Ángel DelValls Casillas, Diana Fernández de la Reguera Tayá, Maria Inmaculada Riba López, and Jesus María Forja Pajares

Abstract The need for short-term measures to reduce the amounts of CO_2 in the atmosphere has led to consider CO_2 sequestration as an essential measure to be able to meet nowadays targets. However, uncertainties related to this option, in particular in relation to control on impurities of the stored gas stream, site selection and characterization, monitoring, allowed leakage rates, estimation of potential impacts and remediation of local damages in the short and long term, etc. have led the international community to develop some guidelines and frameworks within which to regulate this activity. Permanent containment of the storage sites is expected, however it is necessary to determine the risk of leakage to the marine environment and its effects. The application of the Weight-of-Evidence approach for environmental quality assessment in sediments above sub-seabed geological formations for the storage of carbon dioxide can be of paramount importance to determine the effects and potential consequences of the leakage of CO_2. This methodology satisfies the requirements set by the 1992 OSPAR Convention and 1996 London Protocol to ensure permanent containment and to guarantee the integrity of the marine environment and human health.

Keywords Carbon dioxide • Storage • Weight of evidence • Risk assessment • Sediments • Carbon dioxide sequestration • Monitoring • Mitigation • Storage • Marine environment

T.-Á. DelValls Casillas (✉), D.F. de la Reguera Tayá, M.I. Riba López, and J.M. Forja Pajares
Cátedra UNESCO UNIT/WIN/WiCoP, Departamento de Química Física, Facultad de Ciencias del Mar y Ambientales, Campus Río San Pedro s/n, 11510 Puerto Real, Cádiz, Spain
e-mail: angel.valls@uca.es; diana.reguera@uca.es; inmaculada.riba@uca.es; jesus.forja@uca.es

M.I. Riba López
Instituto de Ciencias Marinas de Andalucía, CSIC, Campus Río San Pedro s/n, 11510 Puerto Real, Cádiz, Spain
e-mail: inmaculada.riba@uca.es

P. Duarte and J.M. Santana-Casiano (eds.), *Oceans and the Atmospheric Carbon Content*,
DOI 10.1007/978-90-481-9821-4_8,

8.1 Introduction

The IPCC Fourth Assessment Report (IPCC 2007) concluded that ice cores have shown that global atmospheric carbon dioxide (CO_2), methane and nitrous oxide from human activities have been increasing since 1750, particularly from fossil fuel burning and land use change. The concentration of CO_2, the most important greenhouse gas nowadays, increased from 280 to 379 ppm in 2005. Although annual growth rates vary, the rate of growth annually in the last 10 years has been the greatest since instrumental records of CO_2 started in 1960. In addition, the use of coal by emergent economies as the main source of energy together with an increasing demand on transport and energy worldwide will continue increasing the level of CO_2 in our atmosphere if no further actions are taken. The IPCC (2007) warn that global climate warming is now 'unequivocal' and that urgent measures to reduce greenhouse gases in the atmosphere need to be taken.

The emission reduction of greenhouse gases is going to be costly. However, according to Stern (2007), if no measures are taken and climate change continues to be ignored, it will finally affect the long-term economic growth of all countries and it will be either impossible or extremely difficult to revert the changes generated. Therefore, any early action will fully overcome the costs. Also, as stressed in the 14th conference of parties to the UN Framework Convention on Climate Change and fourth meeting of parties to the Kyoto Protocol the transition to a low carbon society entails not only costs but also important economic opportunities.

At the international level, different measures to reduce atmospheric CO_2 are being proposed. Apart from the economic and political viability of these measures there is a global concern about their environmental viability. CO_2 sequestration in marine geological formations is among the measures that are under study. Nowadays, there are several currently ongoing projects and more than 3 million tonnes of CO_2 are injected annually for the purpose of sequestration (Benson 2006 and references therein). Even though there is a general scientific agreement on the economic and environmental viability of this option in the short-term, there is concern about the potential long-term impacts and their economic cost. Those concerns have led to the 1996 London Protocol to the 1972 Convention on the Prevention of Marine Pollution by Dumping of Wastes and Other Matter and the 1992 OSPAR Convention for the Protection of the Marine Environment of the North-East Atlantic to regulate this activity. Both Conventions have been amended to allow the storage of CO_2 in sub-seabed geological formations and have developed a comprehensive risk assessment and management framework and guidelines to guarantee the integrity of the marine environment.

In the same vein, the European Commission proposed a new Directive to regulate the geological storage of carbon dioxide and to recognise stored CO_2 as non-emitted in emissions trading. However this Directive is still under discussion among the European Countries because a number of regulatory gaps and ambiguities persist (EU Directive CCS 2008). Due to the growing number of ongoing projects and interest in this activity, at national and state level new legislation is also being proposed (e.g. Australia, USA).

A proper site selection and characterization is a key step to ensure permanent containment (London Protocol 2007). However, an adequate monitoring program is a requirement to guarantee that no leakage occurs. Also, in the case of leakage, monitoring will be necessary to determine possible impacts on the environment and human health as a decision-making management tool, but also for the purpose of appropriate accounting for inventory and trading of carbon credits.

The main objective of this work is to describe the importance of environmental monitoring in the CO_2 sequestration under the seabed as part of the monitoring program. In addition, it is proposed that sediment quality assessment using weight-of-evidence approaches be used, as well as modifying and adapting different lines of evidence of the integrated method. This initiative is in agreement with the monitoring requirements set in the international conventions.

8.1.1 Carbon Dioxide Storage in Sub-Seabed Geological Formations

According to the IPCC (2005), carbon dioxide storage in sub-seabed geological formations consists in the capture and separation of CO_2 from industrial and energy-related sources, transport to a storage site and long-term storage in a formation placed under the seabed. As the CO_2 is still emitted, even though it is isolated from the atmosphere, there is a general controversy to consider this process in the Joint Implementation Projects or the Clean Development Mechanisms of the Kyoto Protocol. However, the IPCC (2007) warned that evidence shows that current mitigation policies for climate change and related sustainable development practices are still insufficient to stop the growth of greenhouse gases over the next decades. There is strong evidence that a portfolio of greenhouse gases emissions mitigation options (e.g. shifting to more nuclear power, carbon dioxide sequestration, bio-energy, bio-energy together with carbon sequestration, moving to renewable energy generation, increasing energy efficiency and better land-use practices etc.) will be more effective than relying too heavily on one or a few options (IPCC 2007). Reasons for this include: reduced investment risk (Laurikka and Springer 2003), limitations of particular options or technologies, different regions and sectors need different approaches, and over-dependence on one resource will eventually incur higher costs due to depletion (Van Vuuren et al. 2007).

In addition, many models suggest that the primary source of energy will continue to come from fossil fuels until at least the middle of the century. CO_2 storage offers the possibility of reducing the cost of meeting stabilisation targets as well as increasing the flexibility by which this can be achieved, as it enables the continued use of fossil fuels with low emissions. However, it should not be regarded as the sole mitigation option but rather as part of a range of mitigation options that should include increasing energy efficiency, switching to lower carbon options like natural gas, renewable energy and nuclear energy, enhancing natural biological sinks and reducing non-CO_2 greenhouse gas emissions (IPCC 2005).

8.2 Requirements

8.2.1 Risk Assessment and Management

In order to protect the environment and human health, CO_2 sequestration in sub-seabed formations needs to be regulated. At the present date this activity has been regulated at an international level by the 1992 OSPAR Convention and the 1996 London Protocol. Both conventions have developed Guidelines and a Framework for Risk Assessment and Management of storage of CO_2 in sub-seabed geological formations. These Guidelines are legally binding for the contracting parties of these Conventions for the protection of the marine environment. Also, there is the compromise of the Barcelona Convention to develop similar guidelines and framework (Almeria Declaration of the Barcelona Convention 2008). Therefore, there is an agreement within the requirements developed by different international conventions to establish and protect the environmental quality in the marine environment.

A brief schematic of the contents of this risk assessment and management framework developed in the London Convention and Protocol and OSPAR Convention is included in the Table 8.1 (OSPAR Convention 2007).

This framework is considered an iterative process, the intensity of which will decrease with time for well-selected and managed storage sites (OSPAR Convention 2007). A similar framework was included in the proposed EU Directive on carbon capture and storage (2008). A brief description of the steps of the risk assessment and management framework is included below (London Convention and Protocol 2006; OSPAR Convention 2007; EU Directive CCS 2008; Reguera et al. 2008):

1. *Problem Formulation*: Defines the area and the scope of the activity.
2. *Site selection and Characterization*: Assesses how much CO_2 can be stored at a site and demonstrates permanent containment. Also it helps to establish a baseline for management and monitoring.
3. *Exposure Assessment*: Determines exposure processes and pathways, the likelihood of exposure and the scale of exposure.

Table 8.1 The different steps of the risk assessment and management framework applicable to each phase of the CO_2 storage project (OSPAR 2007)

	Problem formulation	Site selection & characterisation	Exposure assessment	Effects assessment	Risk characterisation	Risk management (monitoring & mitigation)
Planning	☑	☑	☑	☑	☑	☑
Construction		☑	☑	☑	☑	☑
Operation		☑	☑	☑	☑	☑
Site-closure			☑	☑	☑	☑
Post-closure			☑	☑	☑	☑

4. *Effects Assessment:* Demonstrates that, in the event of leakage, storage does not lead to significant adverse consequences for the marine environment and human health. In addition, it determines the sensibility of species and communities and the scale of exposure.
5. *Risk Characterization*: Identifies potential hazards related to the activity, estimates the probability of these hazards occurring and the severity of effects posed to exposed species and ecosystems and the risks to human health, and describes the risk estimate in the context of the significance of any adverse effects. It also identifies and summarizes the uncertainties, assumptions and qualifiers in risk assessment.
6. *Risk Management (including Monitoring and Mitigation)*: Demonstrates how an event of leakage would be managed in order to prevent significant adverse consequences for marine environment and human health, maximizes the intended isolation and minimizes the effects of possible leaks of CO_2, incidental associated substances and substances mobilized by the CO_2stream.

It is important to remark that, in all phases of these frameworks, monitoring is mandatory to verify the integrity of the environment and for accounting purposes. In addition, in the proposed EU Directive for CO_2 capture and storage (2008), article 13 is about requirements for monitoring of the injection facilities, the storage complex (including the CO_2 plume), and the surrounding environment. However, in any of those regulations there are no references about the monitoring systems that should be used, the frequency or the resolution that they should have. As monitoring is one of the key enabling technologies for CO_2 storage (Benson 2006), it is necessary to define the precision and detection levels that this technology should provide to not only guarantee the environment and human health but for the purpose of appropriate accounting for inventory and trading of carbon credits. The geological characteristics of the possible places of storage are widely variable and at the present time there is a small number of monitoring programs capable of either identifying or quantifying leaks of CO_2 from the storage operations in geological formations (IPCC 2007; Klusman 2003; Wilson and Monea 2004).

8.2.2 Main Risks to the Marine Environment

The main risk of the storage of CO_2 in sub-seabed geological formations to the marine environment is leakage of the injected CO_2 stream. High CO_2 levels in the environment may impair respiration in organisms (asphyxiation), lower the pH in animal body fluids (acidosis) and increase the concentrations of CO_2 in body fluids (hypercapnia) (OSPAR Convention 2005). In addition, the changes in ocean chemistry due to the increased concentration of CO_2 from leakage may negatively affect the calcification rates of calcareous organisms (e.g. phytoplankton, corals, shellfish, etc.). The acidification of the environment might enhance the toxic effects of the contaminants and make them more bioavailable (Riba et al. 2003a, 2004). A conceptual model of potential environmental pathways and effects is represented

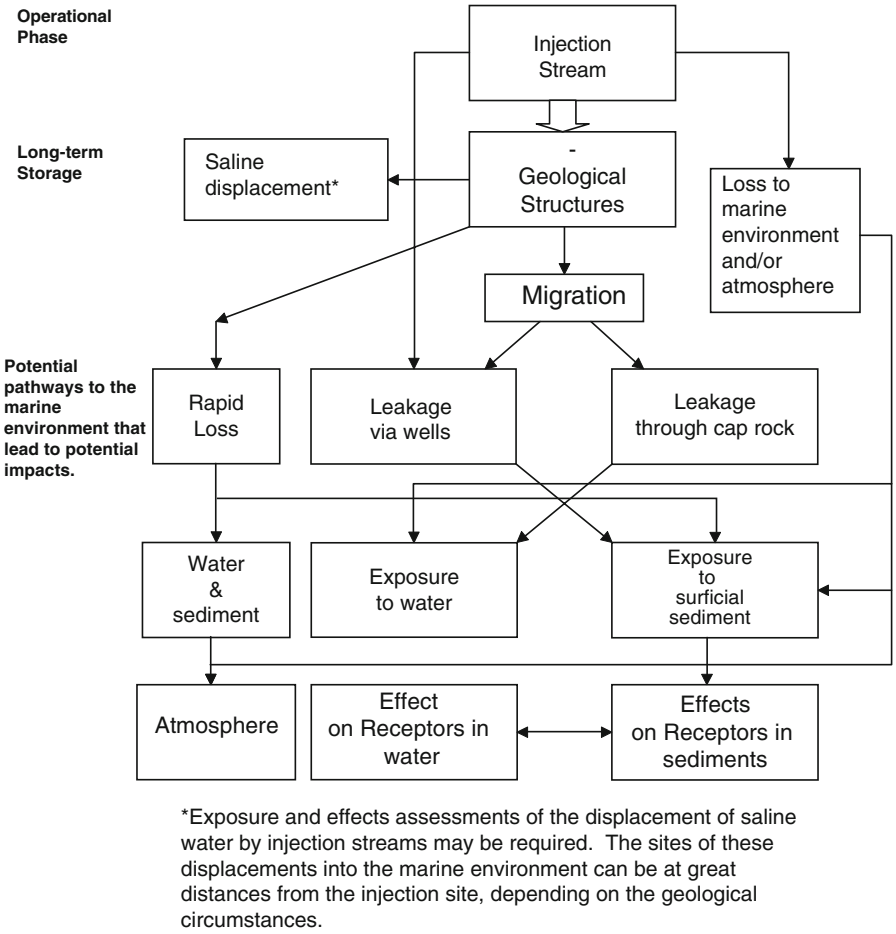

Fig. 8.1 Conceptual model of potential environmental pathways and effects (London Convention and Protocol 2006)

in Fig. 8.1 (from London Convention and Protocol 2006). At low pH, species might be killed if they are very sensitive to pH changes and other species will then prosper. For those that tolerate broader ranges of pH they might change their behavior, decrease the reproduction rates, etc. Therefore the composition and the ecological function of the ecosystem will change. The capacity of an ecosystem to recover from a leak of CO_2 will depend on the spatial and time scale of the leakage and the sensitivity of the ecosystem. However, the ecological function will probably return before biodiversity (Findlay et al. 2008). Nevertheless, in comparison with atmospherically driven acidification, the effects of leakage will be regional instead of global (Blackford et al. 2008).

Nowadays, effects data from exposures to increased CO_2 concentrations is available, but is mostly scarce, scattered and limited in detail (IPCC 2005). Existing field data are mainly limited to deep-sea situations although currently also research is being carried out in shallow waters (OSPAR Convention 2007) The international conventions on the protection of the marine environment stated that the qualitative assessment of environmental effects is currently possible, but further research is needed for quantitative assessments (OSPAR Convention 2007; London Convention and Protocol 2006). Besides, the effects of global acidification on the marine environment might differ from those from acidification due to leakage of CO_2 as there are other substances added to the CO_2 stream, which may cause also adverse environmental effects. Those substances are considered incidentally associated substances derived from the source material and the capture, transport and storage processes used, consisting of:

- Source and process derived substances; and
- Added substances (i.e. substances added to the CO_2 stream to enable or improve the capture, transport and storage processes) (London Protocol 2007; OSPAR Convention 2007).

According to the IPCC 2005, the amount of these substances can be very small but the stream composition varies depending on the fuel characteristics, the industrial process involved, the choice of capture technology and the level of fuel cleaning. At the international level there is no limit on the amount of these substances in the injected stream or the minimum percentage of CO_2 that it should have.

However, the need to better understand the effects of leakage to marine organisms has led internationally to some research groups to simulate in laboratory conditions different leakage scenarios (Riba et al. 2003a, b, 2004, 2006; Miles et al. 2007; Findlay et al. 2008; Widdicombe and Needham 2007; Spicer et al. 2007).

In addition, there are also other risks such as migration of methane (CH_4), which has a stronger potential as a greenhouse gas than CO_2, or seismic events due to the changes in pressure in the geologic formation originated by the injection process and brine displacement (Damen et al. 2006). For stored streams with a high percentage of CO_2 it is expected that some of the CO_2 will leak due to the buoyancy effects of the separated fraction of CO_2, the induced pressure gradients of the injection and the nature of the strata that stop the migration of CO_2. Leakage could also impact aquifers, superficial waters and lands (Bruant et al. 2002). Also, Wallmann (2008) determines that during the operational phase (short-term) of the storage site the risk of leakage is small but the risk of leakage of natural gas (mainly methane) and formation waters (mainly brine or seawater) increases considerably. The (long term) post-operational phase of the storage site increases the risk of leakage of CO_2 and associated substances. Nevertheless, according to the IPPC 2005 for well-selected, designed and managed storage sites, the vast majority of the CO_2 (99%) is very likely[1] to be retained over 100 years and the fraction retained is likely[2] to exceed

[1] The expression 'very likely' used in this statement indicates a probability between 90–99% (IPCC 2005).

[2] The expression 'likely' indicates a probability between 66–90% (IPCC 2005).

Table 8.2 Information included in the guidelines for risk assessment and management of storage of CO_2 streams in sub-seabed geological formations, developed by the London Convention Protocol (2006) and OSPAR Convention (2007). The intention is to be able to demonstrate that the site characteristics are consistent with the ultimate objective of permanent containment and protection of the marine environment, human health and other legitimate uses of the maritime area

Issues to include in the risk assessment	Parameters to identify, qualify and – where possible – quantify in the risk assessment
Characterisation of the injected CO_2 stream	Type and properties of other substances Concentrations of other substances
Location and geographical factors	Water depth, formation depth Human health and safety
Existence of amenities, biological features and legitimate uses of the maritime area	Areas of special ecological, economical or scientific importance, e.g.,: • European marine sites • OSPAR MPA's, • Sanctuaries • (Sensitive) species, communities or habitats • Breeding areas • Potable or irrigation water resources • Fishing areas
Regional geological setting	Regional geology, hydrogeology, hydrology, stratigraphy and structure Regional tectonics and seismicity Faults and fractures
Historical uses of the area	Man-made structures, including: • Integrity of active and abandoned wells with respect to CO_2 that are likely to be affected by the injection process ○ Proximity to other wells (hydrocarbon producers, former or present) or fields ○ Proximity to potable, irrigation or industrial water producing wells ○ Proximity to other injection wells ○ Age, depth and condition of the wells ○ Geometry of plugs and casing and composition of plugs of abandoned wells Conversion of existing well for injection: information is needed on well age, its construction details, and its history
Reservoir/seal evaluation	Geological interpretation • Stratigraphic interpretations and well-log cross sections of the reservoir intervals • Reservoir/seal heterogeneity • Temperature, pressure, fluid characteristics (salinity) Geophysical mapping • 3-D maps of potential migration pathways (faults) • Structure and thickness of formations and cap rocks Petrophysics • Permeability, relative permeability (injectivity) • Porosity • Capillary pressure • Mineralogy Hydrodynamics • Displacement of formation water • Vertical hydraulic gradient Sealing capacity of cap rocks • Seal thickness • Capillary entry pressure

(continued)

Table 8.2 (continued)

	Faults • Location, orientation and properties of faults or fractures that are likely to intersect the formation Geomechanics and geochemistry • CO_2 stream – water – rock interaction • Stress, stiffness and strength • Potential of the injected fluid to cause plugging of the formation • Compatibility with injected formation chemistry • In-situ stress profile in the various layers Other components in the input-stream Reservoir simulations • Short-term behaviour: formation response (pressure changes for a given injection rate) • Long-term behaviour: formation containment • Sufficient capacity of the formation for planned CO_2 storage Data quality • History, current status and age of information available on the geological formation
Marine environment characterization	Ocean current and see floor topography in the region Physical, chemical and biological characteristics of seabed, sediments and overlying waters: • Natural fluxes of CO_2 in the seabed and across the seabed surface • Chemical characteristics of the seawater • Nutrients and other substances (potential contaminants/ pollutants) • Biological communities and biological resources ○ composition, structure, dynamic
Economic/regulatory factors	Economic feasibility Impact on other sub-seabed resources such as oil and gas extraction and other natural gas/CO_2 storage sites Regulatory framework Applicable regulations, codes and standards, and regulatory restrictions and restraints

99% over 1,000 years. In Table 8.2, there are some of the suggested parameters that should be considered for an adequate site selection and characterization, according to the international conventions of the protection of the marine environment, that could contribute to reducing the risks of leakage (OSPAR Convention 2007; London Convention and Protocol 2006).

There is a strong debate among the scientific community and the policymakers on the need to establish a maximum acceptable leakage rate to abate long-term global warming and also to protect marine life. The global average emission of CO_2 from the marine floor is +150 TCO_2/km^2 year (Luff and Moll 2004). Therefore, Wallman (2008) proposes 10% of the natural benthic CO_2 emission rates. This maximum leakage rate would guarantee the integrity of the marine environment and would give greater credibility to the CO_2 storage projects in sub-seabed geological formations, as the CO_2 stored would then be considered as non-emitted.

8.2.3 The Integrated Method as a Monitoring Tool of the Marine Environment

There has been limited experience of the processes of monitoring, verification and information of the rates of leakages and uncertainties associated with the storage of CO_2 (IPCC 2007). Even though there is a wide range of monitoring systems, there is no regulation in relation to which monitoring systems should be used, their frequency or their minimum detection limit. Depending on the purpose of the monitoring, different monitoring systems are available. In order to monitor the effects of the leakage of CO_2 streams in the marine environment, it is necessary to understand the processes and mechanisms that control those leakages in the different types of geological formations in which it is possible to store CO_2. Besides, it is necessary to understand the behavior of the environment, species and ecosystems when they are exposed to CO_2 and the incidentally associated substances. Several previous studies have used the integration of different lines of evidence as an effective methodology to identify polluted areas (Matthiessen et al. 1998; Thompson et al. 1999; Martín-Díaz et al. 2005; Riba et al. 2006; Morales-Caselles et al. 2007). Therefore it is necessary to apply an integrated method (DelValls et al. 1998; Delvalls and Chapman 1998) to be more effective and capable of detecting minor and diffuse leaks of CO_2. This method will allow control of those leaks in considerable extensions of the seabed and will contribute to reduce impacts on the environment and human health. Also, it will help to improve our knowledge of the effects of leakage of CO_2 and incidentally associated substances in the marine environment in the short and long-term (DelValls 2007). Likewise, it can be a system for early alert of leakages and other impacts of the storage of CO_2. Furthermore, it can contribute to verifying the permanent containment of the CO_2 sequestration in geological formations for accounting purposes.

The use of weight-of-evidence integration of the different lines of evidence (LOEs) to monitor the sediment quality in the areas selected to store CO_2 will fulfill the requirements of the international conventions for protection of the marine environment set in the framework and guidelines developed. The leakage of CO_2 will progressively acidify the sediments and therefore the mobility of metals will also increase. In this sense, the LOEs of the integrated method will be contamination of sediment, speciation of metals, bioaccumulation of metals, toxicity, etc. The integrated method is based on the application of a weight-of-evidence approach (WOE). The WOE includes the physicochemical and ecotoxicological characterization of sediments, the determination of biomarkers of contamination and the bioavailability of contaminants measured using laboratory and field bioassays and identifying biomagnification processes in a synoptic approach using field collected sediment and biological samples. A schematic of the different WOEs of the integrated model is included in Fig. 8.2 (DelValls 2007). If leakage of CO_2 is observed or suspected to extend to the seafloor in sensitive or endangered habitats and ecosystems, this method will allow us to determine to what extent this leakage is affecting the marine environment. Besides, this method will allow measuring the effect of

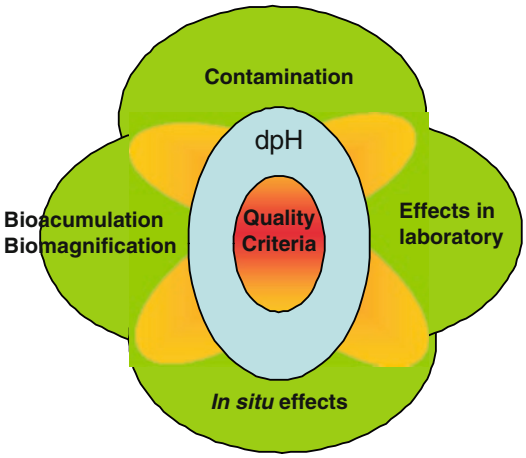

Fig. 8.2 Integrated method adapted for the monitoring of CO_2 storage projects (DelValls 2007)

small and diffuse leakage in the short and long-term (DelValls 2007). Moreover the effects of the incidental associated substances and the substances mobilized by the injection and storage of CO_2 streams can also be assessed.

The results of the application of this method can be integrated in two different ways: (a) a classical use of statistical analysis with ANOVA and multivariate analysis (MMA) or (b) by neural network analysis (NNA) which allows predictive identification of non-linear relationships (DelValls et al. 1998; DelValls and Chapman 1998). Also, it develops sediment quality values (SQGs) by linking the set of data on contamination, toxicity and field effects. In addition, tissue quality values (TQGs) can also be obtained by linking the body burdens and the sublethal effects using biomarkers of exposure and effects in the tissue of different organisms. All these results will help to design a Tier testing for the development of a decision-making tool in the risk assessment and management of CO_2 storage sites. Also, they will provide useful information when remediation and mitigation procedures are required.

The degree of toxicity of the sediments caused by the leakage should be determined by the performance of bioassays in situ and in laboratory conditions. Those bioassays will allow us to determine and quantify the exposure pathways of the contaminants and their negative effects (changes in reproduction or growth patterns, mortality, biomarkers of effect, etc.). In addition, the determination of the degree of bioaccumulation and biomagnification of the different contaminants will be a key parameter to establish the risk of contaminant transference through the trophic chain and therefore the risk for human health.

In relation to the in situ bioassays, so far no leakage rates have been detected in the ongoing projects of CO_2 sequestration (Benson 2006). Therefore, no information of the effects of leakages in the environment is yet available. The integrated method purposes different approaches that can be used depending on the characteristic of

the environment under study: (a) In situ releases of CO_2 streams to observe the behavior of the stream (Adams et al. 2006; Brewer et al. 2006) and its effects on the marine environment; (b) Use natural analogues to understand the consequences of the release of significant amounts of CO_2 (Benson et al. 2002; Summers et al. 2004); or (c) to realize in situ experiments in either natural analogs or in environments with a specific pH variation (e.g. estuaries, natural acidic environments).

Some examples of the results of the integrated application of WOEs have been reported by different authors (DelValls and Chapman 1998; Riba et al. 2003b; DelValls 2007; Martín-Díaz et al. 2008). This method gives very valuable information for management of the site so as to provide environmental quality criteria that allow a rapid and reliable identification of risks.

8.2.4 Final Remarks

The need to reduce greenhouse emissions rapidly has led many countries to begin CO_2 storage projects on land and offshore even though there are numerous aspects that still need to be investigated, processes that must be understood and technologies that must be developed (IPCC 2005). Determination of the safety of CO_2 storage in sub-seabed geological formations is based on a proper site selection and characterization and an appropriate monitoring of the stored CO_2. Even though there is a lack of requirements for the methodology, frequency and accuracy of the monitoring systems that should be used to guarantee the integrity of the marine environment and for accounting purposes of emissions, application of the integrated method as a monitoring tool will provide the necessary information about the behavior of this gas and its effects on the surrounding environment and will provide useful information when remediation and mitigation procedures are required. In relation to the in situ bioassays, more research is required to gain knowledge about the different options proposed for this method. Moreover, the application of the integrated method can be a key step for an adequate environmental risk assessment and management of storage sites and will fulfill the requirements set in the guidelines and framework developed by the London Protocol and the OSPAR Convention. Although, further research is required on the different monitoring systems of the marine environment, the exposure pathways and the effects on marine organisms, the WOEs can be applied in current CO_2 projects to determine their effects on the marine environment.

Acknowledgments This research was supported by grants funded by the Spanish Ministry of Environment during years 2006 and 2007. Also the Ministry for Science and Innovation partially funded this research through grants CTM2008-06344-C03-03/TECNO y CTM2008-06344-C03-02/TECNO and the 'Junta de Andalucia' through Excellence projects RNM-3924. Diana Fernandez de la Reguera thanks the Spanish Ministry of Science and Education for her research fellowship (FPI). Dra. Inmaculada Riba thanks the Spanish program 'Ramón y Cajal' for supporting her research and also thanks the progamme 'Jose Castillejo' for supporting her participation in this chapter during her stay at IPIMAR Lisbon.

References

Adams EE, Chow AC, Brewer PG, Peltzer ET, Walz P, Tsouris C, McCallum SD, Szymcek P, Summers JS, Bergman P, Johnson K (2006) Direct injection of CO_2 hydrate composite particles for ocean carbon storage: Field experiments and plume modelling. From proceedings of the Greenhouse Gas Control Technologies Conference, Trondheim, Norway

Almeria Declaration of the Barcelona Convention (2008) Annex III COP 15. Almeria. Spain. Available online at:www.cop15map.com/docs/en/Annex%20III%20Almeria%20Declaration.doc

Benson SM (2006) Monitoring carbon dioxide sequestration in deep geological formations for inventory verification and carbon credits. Soc Petrol Eng SPE 102833:1–14

Benson SM, Hepple R, Apps J, Tsang CF, Lippmann M (2002) Lessons learned from natural and industrial analogues for storage of carbon dioxide in deep geological formations, Report No. LBNL-51170, Berkeley, E.O. Lawrence Berkeley National Laboratories, Berkeley, CA

Blackford JC, Jonesa N, Proctorb R, Holtb J (2008) Regional scale impacts of distinct CO_2 additions in the North Sea. Mar Pollut Bull 56:1461–1468

Brewer PG, Chen B, Warzinki R, Baggeroer A, Peltzer ET, Dunk RM, Walz P (2006) Three-dimensional acoustic monitoring and modeling of a deep-sea CO_2 droplet cloud. Geophys Res Lett 33:L23607. doi:10.1029/2006

Bruant R, Gusgua AG, Celia M, Peters C (2002) Safe storage of CO_2 in deep saline aquifers. Environ Sci Technol:241–245

Damen K, Faaij A, Turkenburg W (2006) Health, safety and environmental risks of underground CO2 storage – overview of mechanisms and current knowledge. Clim Change 74:289–318

DelValls TA (2007) Diseño y aplicación de modelos integrados de evaluación de la contaminación y sus efectos sobre los sistemas marinos y litorales y la salud humana. Ministerio de la Presidencia. Centro para la Prevención y Lucha contra la Contaminación Marítima y Litoral (CEPRECO). Serie Investigación, Madrid

DelValls TA, Chapman PM (1998). Site-specific sediment quality values for the Gulf of Cádiz (Spain) and San Francisco Bay (USA), using the sediment quality triad and multivariate analysis. Cienc Mar 24:3313–3336

DelValls TA, Forja JM, González-Mazo E, Gómez-Parra A (1998) Determining contamination sources in marine sediments using multivariate analysis. Trends Analyt Chem 17:181–192

EU Directive CCS (2008) Proposal for a directive of the European Parliament and the council on the geological storage of carbon dioxide and amending Council Directives 85/337/EEC, 96/61/EC, Directives 2000/60/EC, 2001/80/EC, 2004/35/EC, 2006/12/EC and Regulation (EC) No 1013/2006

Findlay HS, Kendall MA, Spicer JI, Turley CM, Widdicombe S (2008) Novel microcosm system for the investigating the effects of elevated carbon dioxide and temperature on intertidal organisms. Aquat Biol 3:51–62

IPCC (2005) Special report on carbon dioxide capture and storage. Prepared by working group III of the United Nations Intergovernmental Panel on Climate Change (IPCC). In: Metz B, Davison O, de Coninck H, Loos M, Meyer L (eds). Cambridge University Press, Cambridge, UK, pp 431

IPCC (2007). Climate change 2007: Synthesis report. Contribution of working groups I, II and III to the fourth assessment report of the United Nations Intergovernmental Panel on Climate Change. Core Writing Team, Pachauri RK, Reisinger A (eds). IPCC, Geneva, Switzerland, pp 104

Klusman R (2003) Evaluation of leakage potential from a CO2 EOR/Sequestration project. Energy Conv Manag 44(12):1921–1940

Laurikka H, Springer U (2003) Risk and return of project-based climate change mitigation: A portfolio approach. Glob EnvironChan 13:207–217

London Convention and Protocol (2006) Risk assessment and management framework for CO_2 sequestration in sub-seabed geological formations. London Convention on the prevention of Marine Pollution by Dumping of Wastes and Other Matter 1972 and 1996 Protocol Thereto

London Protocol (2007) Specific guidelines for the assessment of carbon dioxide streams for disposal into sub-seabed geological formations. 1996 London Protocol on the prevention of Marine Pollution by Dumping of Wastes and Other Matter

Luff R, Moll A (2004) Seasonal dynamics of the North Sea sediments using a three-dimensional couple water-sediment model system. Cont Shelf Res 24:1099–1127

Martín-Díaz ML, Villena-Lincoln A, Lamber S, Blasco J, DelValls TA (2005) An integrated approach using bioaccumulation and biomarker measurements in female shore crab, Carcinus maenas. Chemosphere 58:615–626

Martín-Díaz ML, Jiménez-Tenorio N, Sales D, DelValls TA (2008) Accumulation and histopathological damage in the clam Ruditapes philippinarum and the crab Carcinus maenas to assess sediment toxicity in Spanish ports. Chemosphere 71:1916–1927

Matthiessen P, Bifield S, Jarrett F, Kirby MF, Law RJ, McMinn WR, Sheahan DA, Thain JE, Whale GF (1998) An assessment of sediment toxicity in the River Tyne Estuary, UK by means of bioassays. Mar Environ Res 45(1):1–1 5

Miles H, Widdicombe S, Spicer JI, Hall-Spencer J (2007) Effects of anthropogenic seawater acidification on acid-based balance in the sea urchin Psammechinus miliaris. Mar Pollut Bull 54:89–96

Morales-Caselles C, Riba I, Sarasquete C, DelValls TA (2007) Using a classical weight-of-evidence approach for 4-years monitoring of the impact of an accidental oil spill on sediment quality. Environ Int 34(4):514–523

OSPAR Convention (2005) The Royal Society of the United Kingdom. Ocean acidification due to increasing atmospheric carbon dioxide. The Royal Policy Document 2005. OSPAR Convention for the Protection of the Marine Environment of the North-East Atlantic

OSPAR Convention (2007) Guidelines for risk assessment and management of storage of carbon dioxide streams in sub-seabed geological formations. OSPAR Convention for the Protection of the Marine Environment of the North-East Atlantic

Reguera FD, DelValls TA, Forja JM (2008) Carbon dioxide storage in marine geological formations. Risk assessment and management requirements in the international conventions on the protection of the marine environment. From the proceedings of the 7º Congresso Ibérico e 4º Iberoamericano de Contaminação e Toxicologia Ambiental (CICTA 2008). Lisboa, Portugal

Riba I, García-Luque E, Blasco J, DelValls TA (2003a) Bioavailability of heavy metals bound to estuarine sediments as a function of pH and salinity values. Chem Spec Bioav 15(4):101–114

Riba I, Zitko V, Forja JM, DelValls TA (2003b) Deriving sediment quality guidelines in the Guadalquivir estuary associated with the Aznalcóllar mining spill: A comparison of different approaches. Cienc Mar 29(3):261–274

Riba I, DelValls TA, Forja JM, Gómez-Parra A (2004) The influence of pH and salinity on the toxicity of heavy metals in sediment to the estuarine clam Ruditapes philippinarum. Environ Tox Chem 23(5):1100–1107

Riba I, DelValls TA, Reynoldson TB, Milani D (2006) Sediment quality in Rio Guadiamar (SW, Spain) after a tailing dam collapse: Contamination, toxicity and bioavailability. Environ Int 32:891–900

Spicer JI, Raffo A, Widdicombe S (2007) Influence of CO2-related seawater acidification on extracellular acid-base balance in the velvet swimming crab Necora puber. Mar Bio 151:1117–1125

Stern N (2007) The economics of climate change. Cambridge University Press, Cambridge. 712 pp

Summers J, Smith C, Vetter E, Bergman P, Adams E, Akai M (2004) Results of international field experiment on a natural CO2 analogue. From the proceedings of the Seventh International Conference on Greenhouse Gas Control Technologies, Vancouver, Canada

Thompson B, Anderson B, Hunt J, Taberski K, Phillips B (1999) Relationships between sediment contamination and toxicity in San Francisco Bay. Mar Environ Res 48:285–309

Van Vuuren D, Den Elzen M, Lucas P, Eickhout B, Strengers B, Van Ruijven B, Wonink S, Van Houdt R (2007) Stabilizing greenhouse gas concentrations at low levels: An assessment of reduction strategies and costs. Clim Chang 81:119–159

Wallmann K (2008) Maximum acceptable leakage rate to abate long term global warming and to protect marine life. From the proceedings of the Workshop on Sub-Seabed Carbon Dioxide Storage. How to store CO_2 safely for the marine environment - from planning to eternity? Umweltbundesamt. Berlin, Germany

Widdicombe S, Needham HR (2007) Impact of CO2 induced seawater acidification on the burrowing activity of *Nereis virens* (Sars1835) and sediment nutrient flux. Mar Ecol Prog Ser 341:111–122

Wilson M, Monea M (2004) Weyburn CO_2 monitoring and storage project summary report 2000–2004. From the proceedings of the 7th international conference on green house gas control technologies. IEA GHG, Vancouver, Canada

Index

A
Abril, G., 52, 53
Acidification, 48, 54, 61, 62, 64–67, 77–80, 87, 94, 109, 113–127, 159–161, 168
Agricultural fertilizers, 47, 53, 54, 59–61
Air-sea exchange, 23, 24, 45
Alkalinity, 56, 60, 63, 80, 94, 95, 97–100, 102, 107, 109
Allerød event, 1–3, 8, 11–13, 16, 19
Amyot, M., 147
Andersson, A.J., 54
Aragonite, 61, 63, 93, 107–110
Atmosphere, 11, 23–25, 28, 32, 42, 47, 50, 52, 55, 56, 61, 79, 89, 93, 95–97, 103, 107, 109, 110, 114, 119, 132–134, 144–147, 155–157, 160
Atmospheric deposition, 48, 52–54, 59–61, 144

B
Bakker, 24
Balch, W.M., 64
Barros, N., 23–45
Bates, N.R., 57, 65
Bölling, 1—3, 8, 11–13, 16
Bioaccumulation, 113–127, 137, 164, 165
Bioavailability, 94, 114, 115, 123, 125, 126, 164
Björck, S., 12, 13
Blasco, J., 113–127
Bopp, L., 52
Borate, 100–106
Borges, A.V., 24, 47–67
Borges, M.F., 78
Brogueira, M.J., 77–90
Buffer capacity, 93, 94, 103, 105–107, 110, 118, 119
Byrne, R.H., 98

C
Cabeçadas, G., 77–90
Cabeçadas, L., 77–90
Caçador, I., 140
Caetano, M., 131–147
Cai, W-J., 24, 49, 50
Calcifying organisms, 77, 79, 94, 110
Calcite, 61, 63, 89, 93, 107–110
Calcium carbonate, 48, 89, 93, 94, 106–110
Canário, J., 131–147
Carbonate, 48, 53, 54, 60–66, 79, 87, 89, 93, 94, 96, 97, 100, 102–110, 118
Carbonate chemistry, 48, 53, 54, 61–66, 79, 89, 93, 108, 109
Carbon dioxide, 23–45, 47–67, 93, 95–100, 113–116, 119, 126, 155–166
  capture, 114
  fluxes, 47–67
  sequestration, 127, 157
Carvalho, R., 4, 23–45
Chapman, P.M., 120, 121
Chen, C.T.A., 24, 49, 53
Chen, S.T., 82
Chlorophyll-*a*, 55, 77–80, 84–86, 102
Clams, 115–126
Clayton, T.D., 98
Climate change, 2, 7, 13, 16, 24, 25, 47, 48, 55, 57, 59, 65, 77–90, 107, 109, 114, 131–147, 156, 157
Climate variability, 1–16
Coastal environments, 24, 48, 50, 61, 62, 64, 79, 143, 144
Coastal ocean, 47–67
Coastal upwelling, 48, 51, 53–57, 77–79
Coastal zone, 23–45, 60, 135, 137, 142, 145, 146
Contaminant, 114–116, 123, 127, 131–147, 159, 163–165
Copin-Montégut, C., 65

D
da Cunha, L.C., 60
Deglaciation, 1–16
DeGrandpre, M.D., 65
DelValls, T.A., 119, 120, 155–166
Desprat, S., 7
Dickson, A.G., 63, 81, 97, 100, 101
Doney, S.C., 61
Douglas, T.A., 134
Douro estuary, 3–6, 10, 15, 16
Drago, T., 1–17
Dryas episode, 1
Duarte, P., 23–45

E
Ekman, 55
El-Rayis, O.A., 120
Emission, 23–45, 47, 52, 57, 98, 110, 114, 156, 157, 163, 166
Engel, A., 79
ESTOC, 93–107, 109, 110
Estuarine sediments, 114, 115, 138
Estuary, 2–6, 10, 15, 16, 61, 77, 80, 83, 85, 87, 89, 117, 118, 121, 123–126, 138, 140, 142–147

F
Fabry, V.J., 61
Feedbacks, 11, 47–67
Fennel, K., 61
Ferreira, A.M., 131–147
Fiuza, A.F.G., 78
Forest, 1, 10–12, 14–16, 24, 27, 29, 38, 66, 142
Forja, J.M., 120, 155–166
Frankignoulle, M., 24, 56, 65
Freitas, M.C., 1–17

G
García-Luque, E., 113–127
Glacial-interglacial transition, 1, 2, 10–11, 14, 16
Global change, 47–67, 134
Global warming, 2, 23, 24, 53, 55, 57, 62, 66, 113, 116, 137, 163
Gómez-Parra, A., 120
González-Dávila, M., 93–111
Goyet, C., 81, 97
Green house gases, 47
Gypens, N., 60, 63

H
Heinrich, 7–10, 16
Hirst, A.C., 57
Ho, K.T., 121
Holocene, 1, 3, 8, 9, 14–16
Hydrological cycle, 47, 53, 54, 59–61, 134, 144

J
Jahnke, R.A., 49
Jiang, L-Q., 50

K
Kalman, J., 113–127
Kleypas, J.A., 61, 94
Kuss, J., 65

L
Land use, 24, 30, 47, 53, 54, 59–61, 156, 157
Le Corre, P., 80
Loring, D.H., 120
Luoma, S.N., 121

M
Mackenzie, F.T., 52, 60
Marine ecosystem, 47, 78, 109, 131–133
Marine environment, 114, 115, 137, 155, 156, 158–166
Mehrbach, C., 63, 100, 101
Mercury, 131, 134–138, 146, 147
Merico, A., 66
Metals, 94, 113–117, 119, 121–127, 131, 137, 139–142, 164
Metropolitan area, 23–45
Millero, F.J., 63, 93, 97, 98, 100, 101
Mintrop, L., 99
Mitigation, 126, 157–159, 165, 166
Model, 23, 25, 27, 29–35, 41, 42, 44, 45, 52, 54, 55, 57, 60, 61, 63, 64, 79, 80, 94, 98, 109, 113, 116, 120, 132, 134, 143, 157, 159, 160, 164
Monitoring, 24, 27, 33, 35, 45, 114, 155, 157–159, 164–166
Mount, D.I., 118
Mount, D.R., 118
Mucci, A., 63

N
Naughton, A.F., 3
Naughton, F., 1–17
Nogueira, E., 78
Nogueira, M., 77–90
North-western Iberian peninsula, 1–16
Nutrients, 48, 52–54, 59, 60, 65, 77–80, 82–85, 87, 89, 95, 137, 163

O
Ocean, 2, 5, 10, 23, 25, 32, 33, 35, 42, 44, 47–67, 77–79, 81, 87, 89, 90, 93–96, 98, 100–103, 106–110
Ocean acidification, 48, 54, 61, 62, 64–67, 77, 94, 109, 114
Oliveira, A.P., 77–90
Omar, 65

P
Park, O., 33
Parsons, T.R., 81
Particulate metals, 131, 142
Paulmier, A., 56
Peliz, A.J., 78
pH, 61–65, 77, 79–81, 89, 90, 93–110, 113–122, 124, 127, 137, 159, 160, 166
Phytoplankton, 55, 64–66, 77–90, 109, 159
Plattner, G-K., 55
Poissant, L., 131–147
Pollen, 2–5, 7–16
Polychlorinated biphenyls, 144–146
Polycyclic aromatic hydrocarbons, 141

R
Rantala, R.T.T., 120
Raven, J., 61
Regional scale, 23, 33
Reguera, F.D., 155–166
Renssen, H., 13
Revelle factor, 93, 104, 106–107, 110
Riba, I., 113–127, 155–166
Riebesell, U., 65
Risk assessment, 114, 126, 156, 158–159, 162, 165, 166
River, 3–5, 10, 13, 14, 25, 48, 50, 52–54, 59, 60, 62, 63, 67, 77–80, 82–84, 86, 87, 89, 113, 115, 117, 118, 121, 123, 133, 135, 136, 141–147
Rosa, 4
Roy, R.N., 82

S
Salisbury, J., 62
Salt marshes, 52, 66, 118, 131, 139–141
Sanchez-Goñi, M.F., 1–17
Santana-Casiano, J.M., 93–111
Sarmiento, J.L., 57
Saturation state, 61, 63, 79, 93, 107, 108, 110
Schiettecatte, L-S., 50
Schneider, B., 65
Sea level, 2, 3, 5, 13, 16, 47, 66, 131, 132, 139–141
Seawater, 48, 53, 54, 60–66, 77, 80, 87, 89, 93–110, 161, 163
Sedimentation, 3, 13, 139
Sediment quality, 116, 157, 164, 165
Sediments, 13, 15, 61, 67, 78, 109, 113–117, 119–127, 131, 133, 137–147, 155–166
Seok, M., 33
Stern, N., 166
Storage, 114, 115, 117, 126, 127, 155–166
Strickland, J.D.H., 81
Stuiver, M., 5

T
Takahaschi, M., 82
Temperature, 2, 5, 11–16, 27, 30, 33, 41, 47, 53, 55, 58–60, 63, 66, 79, 80, 83–86, 95–98, 104, 107, 109, 119, 131–134, 137–140, 146, 162
Thomas, H., 49, 50
Time series station, 94–96, 98, 110
Total inorganic carbon, 94, 97, 100, 101, 107
Tréguer, P., 80
Tsunogai, S., 49
Tyrrell, T., 66

V
Vale, C., 113–127, 131–147
Vegetation, 1–3, 5, 7, 8, 10–12, 14–16, 139

W
Walker, M.J.C., 12, 13
Wallmann, K., 161, 163

Walsh, J.J., 49
Wang, S.L., 65
Waste water inputs, 53, 54, 59–61
Weight of evidence, 115, 155–166
Weiss, R.F., 82
Wind, 5, 24, 27, 28, 30, 32, 33, 40, 41, 44, 49, 54, 55, 57, 77, 78, 80, 139, 140, 147

Z
Zn, 113–127, 140